

THESIS FOR THE DEGREE OF DOCTOR OF PHILOSOPHY

# Three Phase Controlled Fault Interruption

Using

# High Voltage SF<sub>6</sub> Circuit Breakers

by

RICHARD THOMAS

Division of Electric Power Engineering  
Department of Energy and Environment  
Chalmers University of Technology  
Göteborg, Sweden, 2007

---

Three Phase Controlled Fault Interruption Using High Voltage SF<sub>6</sub> Circuit Breakers

RICHARD THOMAS

© RICHARD THOMAS, 2007.

Division of Electrical Power Engineering

Department of Energy and Environment

Chalmers University of Technology

ISBN 978-91-7291-976-1

ISSN 0346-718X

Ny serie nr. 2657

SE-412 96 Göteborg

Sweden

Telephone: +46 (0)31 - 722 1000

Printed by: Chalmers University of Technology, Reproservice

Göteborg, Sweden, 2007.

---

## Abstract

A method is presented for implementing controlled fault interruption, using high voltage, SF<sub>6</sub> circuit breakers on three phase high voltage power networks. The main goal of the method is to synchronize the opening or trip commands to each phase of a circuit breaker with respect to target current zero times so that each phase will interrupt with a preselected arcing time. Benefits of this approach include reduction in the electrical wear rate of the circuit breaker, in addition to providing potential to optimize existing interrupter technologies and facilitate new interruption techniques.

A generic structure for controlled fault interruption algorithms is proposed, aimed at utilizing synergies with existing digital power system protection methods. The proposed method is based on estimating the future behavior of the currents in each phase, using a generic model. The parameters of the model of the currents are obtained using least mean squares regression. Novel features of the proposed method include the use of analysis-of- variance tests to validate the model for targeting instant selection, provision of algorithm failure bypass control, identification of multiphase fault types and detection of the fault inception instant. A comprehensive range of future work proposals is also provided.

Simulations have been made using the proposed method for a range of multiphase fault cases than may occur on a three phase power network. The results indicate that the method is capable of discriminating between different fault cases and estimating target current zero times within  $\pm 0.5$  ms, within typical protection system response times of 5 to 20 ms, even with large random noise distortion of the measured current signals.

High power experiments have also been conducted to investigate the stability of the minimum arcing times of a high voltage, SF<sub>6</sub> circuit breaker, operated at 80% of its normal opening speed, for a wide range of fault current interruption duties. The results of these experiments confirm the viability of controlled fault interruption from the perspective of minimum arcing time stability, in addition to indicating significant potential for circuit breaker optimization by using the controlled fault interruption technique to restrict the required arcing time window and thereby also the required interrupter operating energy.

### Keywords:

circuit breakers, controlled switching, fault interruption, high voltage, hypothesis testing, least mean squares regression, power system protection

# Acknowledgements

I extend my sincere thanks for the generous financial support provided for this project by my employer, ABB AB (50%), the Swedish Energy Authority (Svenska Energimyndigheten) (40%) and Elforsk AB (10%) through the ELEKTRA programme project nr. 3679. Special thanks also to Sven Jansson and the staff at Elforsk AB for providing the administrative support of this project.

I am very grateful to my supervisor, Dr Carl-Ejnar Sölver (ABB AB), for his patient guidance, excellent advice and unfailing support. To Professors Jaap Daalder and Gustaf Olsson I offer many thanks for their excellent support as my examiners and to whom I grateful for many interesting discussions and valued critical opinions. I have also been extremely fortunate in having had the support and guidance of an excellent reference group, containing an exceptional depth of knowledge and breadth of experience that has been generously shared at all times - special thanks to all the reference group members including, Dr Sture Lindahl (Gothia Power AB), Per Jonsson (ABB AB), Lars Wallin (Svenska Kraftnät) and Anders Holm (Vattenfall Utveckling).

Many thanks also to the staff of the ABB High Power Laboratory in Ludvika, Sweden, for their expert assistance in the preparation and execution of the high power experiments described in this thesis.

To my friends and colleagues at ABB - thank you for your support, not only during this work, but for all the memorable and rewarding times I have had during the past nine years in Ludvika. To all the great friends amongst the fellow doctoral students and staff at Chalmers - thank you very much for your great support and many very happy memories of life in Göteborg. It has been a privilege to work with so many highly skilled and dedicated professionals and I consider myself very fortunate to count many as close friends.

Not least of course, my deepest thanks to my family, spread far and wide around the globe, for their unfailing love and support - thank you! It has been a wonderful opportunity to live in Sweden, work with ABB and study at Chalmers - I hope that this thesis, at least in some small way, proves worthy of all the wonderful support you given.

*“Grant me the serenity to accept the things I cannot change,  
The courage to change the things that I can,  
And the wisdom to know the difference.”*  
- Reinhold Niebuhr

*“Perfection is achieved, not when there is nothing left to add,  
but when there is nothing left to take away.”*  
- Antoine de Saint-Exupery

# Table of Contents

<b>Abstract</b> .....	<b>iii</b>
<b>Acknowledgements</b> .....	<b>iv</b>
<b>Abbreviations</b> .....	<b>vii</b>
<b>Symbols &amp; Nomenclatures</b> .....	<b>viii</b>
<b>1 Introduction</b> .....	<b>9</b>
1.1 Definition of controlled fault interruption .....	9
1.2 Thesis goals .....	13
1.3 Motivations for controlled fault interruption research .....	14
1.4 Scope of work .....	15
1.5 Thesis structure .....	22
1.6 List of publications .....	23
<b>2 Three phase fault interruption theory</b> .....	<b>25</b>
2.1 Applied power system model .....	26
2.2 Multiphase fault behaviors .....	31
2.3 Fault cases and power system configurations requiring further investigation .....	39
<b>3 High power experiments</b> .....	<b>45</b>
3.1 Experimental considerations .....	45
3.2 Disclaimer .....	46
3.3 Experiment objectives .....	47
3.4 Test object description .....	48
3.3 Applied high power interruption test duties .....	54
3.4 Experimental method .....	55
3.5 CFI arcing window results .....	64
3.6 Implications for controlled fault interruption .....	70
<b>4 Three phase controlled fault interruption - General theory</b> .....	<b>71</b>
4.1 General requirements and constraints on CFI .....	71
4.2 CFI current zero targeting strategies .....	73
4.3 Prior art and research relevant to CFI .....	77
4.4 General CFI and protection system process interactions .....	78
4.5 CFI and protection system synergies and differences .....	80
4.6 Overall comparison of CFI and distance protection schemes .....	89
4.7 Proposed CFI process structure for three phase networks .....	91
<b>5 Three phase controlled fault interruption - Proposed method</b> .....	<b>93</b>
5.1 Overall proposed CFI process .....	93
5.2 Applied fault current models and parameter estimation method .....	96
5.3 Analysis of variance (F0) tests .....	99
5.4 Synchronizing target selections .....	106
5.5 Simulation examples of proposed method .....	108

## Table of Contents

<b>6 Three phase controlled fault interruption - Simulation tests .....</b>	<b>115</b>
6.1 Description of simulation program structure .....	115
6.2 Performance indicators used for CFI algorithm assessment .....	115
6.3 Parameter values used for CFI simulations .....	120
6.4 Single parameter set CFI simulation examples .....	125
6.5 Baseline “ideal” CFI simulation results .....	131
6.6 Multiple run parameter set CFI simulation results - with signal noise .....	135
<b>7 Future work proposals .....</b>	<b>147</b>
7.1 Fault current model and parameter estimation technique comparisons .....	147
7.2 Parameter variation sensitivity analyses .....	151
7.3 CFI implementation and simulation on large scale power system models .....	155
7.4 Field trialing of current prediction method .....	157
7.5 Current interruption technologies based on CFI .....	159
<b>8 Conclusions .....</b>	<b>161</b>
8.1 Fulfilment of thesis goals .....	161
8.2 Novel contributions of the work .....	162
8.3 Results summary .....	165
8.4 Areas for further development .....	165
8.5 Closing remarks .....	166
<b>References .....</b>	<b>167</b>
<b>Appendix A - EMTDC/PSCAD fault model description .....</b>	<b>174</b>

# Abbreviations

The following is a list of abbreviations used throughout this thesis:

AC	alternating current
A/D	analogue-to-digital (conversion)
ANOVA	analysis-of-variance
ANSI	American National Standards Institute, Inc.
CB	circuit breaker
CFI	controlled fault interruption
CIGRÉ	International Council on Large Electric Systems
CT	current transformer
DC	direct current
DFT	discrete Fourier transform
FPTC	first-pole-to-clear
GPS	global positioning system
HV	high voltage
IEC	International Electrotechnical Commission
IEEE	Institute of Electrical and Electronic Engineers
LES	least error squares
LMS	least mean squares
LC1	line-charging breaking current test duty (circuit no.1) as per IEC 62271-100 (2003)
L <sub>90</sub>	short-line fault test duty applying 90% of rated symmetrical fault current as per IEC 62271-100 (2003)
max	maximum
min	minimum
OoP	out-of-phase fault test duty for 180 degree phase opposition as per IEC 62271-100 (2003)
RDDS	rate of decline of dielectric strength
RRDS	rate of rise of dielectric strength
RRRV	rate of rise of recovery voltage
S/H	sample-and-hold
SF <sub>6</sub>	sulphur hexafluoride
SLF	short-line fault;
TRV	transient recovery voltage
T30	short-circuit test duty applying 30% of the rated symmetrical fault current as per IEC 62271-100 (2003)
T60	short-circuit test duty applying 60% of the rated symmetrical fault current as per IEC 62271-100 (2003)
T100a	asymmetrical short-circuit test duty applying 100% of the rated symmetrical fault current as per IEC 62271-100 (2003)
VT	voltage transformer
WGN	white gaussian noise
WLMS	weighted least mean squares

# Symbols & Nomenclatures

The following is a list of symbols and nomenclature used throughout this thesis:

$\alpha$	fault initiation angle with respect to driving source phase voltage
$\Delta$	difference (delta)
$\gamma$	source voltage reference angle, relative to reference source phase voltage
$\phi$	fault current phase angle
$\pi$	$\pi = 3.14159\dots$
$\sigma$	standard deviation
$\tau$	time constant of fault current exponentially decaying component
$\omega$	power system angular frequency
$dx(t)/dt$	derivative of $x(t)$ with respect to $t$
$\mathbf{X}$	matrix “X”
$\mathbf{x}$	vector “x”
$\mathbf{X}^T$	transpose of matrix “X”
$\mathbf{v}^T$	transpose of vector “x”
R	resistance
L	inductance
C	capacitance
X	reactance
$f$	power system time frequency
$i$	instantaneous current as function of time, i.e. $i(t)$
$u$	instantaneous voltage as function of time, i.e. $u(t)$
$t$	time
$e$	exponential function

## Subscripts:

S	source
L	load
F	fault
PK	peak
$x$	phase designations

## Superscripts:

$\hat{a}$	estimated values of variable “a”
-----------	----------------------------------



# 1 Introduction

As described in the licentiate thesis [1], controlled switching of well defined load applications, such as shunt capacitor and reactor banks, has become a widely accepted practice for switching transient mitigation on high voltage alternating current (HV AC) power systems [11], [12], [13], [14], [53]. Controlled switching for fault interruption has only been restricted to a few theoretical studies [2], [17], or experimental installations e.g. American Electric Power experimental breaker described by Garzon [3], though there do exist a number of patents directed within this area, both for conventional arc-based interrupters [55], [56] and power electronic-based interrupters [54].

## 1.1 Definition of controlled fault interruption

Controlled fault interruption (CFI) aims to synchronize the trip command(s) to a circuit-breaker with respect to target instants e.g. future current zero crossings, so as to achieve a selected (or “optimum”) arcing time for interruption. The primary goal of CFI is to avoid longer arcing times that add to the stress and wear on a circuit breaker, without necessarily providing a higher probability of successful interruption.

The concept of CFI is illustrated in Figure 1.1 for a single phase earth fault. In the case of a direct or “non-CFI” protection trip operation, the protection system will issue its trip command to the circuit breaker after the protection operation time,  $t_{\text{PROT}}$ . The circuit breaker arcing contacts will begin to separate at the circuit breaker opening time,  $t_{\text{OPEN}}$ , after the trip command. The current will then be conducted by the arc between the arcing contacts and interrupted at the first current zero in each phase that occurs after the required minimum arcing time,  $t_{\text{MIN\_ARC}}$ . The minimum arcing time constraint is dictated by the required contact gap and mass flow of interrupting medium (e.g.  $\text{SF}_6$  gas) in the contact gap region at current zero in order to extinguish the arc thermally and provide the necessary dielectric withstand against the subsequent transient recovery voltage that will develop between the open contacts after current extinction.

As can be seen in the example shown in Figure 1.1 the interruption current zero is not necessarily the first current zero that occurs after arcing contact separation. This is due to both the minimum arcing time constraint and the random, non-synchronized relative timing of arcing contact separation and current zero occurrence. In the direct tripping case an arcing time,  $t_{\text{DIRECT\_ARC}}$ , occurs that is somewhat longer than the minimum arcing time. This longer arcing time does not necessarily increase the probability of successful interruption, compared to the minimum arcing time and at worst only contributes to additional electrical contact wear.

In contrast to direct tripping, CFI control delays the issuing of the trip command after  $t_{\text{PROT}}$  so that the circuit breaker will open and experience an arcing time,  $t_{\text{CFI\_ARC}}$ , that is close to the minimum arcing time. The CFI control requires that the target interruption current zero time be accurately estimated within the protection operation time,  $t_{\text{PROT}}$ , so that the required waiting time for the CFI trip command can be calculated and have no delay in the total fault clearing time. The targeted arcing time,  $t_{\text{CFI\_ARC}}$ , is slightly longer than  $t_{\text{MIN\_ARC}}$ . The additional arc margin in  $t_{\text{CFI\_ARC}}$  is to cater for minor variations in  $t_{\text{OPEN}}$ ,  $t_{\text{MIN\_ARC}}$  and possible errors in the estimation of the target interruption current zero time.

It is important to note that the *CFI control is complementary to the protection system and not a replacement*. The protection system retains its critical role of determining whether or not the circuit breaker must be tripped. The CFI control simply aims to synchronize the eventual trip command to achieve interruption with a non-excessive and more desirable arcing time. The functional relationship between the protection system and the CFI control is illustrated in Figure 1.2.

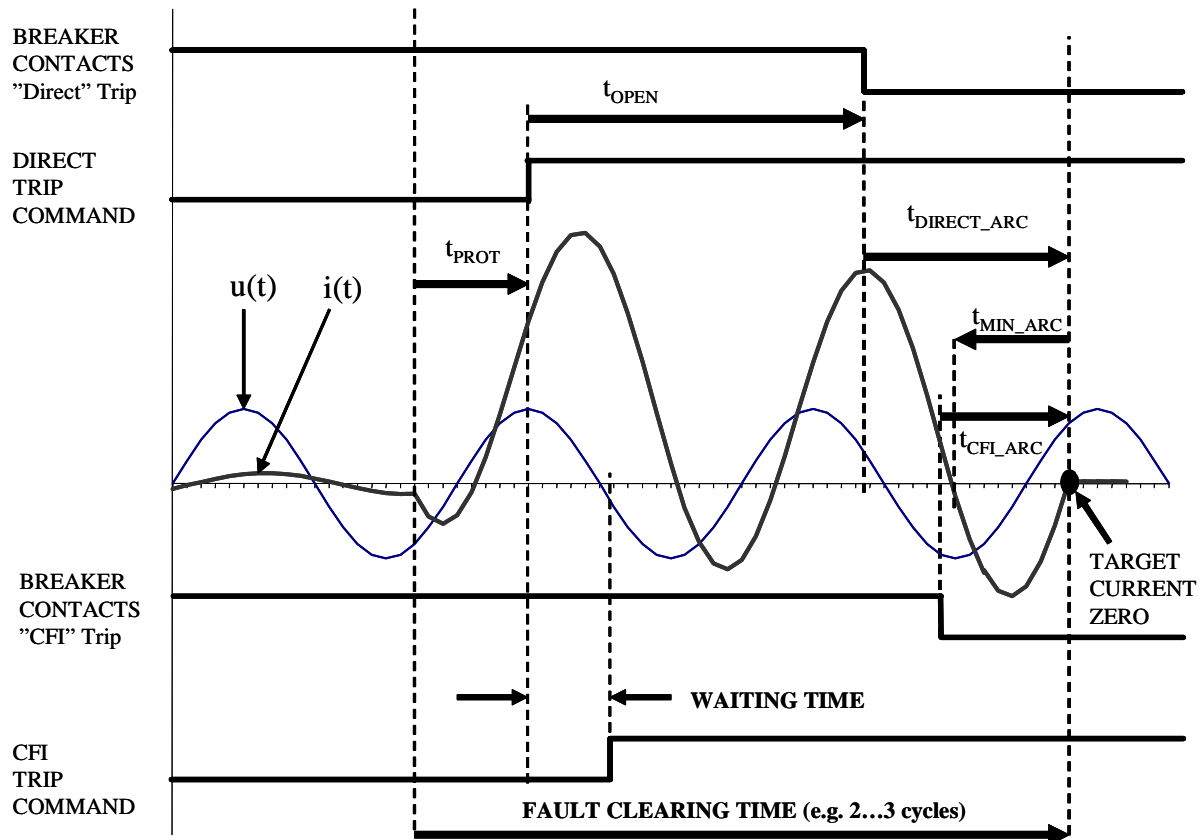


**Figure 1.1 : Comparison of direct and controlled fault interruption (single phase)**

In the implementation of CFI, as proposed in both the licentiate and this thesis, the protection and CFI systems process the same voltage and current data, but for different purposes. The protection system processes the data to determine if the criteria for a protection operation are met and that operation of the associated circuit breaker(s) is required. The CFI system processes the data to make an estimation of viable interruption current zero times. As indicated in Figure 1.2, the proposed CFI method includes a validation check of the target estimations and in the event of an insufficiently reliable result can force the waiting time to zero and divert the circuit breaker control to direct tripping. An alternative CFI bypass strategy can be to divert the tripping to back-up protection and circuit breaker operation. Selection of the preferred bypass strategy is dependent on whether or not the associated circuit breaker is critically dependent on CFI control to achieve interruption i.e. can the circuit breaker interrupt with a “full” or only a “restricted” arcing time window.

A further point to note from Figure 1.2 is that as the protection and CFI systems process the same voltage and current signal data, they can operate within the same hardware platform. In other words, a CFI algorithm can be embedded within an existing digital protection relay without need of additional hardware. This offers both cost and performance benefits. As will be shown later in this thesis there are significant potential synergies to be gained from the protection and CFI systems using the same data signal processing platform. In addition it will be shown that while the functions and objectives of the protection and CFI systems are separate and different, they share a large amount of common data e.g. distance protection schemes that make estimation of the fault current phase angle. This common data link offers potential benefits in the research and development of both protection and CFI systems.

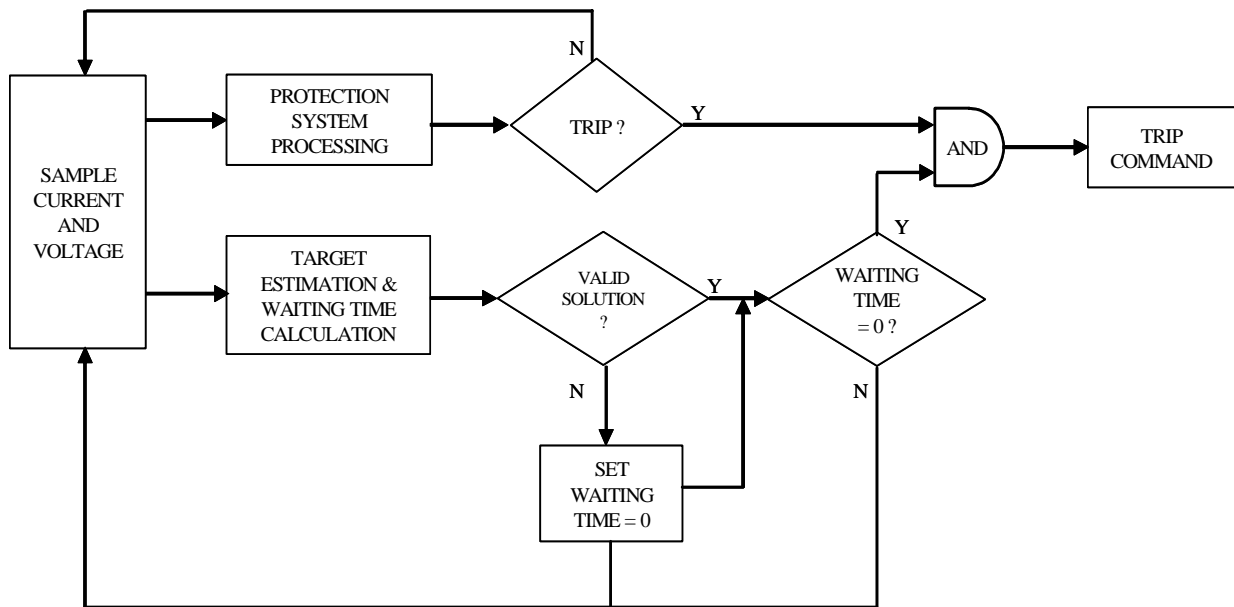


**Figure 1.2 : Functional relationship between protection and controlled fault interruption systems**

As stated earlier, CFI has yet to reach the same implementation status as controlled load switching. While both applications fall generally under the umbrella of controlled switching and have some common aspects, they have substantially different objectives and constraints. A summary comparison of controlled load switching and CFI is presented in Table 1.1. The strongest common link between controlled load switching and CFI is reliance on known, stable and consistent circuit breaker operating times. The most notable differences between the two applications are the complexity of synchronizing target identification, calculation time constraints and the consequences of control system failure.

While there are applications within controlled load switching, e.g. energizing of shunt compensated lines, that have complex non-periodic targets, the time to reach a target solution is typically non-critical, at least compared to the quarter to one cycle time of a protection relay operation. The consequences of a failure of the controlled switching scheme is also a significant difference between the load switching and fault interruption applications. The potentially severe consequences of a CFI system failure should not be under- nor overstated, but considered in the context of the application. The reliability demands on a CFI scheme should be considered in the

context of protection system operation terms such as dependability and security. Dependability of a protection system has been defined as the probability that the system will operate correctly for all cases of its *intended* application, over given time period, whereas security is considered as the probability that the system will not operate incorrectly in any case, over a given time period [4]. CIGRÉ WG 34.01 provide quantified definitions of these performance indices [8].

**Table 1.1: Summary comparison of controlled load switching and controlled fault interruption**

	Characteristic	Requirements / Consequences	
		Controlled Load Switching	Controlled Fault Interruption
1	Main purpose	Switching transient mitigation	Arcing time control
2	Main benefits	Reduction in switching overvoltage magnitudes Avoidance of re-ignitions on inductive current interruption Increased margin against capacitive current restrike risk	Reduction in interrupter electrical wear rate Potential for circuit breaker design optimization Facilitation of new interruption technologies
3	Frequency of use	Can be daily for shunt capacitor / reactor banks or infrequent for transformers and lines.	Typically infrequent, dependent on fault occurrence rates.
4	Target selection and identification	Mostly simple, periodic targets (except for compensated lines and some transformer applications)	Target times vary significantly due to fault current asymmetry and range of fault types
5	Target and control calculation complexity	Relatively simple for periodic targets (except for compensated lines and some transformer applications)	Can be as complex as for protection system decisions due to range of possible fault type behaviors.
6	Calculation time	No major constraint. Load switching is not "time critical". Can allow several cycles of calculation time.	Time critical. Ideally must be done within protection response time, which can be as low as 0.25 cycle.
7	Circuit breaker operating time consistency	Important. Generally aimed at +/- 0.5 ms	Important. Generally aimed at +/-0.5 ms
8	Circuit breaker arcing time consistency	Some importance for interruption of small inductive (or capacitive) loads, but +/- 1 ms tolerance is manageable.	Important. Can vary according to fault type. Ideally needs to be known to +/- 1 ms tolerance.
9	Failure consequences	Low to moderate. Power system should be designed to manage non-controlled switching.	Moderate to severe. Worst case failure to interrupt fault, resulting in reliance on back-up protection and potential wider scale system interruption than otherwise necessary.

In summary the critical requirements for a viable CFI scheme include:

1. Ability to identify target interruption current zero times, with reasonable accuracy, for a full range of multiphase fault types within the nominal protection response time;

2. Provision of a “back-up” facility in the event of CFI system failure;
3. Knowledge and stability of circuit breaker mechanical performance;
4. Knowledge of circuit breaker (minimum) arcing time behavior;
5. Knowledge and appropriate design of data measurement, sampling, processing and control;

The first demand above has already been examined in detail for single phase fault currents in the licentiate thesis with good results. Target current zero times could be identified within  $\pm 0.5$  ms accuracy, even with onerous signal noise. The second requirement was also addressed in the licentiate thesis with the use of an analysis of variance test to verify the validity of the synchronizing target and regulate control of the algorithm. This thesis will describe a further development of the licentiate method to manage the basic range of multiphase fault combinations that can occur on a three phase HV AC network.

The requirement for known and stable mechanical operating time performance is common with conventional controlled load switching for transient mitigation and is generally achievable with most modern HV circuit breakers [50]. The most common applications of controlled load switching, including shunt capacitor and reactor bank operation tend to involve frequent (e.g. daily) switching and reference type tests such as the IEC class M2 10,000 operation mechanical endurance test [5] can provide good base data for assessing the suitability of a circuit breaker to such controlled load switching applications. Fault switching tends to be significantly less frequent and in addition the potential variation in fault type and fault current levels may impact significantly on the minimum arcing time constraints applicable in each case.

## 1.2 Thesis goals

This thesis has two main goals:

1. Extension of the single phase CFI method outlined in the licentiate thesis to three phase application with associated simulation analyses of algorithm performance under a range of system fault conditions.
2. High power experiments to investigate aspects of circuit-breaker performance related to both the application and potential benefits of controlled fault interruption.

HV AC fault interruption using circuit breakers is an inherently broad, complex and multi-disciplinary topic. It has been necessary therefore to limit the scope of this work within a set of acceptable problem boundaries, that offer sufficient scope for the work to be a useful foundation for further research to be conducted on this interesting and important topic. The scope limitations of the CFI solution presented in this thesis are described in more detail later in this chapter.

### 1.3 Motivations for controlled fault interruption research

The licentiate thesis identified several motivations for the study of CFI, including reduction in the rate of electrical wear of interrupters and as a means to facilitate new interruption technologies such as those based on solid state devices requiring commutation control. The results of the licentiate work indicated that it is feasible with a simple single phase current model to predict current zero times within  $\pm 0.5$  ms, under a wide range of asymmetrical current conditions and in the presence of large signal noise. The challenges set for this thesis work have been to extend the licentiate CFI method to manage fault cases on a three phase network and study the minimum arcing time behavior of an HV SF<sub>6</sub> circuit breaker, in conjunction to investigating the potential to optimize such a circuit breaker by reduction in its required operating energy by using CFI.

It shall not be overlooked that HV AC circuit breakers with arc based interrupters have been successfully used virtually since the advent of electric power systems in the late nineteenth century. Numerous interrupter designs, using air, oil, vacuum or SF<sub>6</sub> have been applied and continue in service around the world today [3], [34], [40]. International and local service reliability studies have been conducted on HV AC breakers and all have demonstrated that while the specific reliability and performance of different arc based interrupters, their media and mechanisms may vary, overall breakers have evolved to be very reliable given the onerous nature of their primary function of current interruption on command [35], [36], [37].

The vast majority of modern HV AC breakers use either vacuum (medium to high voltage applications) or SF<sub>6</sub> (high to ultra high voltage applications) as the interrupting medium. Such breakers generally have type test proven ratings to interrupt fault currents within two to three power frequency cycles. Modern vacuum and SF<sub>6</sub> breakers are designed, tested and expected to perform reliably in a wide range of environments, for decades and thousands of operations without need of major maintenance. Advanced tools exist for optimization of both the electrical and mechanical design and testing of such breakers [32], [33], [41], [42], [45]. HV AC circuit breakers work and work well. This poses the important question: Why complicate the control of HV circuit breakers by implementing CFI?

The easiest potential benefit to recognize is reduction in interrupter wear from avoiding longer than necessary arcing times [16]. As will be shown, such savings do incur other costs e.g. longer total fault clearing times in some cases. However this benefit is potentially the least of all. As stated earlier, the main benefit of interrupting with a selected arcing time is to avoid longer arcing times that may place additional stress or wear on an interrupter, without necessarily contributing to the probability of a successful interruption. An important consequence of the lack of synchronization of direct trip commands with respect to the eventual interruption current zeroes is that circuit breakers must be designed and type tested to verify their rated performances for a wide range of possible arcing times.

Interruption of capacitive currents involves a large number of type test operations down to near zero arcing time to verify the restrike probability of the circuit breaker. For higher current interruptions, ranging up to full symmetrical fault current rating the type tests are normally limited by international standards [5] to verification of the minimum, maximum and medium arcing times. The typical fault current arcing time range (or “window”) for a modern HV SF<sub>6</sub> circuit breaker ranges from 10 ms minimum to 20 ms maximum arcing times. At the same time,

cost optimization constraints require that circuit breakers fulfil their interruption ratings with a minimum of material and operating energy, while providing their functions reliably over as long as possible intervals without need of maintenance. Additional potential benefits of implementing a CFI scheme may therefore include:

1. Optimization of circuit-breaker design; freedom to design to narrow arcing time window(s);
2. Prediction of future current zeroes, leading to possibility for improved (faster) breaker failure detection;
3. Facilitation of new high-voltage interruption technologies e.g. “arc-free” (power electronic) interrupters, alternative interruption media to SF<sub>6</sub>;

The optimization of arc interrupter designs and facilitation of new interruption technologies may prove to eventually provide far greater overall and long term benefit in terms of cost, performance, health and environmental terms.

## 1.4 Scope of work

The primary focus of this work is the development of a method for synchronizing the trip commands of a HV AC circuit breaker to predicted current zero crossings in order to achieve a predetermined (“optimum”) arcing time, within the context of three phase AC networks.

HV AC fault interruption on three phase networks is a broad topic and by necessity the work described here has been limited in its scope in order to provide a manageable and useful focus for continued research. The chosen scope limitations for this work are summarized in four main areas described below:

### 1.4.1 Power system configuration:

While in principle applicable to three phase AC networks from MV to UHV levels, the primary focus of this work has been on application within HV to UHV transmission networks typically operated between 72-800 kV at 50 or 60 Hz. Figure 1.3 illustrates the areas within a classical, hierarchal power system where the proposed method can be expected to function without major enhancements and those applications where further work is required to both determine the requirements and develop a viable method for controlled fault interruption.

Essentially the focus of this work has been on circuit breakers within the transmission and sub-transmission parts of a classic network. Some specific exceptions indicated in Figure 1.3 include the boxed areas numbered 1, 2 and 3.

Boxed area 1 refers to circuit breakers located close to large generators where sub-transient reactance effects during faults can result in “missing” current zeros due to the transient exponential change in fault current magnitude, imposed in addition to the transient exponential DC offset present in a fault current [26], [31]. It can also be noted that HV generator circuit breakers are governed by a dedicated (ANSI) standard [10].

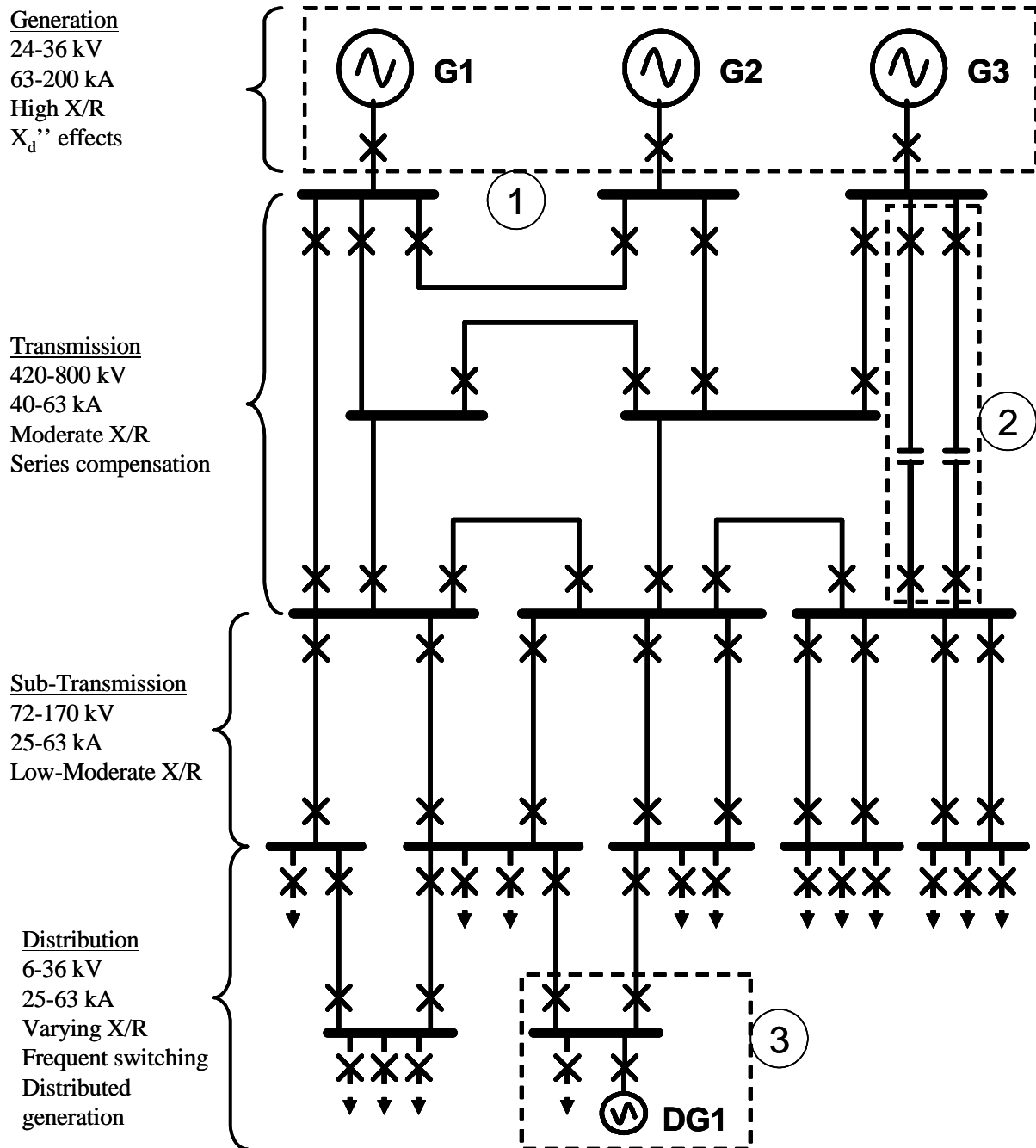


Figure 1.3 : Classical hierarchal power system

Boxed area 2 refers to series compensated lines, typically found in EHV transmission systems at 500 to 800 kV over long distances (e.g. 500 km). Faults on series compensated lines can exhibit both sub-synchronous resonances [51] and missing current zero transient periods [52], neither of which effects have been included within the scope of the CFI solution presented in this thesis.



Boxed area 3 refers to network cases found more typically in the traditional distribution network, including distributed generation stations or large industrial sites with large motors. Distributed generation can vary from combined cycle, gas turbine to wind turbine systems that may each exhibit special behaviors during fault conditions that have not been considered in detail in this thesis.

Transmission networks tend to have a meshed network configuration, resulting in that normally at least two (2) circuit breakers will be required to operate to fully isolate a faulted part of the network e.g. overhead transmission line. Busbar trip operations are a more extreme example of parallel circuit breaker operation and current interruption. Such parallel circuit breaker operation has not been explored in explicit detail in this work, though reference to its implications for the implementation of the proposed CFI scheme is discussed, in addition to suggestions for future work in this area.

Most transmission systems are effectively earthed networks, though at lower transmission and sub-transmission levels non-effectively earthed networks can be in use. The work described here has considered the implications of phase shifts occurring in the last phases to interrupt due to the absence of a zero sequence return path, but only in the context of three phase unearthed faults on an effectively earthed network. The main assumption applied in this work has been that the power system is effectively earthed on at least one side of the breaker.

Following from the focus on effectively earthed transmission systems, it has also been assumed that the system can effectively be modelled as an infinite bus symmetrical source. Such an assumption is typical in general short-circuit analyses and power system studies, though it must be recognized that in dealing with “faulted” networks, abnormal, unbalanced system conditions cannot be ignored. Two critical conditions for this particular research drawn from the infinite symmetrical bus model are:

1. the driving source voltages maintain their balanced phase relationships during a fault
2. the breaker to fault impedance is significantly greater than the source to breaker impedance (e.g. 10:1 ratio) and as such the phase angle difference between the ideal source voltage and the voltage measured at the breaker is “small” (i.e. less than 20 electrical degrees)

Even within the “general” network considered for this work different neutral point earthing arrangements do exist e.g. delta-star transformer winding arrangements. The effects of power transformer winding arrangements on fault current behavior have not been studied in detail in this work, as it has been assumed that the currents used for prediction of future current zero times are those measured directly at the associated circuit breaker location.

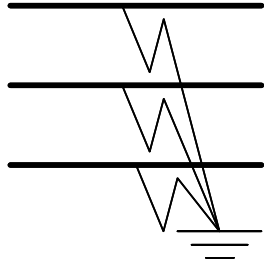
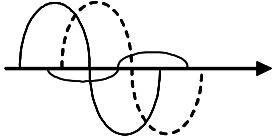
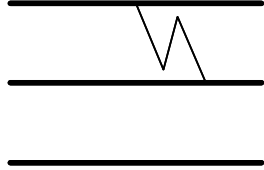
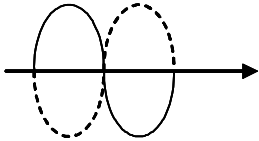
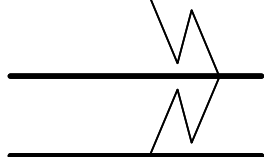
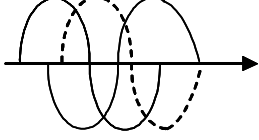
While the above cases have been excluded from specific consideration within the scope of this work, it is by no means to imply that such cases are either unimportant nor unable to be solved for CFI. Rather it has simply been to provide a manageable scope to the work to focus on extension of the CFI method from the licentiate to application on basic three phase network multiphase fault cases. In essence this focus is considered the next logical step before possible future work to research CFI solutions to the more complex fault scenarios associated with the excluded network cases described above.

### 1.4.2 Fault current behavior:

Fault currents can be classified in many ways and in respect of CFI, three main classifications can be considered:

1. Bolted terminal or short-circuit faults classed by phase (p) / earth (e) combinations i.e. p-e, pp-e, ppp-e, pp or ppp
2. Faults classed according to circuit type, influencing circuit breaker interruption stresses i.e. terminal faults, short-line faults, out-of-phase, high DC components
3. Classification according to the interruption behavior, particularly with respect to current zero timings, as described in Table 1.2

**Table 1.2: Classification of fault currents according to interruption behavior**

	Fault type	Description	Interruption behavior
1	1-, 2-, 3-phase to earth faults  Currents behave "independently"		
2	phase-to-phase unearthed faults  Fault currents in phase opposition		
3	3-phase unearthed faults  Last phases to interrupt shift into phase opposition after first phase interrupted		

The first classification grouping, according to multiphase fault combinations is the primary focus of the CFI method described in this thesis. A method is included to discriminate between

two phase earthed and unearthed faults. In addition a method for management of phase shift in last phases to clear in unearthed three phase fault cases will be described and demonstrated.

The second fault classification method, according to circuit type and interruption stresses is most relevant to the design and arcing time performance limits of the circuit breaker interrupter. Figure 1.4 provides examples of some of the different interruption stresses that a circuit breaker must manage. The upper graph in Figure 1.4 shows interruption of a small capacitive current, with the characteristic (1-cosine) recovery voltage after current zero interruption. The thermal stress for small currents is correspondingly very low, so that an HV circuit breaker can normally achieve thermal interruption at near zero arcing time. However a near zero arcing time, corresponds to near zero contact gap at the current zero and in the case of capacitive current interruption, the peak of the recovery voltage can reach over three times the normal AC peak voltage and thus places a very high dielectric stress on the interrupter.

The lower three graphs in Figure 1.4 show, from top to bottom, symmetrical fault current, short-line fault and asymmetrical fault current interruption and associated transient recovery voltages (TRV), based on IEC standard type test circuits. Each of these interruptions is characterized by fault level currents and the very fast rising TRV caused by the inductive nature of the power system. Such interruptions place both high thermal and dielectric stresses on the interrupter. The short-line fault is a special case, characterized by an especially severe initial rate of rise of recovery voltage (shown expanded in the inset graph) which is caused by travelling wave reflections between the open circuit breaker and the fault location. The performance of an SF<sub>6</sub> HV AC circuit breaker with respect to these interruption duties is examined in greater detail in Chapter 3, within the high power experiments.

The third fault classification method is a derivative of the first classification method, as described in Table 1.2, but with particular focus on the order and timing of the interruption current zeros. Type 1 and 2 faults differ in the configuration of the power system source voltage driving the fault, but the fault current phase angle and current zero behavior remain consistent as each phase is interrupted. Type 3 faults represent the case where the driving source voltage and current zero behavior change after the first phase is interrupted. Due to the absence of a zero sequence return path, once the first phase is interrupted the remaining two phases shift into phase opposition - in effect changing into an equivalent phase-to-phase fault. Such behavior presents a particular challenge to the implementation of CFI on three phase networks.

The licentiate included a detailed analysis of the method of using a modelled approximation of the measured fault current for single phase faults over a complete range of fault inception voltage phase angles and fault current time constants. The three phase CFI method described here is based on a very similar model and will be shown to exhibit similar robustness and versatility for inception angles and time constants, though the range of time constants actually tested and presented here is limited, simply for reasons of practical necessity.

In addition, following from the assumption of an infinite bus transmission network, it is assumed the fault current magnitude is several times larger than the pre-fault load current magnitude. Consideration of fault current types influencing circuit breaker interruption performance has been in part made in the experimental part of the work, but for the algorithm development it has been assumed that for the simulated fault cases a well defined and consistent minimum arcing time behavior is known for the applied circuit breaker.

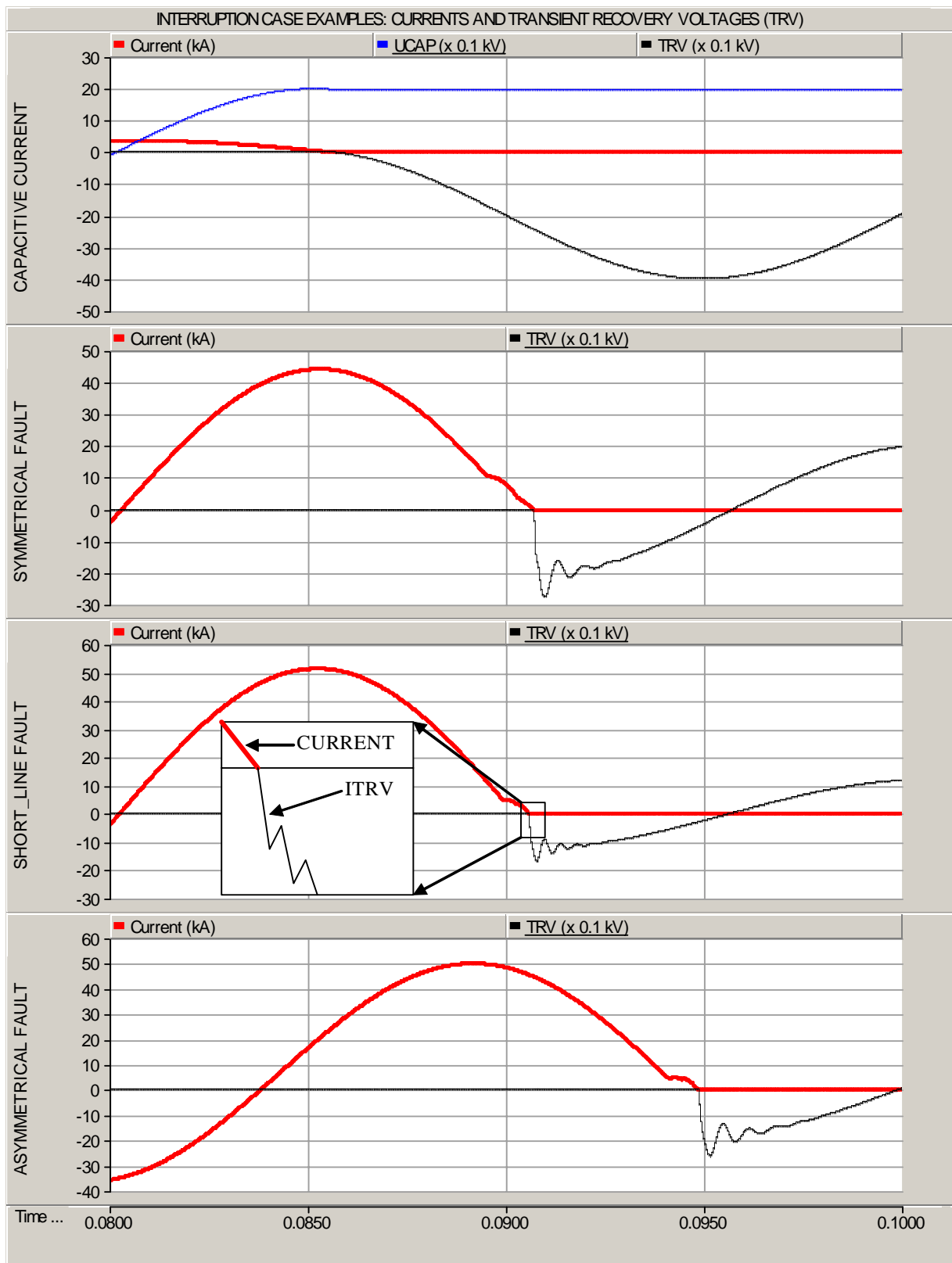


Figure 1.4 : HV AC interruption case examples (over 20 ms snapshot)

### 1.4.3 Circuit breaker behavior:

Understanding of circuit breaker current interruption and mechanical functions and behavior is of course critical to the development and application of a CFI scheme. Several aspects of circuit breaker behavior critically affect CFI implementation:

1. Minimum arcing times for different current interruption duties;
2. Mechanical operating time stability;
3. Influence of electrical wear from successive interruption on interrupter materials;

Minimum arcing time behavior will be examined in detail within Chapter 3. Mechanical operating time stability is a well documented requirement for controlled switching and can be verified by type tests [11], [50]. The influence of electrical wear of interrupters is an important consideration that has attracted considerable focus [7], [22], [23], [24], [25], [49] and will be examined in Chapter 3.

In the transmission system context of this work, focus is placed on modern SF<sub>6</sub> HV AC circuit breaker designs and behaviors. In particular the work in this thesis assumes tripping of all phases for every interruption, though with single phase operation control, common at the higher transmission voltage levels. At lower transmission voltage levels, circuit breakers are often mechanically arranged for simultaneous three pole operation (otherwise referred to as “ganged” operation). Ganged operation forces additional constraints on the implementation effectiveness and practicality of CFI due to the wide variation in possible current zero times between phases during fault conditions.

### 1.4.4 Protection system performance:

The CFI scheme described here is *not* proposed as an alternative or replacement power system protection scheme. Rather it is proposed as a method to augment or optimize the fault current interruption process. It should however be noted that there can be aspects of the proposed method that might offer interesting features for inclusion in distance protection schemes e.g. the use of analysis of variance tests as a parameter or model validation tool and control augmentation feature.

Line protection schemes in transmission networks are typically equipped with distance protection relays. Distance protection schemes calculate apparent impedance data which is very similar information (e.g. X/R ratio) to that used by the proposed CFI scheme to model asymmetrical fault currents.

While there exist data calculation synergies between digital distance protection algorithms and the proposed CFI scheme, the extracted data is applied in different ways and for different purposes. Distance protection is aimed at determining if the measured apparent current and impedance are within defined fault criteria, necessitating a circuit breaker operation. The CFI scheme is focussed on continually updating its modelling of currents to predict future current zero times for synchronizing any eventual trip command to the circuit breaker in order to achieve a predetermined arcing time. In short, the protection system determines if the measured system values constitute a fault condition and hence if circuit interruption is required, while the CFI scheme aims to optimize the interruption process. The operating time and total fault clearing time associated with protection operations are major constraints on a CFI algorithm as the use of CFI

should not result in any (significant) prolongation of the total fault clearing time, in the interests of maintaining power system transient stability.

Detailed analysis of protection schemes is outside the scope of this work. However references are made to the similarities in system data extraction and calculations used in modern distance protection algorithms and the proposed CFI scheme.

#### **1.4.5 Data measurement, processing and control:**

Following on from the single phase method described in the licentiate, the CFI method for three phase network application described in this thesis is also based on an approach whereby the algorithm could be embedded directly into existing modern digital protection relays and thereby utilize the same current and voltage measurements, filters and signal processing hardware.

The implications of the above scope limitations and assumptions are addressed in more detail where relevant within the body of the thesis.

### **1.5 Thesis structure**

This thesis is a continuation and extension of the CFI scheme described in the licentiate [1]. The licentiate contains substantial background material that is relevant to the work presented herein. The specialized nature of this research is such that there is little direct comparative published academic literature dealing with this specific topic. The work involves consideration of a combination of power system topics including fault current modelling, protection systems, circuit breakers, data measurements and control systems. Literature has therefore been surveyed and referenced from each of these areas with consideration of the implications for CFI development and implementation. Chapters 2, 3 and 4 described below include literature survey material.

The thesis is structured in chapters, summarized as follows:

- Chapter 2 - Three phase fault theory: The applied model for fault currents in a three phase system is described. Three phase system fault combinations are described, including influence of system earthing configurations on fault and current interruption behavior. The key parameters affecting the modelled current behavior are defined.
- Chapter 3 - High power experiments: This chapter focuses on high power experiments conducted to obtain additional data to support both the arcing time selection and potential benefit motivations for CFI. A summary description of HV AC three phase interruption process, based on SF<sub>6</sub> interrupters is provided, with particular focus on minimum arcing time behaviors for different current interruption duties. A brief description of the applied high power synthetic testing process is given. The applied tests and results are described with focus on their particular relevance for CFI research.
- Chapter 4 - Controlled fault interruption - Overview: An overall description of the CFI process is provided. Requirements for successful CFI implementation are described. Comparison, including a literature survey, is presented between distance protection, previous CFI methods and the proposed method. The boundaries and system assump-

tions applied to the present work are defined. The novel features introduced by this research are described.

- Chapter 5 - Three phase controlled fault interruption - Proposed method: This chapter provides the detailed description of the proposed three phase CFI method, as further developed from the previous single phase scheme described in the licentiate thesis [1]. Modifications to the least means square method applied for fault current phase angle estimation are described. In addition, modifications in the application of the analysis of variance current model check function for fault inception detection and multi-phase fault type identification are described. Simulation examples are provided for a range of multi-phase fault cases to illustrate the details of the proposed CFI process.
- Chapter 6 - Three phase controlled fault interruption - Simulation tests: MATLAB simulations of the proposed scheme are provided covering the range of three phase system fault combinations for different system earthing configurations. Specific measures of performance for the CFI scheme are defined. Behavior of the proposed method with respect system parameter variations are presented.
- Chapter 7 - Future work proposals: This chapter outlines further research topics that should be undertaken to complement and improve the existing work on CFI for three phase AC networks.
- Chapter 8 - Conclusions: The main conclusions are summarized with respect to the undertaken work, including assessment of fulfillment of the goals set for the work.
- Chapter 9 - References: All references in the thesis are numbered and listed in this final section.
- Appendix A - EMTDC model descriptions for three phase network fault cases: Description of the circuit models used for the simulation of three phase fault cases described in Chapter 2.

## 1.6 List of publications

The following conference papers have been presented and published, based on the Licentiate thesis describing the single phase controlled fault interruption method:

- Thomas R., Daalder J., Sölver C-E., “An Adaptive, Self-Checking Algorithm for Controlled Fault Interruption”, Paper 0134, CIRED 2005, 18th International Conference on Electricity Distribution, Turin, 6-9, 2005.
- Thomas R., Daalder J., Sölver C-E., “An Adaptive, Self-Checking Algorithm for Controlled Fault Interruption”, Paper IPST05-011, IPST’05, 6th International Conference on Power System Transients, Montreal, June 19-23, 2005.
- Thomas R., Daalder J., Sölver C-E., “An Adaptive, Self-Checking Algorithm for Controlled Fault Interruption”, Paper 419, PSCC 2005, 15th Power Systems Computation Conference, Liege, 22-26 August, 2005.

The following conference papers have been presented and published in connection with this PhD thesis:

- Thomas R., Sölver C-E., “A Method for Controlled Fault Interruption for Use with HV SF<sub>6</sub> Circuit Breakers”, IEEE PowerTech 2007 conference, Lausanne, Switzerland, July 2-5, 2007.
- Thomas R., Sölver C-E., “Application of Controlled Switching for High Voltage Controlled Fault Interruption”, CIGRÉ SC A3 International Technical Colloquium, Rio de Janeiro, Brazil, September 12-13, 2007.

The following transaction journal papers and conference abstract submissions have been submitted in connection with this PhD thesis and are under review:

- Thomas R., Sölver C-E., “Experimental Investigations for High Voltage Controlled Fault Interruption”, submitted to IEEE Transactions on Power Delivery on March 6, 2007.
- Thomas R., Sölver C-E., “A Method for Controlled Fault Interruption Based on Predictive Current Behavior”, abstract submitted to DPSP, 9th International Conference on Developments in Power System Protection, Glasgow, on July 19, 2007.

The following patent applications have been submitted for both the single and three phase methods of controlled fault interruption described by the Licentiate and PhD theses:

Patent Cooperation Treaty (PCT):

Title: An apparatus and a method for predicting a fault current

Applicant: ABB Technology Ltd, Affolternstrasse 44, CH-8050, Zurich.

Inventor: Richard Thomas

International Publication No: WO 2006/043871 A1

Priority date: 22 October, 2004.

Publication date: 27 April, 2006.

European Patent Office:

Title: A method and an apparatus for predicting the future behavior of currents in current paths

Applicant: ABB AB, Västerås, Sweden.

Inventor: Richard Thomas

Application No: 06125262.3-

Filing date: 1 December, 2006.



## 2 Three phase fault interruption theory

One of the main goals of this work has been to extend the application of the CFI method described in the licentiate [1] to application on three phase HV AC networks. It is therefore necessary to describe and examine fault current and interruption behavior for three phase power systems. In particular this chapter will focus on presenting a modified form of the fault current model used in the licentiate, that in turn is used as the basis for the proposed three phase CFI algorithm.

First it is important to differentiate between fault type classifications relevant to HV AC power systems in general, in contrast to the fault type classifications that are used for HV AC circuit breakers from the perspective of specific interruption stresses. In power systems theory it is typical to focus on classification of faults according to the number of phases affected and whether or not the fault case involves an earth (or zero sequence) component. There also special fault or power system failure cases, that may require circuit breaker operation and while possibly abnormal current behavior, not necessarily “classic” fault currents, e.g. load rejection operations and out-of-phase synchronization failures.

For the study of current interruption, particularly with respect to HV AC circuit breakers, faults types are more typically classified with respect to current magnitude, level of asymmetry and other circuit parameters affecting both the current and the transient recovery voltage behavior. Type testing of HV AC circuit breakers requires such detailed classification and fault type definitions and will be assessed in greater detail in Chapter 3.

In this chapter the focus is on generic, classical fault behavior according to number of phases and earth connections involved. Though the CFI method proposed by this thesis implements interruption for all three phases with single phase control, it is nevertheless important for the algorithm to differentiate between different phase and earth fault combinations, primarily with respect to the frames-of-reference for the applied current model, according to which phases are faulted and whether or not an earth connection is involved.

It should also be noted that the described system fault behaviors will focus on the voltages and currents as seen immediately at the circuit breaker associated with fault interruption. The analysis of fault current interruption behavior is focussed on a specific circuit breaker interrupting its through current, as indicated by Figure 2.1. In this respect, the fault current analyses presented in this chapter differ slightly from “conventional” power system or protection system fault study focus in that the eventual full interruption of the fault current *at the fault location* is of less interest. In meshed power systems it is likely that at least two circuit breakers will operate to interrupt a fault e.g. the circuit breakers at either end of a faulted line. However in the context of this thesis, the interest is only on each of these circuit breakers in “isolation”. This approach is used simply for convenience and should not be mistaken as to mean that parallel circuit breaker operation is “irrelevant” or without effect in the context of a full implementation of CFI. The potential consequences of parallel circuit breaker operation, and the use of voltage and current signals obtained at the circuit breaker location on the applied fault current model will be discussed at the end of this chapter. Note that in Figure 2.1 the circuit breaker is drawn for single phase operation, though in all the interruption cases considered here, trip commands are sent to all three phases.

The chapter will begin with a description of the general three phase fault current model and then proceed to analysis of the current and interruption behavior for the basic multiphase fault cases and conclude with a review of factors and fault conditions not included in the scope of this work, but require further investigation in the context of CFI.

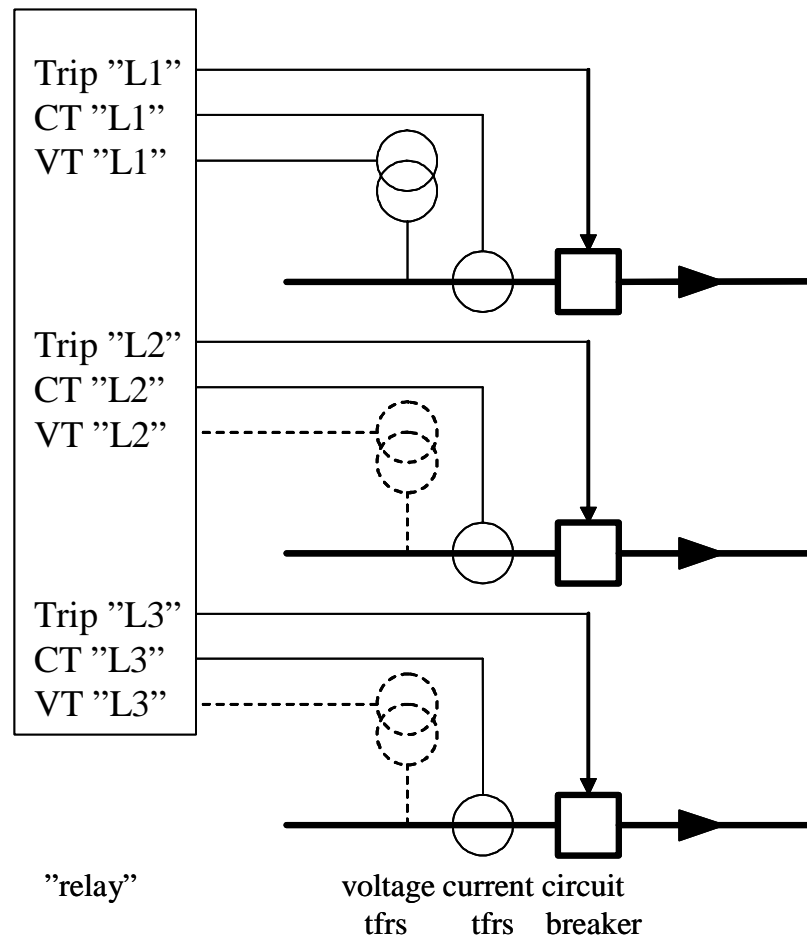


**Figure 2.1 : Measurement and control scope of study for a specific CFI circuit breaker**

## 2.1 Applied power system model

In order to focus on development of the CFI scheme to manage the fundamental range of fault cases that can arise in a three phase HV AC network, a simplified power system model has been used, similar to that described in the licentiate and as illustrated in Figure 2.2. Attention has been placed on the control of a single, three phase circuit breaker located between a common source and the fault location. The source for the model is assumed to be ideal (i.e. symmetrical, earthed, infinite bus). While not dissimilar in its simplicity to models applied for basic fault theory development, there are obvious limitations to such a model, which will be discussed briefly later in this chapter. It is assumed that in the case of a fault, the fault location impedance in the faulted phases is zero i.e. non-arcing faults.

The method of symmetrical components [19], [27] is typically applied to the study of multiphase faults in three phase networks. An important assumption in the applied model related

to it being effectively earthed is that the positive and zero sequence impedances are “equal” - the main consequence of this for CFI being that for earthed faults, each phase interrupts independently of the other phases.

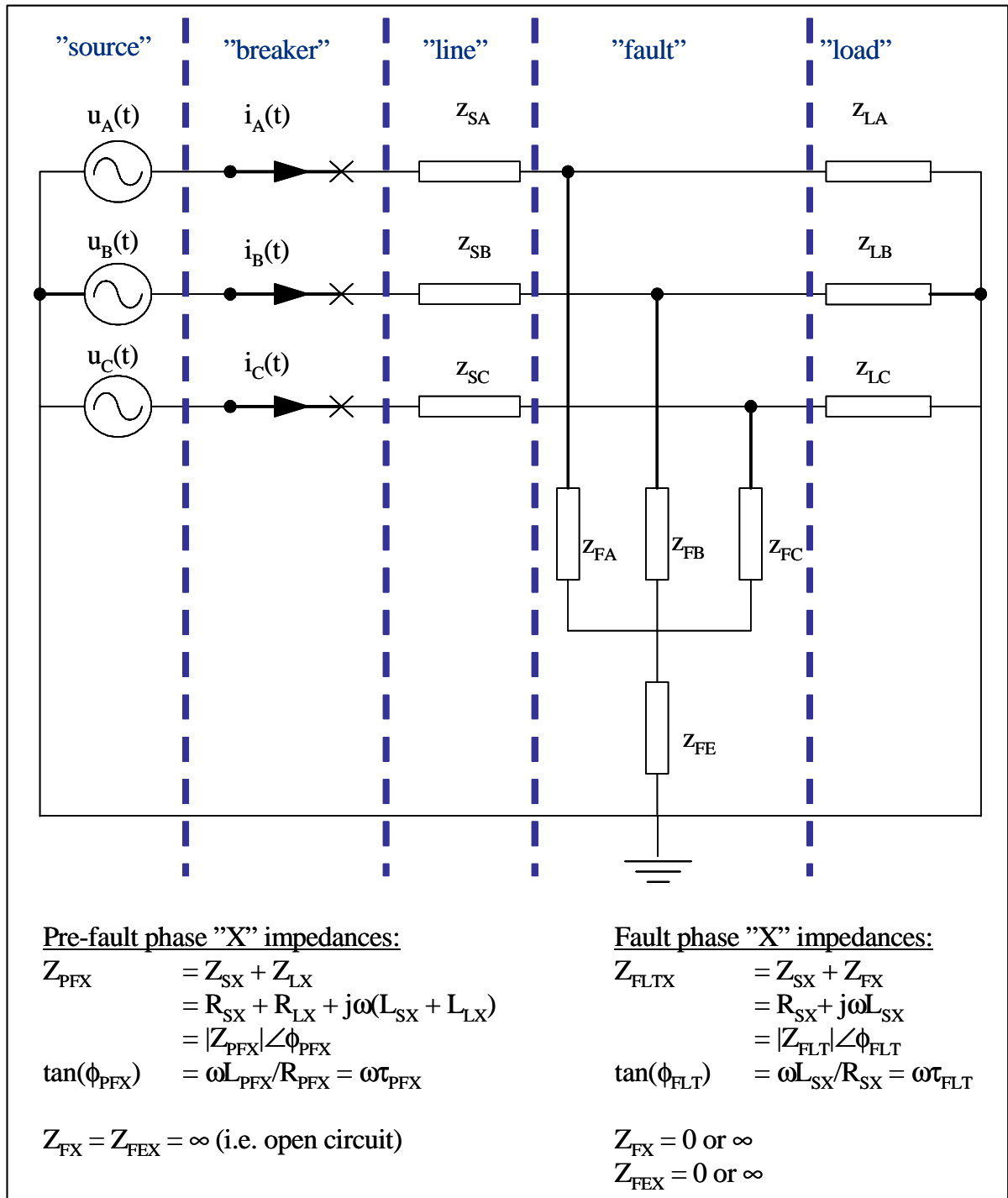


Figure 2.2 : Applied power system model

The symmetrical components method has not been used for this work and will not be presented here. As the symmetrical components method is phasor based, its most common use is for the evaluation of the “steady state” fault levels that might be seen in a power system. For CFI the focus is on the transient behavior of the fault current and therefore an analytical fault current model approach has been used here, following on from the same type of model used in the licentiate.

For the three phase system described by Figure 2.2 the driving source phase-to-earth (“phase”) and phase-to-phase (“line”) voltages can be generically defined by {2.1},

$$u_X(t) = U_{PKX} \cdot \sin(\omega \cdot t + \alpha_X + \gamma_X) \quad \{2.1\}$$

where “X” sub-script is the phase designation (e.g. “A”, “B”, “C” or “L1”, “L2”, “L3” or “R”, “S”, “T” etc) respectively and  $\alpha_X$  is the respective source voltage phase angle at which a fault begins (at a time,  $t = 0$ ) in any phase. For the case of using “A” phase as the main reference phase with respect to a common time base and a positive phase rotation of “A-B-C” phases, the associated  $\gamma_X$  values for all phase-to-earth and phase-to-phase voltages are as indicated in Figure 2.3. The associated phase-to-earth definitions of  $\alpha_X$  are shown in Figure 2.4.

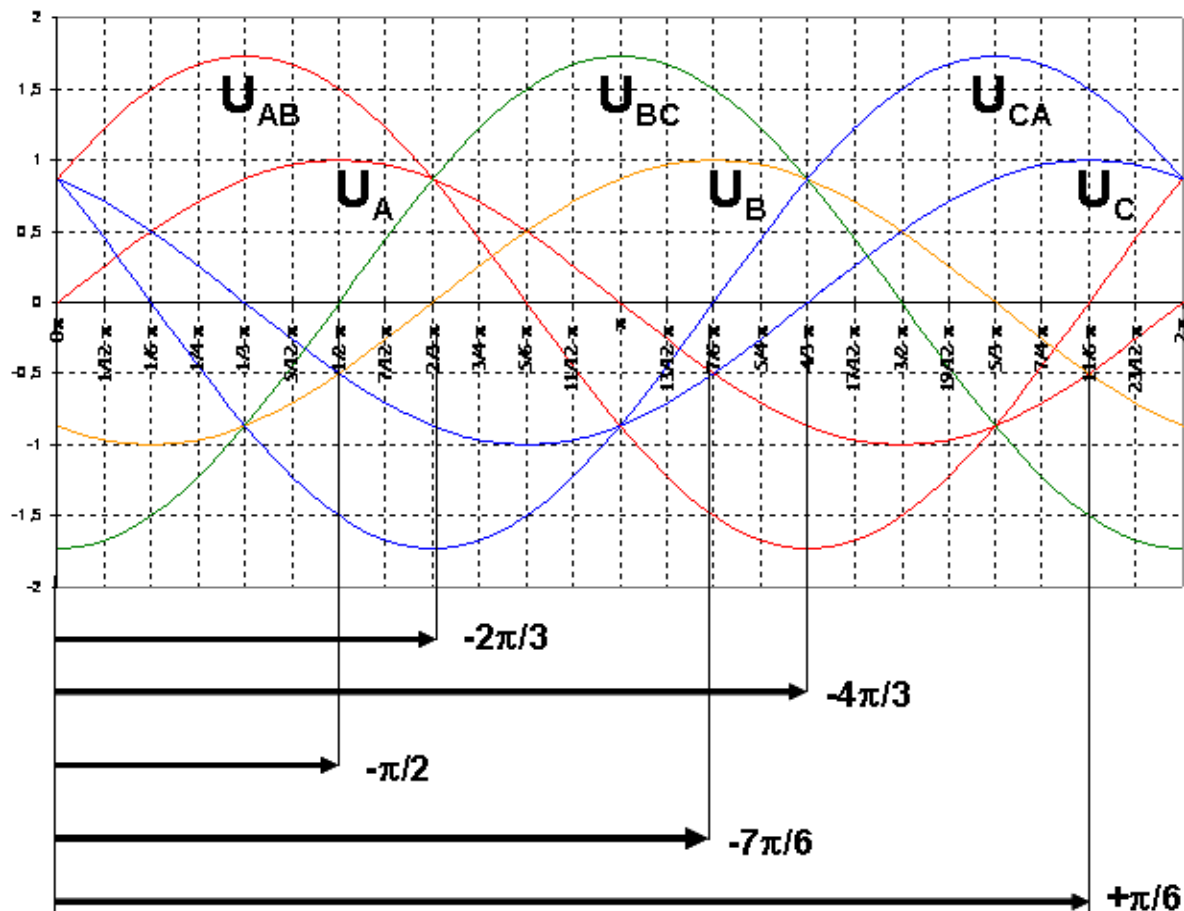


Figure 2.3 : Reference  $\gamma_X$  values using “A” phase as reference voltage

The fault currents in each phase can be described with respect to their associated driving source voltages as follows. Let the source-to-fault impedance,  $Z_X$ , for each phase “X” is defined as,

$$Z_X = Z_{SX} + Z_{FX} = R_X + j\omega L_X \quad \{2.2\}$$

where  $Z_{SX}$  is the normal source-to-fault location impedance and  $Z_{FX}$  is the equivalent fault location impedance, including earth impedances.

Following from {2.1} and {2.2} the generic fault current model can be derived (e.g. from Laplace transformations - see Greenwood [20]) to {2.3},

$$i_X(t) = I_{FX} \cdot [\sin(\omega \cdot t + \alpha_X + \gamma_X - \phi_X) - \sin(\alpha_X + \gamma_X - \phi_X) \cdot e^{(-t/\tau_X)}] + I_{PF\alpha_X} \cdot e^{((-t)/\tau_X)} \quad \{2.3\}$$

where,

$$I_{FX} = U_{PKX}/|Z_X| \quad \{2.4\}$$

$I_{PF\alpha_X}$  is the instantaneous value of the pre-fault load current at the moment of fault inception

$$\phi_X = \tan^{-1}(\omega L_X/R_X) \quad \{2.5\}$$

$$\tau_X = L_X/R_X = \tan(\phi_X)/\omega \quad \{2.6\}$$

The above model works equally well for ungrounded two phase faults, provided the appropriate line voltage for the faulted phases is used as the reference driving source voltage with associated adjustment of  $\gamma_X$  and  $\alpha_X$  values as shown in Figure 2.4. It should be easily apparent that {2.3} takes the same general form as that used for the fault current model used in the licentiate {2.7}:

$$i_X(t) = I_{FX} \cdot [\sin(\omega \cdot t + \alpha_X - \phi_X) - \sin(\alpha_X - \phi_X) \cdot e^{(-t/\tau_X)}] + I_{PF\alpha_X} \cdot e^{((-t)/\tau_X)} \quad \{2.7\}$$

The only apparent difference between {2.3} and {2.7} is the inclusion of the voltage reference angle term,  $\gamma_X$ . In effect the  $\gamma_X$  term simply provides the necessary phase angle adjustment to allow the currents in all phases to be modelled using a common timebase frame of reference. As shown in Figure 2.4, the sum  $(\alpha_X + \gamma_X)$  is the same for all three phases. However it should be noted that {2.3} is only valid for each phase in the event that the correct respective and appropriate  $\gamma_X$  and  $\alpha_X$  values are used. This is particularly evident when modelling the different fault current behaviors that occur in faulted phases of double phase-to-earth versus phase-to-phase unearthed faults are considered. The relevance of correct  $\gamma_X$  and  $\alpha_X$  value estimation will become further evident when the proposed three phase CFI algorithm is presented in further detail in Chapters 4 and 5.

It is important to note the potential problems in accurate practical measurement of  $\gamma_X$  and  $\alpha_X$  values. Figure 2.1 indicated that the focus of study for this CFI research is on the currents flowing through a specific CFI circuit breaker with the associated implication that the CFI solution is based on the currents and voltages measured at the circuit breaker location. The power system model described by Figure 2.2. and used to derive {2.3} is based on the “ideal” source voltages i.e.  $u_{SX}(t)$ . The voltage measured at the circuit breaker,  $u_{MX}(t)$ , will of course differ in

both magnitude and phase angle to the ideal source voltage, due to the ideal source-to-breaker impedance - see Figure 2.5. It is the phase angle differences between these voltages that has the most bearing on the fault current model. If the source-to-breaker impedance can be assumed to be reasonably “constant”, then load and fault flow studies could provide an estimation of the ideal versus actual phase angle differences at each circuit breaker location, which could then be used as adjustment factors in the estimated  $\gamma_X$  and  $\alpha_X$  values are used by the CFI algorithm. For the purposes of this work the assumption of the infinite bus network behind the circuit breaker is important in the context of assuming the ideal source and measured-at-breaker voltages have a negligible phase angle difference.

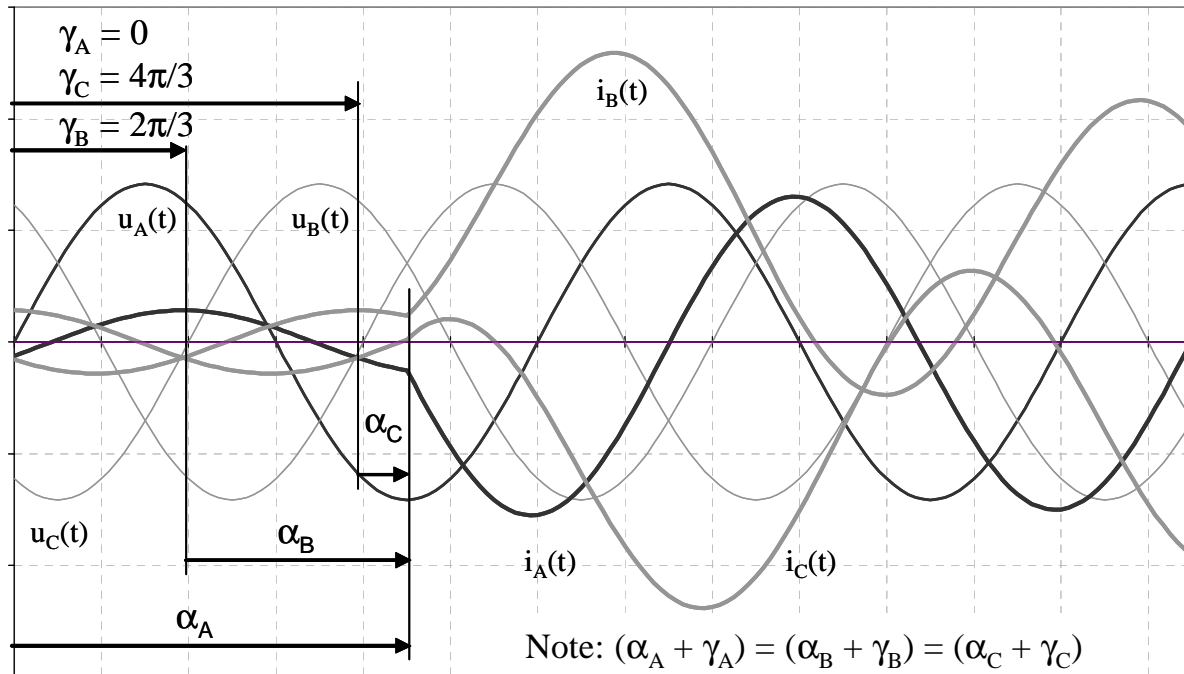


**Figure 2.4 : Example of phase-to-earth  $\gamma_X$  and  $\alpha_X$  relationships for three phase fault**

While the power system model described above is extremely simple, the resultant fault current equation {2.3}, is sufficiently accurate to describe typical fault currents within a transmission and distribution system, moderately removed from any generators or motors that may contribute with additional transient and sub-transient reactance effects. However it can also be noted that there does not exist a single “universal” power system protection solution to cover all possible fault events. Application-specific protection schemes are necessarily used in all power systems in order to provide a sufficiently robust and reliable coverage and management of possible fault events e.g. distance protection for lines, differential protection for transformers, generators and motors, overcurrent relays, under/overvoltage protection, frequency monitoring protection etc. In a similar way it is reasonable to expect that application-specific CFI solutions are more likely than any single “universal” CFI algorithm that could manage all possible fault current behaviors.

It should also be noted that the above fault current model neglects mutual inductance effects between the phases or adjacent circuits, which can be equated to an assumption of perfectly symmetrical transposed lines. As the model and eventual CFI algorithm are based on phase-

specific measurements and parameter value estimations, the effects of impedance unbalance between the phases should be minimal. However as noted in [8], while the positive and negative sequence mutual coupling terms for parallel lines are normally negligible, this is not necessarily so for the coupling between positive and zero sequence mutual coupling terms and can be significant in terms of the influence on the correct function of earth fault protection schemes.

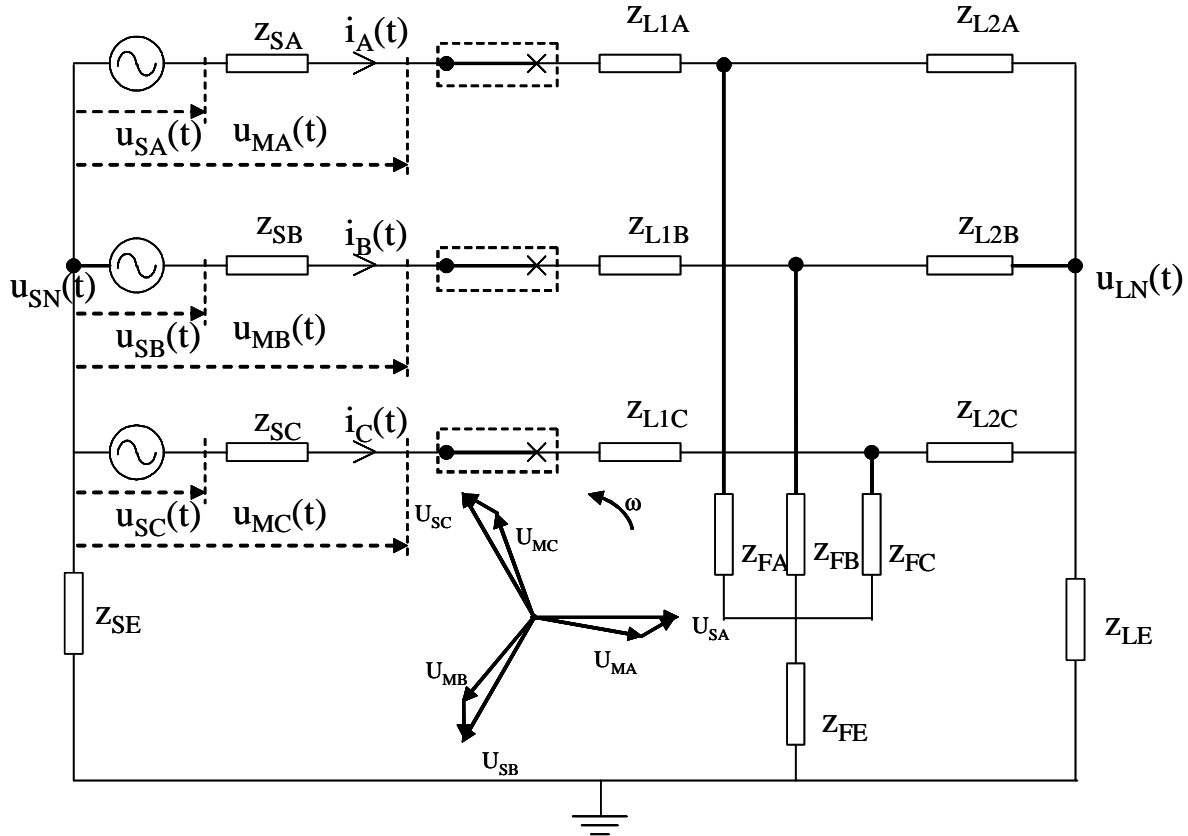


Figure 2.5 : Illustration of the relationship between “ideal” and measured source voltages

## 2.2 Multiphase fault behaviors

The eleven possible fault combinations that can arise in the three phase AC power system described by Figure 2.2 can be grouped into four main types, according to the general behavior of the fault currents up to and including interruption, as listed in Table 2.1. Type 1 faults are all variants of phase-to-earth faults and can essentially be managed by the single phase CFI algorithm described in the licentiate applied on an independent per phase basis, without modification (assuming effectively earthed source and negligible mutual coupling between phases). Type 2 faults are phase-to-phase faults without earth connection. In these cases the single phase-to-earth current model must be modified as the driving source voltage is the phase-to-phase voltage. The Type 3 fault is a three phase to earth fault and in effect should behave the same as Type 1 faults. The reason for its separate classification here is to highlight the similarity of this fault case to that of Type 4. Type 3 and Type 4 faults only differ in behavior *after* the first phase current has been interrupted.

Table 2.1 also summarizes reported fault type occurrence rate distributions at various rated voltage levels, as published in Annex A of IEC technical report TR 62271-310 on electrical endurance testing of high voltage circuit breakers [7]. The reported fault rate distributions are the results of a limited international survey conducted cooperatively by CIGRÉ working group WG 13.08 and IEC study committee 17A, working group 29. (See also CIGRÉ Brochure 140, Chapter 6 [8] for comparative results).

**Table 2.1: Summary grouping of three phase network fault types**

Fault type group	Fault description	Reported fault type occurrence rate distributions (IEC [7])			
		100...200 kV	200...300 kV	300...500 kV	550 kV
1	A-E	65%	74%	83%	90%
	B-E				
	C-E				
	A-B-E	29%	20%	14%	10%
	B-C-E				
	C-A-E				
2	A-B	6%	6%	3%	0%
	B-C				
	C-A				
3A	A-B-C-E	6%	6%	3%	0%
3B	A-B-C				

The above table clearly shows the predominance of single phase-to-earth faults within transmission systems, which is intuitively to be expected considering also the predominant use of overhead lines and the large phase clearances required for such systems. Unfortunately there is little comprehensive survey information available on the distribution between earthed and unearthed multiphase faults, however as can be seen in Table 2.1 such faults can comprise between 10% to 35% of the total number of faults seen on high voltage transmission networks and are thus necessary to study for the purposes of CFI.

Each of the four fault type groups described in Table 2.1 will now be presented in further detail by way of simulated case examples. The purpose of these examples is to present the current zero behavior of each of the fault types, which has lead consequently to the specific approach used in the CFI method described later in this thesis. The presented cases are the results of simulations conducted in EMTDC [48] using a simple single source transmission line model that is described in further detail in Appendix A.



### 2.2.1 Double phase-to-earth faults

As shown the example two phase to earth fault in Figure 2.6 the currents in each phase effectively behave independently and thus can be processed and managed on an individual, independent basis.

### 2.2.2 Phase-to-phase (unearthed) faults

The currents in the faulted phases are effectively flowing in their own circuit loop and can be considered as being in phase opposition as shown in the example in Figure 2.7. As the faulted phases form their own circuit, both phases will interrupt at the same current zero time.

As mentioned earlier, the phase-to-phase fault currents can be modelled by the same form of equation {2.3}, with appropriate values of  $\gamma_{XX}$  and  $\alpha_{XX}$ , based on the associated phase-to-phase (or “line”) equivalent driving source voltage (double letter subscripts are used to discriminate from phase-to-earth  $\gamma_X$  and  $\alpha_X$  values with single letter subscripts).

### 2.2.3 Three phase earthed faults

Three phase earth faults, on an earthed source system, behave in the same manner as single phase or double phase to earth faults, as shown in Figure 2.8. Each current will interrupt at its own current zero, independent of the other phases and CFI can be implemented on a three-by-single phase basis. The relevance of illustrating this fault case separately is the similarity of the current behaviors to that of the three phase unearthed fault, up until the first phase is interrupted, as is shown in the next section.

### 2.2.4 Three phase unearthed faults

The fourth fault type, a three phase fault without earth connection, differs from the other types most particularly with regard to the interruption behavior of the three phases. Figure 2.9 illustrates interruption of both three phase earthed and unearthed faults occurring at the same fault inception voltage phase angle. Up until the first phase is interrupted, all three currents in the unearthed three phase fault behave in the same manner as for a three phase-to-earth fault, as described by the equivalent circuit shown at the top of Figure 2.10. After the first phase interrupts, there is no zero sequence path in the unearthed fault case and the remaining currents undergo a phase shift to come into phase opposition, in to a similar relationship were these two phases undergoing a phase-to-phase fault, as described by the equivalent circuit shown at the bottom of Figure 2.10.

This change of current behavior after the first phase interrupts poses particular challenges to the CFI algorithm, as it is very difficult to discriminate between the three phase unearthed and three phase earthed fault cases *before* the first phase is interrupted, but this is also far too late for the CFI algorithm to react, as it must make its determination of target current zeroes within the response time of the associated protection system and ideally achieve interruption within the same total fault clearing time as would occur for a “direct”, non-CFI trip operation.

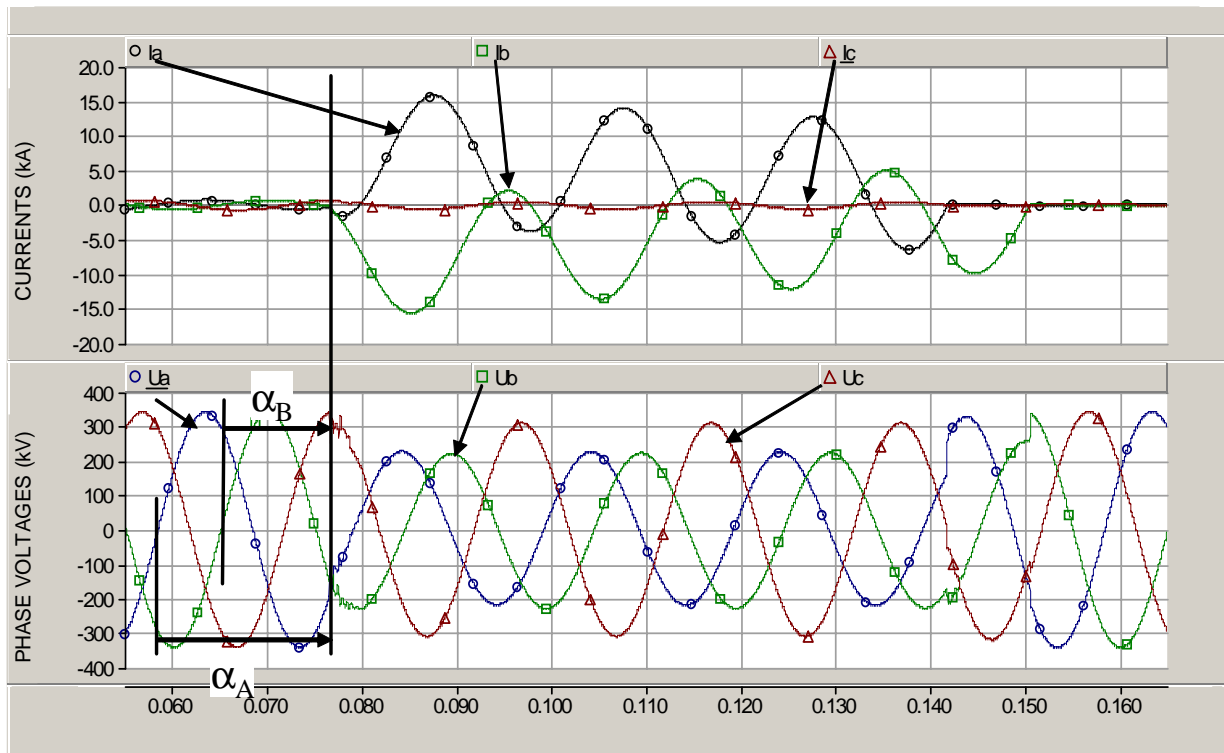
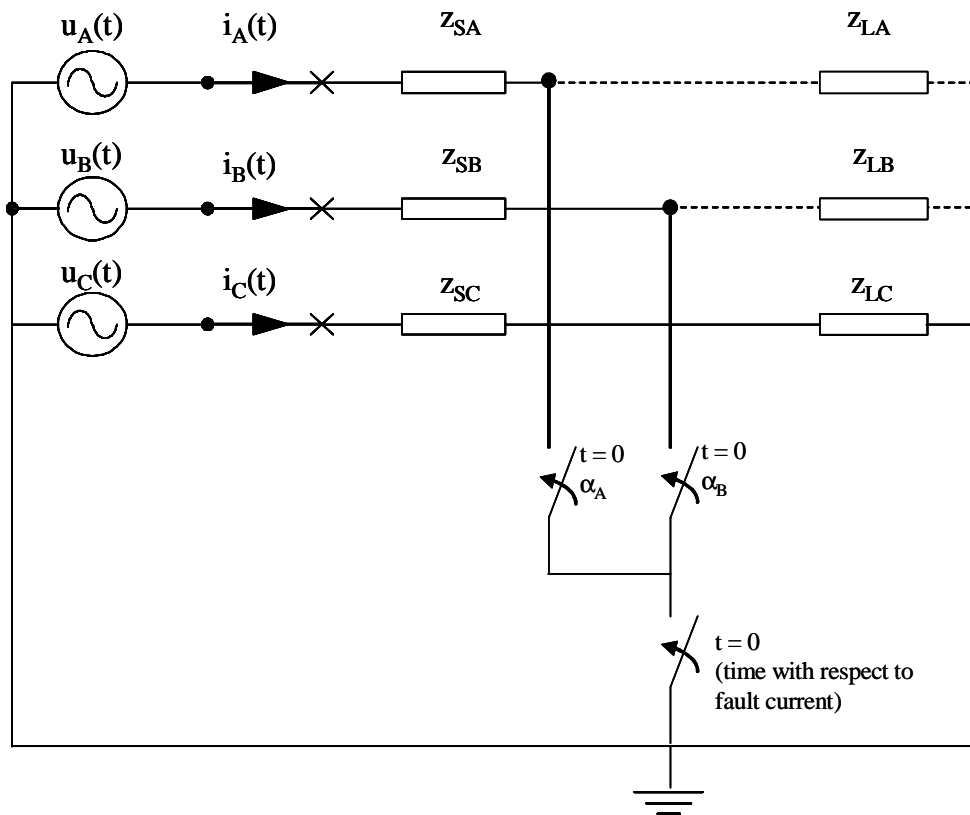


Figure 2.6 : Double phase-to-earth fault example

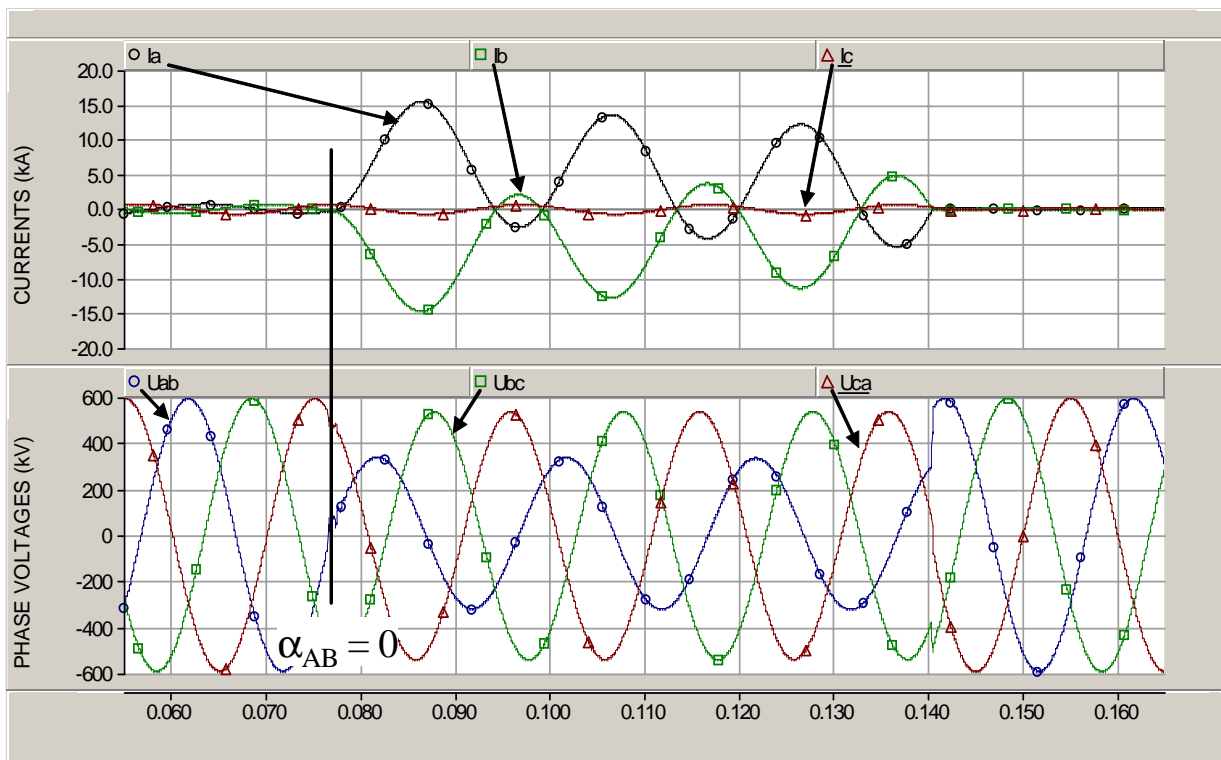
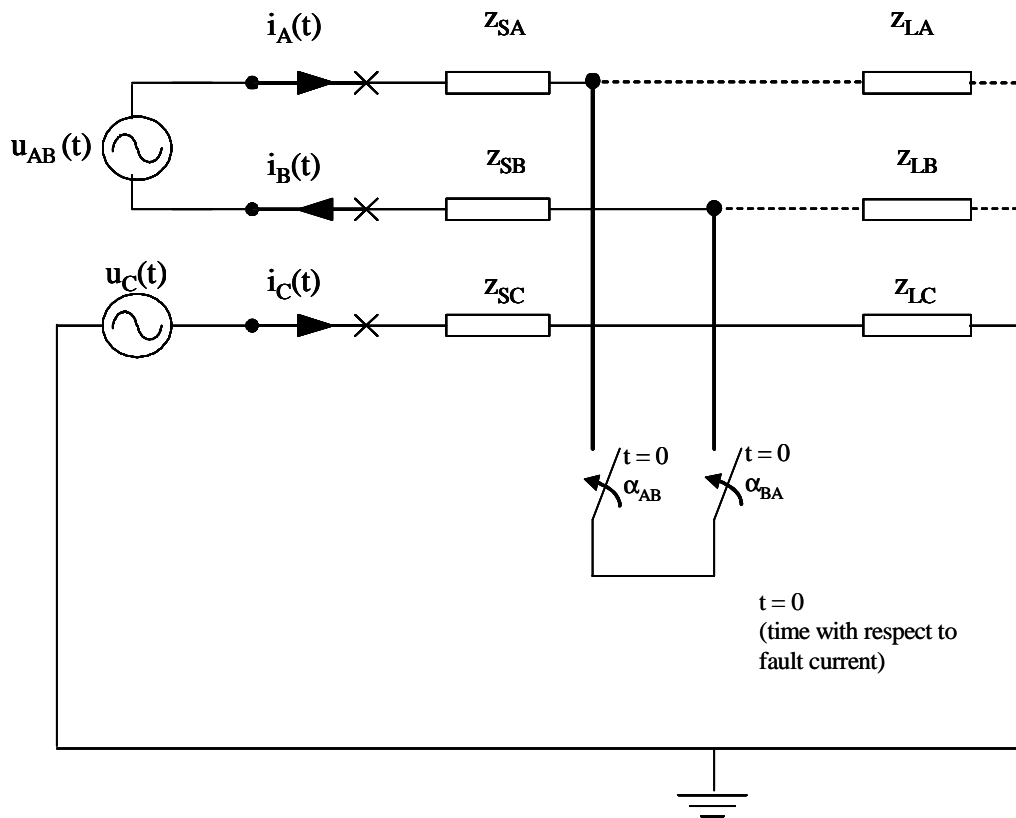


Figure 2.7 : Phase-to-phase, unearthed fault example

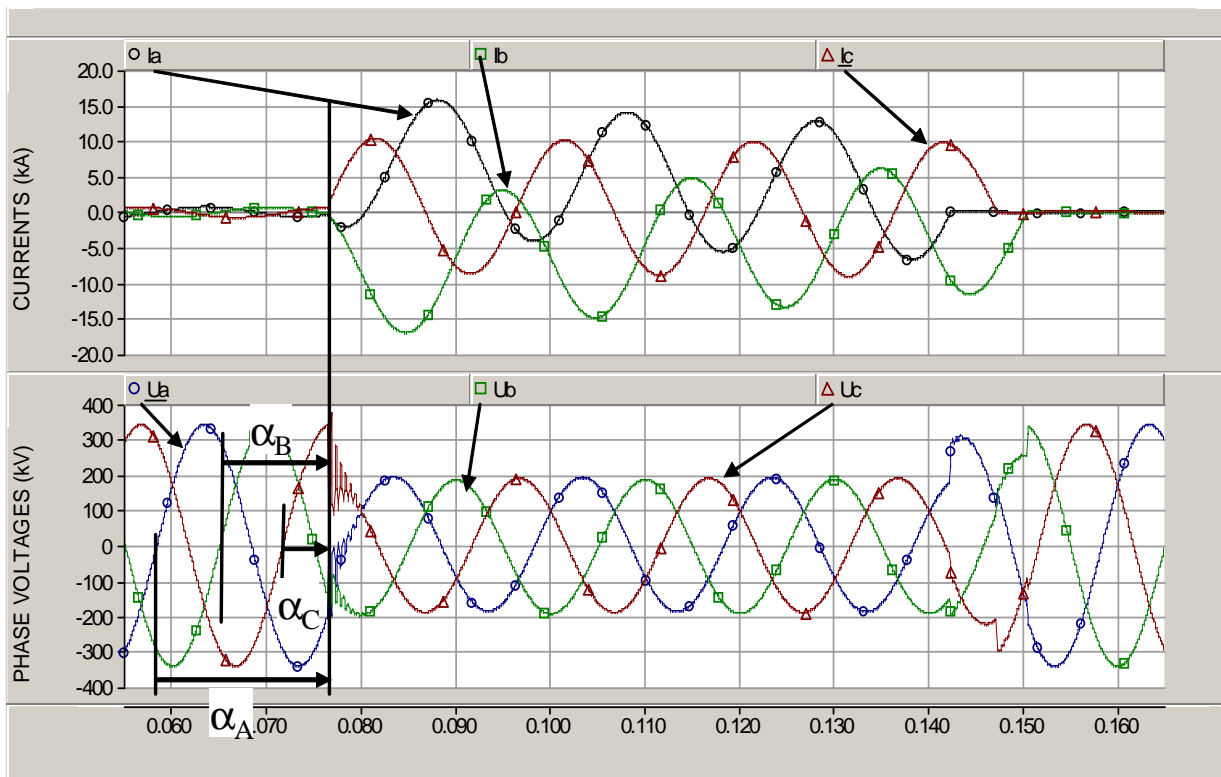
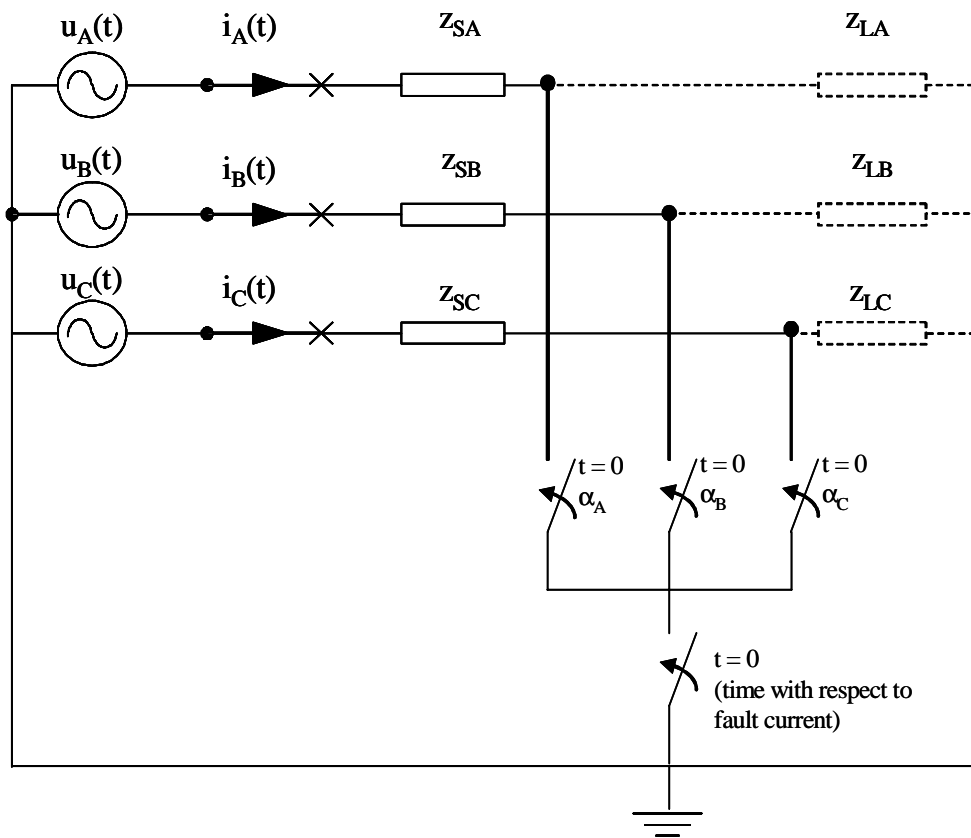


Figure 2.8 : Three phase earth fault example

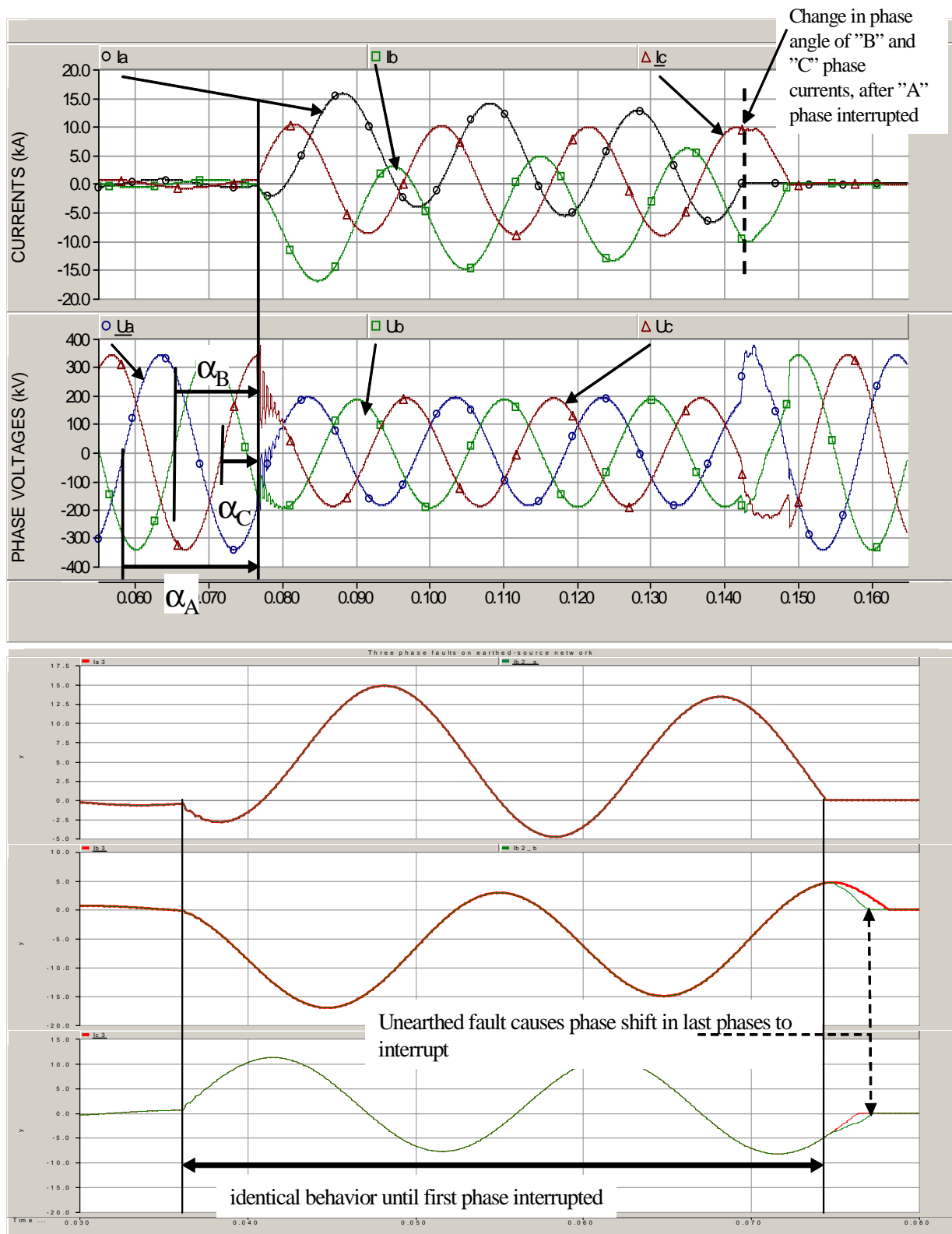


Figure 2.9 : Three phase unearthed fault example

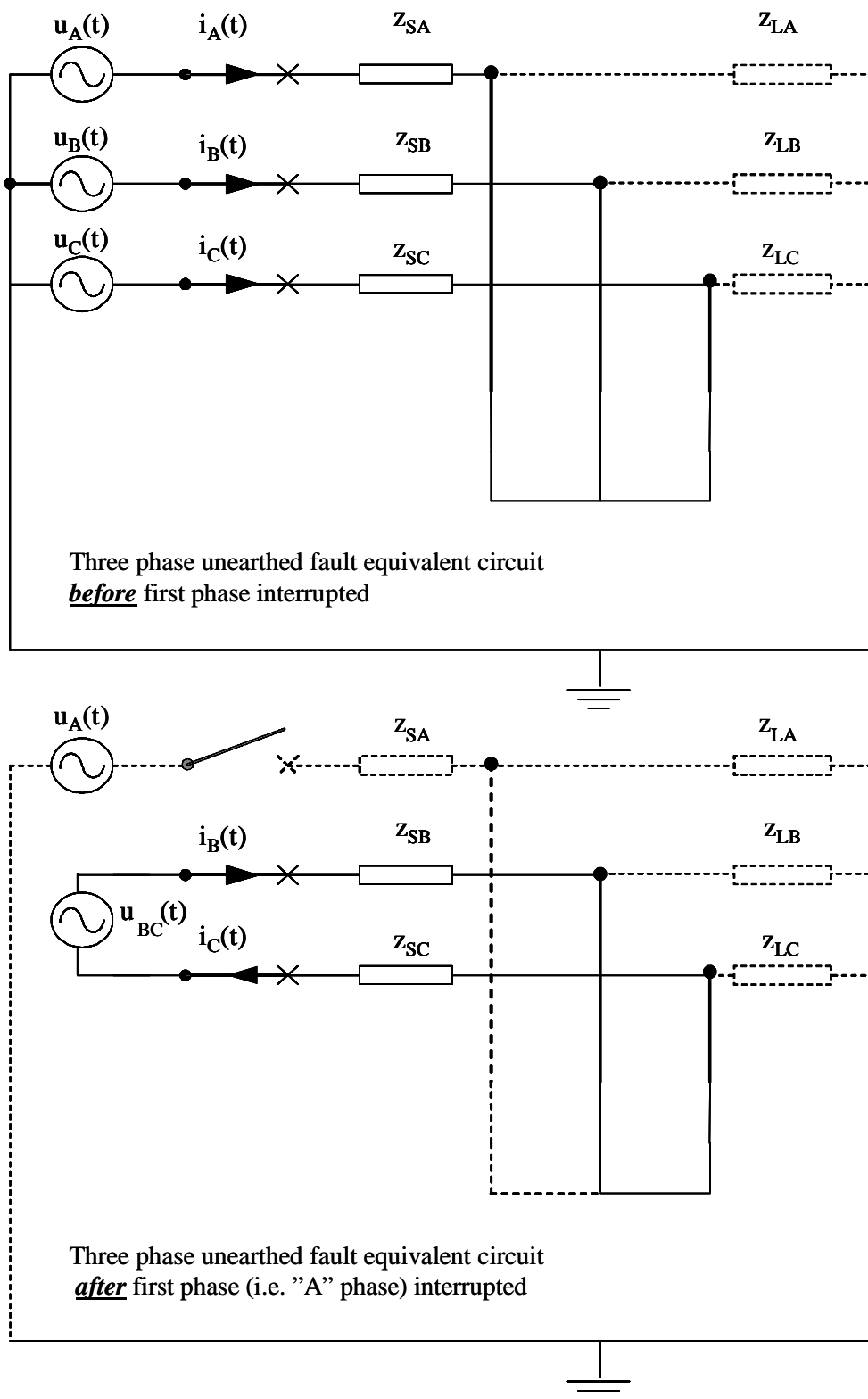


Figure 2.10 : Three phase unearthed fault interruption equivalent circuits; before first phase interrupted (top) and after first phase interrupted (bottom)

### 2.2.5 Multiphase fault type behavior implications for CFI method

There are two main considerations for the implementation of CFI on a three phase network that can be reasonably modelled as per Figure 2.2 and equation {2.3}. First is the identification and discrimination between double phase-to-earth and phase-to-phase unearthed faults, so that appropriate  $\gamma_X$  and  $\alpha_X$  values can be used in applying a model such as described by {2.3} to estimate fault current phase angle,  $\phi_X$ , and time constant,  $\tau_X$ . Second is developing a viable strategy for management of three phase faults, where it can be difficult to reliably discriminate between earthed and unearthed fault cases, within the normal sampling and required protection response time following fault inception.

Both of the above aspects emphasize the importance of multiphase fault type identification to the implementation of a CFI method on a three phase network. Several different methods of fault type identification exist in conjunction with protective relay designs and could potentially be applied also in the CFI context, as will be described further in Chapter 4. The proposed CFI method, described further in Chapter 5, applies a model comparison based method to facilitate the appropriate targeting and control strategy, expanding on the analysis-of-variance test method applied in the single phase CFI method described in the licentiate.

## 2.3 Fault cases and power system configurations requiring further investigation

As stated in the introduction, the scope of power network configuration considered for this work has been restricted to focus on the more general circuit breaker applications that are to be found in a typical transmission or sub-transmission earthed network. This has been intentional in order to first develop the CFI method to basic three phase fault management prior to possible further development to manage more complicated network configuration and associated fault cases. Some of the special application cases, particular to higher voltage transmission networks, requiring future work are briefly described below.

### 2.3.1 Power transformers

The simple three phase circuit described by Figure 2.2 has no power transformers included, implying that the source-to-breaker impedance would include the equivalent impedances of any transformers present in this part of the circuit. It is however important to recognize the additional effects, such as the magnetic circuit response and phase shifting effects that transformers will have on fault currents, as potential challenges to the practical implementation of a CFI scheme.

#### 2.3.1.1 Magnetizing inrush currents

Magnetizing inrush currents can be heavily distorted by (mainly 2nd and 3rd) harmonics and in some cases can cause maloperation of transformer protection relays. The relatively high levels of current distortion that may occur result in a far from sinusoidal waveform and would present a significant problem to the CFI methods described by Pörtl [2] and in the licentiate [1]. Methods exist to mitigate the impact of such currents on protection systems (e.g. harmonic current restraint [21]). It is also possible to mitigate magnetizing currents by using controlled switching for energization of the transformer [15] and in the context of CFI it is suggested that controlled energization presents the best strategy to manage such cases.

### 2.3.1.2 Winding configurations

It is fundamental to the CFI approach proposed in this thesis that the currents used for fault current modelling are measured as those flowing through the associated circuit breaker. This allows power transformer winding configurations (e.g. delta-star or star-delta) to be dealt with as equivalent series impedances. It is however important to note the effect such winding configurations have on the through fault behavior. Some examples are shown in Figures 2.11 to 2.14. Each of the cases here can also be described in terms of symmetrical components, however the following examples are only provided as illustrations of the changes in fault current behaviors that can occur due to one typical type of transformer winding configuration.

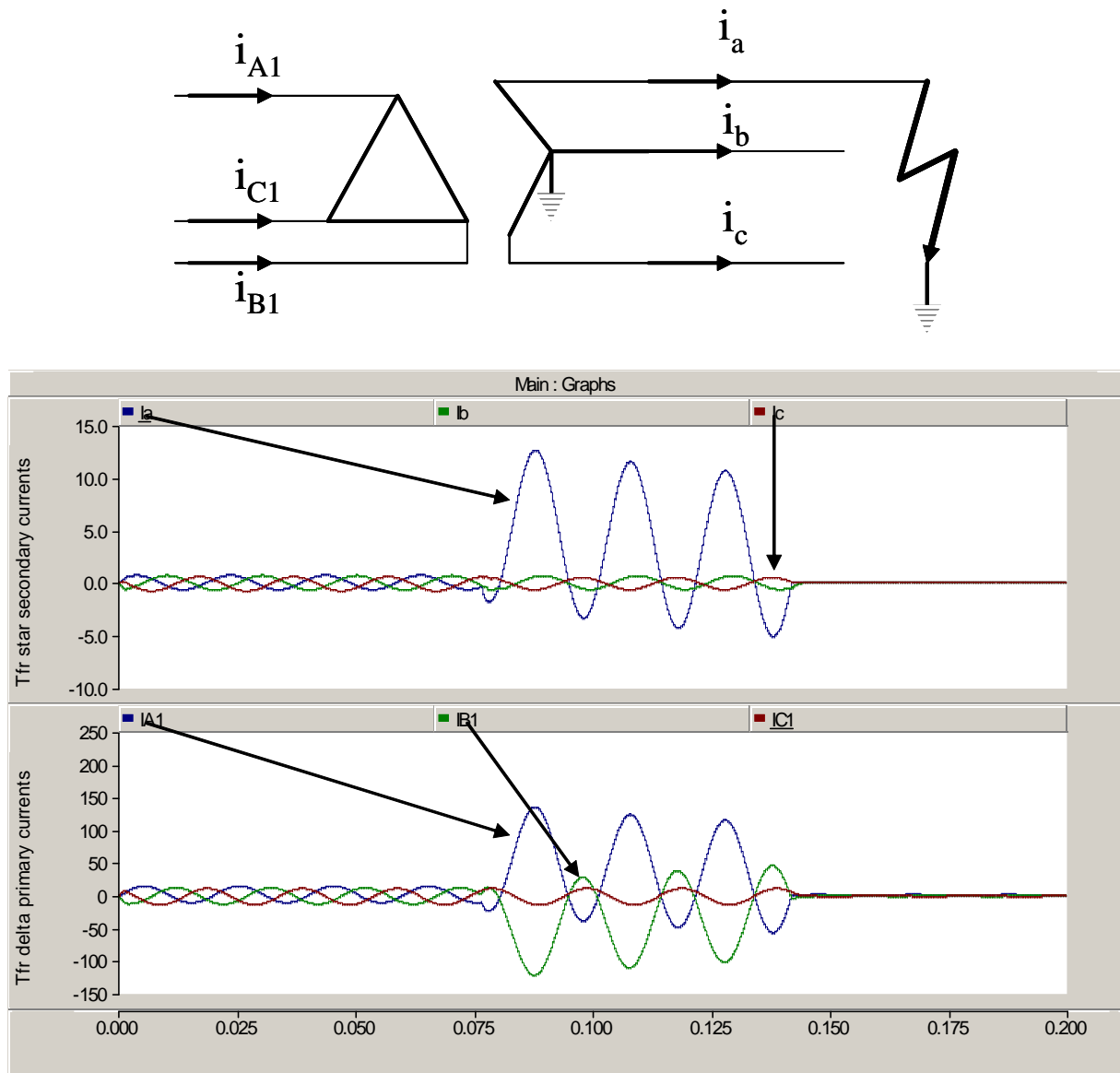
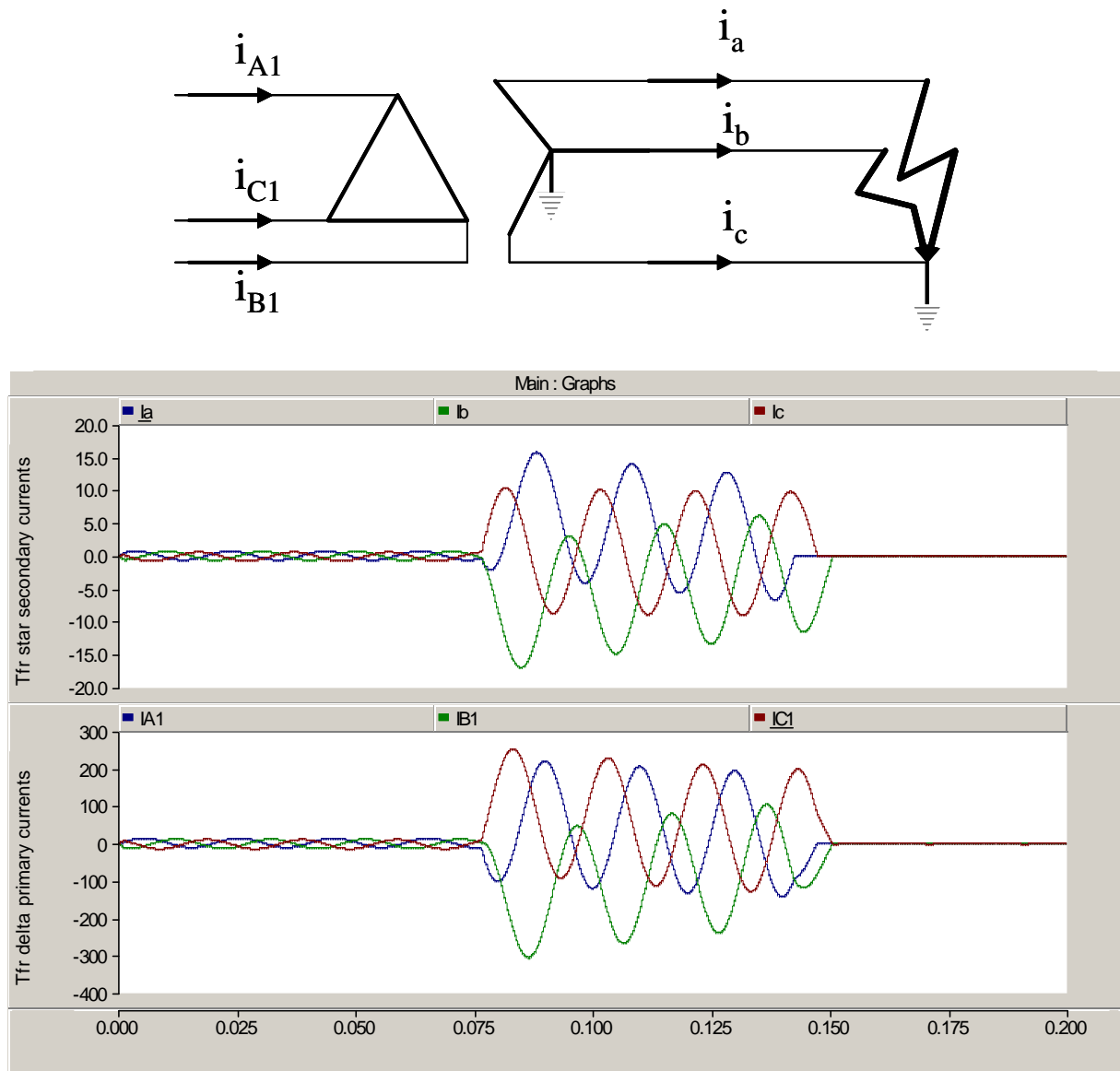


Figure 2.11 : Single phase fault on star side of delta-star transformer



Figure 2.11 shows primary and secondary currents resulting from a single phase-to-earth fault on the secondary (star) side of a delta-star (dY11) transformer. The currents on the delta primary side follow that of a phase-to-phase unearthed fault.

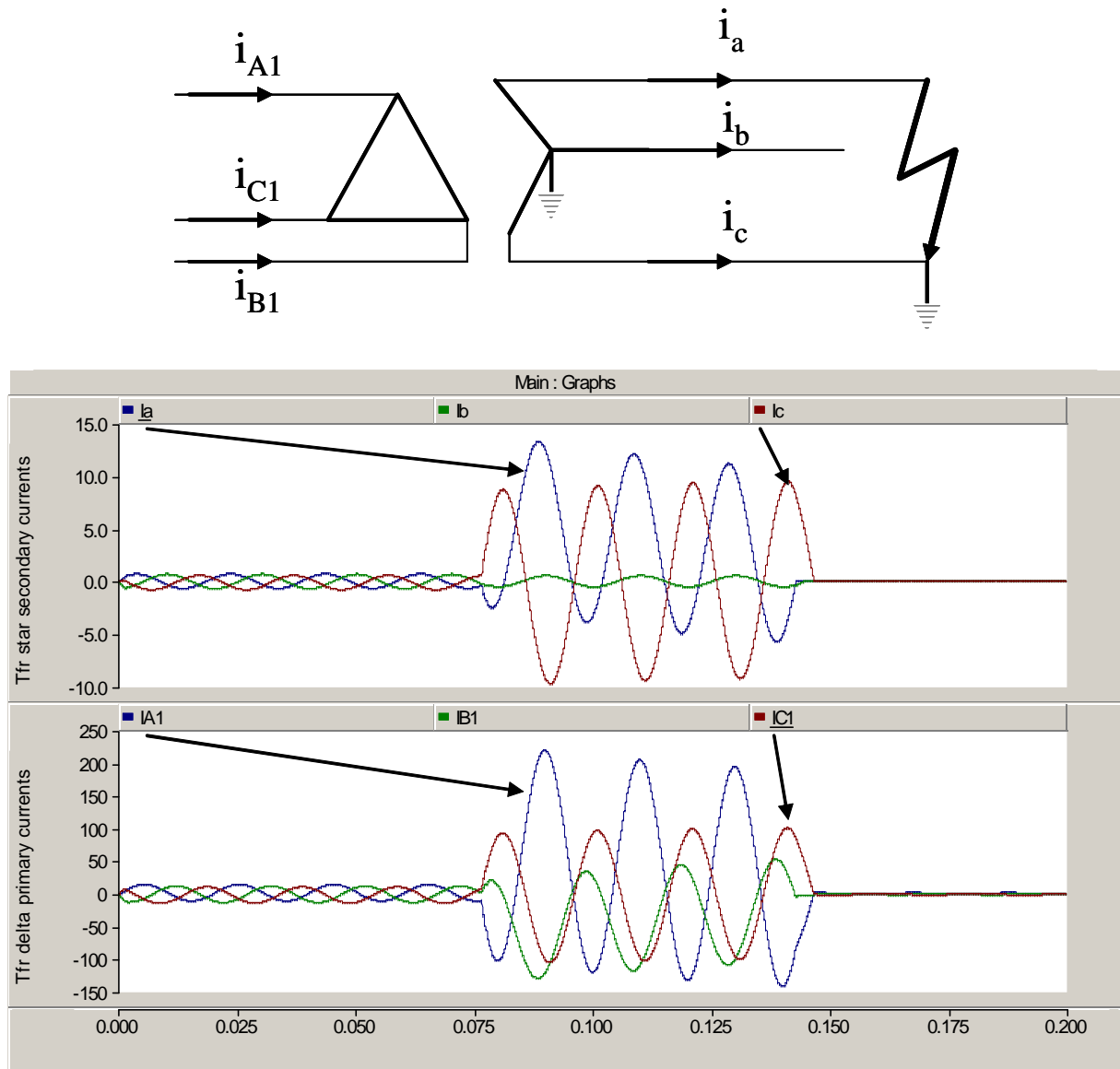
Figure 2.12 shows primary and secondary currents resulting from a three phase-to-earth fault on the secondary (star) side of a delta-star (dY11) transformer. The currents on the delta primary side follow that of three phase unearthed fault.



**Figure 2.12 : Three phase-to-earth fault on star side of delta-star transformer**

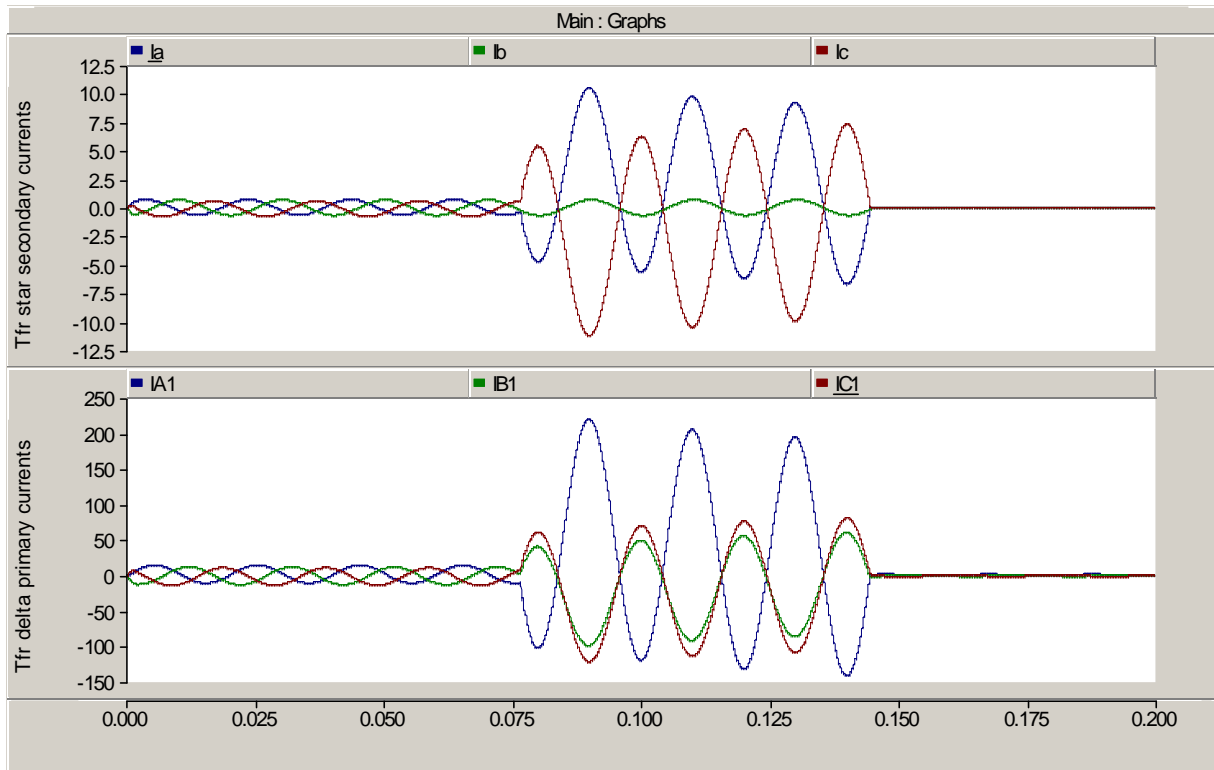
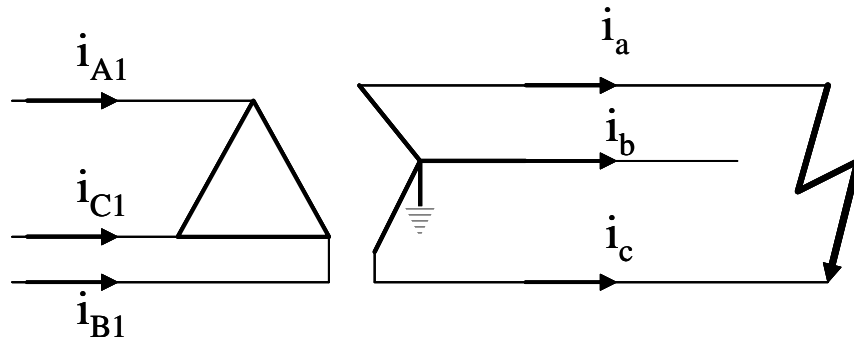
Figure 2.13 shows primary and secondary currents resulting from a double phase-to-earth fault on the secondary (star) side of a delta-star (dY11) transformer. The currents on the delta primary side follow that of a three phase unearthened fault.

Figure 2.14 shows primary and secondary currents resulting from a phase-to-phase (unearthed) fault on the secondary (star) side of a delta-star (dY11) transformer. The currents on the delta primary side follow that of a phase-to-phase unearthened fault with the currents of two of the phases shifted and combining to match the third phase.



**Figure 2.13 : Double phase-to-earth fault on star side of delta-start transformer**

Various strategies might be used to manage CFI coordination for circuit breakers installed immediately either side of and protecting the associated power transformer, including communication between CFI algorithms used on the associated circuit breakers e.g. expected phase interruption timings and sequences.



**Figure 2.14 : Phase-to-phase (unearthed) fault on star side of delta-star transformer**

### 2.3.2 Large generators

Problem of sub-transient reactance causing transient (exponential) change in fault current magnitude (due to change in generator effective source impedance) and thus leading to potential for a time period of “missing” current zeroes. Pörtl proposed “asymmetrical safe-points” as a CFI method to manage this problem.

It may also be possible to extend the {2.3} model to being a higher order equation to model  $X_d''$  effects - but this will lead to more degrees of freedom in applying an LMS solution to estimate the equation parameter values and make this process much more noise sensitive. It should be noted that for large synchronous generators in base load power stations that the connections between the generator and step-up transformer are normally constructed using “phase-isolated busbars”, whereby each phase conductor is housed inside its own earthed enclosure. This is done to avoid the risk of phase-to-phase unearthed or three phase unearthed faults. As such, a CFI scheme for a circuit breaker in such an installation need only focus on solving the single phase-to-earth fault cases.

It should also be noted that in the case of generator circuit breakers, directly connected to large synchronous generators, that additional special interruption stresses exist (e.g. very fast rates-of-rise-of-recovery voltage) that necessitate specially designed circuit breakers, covered by their own specific international standard (ANSI/IEEE C37.013-1997 [10]).

### 2.3.3 Series compensated lines

Faults on series compensated lines can be characterized by the problem of sub-synchronous resonance, wherein sub-harmonic oscillations can occur in the fault current [51] and this would present challenging problem in predicting current zero behavior. Also Hydro-Québec has reported cases of “missing” current zero behavior (similar to that seen near large generators) associated with faults on series compensated lines [52].

### 2.3.4 Parallel breaking operations

Parallel breaking occurs commonly on transmission systems where typically, where the system is at least partly meshed and more than one circuit breaker must interrupt to isolate a faulted section of the system. This can present a challenge to CFI, especially where the interruption by one circuit breaker may alter the power system configuration significantly enough to alter the current behavior in other circuit breaker(s) interrupting the same fault. Where circuit breakers are arranged within well defined protection operation zones it might be possible to use communication between the CFI controllers of each circuit breaker to co-ordinate the interruption e.g. to share targeting information and aim for common interruption targets and thereby mitigate the risk for significant changes in the current behaviors of any specific circuit breaker.

## 3 High power experiments

Since the main objective of CFI is to achieve interruption with a selected or preferred arcing time, it is critical to know the arcing time behavior of the circuit breaker to be controlled. This chapter describes a series of high power experiments conducted to both investigate the stability of minimum arcing times of an HV SF<sub>6</sub> circuit breaker, as well as the potential to utilize CFI to optimize interrupter performance by using a lower opening speed and therefore lower opening energy.

### 3.1 Experimental considerations

Circuit breakers are type tested in accordance with international standards [5], [6], [9], [10] in order to verify the minimum and maximum range of arcing times for different current interruption conditions from small capacitive or inductive currents of less than 100 A up to their full rated asymmetrical fault interruption duty. Partly due to the cost of high power type testing the applied standards normally require only single verified interruption at the minimum, maximum and medium arcing times for each fault test duty. As such there is normally only limited test data on the arcing time performance of a circuit breaker. It is therefore desirable to obtain further experimental evidence to verify the stability of arcing time behavior over a succession of interruptions. If the arcing times can be found to be reasonably stable for a number of interruptions, it provides a sound basis for the potential application of CFI using a restricted, targeted arcing time or window.

High power testing is a complex and expensive process. By its very nature, involving the interruption of large currents, it subjects the tested circuit breaker to electrical wear with each operation and ultimately the interrupter wear limit will be reached. Each test operation (or “shot”), can cost in the order 3000 USD, though as a minimum for a single series of tests shots can cost in the order 25 000 USD (excluding the cost of the tested circuit breaker). Both these factors limit the amount of test data that can normally be obtained within practical limits. As such, while the scope of the experiments conducted here is limited, the results provide some valuable insight to the feasibility of CFI.

As summarized in the introduction, one of the most readily recognized potential benefits of CFI aimed towards the minimum arcing time is the reduction in the rate of electrical contact wear of the interrupter. Using such CFI the circuit breaker could interrupt a larger number of faults before requiring intrusive interrupter maintenance and thereby reducing the overall life cycle cost.

A less obvious potential benefit of CFI is the possibility to optimize the circuit breaker design. The random nature of faults means that circuit breakers designed and tested for a range of possible arcing times, normally in the range of 0.5 to 1.5 cycles. To this extent circuit breakers tend to be sub-optimized from a mechanical perspective as they must be designed with sufficient contact stroke, speed and operating energy to cater for a wider range of arcing times than might be necessary if the trip commands were synchronized with respect to target interruption current zeroes i.e. through use of CFI.

Circuit breaker design is further complicated by the need to cater for a wide range of interruption cases, ranging from small capacitive or inductive currents through to full rated

asymmetrical fault currents. Different interruption duties place different thermal and dielectric stresses on the circuit breaker.

In respect of HV AC SF<sub>6</sub> circuit breakers, much of the development focus of the past decade has been on improvement of interrupter designs such that they shall require mechanical lower operating energy for the same ratings as earlier designs. Lowering the required mechanical operating energy for given interruption ratings offers important benefits by the associated reduction in the mechanical stresses placed on the circuit breaker, which in turn can lead to both lower maintenance requirements (i.e. longer intervals between maintenance work) and higher reliability. Industry surveys (e.g. CIGRÉ [34], [35], [36], CEA [37]) have consistently shown that mechanical failures in HV AC circuit breakers are far more common than failures of interrupters.

Two main development steps in SF<sub>6</sub> interrupter energy reduction have been the introduction of “self-blast” in place of “puffer” interrupters and the more recent use of reciprocal or “double-motion” interrupters, where the relative speed required on the arcing contacts is obtained by using a gear system to obtain movement of both arcing contacts from a single common drive linkage. Though these developments have been shown to be successful through their eventual productification by most of the major HV circuit breaker manufacturers [41], [42], it should not be overlooked that such developments in interrupter design require substantial cross-disciplinary research and investment. It is not the purpose of this chapter, nor this thesis, to attempt a detailed analysis of HV AC interrupter design. However it should be noted that successful interrupter design requires detailed knowledge of gas plasma and arc physics, material science, mechanical and electrical design [43], [44], [45].

It is possible that CFI may provide a means to extend such development in addition to facilitating new interruption technologies. In this context, it was considered of interest within the scope of this thesis to investigate the potential to obtain operating energy savings by the use of CFI, in conjunction with the investigations on the stability of minimum arcing time behavior.

### 3.2 Disclaimer

As indicated in the acknowledgments to this thesis ABB has generously supported the work in this thesis financially, in particular with respect to the cost of the high power experiments described in this chapter. The circuit breaker used in this work is a standard ABB product. However it must be stressed that the circuit breaker was operated in the following experiments well outside its designed operating configuration and the results presented here should in no way be used to infer or extrapolate the performance of the original ABB product. In addition, the conclusions presented in this thesis are those of the author and do not necessarily reflect the opinions or policies of ABB as a company. In order to protect ABB intellectual property associated with the circuit breaker used, only limited data related to the circuit breaker design and operational values can be presented. Interrupter dimensions, contact travel stroke and speeds have been normalized and expressed in percentages referred to the original circuit breaker design nominal values. These restrictions on data publication do not affect the validity of the data of interest from these experiments i.e. arcing time behavior in the context of the CFI research.

### 3.3 Experiment objectives

As described above, two main objectives were set for the high power experiments:

1. confirm stability of minimum arcing times for a range of interruption duties
2. investigate the minimum arcing time behavior at reduced interrupter operation speed (=energy)

Figure 3.1 places these objectives together with primary goal of CFI to achieve interruption with a targeted narrower arcing window in the context of a typical arcing window for a circuit breaker designed for the conventional “direct trip” arcing window capability.

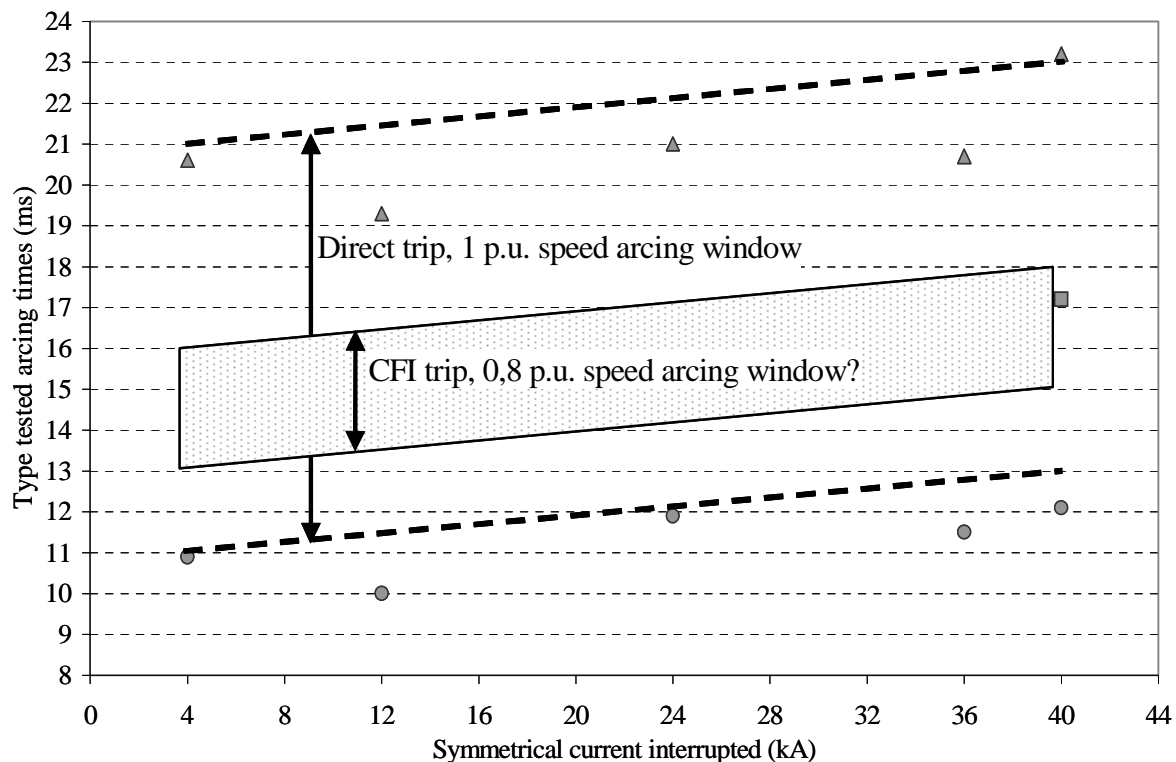


**Figure 3.1: Comparison of direct and possible CFI arcing time windows for 145 kV SF<sub>6</sub> circuit breaker**

The type tested “direct trip” arcing time data shown in Figure 3.1 is for a 145 kV, 40 kA, 50 Hz, SF<sub>6</sub> circuit breaker of the same interrupter design as used for the CFI high power experiments. As can be seen in the graph, the direct trip arcing window is 10 ms wide and the specific arcing time limits generally tend to increase (slightly) with increased current magnitude. This increase is to be expected in the context that the larger the current to be interrupted, the longer contact travel (and thus arcing time) is required for developing the required SF<sub>6</sub> gas pressure and gas flow at current zero to achieve interruption. Nevertheless, given the tenfold range of the symmetrical interrupted currents, the arcing time window limits are very consistent and stable over the full current range.

The narrow shaded band shows the area of interest for the investigation of arcing time behavior and stability for CFI, while also operating the circuit breaker at a substantially lower

than designed opening speed. It was decided to use an opening speed of 0.8 per unit with respect to the designed nominal opening speed of this circuit breaker. This would result in an operating energy reduction also in the range of 20%, allowing for energy required to overcome inherent losses (e.g. friction) in the mechanical system.

As will be explained in further detail with the test object description, it was expected that the minimum arcing times at 0.8 p.u. opening speed would be longer than for the 1.0 p.u. speed minimum arcing times. This is due to the dependence of the required SF<sub>6</sub> gas pressure and density build-up for interruption being linked to a minimum contact travel. The range of arcing times tested at 0.8 p.u. opening speed was set at a 3 to 4 ms spread in order to verify that there would be an acceptable margin retained in the circuit breaker performance to cater for other factors that may affect the targeting and control accuracy of a CFI scheme e.g. spread in circuit breaker opening times, errors in target current zero time estimation.

### 3.4 Test object description

The circuit breaker used for these experiments is shown in Figure 3.2, as it was set up within the test cell of the high power laboratory. It was a three pole operated live tank circuit breaker equipped with so-called “self-blast”, SF<sub>6</sub> interrupters housed within porcelain breaking chambers. The interrupters are each connected by an insulated operating rod housed within the supporting insulators. The operating rods are in turn connected through a simple shaft mechanism at the base of each pole to a common drive shaft that is in turn driven by a motor connected at one end of the breaker. The motor is operated by a digital control system that is described in further detail later.

When configured with its normal designed operating parameters of contact travel and SF<sub>6</sub> gas density, the interrupters on this circuit breaker are rated as indicated in Table 3.1 below, together with the equivalent rating values applied for the CFI experiments.

**Table 3.1: Summary ratings of test circuit breaker**

Breaker type	Opening speed	Rated voltage	Symmetrical breaking capacity	Frequency	SF <sub>6</sub> blocking level	First pole to clear factor
-	p.u.	kV	kA	Hz	MPa abs @ 20°C	(FPTC)
Normal 1	1.0	145	40	50	0.43	1.5
Normal 2	1.0	170	40	50	0.6	1.5
Test Object	0.8	145	40	50	0.6	1.5





**Figure 3.2: HV SF<sub>6</sub> circuit breaker used for high power experiments**  
(Photo courtesy of ABB AB©)

The interrupters used have the same contact stroke for 145 kV and 170 kV applications and only differ in the applied SF<sub>6</sub> blocking density level and length of the support and breaking chamber insulators to cater for the higher dielectric stresses associated with 170 kV. The lower 0.43 MPa abs SF<sub>6</sub> blocking level used at 145 kV also allows the circuit breaker to be used down

to  $-40^{\circ}\text{C}$  with 100%  $\text{SF}_6$  gas, whereas the 0.6 MPa abs  $\text{SF}_6$  blocking level is restricted to use down to  $-30^{\circ}\text{C}$ , due the liquefaction properties of  $\text{SF}_6$ . As the circuit breaker was going to be tested with 20% lower than designed opening speed, it was considered prudent to use the higher 0.6 MPa abs  $\text{SF}_6$  blocking level in combination with the 145 kV, FPTC = 1.5 ratings as the additional  $\text{SF}_6$  was hoped to mitigate the expected increases in minimum arcing times.

The basic design of the self-blast interrupter is shown in Figure 3.3. The moving assembly of the interrupter consists of a puffer cylinder comprised of a fixed volume,  $V_F$ , and a compression volume,  $V_C$ . As the interrupter opens, the puffer cylinder moves downwards, compressing the  $\text{SF}_6$  in  $V_C$ , which passes through a simple flap valve into  $V_F$ . As the arcing contacts separate, the arc blocks the  $\text{SF}_6$  exhaust path from  $V_F$  until a current zero, at which time the pressurized  $\text{SF}_6$  in  $V_F$  will be released and will attempt to extinguish the arc and establish sufficient dielectric strength in the contact gap to withstand the transient recovery voltage (TRV). During the arcing time, heat from the arc will also contribute to the  $\text{SF}_6$  pressure build-up in  $V_F$ . Such designs allow for use of lower interrupter operating energies than "pure puffer" interrupters that rely more fully on pure mechanical compression to achieve the  $\text{SF}_6$  pressure required for interruption.

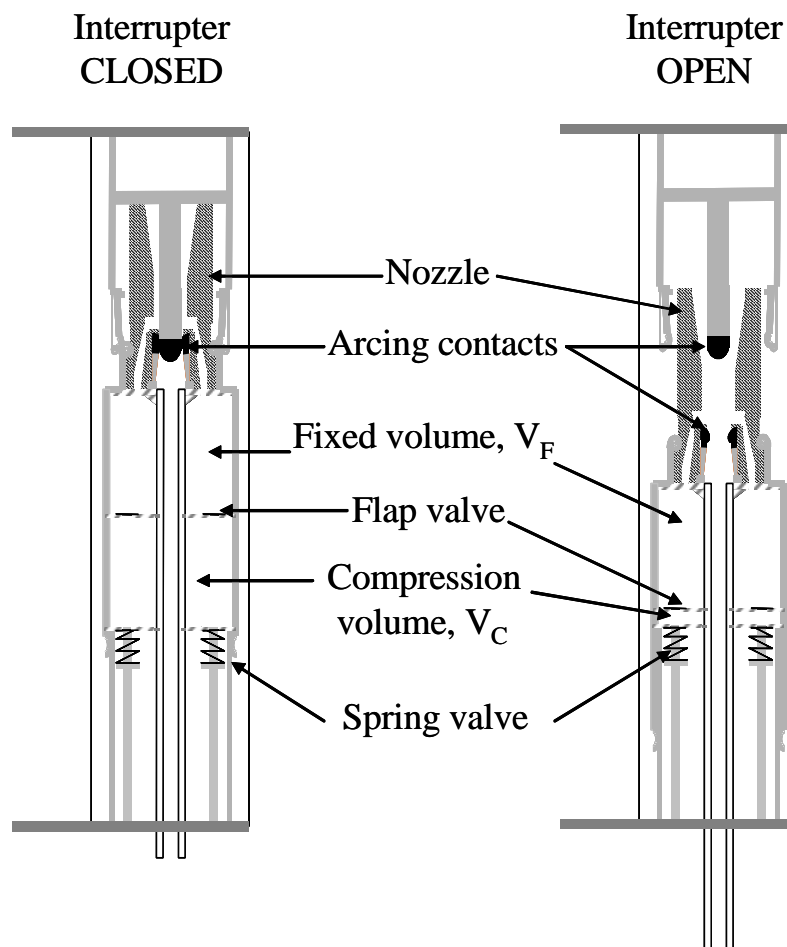


Figure 3.3: Sketch of self-blast  $\text{SF}_6$  interrupter design

The self-blast interrupter is self-regulating in regard to pressure build-up. For low magnitude currents the arc heat contributes little to the pressure build-up in  $V_F$  and the main pressure build up comes via  $V_C$ . At fault current levels, the arc heat is dominant and once the pressure in  $V_F$  exceeds that in  $V_C$ , the flap valve closes and any excess pressure in  $V_C$  is released by the lower spring valve.

The moving contact system of the interrupter is driven by the circuit breaker operating mechanism. In order to easily manage the proposed opening speed reduction and to monitor the resultant operating energy of the circuit breaker it was decided to use an electric motor drive operating mechanism, similar to that described in previously published papers from ABB [38], [39] and by the block diagram shown in Figure 3.4.

The common interphase drive shaft of the circuit breaker is connected directly to the rotor of the drive motor. The motor is a specially dimensioned permanent magnetic synchronous motor, designed to deliver very high torque, but for very short total operating times. The motor is only required to make one half revolution for a close or open operation of the circuit breaker, with total individual operating times less than 100 ms.

The Motor Drive comprises the motor with an integrated resolver for adaptive feedback position control and an IGBT bridge fed from an energy buffer made up of a battery of electrolytic capacitors. The charge on the capacitor bank is maintained via the charging unit connected to the auxiliary supply. The commands to the drive are regulated through the I/O controller to manage normal circuit breaker logic permissive controls and then passed to the motion controller circuit board. The motion controller board contains the programmed parameters for open and closing travel curves and issues the appropriate signals to the IGBT bridge to provide the required current to the motor to achieve the desired closing or opening travel, with feedback control implemented by the continual comparison of the measured travel from the resolver to the stored programmed travel curve requirements. The result of the feedback control is that the Motor Drive provides very stable and consistent travel from operation to operation.

Two additional features of the Motor Drive made it particularly useful for the experiments. Since the contact travel is digitally controlled, it is very easy to adjust the speed of the circuit breaker by adjustment of appropriate parameters stored in the motion controller. This allowed easy and rapid adjustment of the opening speed from 1.0 p.u. to 0.8 p.u. for the experiments. The operating energy consumed by the drive,  $J_{OP}$ , can also be easily measured by the voltage drop on the capacitor bank,  $U_{DROP}$  for each operation ( $J_{OP} = \frac{1}{2} * C * U_{DROP}^2$ ), which is registered by the automatic event log within the drive for every operation. Thus the energy saving from the 20% reduction in opening speed could be directly checked.

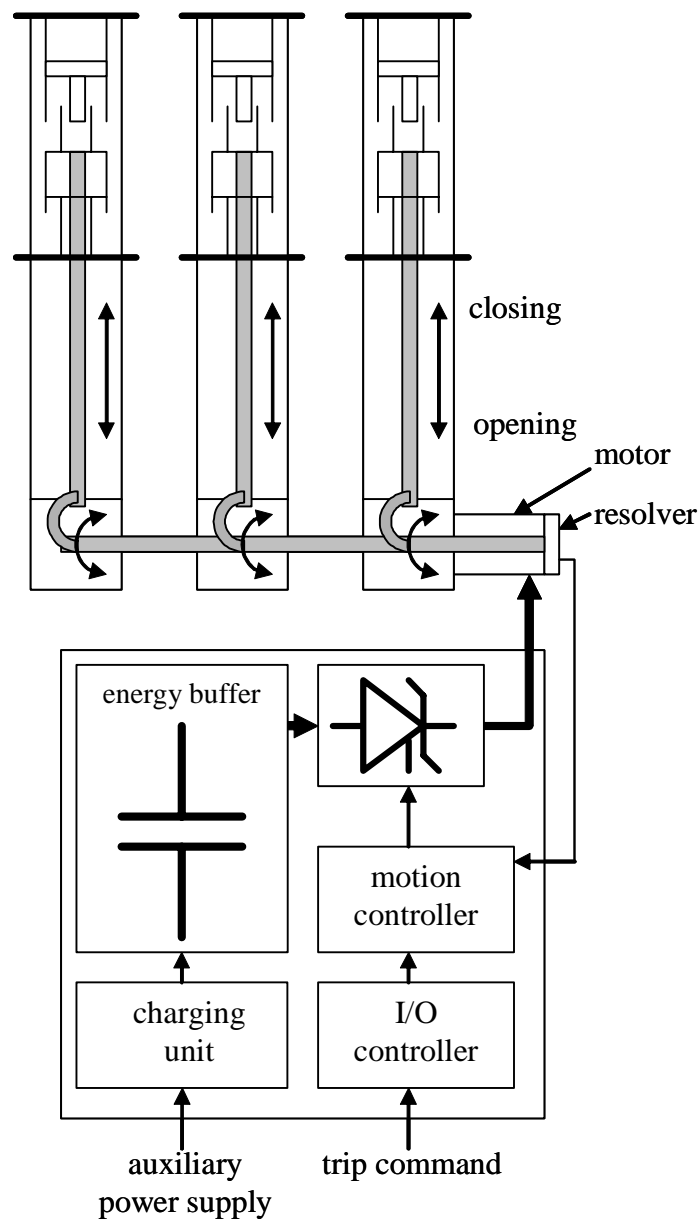


**Figure 3.4: Motor drive operating mechanism**

Figure 3.5 shows normalized and linearized representations of the 1.0 and 0.8 p.u. opening speed travel curves and respective no-load opening times of the test circuit breaker. The contact stroke data has been normalized to per unit values in order to protect ABB proprietary information.

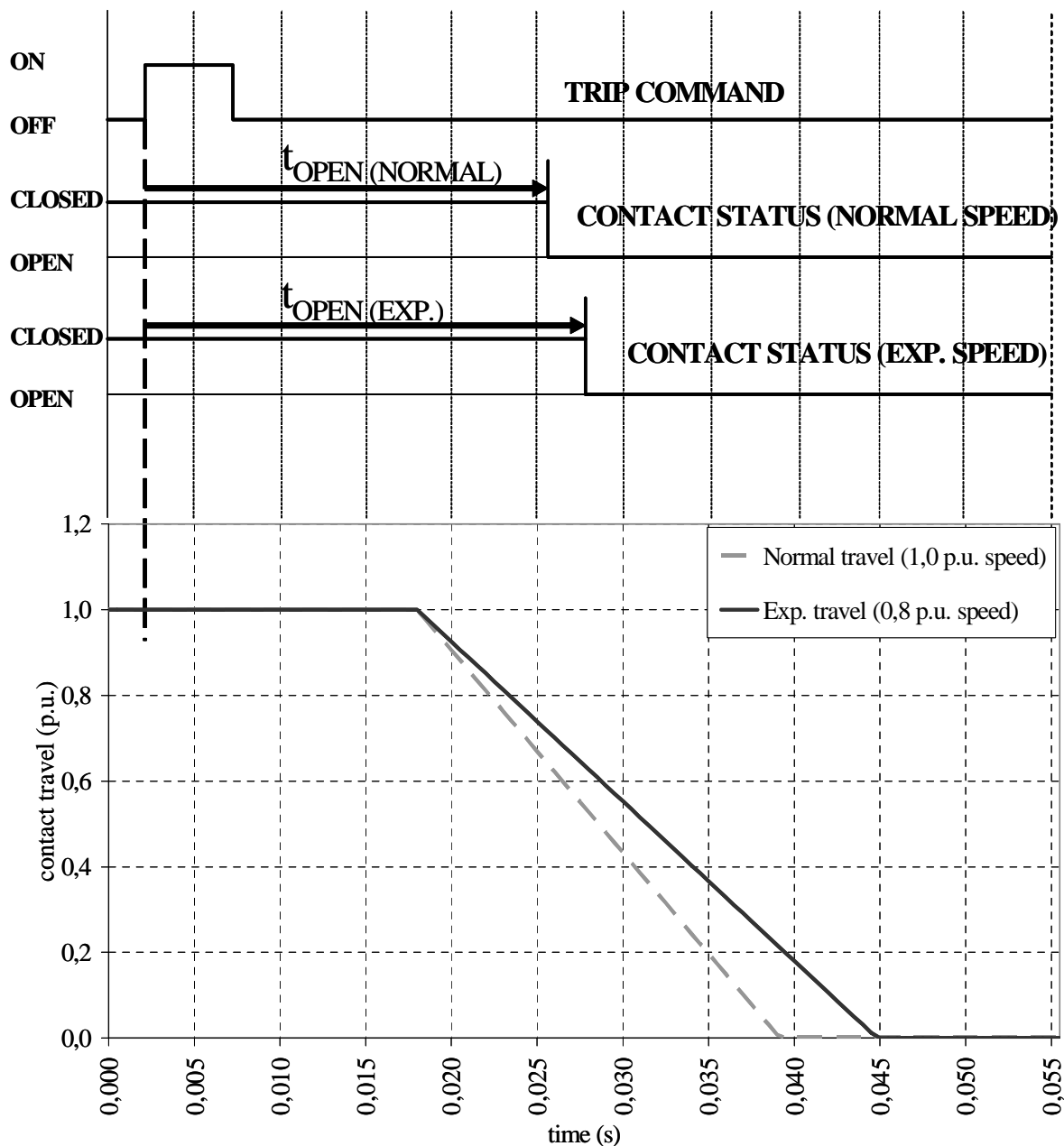
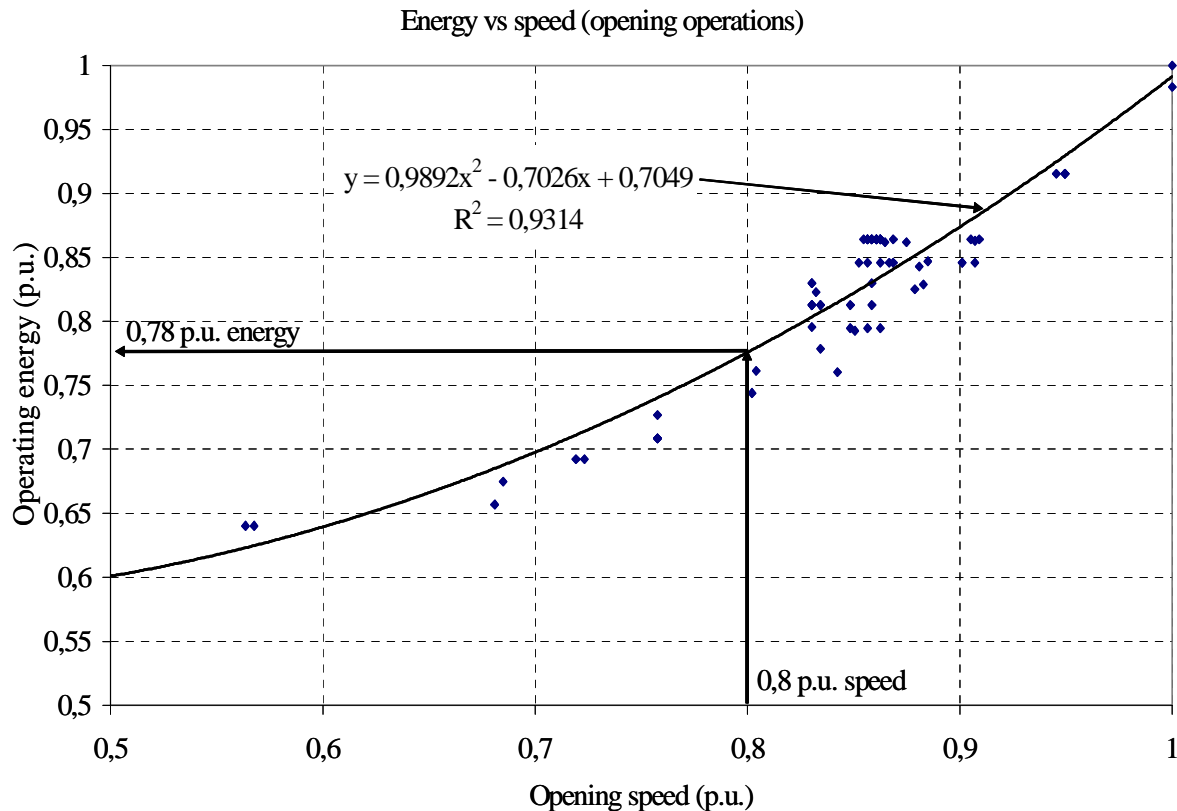


**Figure 3.5: Normal (1,0 p.u.) and experimental (0,8 p.u.) speed travel curves**

Figure 3.6 shows the calculated consumed operating energy of the Motor Drive on opening the three phase circuit breaker for different per unit levels of opening speed. While it might be expected that the operating energy would be equal to  $\frac{1}{2} \cdot m \cdot v^2$  in mechanical terms, there are electrical losses (e.g. resistive losses in cables and motor) and mechanical losses (e.g. friction, gas compression in interrupter, acceleration and braking of moving masses) within the complete moving system of the circuit breaker. Hence there was an approximate 22% saving in total consumed operating energy for a 20% reduction in opening speed. The variations in the plotted

data points about the trend line are due to the fact that they reflect different parameter settings on the Motor Drive, testing different torque as well as speed settings.



Acknowledgements:

Raw data obtained from Motor Drive motion log provided by A. Tengzelius, ABB AB.

Data normalized, plotted and trend line calculated using Microsoft® Excel 2003 by R. Thomas.

**Figure 3.6: Test circuit breaker reference operating energy vs. speed characteristic for no-load opening operations**

### 3.3 Applied high power interruption test duties

A range of IEC standard test duties was chosen to investigate the minimum arcing time stability under different thermal and dielectric stress conditions as summarized below:

1. T100a, asymmetrical fault current major loop ( $X/R = 14$ ;  $I_{sym} = 40$  kA)
2. T100a, asymmetrical fault current minor loop ( $X/R = 14$ ;  $I_{sym} = 40$  kA)
3. L90, short-line fault current ( $I_{sym} = 36$  kA)
4. T30, symmetrical fault current ( $I_{sym} = 12$  kA)
5. LC1, 50 A capacitive current interruption, preceded by T60 symmetrical fault current pre-conditioning interruption ( $I_{sym} = 24$  kA)

The IEC standard test requirement parameters are summarized in Table 3.2, including the transient recovery voltage peak and rate-of-rise-of-recovery-voltage (RRRV) values.

**Table 3.2: IEC 62271-100 standard test parameters**

Test No	Test duty	kA	%DC (current zero)	di/dt current zero (A / $\mu$ s)	TRV peak (kV)	RRRV (kV/ $\mu$ s)	ITRV RRRV (kV/ $\mu$ s)
1	T100a minor loop	40	30-50%	16,17	249	2	n.a.
2	T100a major loop	40	30-50%	17,38	249	2	n.a.
3	L90 short-line fault	36	<20%	15,99	166	2	7,4
4	T60	24	<20%	10,66	266	3	n.a.
5	T30	12	<20%	5,33	273	5	n.a.

The fault current test duties primary test the circuit breaker's thermal interruption capability. All the fault current tests were conducted on the basis of a 1.5 first-pole-to-clear (FPTC) factor, corresponding to a non-effectively earthed 145 kV system.

The capacitive current interruption tests were included to verify the circuit breaker dielectric interruption capability at the reduced opening speed, even allowing for the use of the 0.6 MPa abs SF<sub>6</sub> pressure during the tests. The peak recovery voltage for the capacitive current interruption tests was 332 kV, corresponding to a voltage factor of 1.4. The LC1 tests were limited to six interruptions each at arcing times of 4 ms, 5 ms and 6 ms. Normal IEC capacitive current interruption tests include tests down to near zero arcing time to verify the restrike withstand probability of the circuit breaker under the most onerous dielectric conditions with minimal contact gap after current zero. However the above chosen longer arcing times, centered around a ¼, 50 Hz cycle time were used on the basis that if the circuit breaker was to be operated with a CFI scheme, it would be equally viable to apply controlled interruption for capacitive current interruption also. All the capacitive interruption tests were achieved without re-ignitions or restrikes.

The remaining sections of this chapter will focus on the tests and results of the fault current interruption tests.

### 3.4 Experimental method

While the fault current tests were conducted using IEC standard test circuits and methods, the particular method of testing differed from "conventional" IEC type testing in that the arcing times were restricted to the narrow CFI arcing window of interest to this thesis work. A brief description of the applied current injection synthetic test method will now be presented, followed

by a description of the process used to verify the circuit breaker performance within the chosen CFI arcing window.

### 3.4.1 Current injection synthetic test method

The high power tests were conducted using the current injection method for synthetic testing, in accordance with IEC 62271-100 [5] and IEC 60427<sup>1</sup> [6], at the ABB High Power Laboratory located in Ludvika, Sweden. A detailed description of the synthetic test method is beyond the scope of this thesis and further information can be found in the referenced standards and circuit breaker texts e.g. Flurschein, Chapter 10 [40], Garzon, Chapter 8 [3]. As mentioned by Flurschein, the current injection method was developed nearly simultaneously by Weil and Dobke in Germany and by the Electrical Research Association in the U.K.

Figures 3.7 and 3.8 show the basic arrangement and operation of a current injection synthetic test circuit. Effectively the circuit works by first supplying the power frequency short-circuit current through the circuit breaker under test, TB, and just immediately prior to the targeted interruption current zero connecting the transient recovery voltage (TRV) circuit via triggering of the spark gap, SG, so that as the test circuit breaker interrupts the short circuit current at current zero it will then experience a TRV across its open contact gap. In this way, the current and voltage stresses associated with interruption are provided in parallel by two separate circuits, brought together just before the interruption current zero. This technique provides a similar stress on the circuit breaker as a direct fault interruption, but with a significantly lower total short circuit power requirement on the test laboratory. As the current and voltage stresses are provided by separate circuits, the method is referred to as “synthetic” as opposed to “direct” testing, where the interruption stresses would be provided by a single source and circuit.

The circuit to the left of the circuit breaker under test in Figures 3.7 and 3.8 is the power frequency short-circuit current source. The circuit to the right hand side of the test circuit breaker is the transient recovery voltage and current injection generation circuit. The test procedure can be described in five main steps as illustrated in Figure 3.8. The solid lines indicate “active” circuit parts and the dotted lines indicate “dormant” circuit parts for each step of the test process.

Step 1 is the charging of capacitor  $C_H$  with a DC voltage that will eventually provide the injection current that will in turn lead to the generation of the TRV at the interruption current zero. Once  $C_H$  is charged to the required voltage it is isolated from the DC charging source and the AC power frequency short-circuit current circuit is connected through to the test breaker (Step 2).

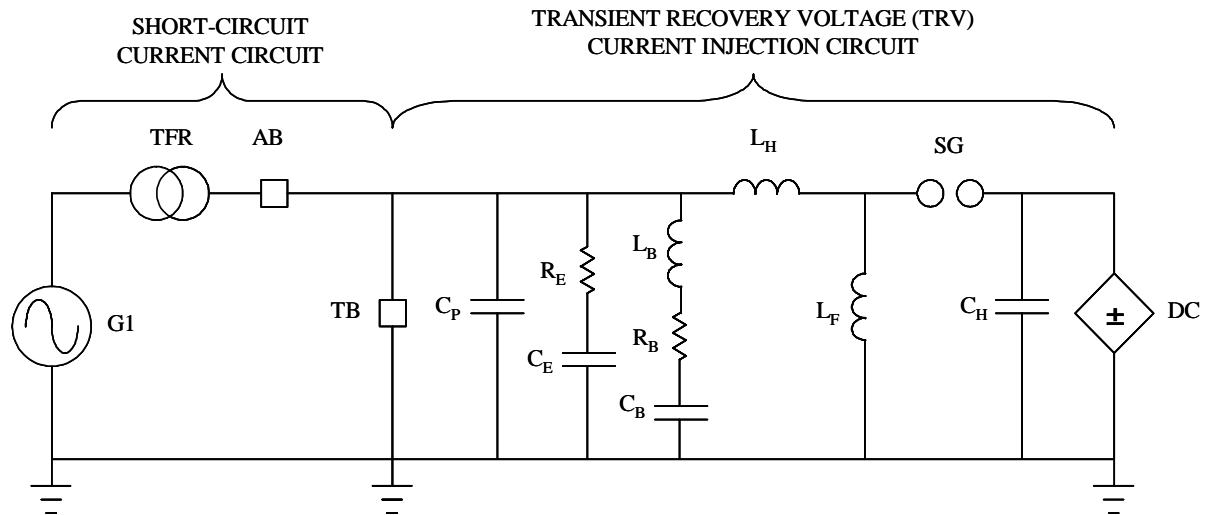
Just prior to the targeted interruption current zero (Step 3), the spark gap in the TRV circuit is triggered, allowing  $C_H$  to discharge through the main reactor of the TRV circuit and deliver the injection current to the test circuit breaker. Now the combined current through the test circuit breaker,  $i_T$ , is the sum of the AC power frequency current,  $i_G$ , from the left hand side circuit and the injection current,  $i_V$ , from the right hand TRV circuit. This leads to a modification of the current through the test circuit breaker as shown in Figure 3.9.

---

1. IEC 60427 (2000) has since been replaced by IEC 62271-101, published in May, 2006. However the testing made for this thesis was made at the time in accordance with IEC 60427.



At instant (1) in Figure 3.9, the spark gap, SG, is triggered, leading to the injection current to flow. Instant (2) indicates the time of the undistorted current zero that would occur from the generator supplied short circuit current. Instant (3) shows the resultant interruption current zero experienced by the test circuit breaker, immediately after which the TRV develops across the test circuit breaker (Step 5 in Figure 3.8).



## LEGEND

G1	SHORT-CIRCUIT A.C. GENERATOR
TFR	TRANSFORMER
AB	AUXILIARY CIRCUIT BREAKER
TB	TEST OBJECT CIRCUIT BREAKER
$C_p, C_b, C_e$	CAPACITORS FOR TRV WAVE SHAPE
$C_H$	CAPACITOR TO SUPPLY INJECTED CURRENT FOR TRV
$L_B$	INDUCTANCE FOR TRV WAVE SHAPE
$L_H$	INDUCTANCE OF HV CIRCUIT
$L_F$	INDUCTANCE FOR POWER FREQUENCY RECOVERY VOLTAGE
$R_E, R_B$	RESISTORS FOR TRV WAVESHAP
$R_B$	RESISTOR FOR TRV WAVESHAP
SG	SPARK GAP FOR HV CIRCUIT, CURRENT INJECTION
DC	DC SUPPLY TO CHARGE $C_H$

**Figure 3.7: Basic current injection synthetic test circuit**

In addition to the importance of the correct short circuit current level, TRV peak and rate-of-rise values for a designated standard type test, it is also important that the synthetic circuit achieve the same  $di/dt$  at the actual interruption current zero, to that which would have occurred for the undistorted generator fed short-circuit current.

In the event the test circuit breaker is unable to interrupt, the auxiliary circuit breaker will interrupt the generator fed short circuit current and the test circuit breaker will then only required to complete an interruption of the remaining injection current oscillations.

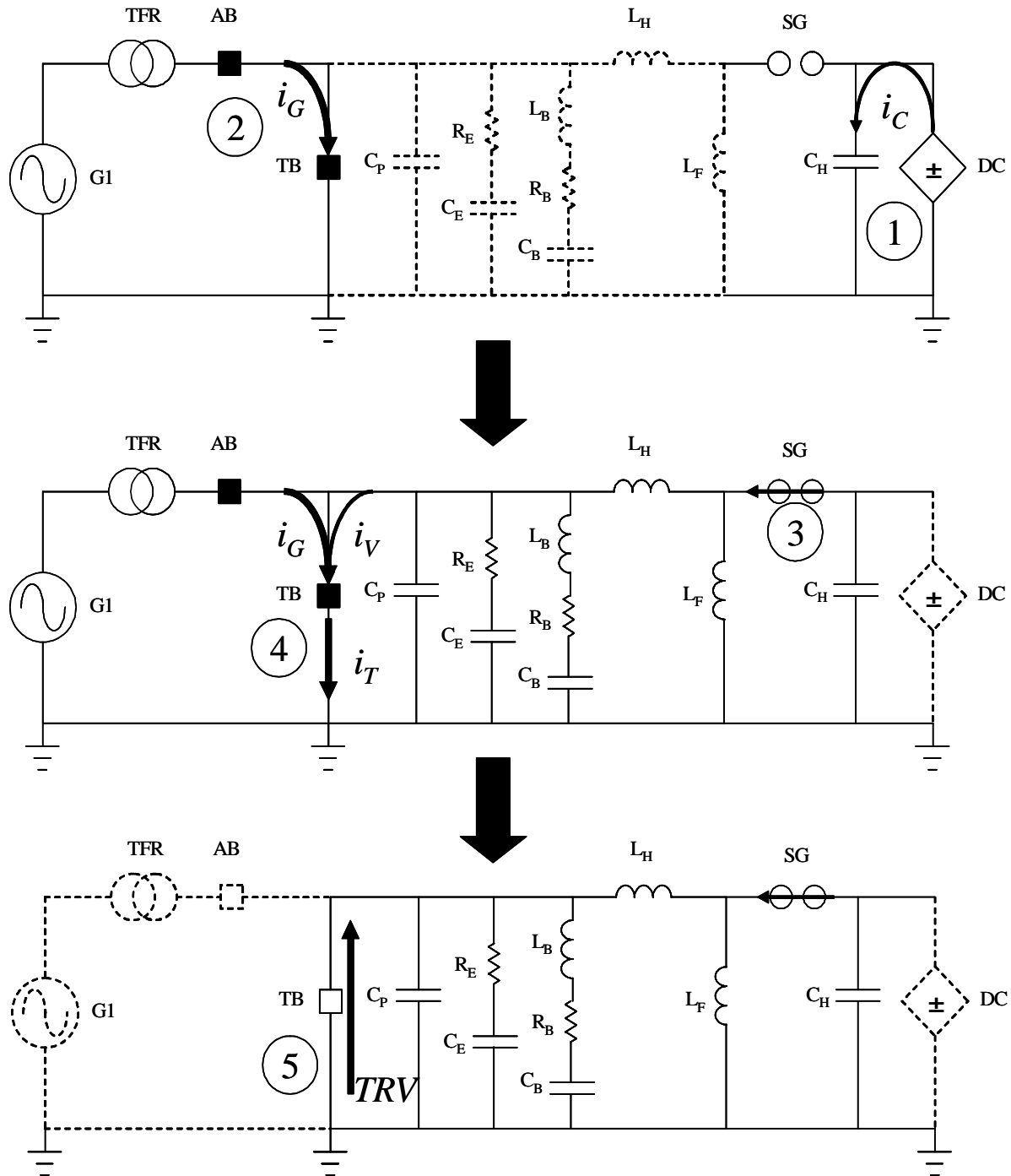
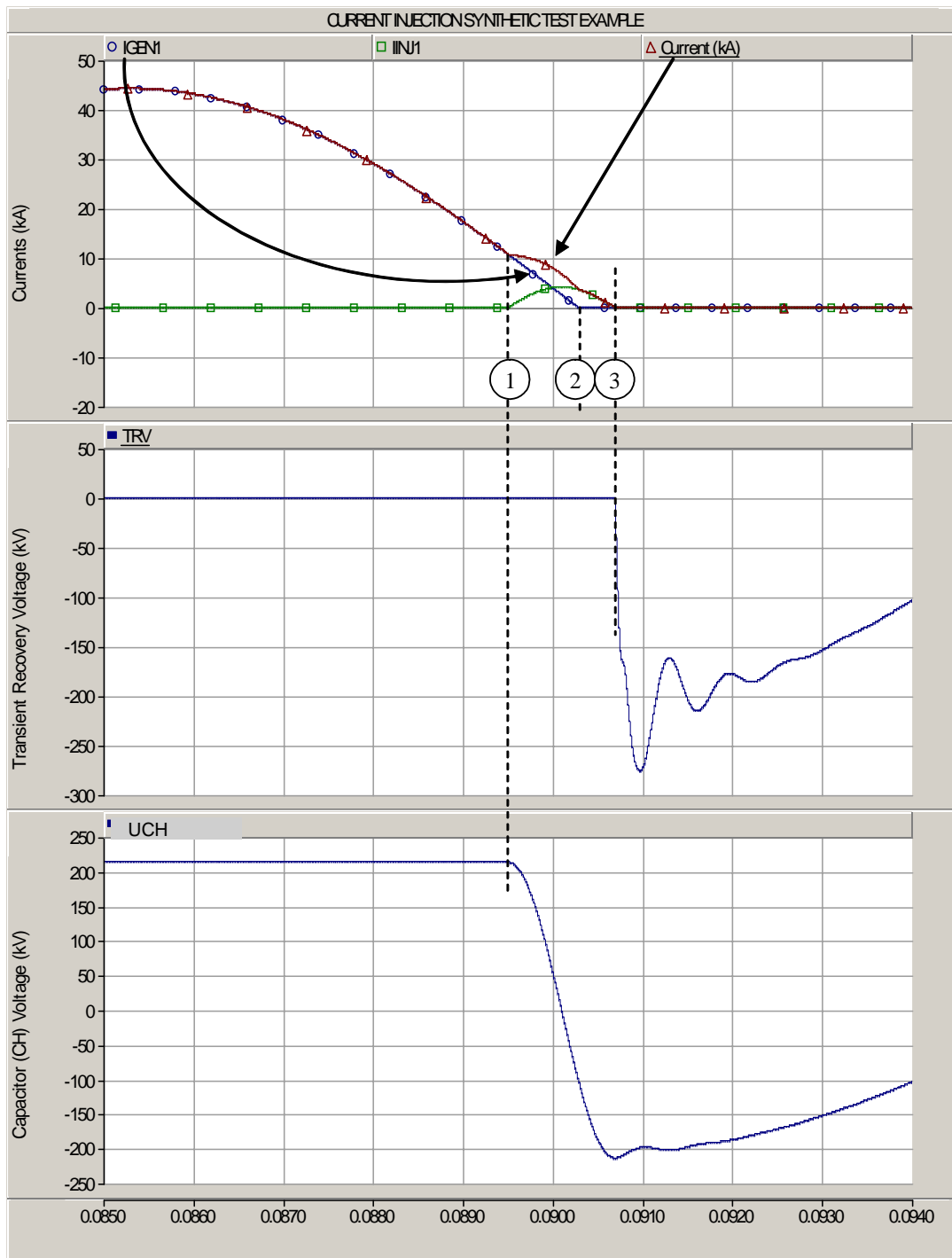


Figure 3.8: Basic operation stages of current injection synthetic testing



**Figure 3.9: Example of current injection co-ordination at current zero**

### 3.4.2 CFI restricted arcing window experimental procedure

Unlike conventional high power type tests, that test the circuit breaker for minimum, maximum and medium arcing times per fault test duty, the experiments conducted for this thesis focussed specifically on the stability around minimum arcing times for a succession of

interruptions. As indicated in the proposed reduced arcing window for CFI shown earlier in Figure 3.1, the investigated arcing time range was from the determined minimum arcing time and up to an additional 3 ms margin.

A separate interrupter contact set was used for each test duty, with the exception of applying both the T60 and LC1 line charging current interruption tests on one contact set. It was proposed to aim for between 6 to 12 interruptions per test duty depending on the current level being interrupted and as such testing each contact set towards the limit of its electrical wear. Given the different magnitudes of currents being tested, different rates of contact and nozzle erosion were to be expected. Part of the normal high power test procedure includes so-called “no-load” tests, where the circuit breaker opening time is measured for reference purposes. The measured no-load opening times are important in programming the targeting and synchronization of the high power synthetic test circuit to achieve verification of specific targeted arcing times.

As the intent was to verify the stability of minimum arcing time behavior with accumulated interruptions, it was also necessary during the test process to make intermediate tests for interruption failure at slightly below the minimum arcing time. The basic concept of the experimental procedure is illustrated in Figure 3.10. The specific order and number of test shots made was modified according to the results obtained during the testing.



**Figure 3.10: Experimental procedure for CFI arc window investigation**

Though no-load opening time verification tests were made during each test series, for practical reasons these were not made after every interruption. As such, the arcing times measured by the laboratory data acquisition system were based on the last prior no-load opening time prior to a series of interruptions and the measured current zero time at each subsequent interruption. With each interruption some arcing contact and nozzle material is burnt off. The accumulated nozzle erosion can influence the minimum arcing time due to the modification of gas flow caused by changes in the nozzle dimensions. The accumulated contact material erosion will result in a reduction in the opening time of the circuit breaker, as illustrated in Figure 3.11.

It is normally not possible to directly measure the opening time of the circuit breaker while it is interrupting a current, (though it could be done if good arcing voltage measurement is available). Hence during interruption testing the opening time is calculated by reference to the contact travel that is measured during each opening operation. The travel curve data is calibrated to the most recent prior no-load opening time to obtain the reference point on the contact travel where the contacts part.

In order to evaluate the arcing times more precisely for each interruption, the incremental effect of contact burn-off on the opening times of the circuit breaker was evaluated against the

summated integral of the absolute value of the arc currents for each test duty as described in Figure 3.12 below. The integral of the absolute value of the arc current was chosen as the independent variable affecting the contact burn-off based on the assumption that for fault currents, the arc voltage is effectively “constant” and the rate of contact burn-off would be proportional to the arc energy [49].

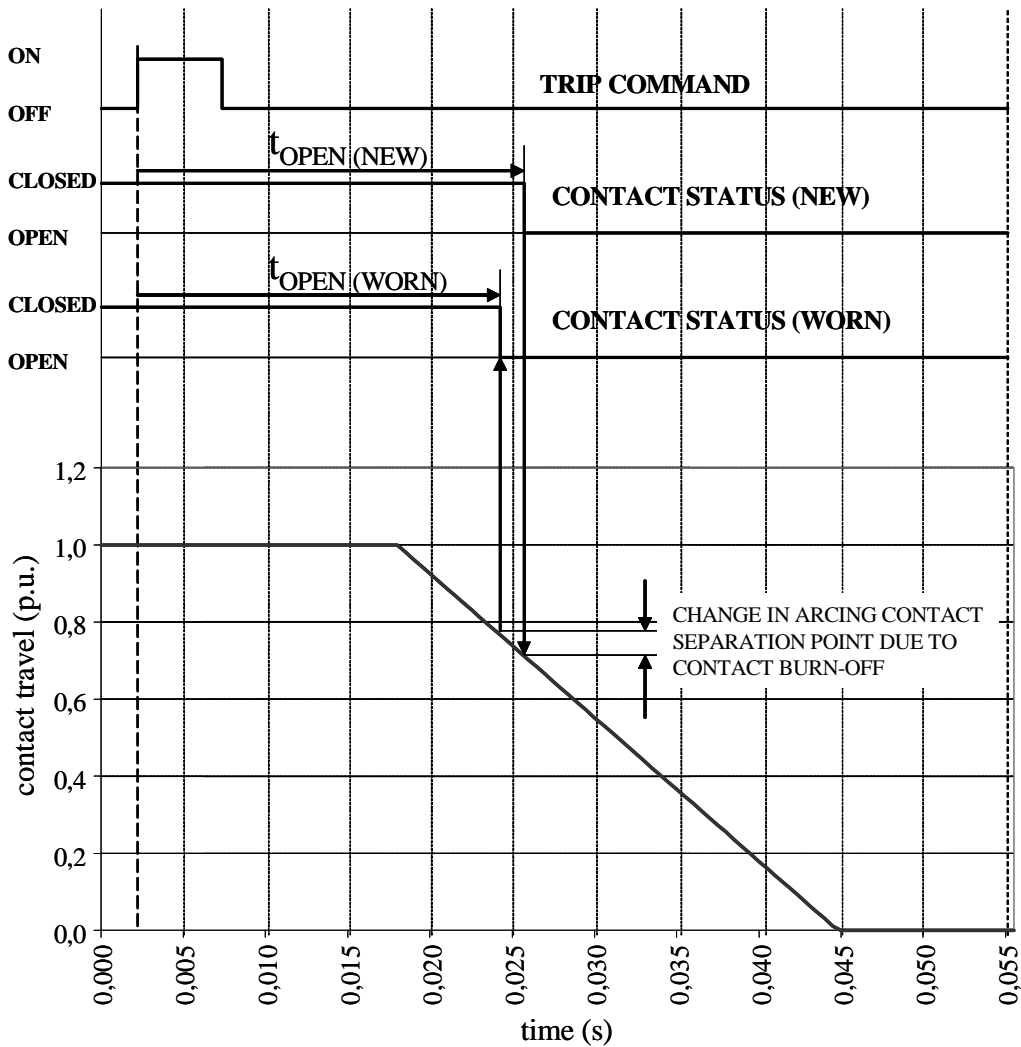
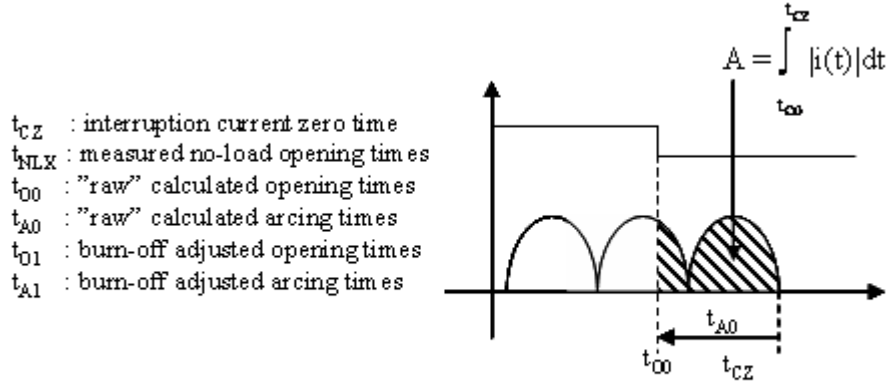


**Figure 3.11: Impact of contact burn-off on circuit breaker opening time**



Test shot	$ I_{SYM} $	Opening times	Arcing times	Arc integrals
0	-	$t_{NLO}$	-	-
1	$ I_{SYM1} $	$t_{O0_1}$	$t_{A0_1}$	$A_1$
2	$ I_{SYM2} $	$t_{O0_2}$	$t_{A0_2}$	$A_2$
.	.	.	.	.
.	.	.	.	.
.	.	.	.	.
X	-	$t_{NLX}$	-	-
		$\Delta t_O = t_{NLX} - t_{NLO}$		$A_{SUM} = \sum A_N$

**Figure 3.12: Evaluation of contact burn-off with respect to summated arc integral**

This was performed in a two stage iteration. First the arc integral sums for each test duty were calculated based on the original estimated arcing times and no-load opening times. The reductions in no-load opening times were then plotted against the associated arc integral sums between each of the no-load operations. The plotted data was combined from all the fault current test duties and a line of best fit interpolation was sought using Microsoft® Excel 2003©. The resultant trend line equation was then used as the basis for adjusting the opening and arcing times for each of the current interruption test shots. The results of the no-load opening time change versus the summated arc integrals is shown in Figure 3.13. The associated adjustment in arcing times with respect to the arc integrals according to the interpolation obtained from the plot in Figure 3.13 is shown in Figure 3.14 (for T100a minor and major loop tests only, as these tests

showed the most contact burn-off). The reduction in opening times due to contact burn-off results in an equivalent increase in the arcing times.

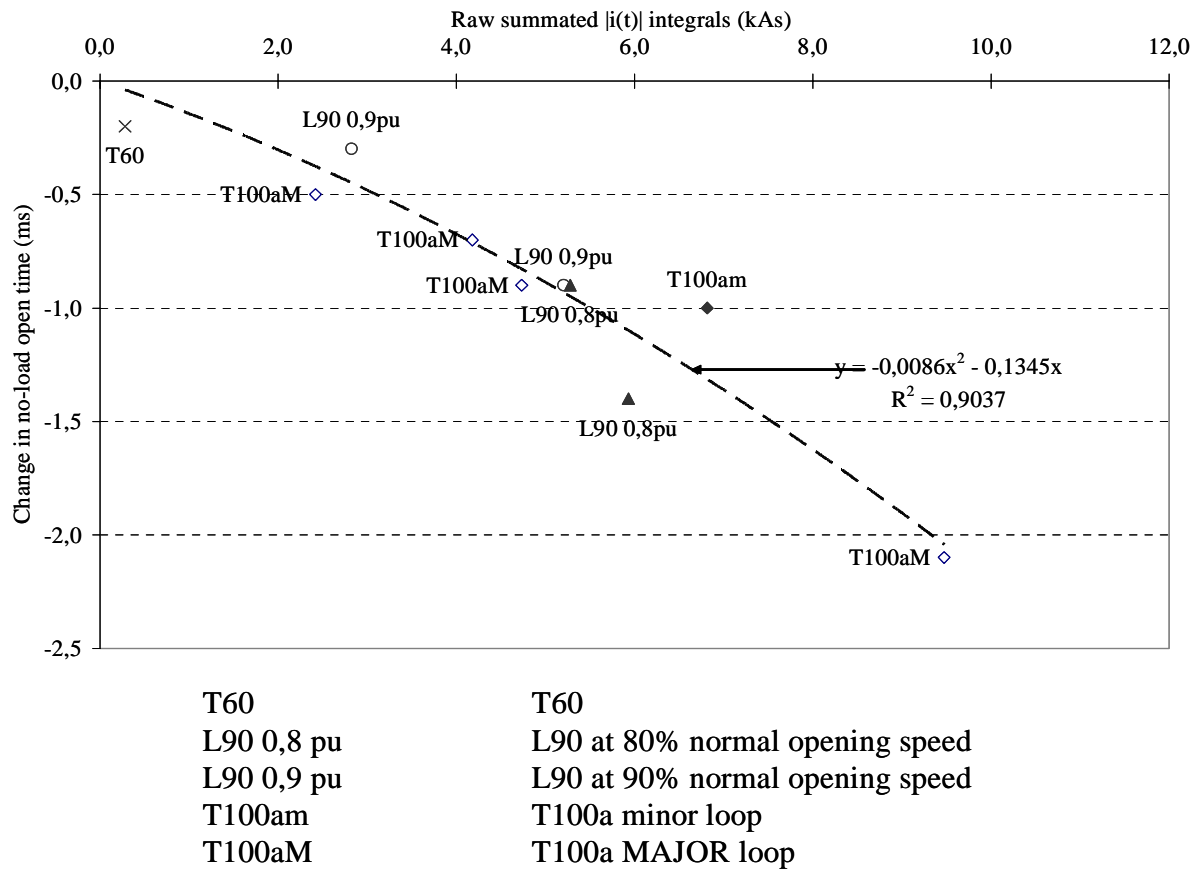


**Figure 3.13: Change in no-load opening time versus summated arc integrals**

The results of this analysis of the impact of contact burn-off on opening and arcing times is relevant for more than just interpretation of the arcing time tests. Establishing a contact wear rate related to the summated arc integrals is potentially very useful for a CFI algorithm as it would permit progressive adjustment of the expected opening times and arcing times of the circuit breaker over its lifetime and enable the CFI algorithm to maintain greater control accuracy and dependability.

The arcing time results presented in the next section of this chapter are all taken from the adjusted arcing times derived from the above procedure. All arcing times have been calculated to 0.1 ms resolution.

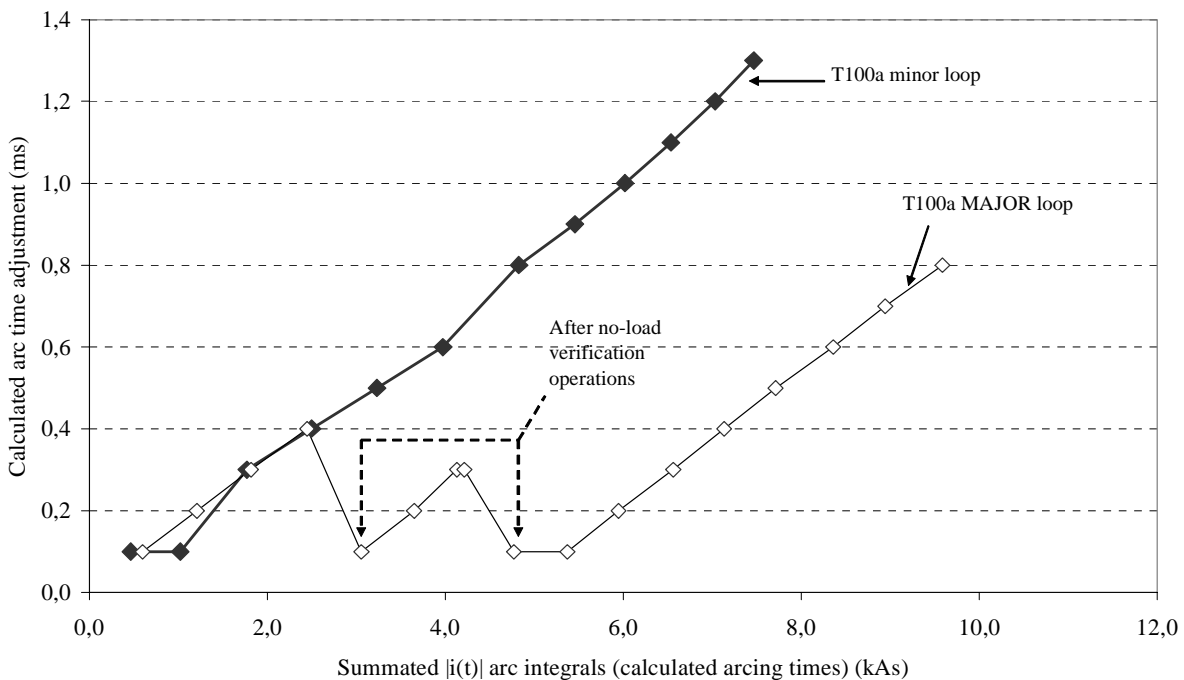


**Figure 3.14: Adjustment in arcing times with respect to summated arc integrals**

### 3.5 CFI arcing window results

The calculated CFI arcing window results are summarized below per fault test duty. The T30, T60 and T100a results are all from interruptions made with 0.8 p.u. opening speed. For L90, results are presented for both 0.8 and 0.9 p.u. opening speed.

Successful interruptions are indicated by a large dot (= “OK”). Unsuccessful interruptions, referred to as “misses” are indicated by “X”. The calculated arcing time values, in milliseconds, are indicated above or below each data point. The arcing time results are plotted based on the sequence of test shots per test duty, with all graphs normalized to 14 interruptions, though not this many interruptions were performed for all test duties.

It must be recognized that it is difficult to establish an “absolute” value for the minimum arcing time threshold to the same accuracy that can be obtained for no-load circuit breaker opening times e.g.  $\pm 0.1$  ms. Establishing the minimum arcing time limit is a process of “hunting” and the limit is only established by obtaining consecutive successful and unsuccessful interruptions. As such an accuracy in the order of  $\pm 1$  ms for the minimum arcing time limit is what can be expected, within the constraints of both the cost and destructive nature of interruption tests, where interrupter contact and nozzle material is burn-off with each operation. The more important result for these tests is to establish that there is a reasonable 2...3 ms interruption window at the reduced opening speed, over a succession of interruptions, from which a target CFI arcing time could be chosen in the mid-range with margin for other statistical variations in the control process.



### 3.5.1 T30 results

Figure 3.15 shows the calculated arcing times for the series of T30 interruptions made on a single contact set. The initial minimum arcing time is approximately 13 ms and after more than 12 interruptions it has decreased to approximately 11 ms, which is a reasonably moderate change in the minimum arcing time threshold for a large number of fault interruptions.

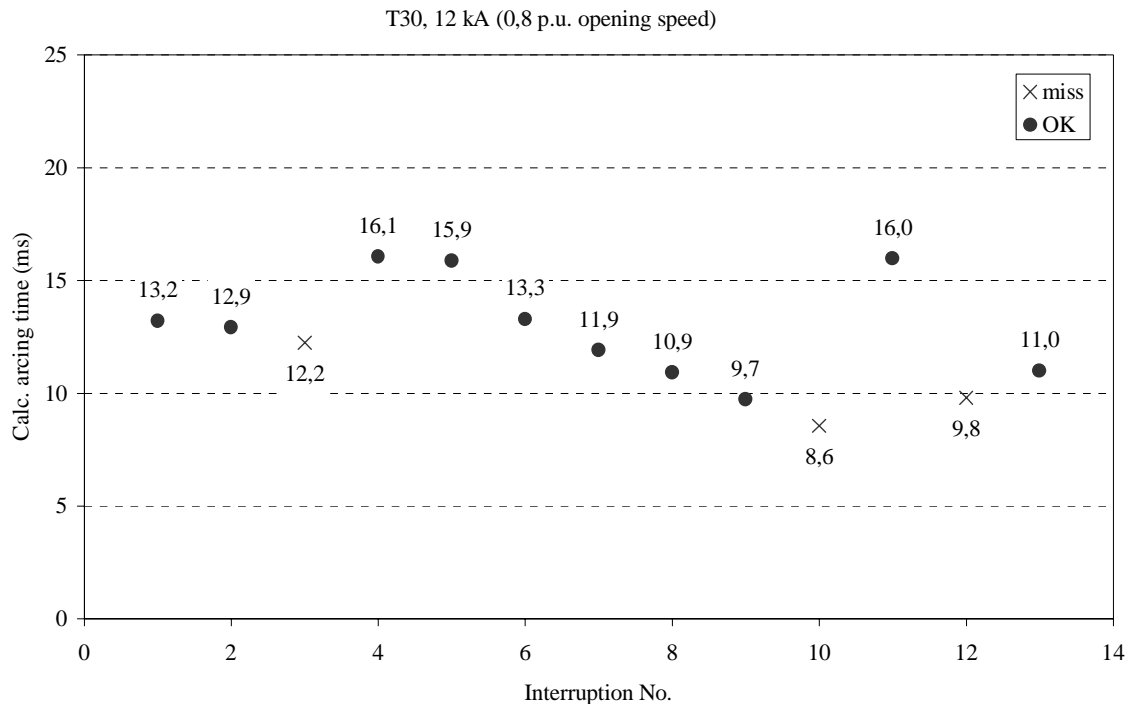


**Figure 3.15: T30, 12 kA, 0.8 p.u. opening speed arcing time results**

Importantly the circuit breaker was also found to interrupt successfully three times at approximately 16 ms over the series of tests. This indicates that there is a viable window of arcing time performance between 13 - 16 ms for this current level. It must be remembered that while CFI aims towards the minimum arcing time end of the arcing window, the target arcing time used should include some margin to allow to statistical spread in the arcing time threshold itself, circuit breaker opening times and errors in the prediction of the target current zero time.

### 3.5.2 T60 results

Figure 3.16 shows the results of the T60, 24 kA symmetrical current interruptions at 0.8 p.u. opening speed. The number of interruptions for this test was intentionally limited as the LC1 capacitive current interruption tests were subsequently made on the same contact set. Though limited to six interruptions, the results indicated a stable interruption window in the range of 14 to 17 ms.

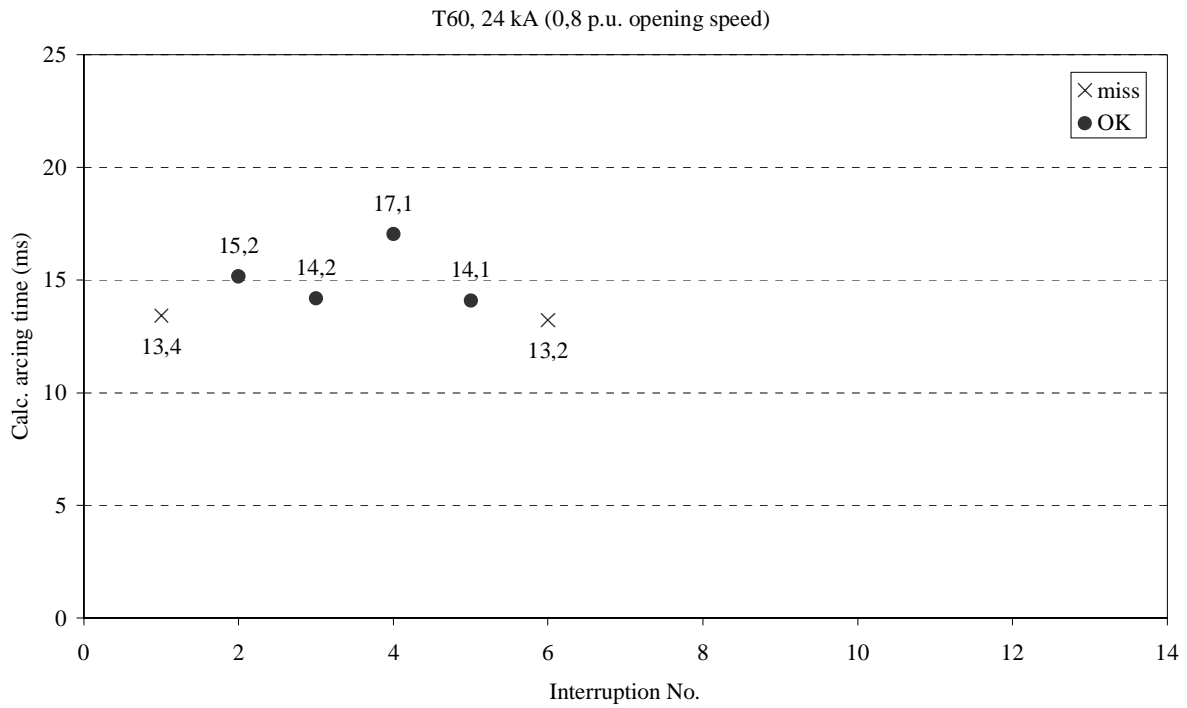


**Figure 3.16: T60, 24 kA, 0.8 p.u. opening speed arcing time results**

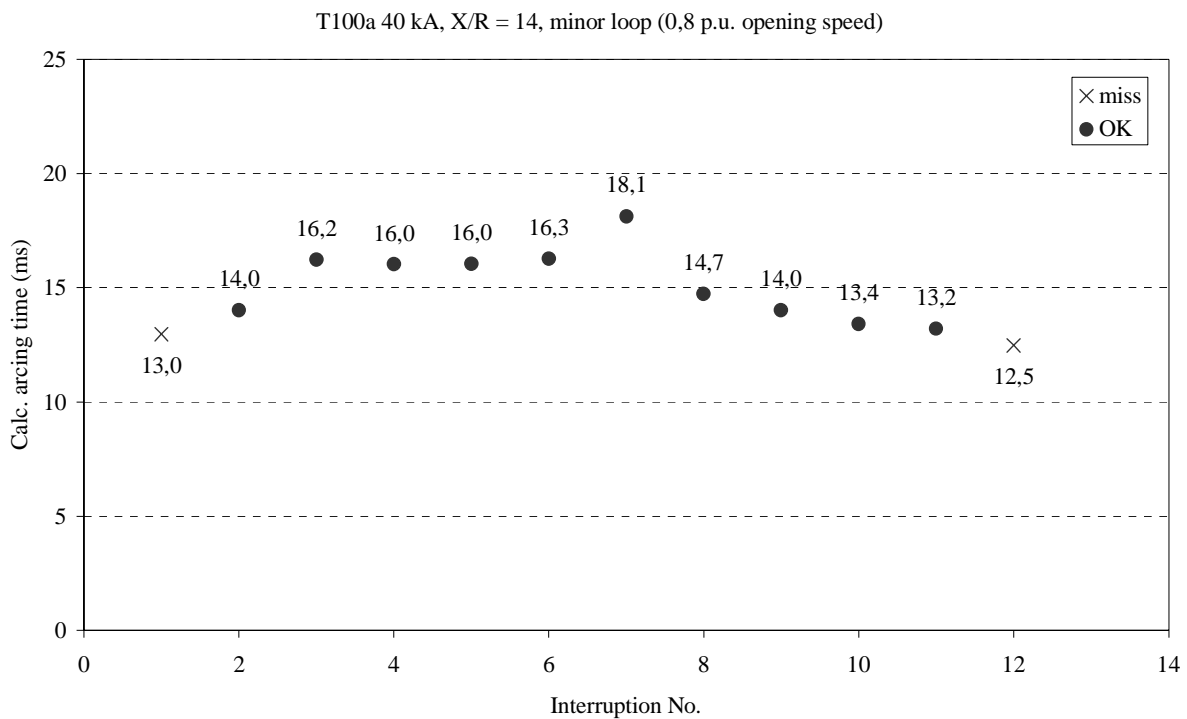


**Figure 3.17: T100a, 40 kA minor loop, 0.8 p.u. opening speed arcing time results**

### 3.5.3 T100a minor loop results

Figure 3.17 shows the results of the T100a, 40 kA minor loop current interruptions at 0.8 p.u. opening speed. These results also show a reasonably good level of stability at the minimum arcing time threshold at approximately 13 ms, even after twelve interruptions. The circuit breaker was also shown to have a consistent capability at 16 ms level and also continued to manage interruption at 18 ms at the seventh interruption.

### 3.5.4 T100a major loop results

Figure 3.18 shows the results of the T100a, 40 kA major loop current interruptions at 0.8 p.u. opening speed. In comparison to the minor loop interruptions the minimum arcing time threshold showed a gradual increase from 12 to 14 ms over the first ten operations, though the circuit breaker was still able to interrupt with over 16 ms arcing time at the 12th interruption. From both the T100a minor and major loop results, a nominal CFI target arcing time of 15 ms would seem to be reasonable, even for ten or more interruptions at 40 kA.

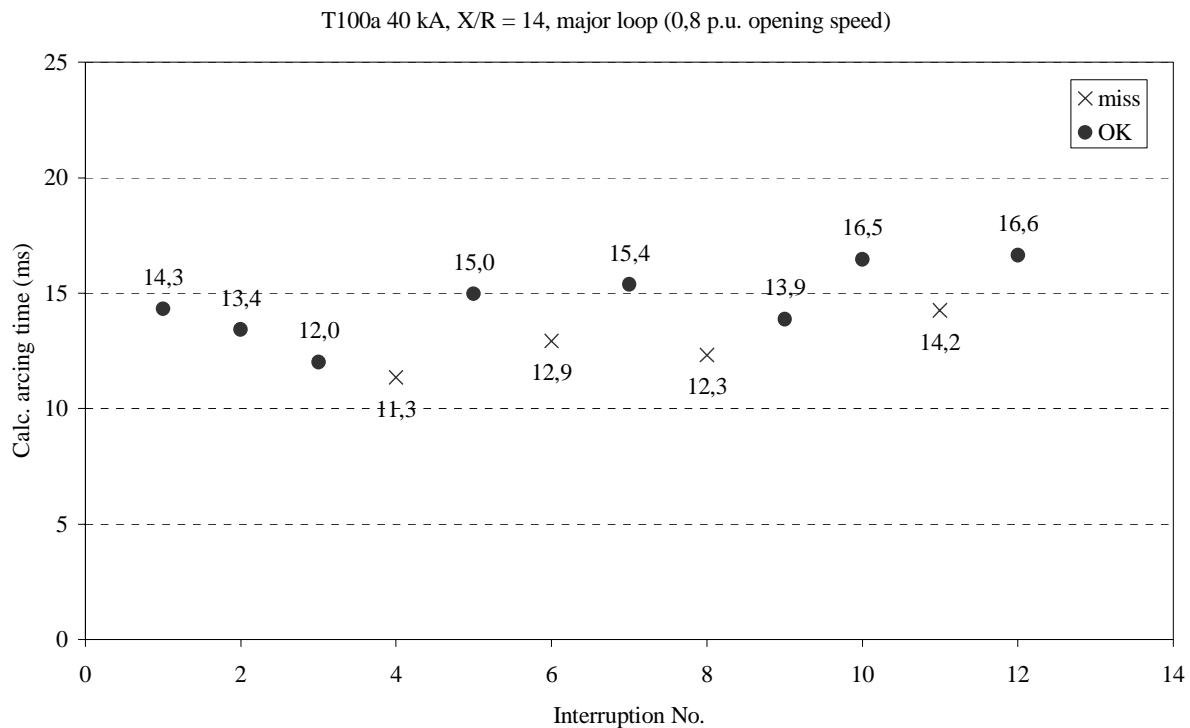


**Figure 3.18: T100a, 40 kA major loop, 0.8 p.u. opening speed arcing time results**

### 3.5.5 L90 results

Figures 3.19 and 3.20 show the results of the L90, 36 kA short-line fault interruptions made at 0.8 p.u. and 0.9 p.u. opening speeds, respectively. It is clearly evident that the short-line fault presented significant difficulties to the interrupter at the 20% lower opening speed. Short-line fault interruption is a particularly onerous thermal interruption duty on a circuit breaker due to the high initial transient recovery voltage waveshape, which represents travelling wave reflections between the fault location and the open circuit breaker contacts.

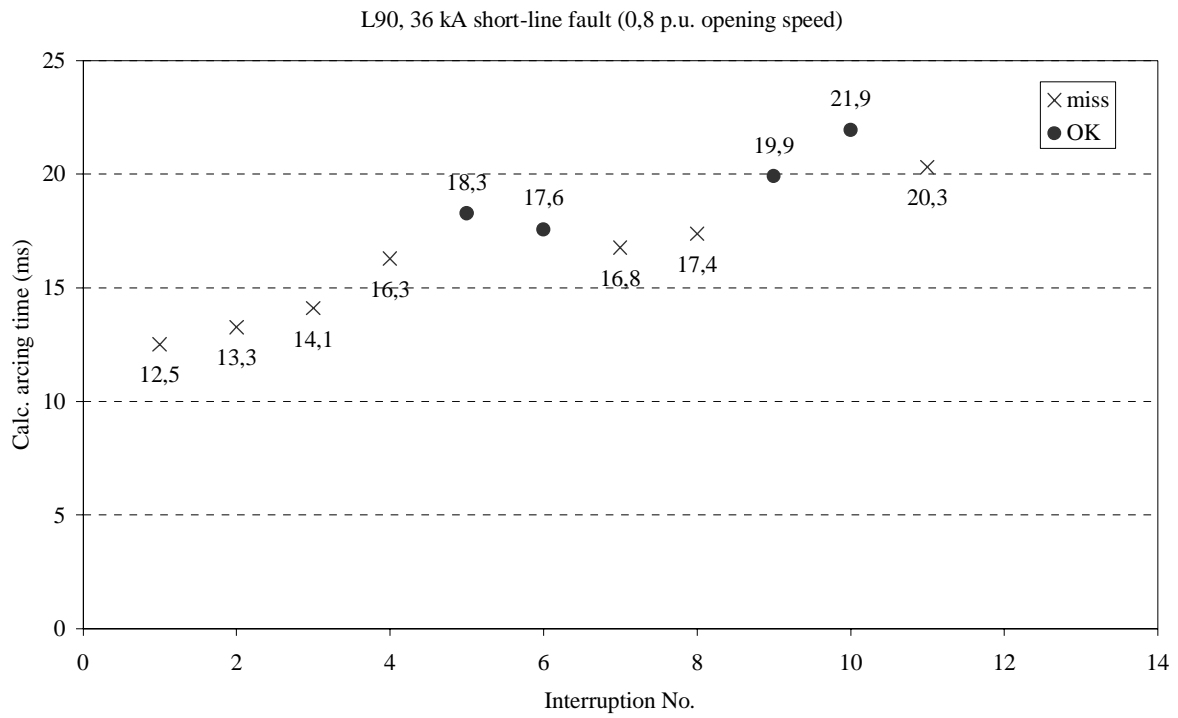


**Figure 3.19: L90, 36 kA short-line fault 0.8 p.u. opening speed results**

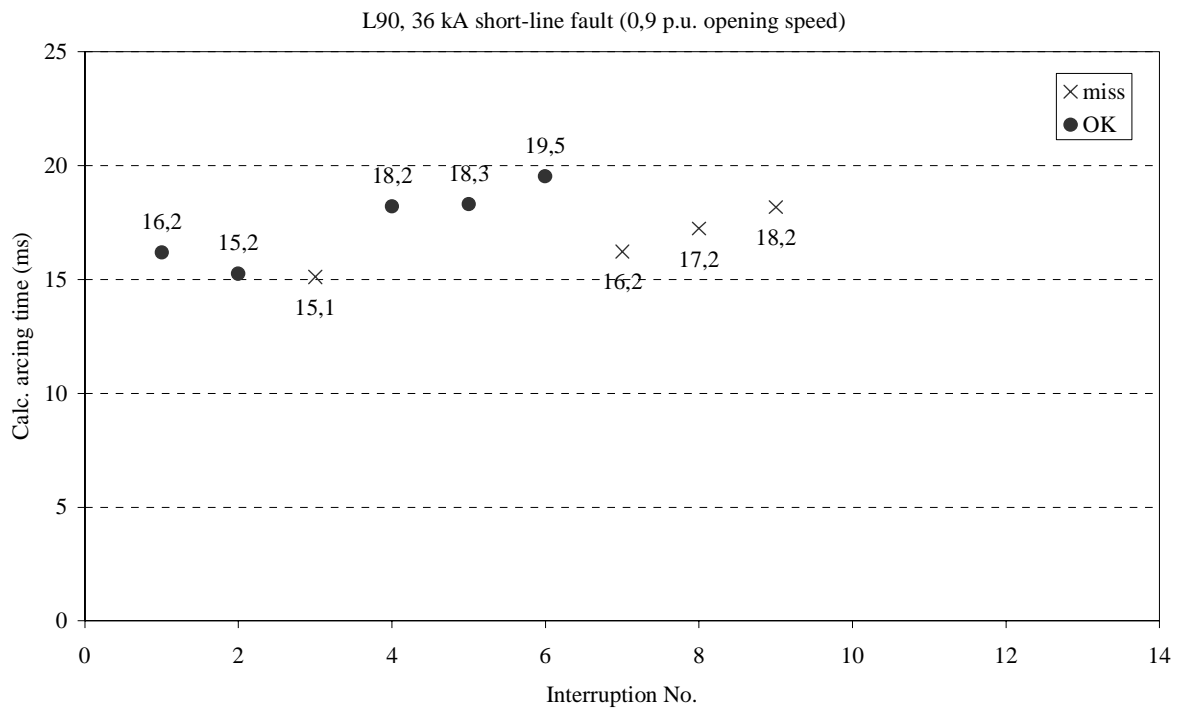


**Figure 3.20: L90, 36 kA 0.9 p.u. opening speed results**

As mentioned earlier, the lower speed was expected to affect the rate of pressure build-up in the compression volume,  $V_C$ , of the interrupter, which in turn feeds  $SF_6$  to the fixed volume,  $V_F$ , until the pressure in  $V_F$  seals the intermediate flap valve. The lower speed therefore leads to an expected increase in the minimum arcing time of the circuit breaker. The impact of opening speed on the minimum arcing time behavior was verified by the repeat of the L90 interruption tests on a new contact set adjust to 0.9 p.u. opening speed. Though the arcing times at 0.9 p.u. speed were also long and not as stable as for the other fault current duties, the lowest successful arcing times were at least 2 ms shorter than for the tests at 0.8 p.u. opening speed.

Nevertheless, the shortest successful L90 arcing time at 0.8 p.u. at approximately 18ms is still at the upper limit of the verified longer arcing times for T100a and T60. While it is possible to see a general trend towards longer minimum arcing times with increasing current magnitude from T30 to T100a, the L90 results fall well outside any simple linear trend. As the short-line fault condition is characterized by the high ITRV travelling wave reflections, it is impractical to reliably identify and discriminate between a near normal terminal fault condition and the short-line fault conditions, until the circuit breaker attempts to interrupt. Hence for the purposes of utilizing CFI to optimize circuit breaker design, it is necessary that the short-line fault arcing times fall within the same range as terminal fault arcing times. These L90 results at the lower than normal opening speed are therefore important in demonstrating that the process of optimizing a circuit breaker through the use of CFI is not a trivial task.

### 3.5.6 Summary comparison of CFI reduced opening speed and normal opening speed minimum arcing times

It is useful to place the reduced opening speed arcing time results in context with respect to the minimum arcing times obtained in earlier type tests of the same interrupter type, operated at its nominal 1.0 p.u. opening speed. Figure 3.21 provides such a comparison (based on ABB proprietary type test reports).

Putting aside the L90 minimum arcing time results, for the other fault current test duties, the 0.8 p.u. average minimum arcing times obtained for T30, T60 and T100a all lie approximately 3 ms above the 1.0 p.u. minimum arcing times. These longer arcing times at the substantially lower opening speed are still below the nominal medium arcing time level for 1.0 p.u. speed and imply that the circuit breaker could be operated with the lower speed without compromising the electrical wear rate of the interrupter. This provides a promising indication that  $SF_6$  interrupters could be further optimized with respect to operating energy by the use of CFI targeting a restricted arcing window in the range of 3...4 ms wide, as opposed to the existing standard requirement to manage a 10 ms (or half cycle) arcing window.

It must however be stressed that adopting such an optimized design approach introduces the need for the circuit breaker to be completely dependent on the CFI algorithm to achieve interruption. As such, the potential savings in operating energy and mechanical stresses on the circuit breaker must be traded against the added control complexity of CFI. The exceptional L90 arcing time results at 0.8 and 0.9 p.u. opening speed also underscore that there would still be significant interrupter design work required to achieve consistent and predictable arcing time behavior at lower interrupter speeds or energies.

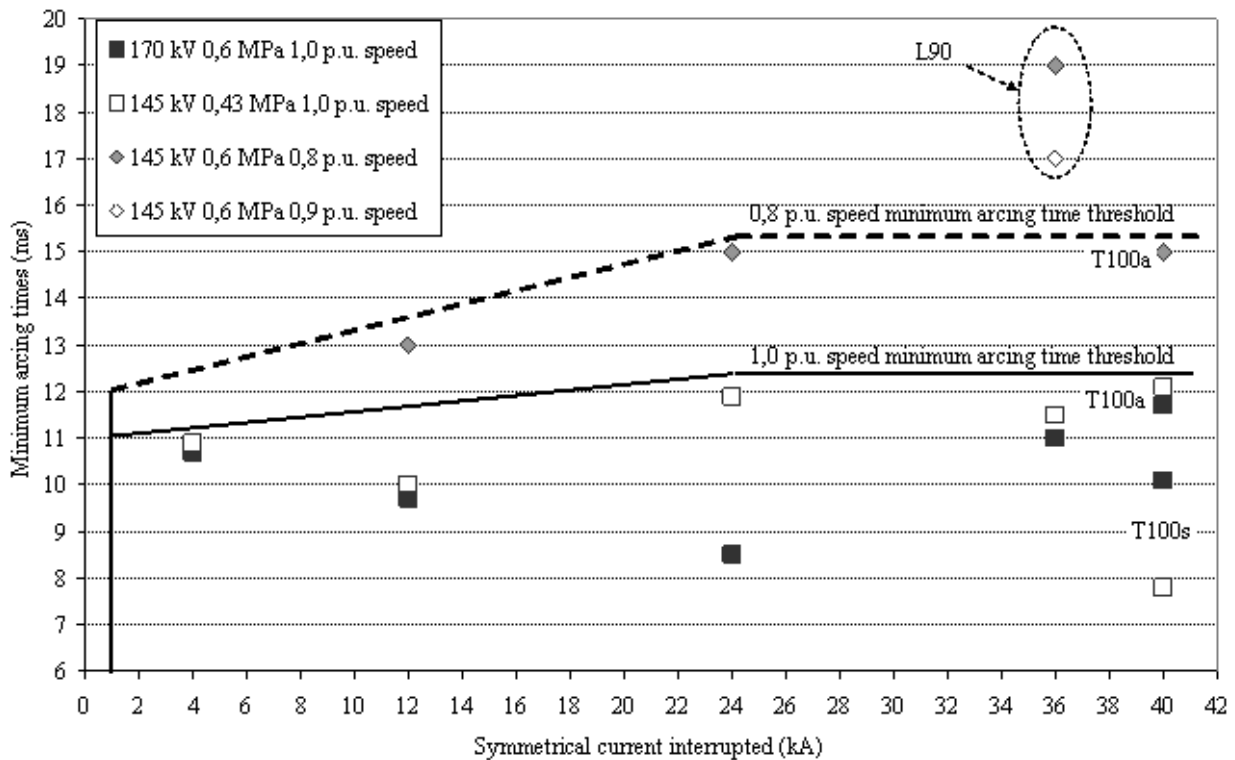


**Figure 3.21: Comparison of 1.0 p.u., 0.8 p.u and 0.9 p.u. opening speed minimum arcing times**

### 3.6 Implications for controlled fault interruption

The presented high power experiments, while limited in their scope, have provided some useful indications of circuit breaker behavior that can be used in support of the further development of CFI. In respect of the main goals of these experiments, it was possible to establish consistent reduced arcing time windows for T30, T60 and T100a test duties in the range of 13...16 ms, which would provide a viable basis for use of a nominal CFI target arcing time of 14...15 ms while still maintaining some margin for statistical variations in other CFI control times.

The above arcing time ranges were also achieved while operating the circuit breaker at 0.8 p.u. of its normal opening speed, with a resultant saving of over 20% in the opening operation energy. This result indicates an interesting potential for the exploitation of CFI to optimize SF<sub>6</sub> interrupter designs to obtain operational energy savings without necessarily compromising on the electrical endurance of the interrupter.

The difficulty in achieving energy optimization of an SF<sub>6</sub> circuit breaker by use of a restricted arcing window is not a trivial task, as evidenced by the substantial increase in minimum arcing times for L90 short-line fault interruptions. Nevertheless the stability of the arcing window limits for the other tested fault duties provides sufficient evidence that use of a CFI target arcing time in the range of 1...2 ms above the type tested minimum arcing time for a specific current level is potentially viable and can be used as a basis for further testing of CFI algorithms.

## 4 Three phase controlled fault interruption - General theory

Application of CFI to three phase networks requires the solution of several problems, including management of 1-, 2- and 3-phase fault behavior for effectively and non-effectively earthed networks. This chapter describes overall strategies that can be employed for CFI on a three phase network, with particular focus on the interaction and synergies with protective relay systems. The following chapter will describe more specific details of the three phase CFI method proposed by this thesis.

### 4.1 General requirements and constraints on CFI

Before reviewing methods that can be applied for CFI on three phase networks it is worth reviewing the main requirements and constraints placed on such a technique. This will provide a context for the later review of possible methods to address particular issues relevant to the CFI process. The following is a revised summary of similar issues presented and assessed in Chapter 5 in the licentiate thesis [1]. In the licentiate it was proposed that various CFI strategies could be classified according to their main goals and requirements, as summarized in Table 4.1.

**Table 4.1: Classification of CFI strategy types according to requirements**

CFI "Type":	1	2	3	4
Arcing time	NON-CRITICAL		CRITICAL	
Optimization	Clearing Time	Arc Energy	Clearing Time	Arc Energy
Accuracy	Moderate e.g. $\pm 1\text{ms}^*$	Moderate	High e.g. $\pm 0.1\text{ms}^*$	High
Security	Moderate e.g. $>95\%^*$	Moderate	High e.g. $>99.9\%^*$	High
Signal Noise Tolerance	Low e.g. $\leq 5\%   \text{WGN}^*$	Low	High e.g. $\leq 20\%   \text{WGN}^*$	High
Response Time	Fast e.g. $\frac{1}{4}\text{-}\frac{1}{2}\text{ cycle}^*$	Moderate e.g. $\frac{1}{2}\text{-}1\text{ cycle}$	Fast	Moderate

\* Note: Examples for "tolerances" shown above are indicative suggestions only.

Non-critical arcing time performance (strategy types 1 and 2) implies that the circuit breaker can interrupt over a normal "full" half cycle arcing window, in accordance with existing international standard requirements. Critical arcing time performance (strategy types 3 and 4) implies that the circuit breaker is designed to interrupt only with a restricted narrow arcing window that therefore is critically dependent on correct CFI function in order to achieve an arcing time within the circuit breaker's capability. As has been seen from the results of the experiments in Chapter 3, optimizing a circuit breaker by use of CFI is not trivial and given the extent of further development work required both on the circuit breaker design and CFI methods it can be expected that any initial use of CFI would be restricted to non-critical arcing time applications,

though the potential for use with non-arc based (e.g. power electronic) interrupters also exists [54].

The primary goal of CFI is interruption of the currents flowing through a circuit breaker with a pre-selected arcing time and without undue prolongation of the total interruption or clearing time. Figure 4.1 shows CFI interruption of a single phase, asymmetrical fault current, highlighting certain critical aspects of the overall process. Important aspects of this figure are the fault inception angle,  $\alpha$ , the fault current phase angle,  $\phi$ , and time constant,  $\tau$ , the protection response time,  $t_{\text{PROT}}$ , and the fault clearing time. The fault clearing time and  $t_{\text{PROT}}$  place specific constraints and demands on a CFI algorithm with respect to its speed of response. The fault inception angle estimation requires an accurate estimation of the fault inception time. The estimations of the fault current phase angle and time constant are critical to the eventual accurate estimation of the target current zero times.

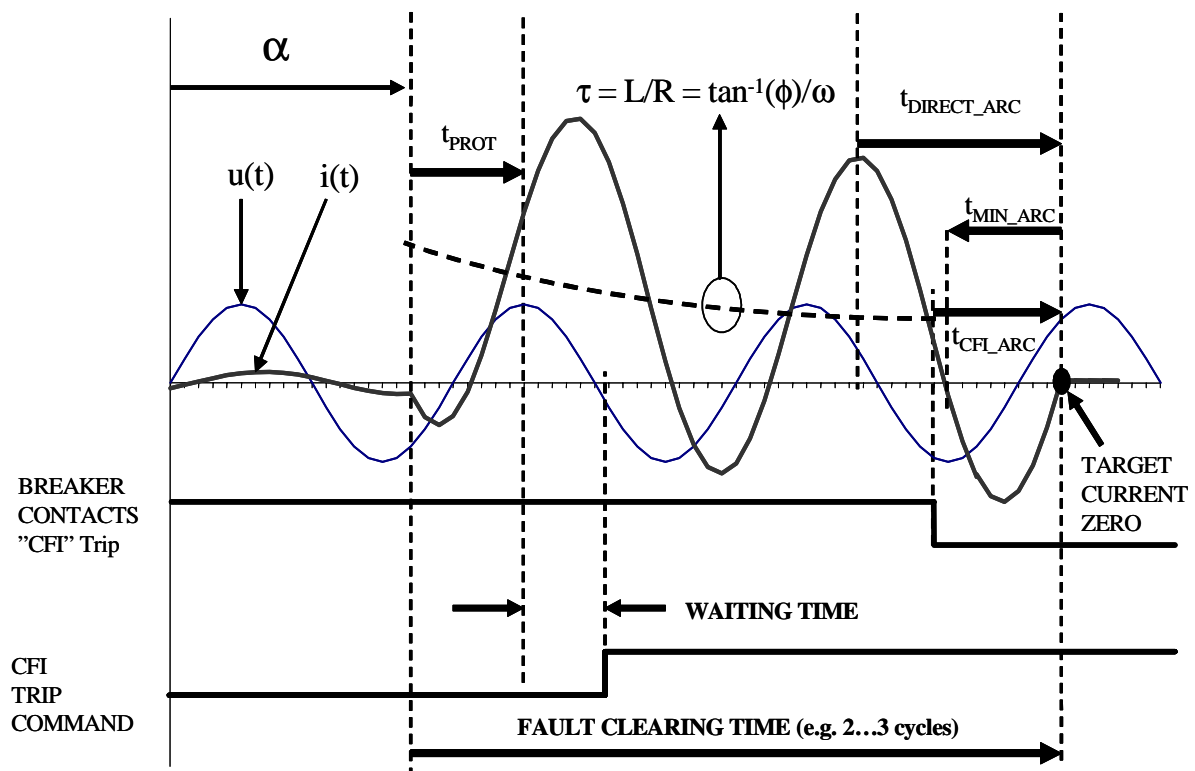


**Figure 4.1: CFI on a single phase asymmetrical fault current**

For CFI to be of most benefit the target arcing time,  $t_{\text{CFI\_ARC}}$ , should be as close to the minimum arcing time,  $t_{\text{MIN\_ARC}}$ , as possible, for a given current magnitude taking into consideration the possibility of the minimum arcing time limit changing with current magnitude, as indicated by the high power experiments described in Chapter 3. Nevertheless some margin should be added to the minimum arcing time to accommodate statistical variation in circuit breaker opening time and errors in the estimation of the target time (e.g. target current zero).



## 4.2 CFI current zero targeting strategies

As described in the scope of work in the introduction, this work has focusses on developing the CFI method for management of the eleven basic multi-phase and earth short-circuit combinations that can arise in a three phase network. Chapter 2 described these fault cases in further detail with particular focus on the current zero and interruption behavior. Table 4.2 presents a summary of the main types of multi-phase fault current interruption behaviors that were assessed in Chapter 2.

For single or double phase-to-earth faults in effectively earthed network conditions (Fault type 1 in Table 4.2), the single phase CFI method can be more or less applied directly per phase without major modification. Assuming single phase control of each phase of the circuit-breaker, each phase can be managed independently of the others.

In the case of phase-to-phase faults (Fault type 2 in Table 4.2), not involving and earth connection, the CFI method needs to be enhanced to cater for a different fault current model, that in principle is the same as for a single phase fault, but referenced to the phase-to-phase voltage of the faulted phases.

Three phase faults with (Fault type 3A) and without (Fault type 3B) earth connection present the additional problem of selecting appropriate target current zero times for the last two phases to interrupt. The behavior of three phase faults involving and not involving earth is, to all practical purposes, identical up until the current is interrupted in one phase. Only after the first phase interrupts, does a distinctive difference arise between the currents of the last two phases to interrupt for three phase earthed and unearthed faults. A CFI scheme must be capable of effectively managing both cases.

In the above context, the phase fault current interruption behavior can considered in two (2) stages:

Stage 1: conduction in each of all three phases prior to first-pole-to-clear

Stage 2: conduction in the last two phases to clear, after the first pole interrupts

The behaviors in each of the above stages is influenced by both the type of fault and the source-to-fault zero sequence impedance (alt. “system neutral earthing”). All faults involving earth connection can effectively be described by single phase equivalent circuits in each phase during both stages 1 and 2 above. Two phase faults without earth connection need to be described in terms of an equivalent “common” single phase circuit, driven by the faulted phases’ line voltage. Three phase faults not involving earth require separate modelling for stage 1 and stage 2 of the interruption process.

As mentioned above, in the event of faults occurring in a completely non-earthed neutral network, the last phases to interrupt will see their currents shift into phase opposition after the first pole interrupts. This is since there is no zero sequence path (or alternatively the zero sequence impedance is “infinite”) and in order to maintain  $I_0 = 0$ , the sum the remaining currents must therefore also be zero.

Table 4.2: Summary of multi-phase fault current interruption behaviors

Fault type	Equivalent circuit	Current interruption behaviors
1		
2		
3A		
3B		

A key problem for a controlled fault interruption scheme is selecting the appropriate current behavior model for interruption stages 1 and 2 above. Even if the network earthing configuration can be assumed to be a known input to the CFI process, the possibility of two and three phase unearthed faults still needs to be considered (even if the occurrence of such faults in HV networks is exceptionally rare).

It is comparatively simple to develop a CFI system to provide target estimation for the possible combinations of fault behavior during stage 1 of the interruption process. It is more difficult to develop a robust CFI system to manage possible stage 2 behaviors, as there are cases where stage 1 behavior is the same (e.g. phase-to-earth faults), but stage 2 behavior can be different (e.g. three phase unearthed faults).

Stage 1 behavior can be determined directly by the CFI algorithm, prior to it sending the trip command to the breaker. Exact stage 2 behavior may only be apparent after the first pole interrupts, by which time it is normally too late for the CFI system to react, particularly in the case where three phase trip commands are issued and total fault clearing times are to be kept as short as possible for system transient stability reasons.

One method to manage indeterminate stage 2 interruption behavior is to apply a compromise targeting solution, as illustrated in Figure 4.2, whereby the two possible behaviors of the last phases to clear are estimated and the earliest estimated current zero in each phase (e.g. ZC2 and ZC3) are then used as the targets for each phase. This will result in one of the phases interrupting at its target, while the remaining phase will see a slightly longer than targeted arcing time, but normally only with a prolongation in the order of 1-2 ms which should still be within the restricted arcing window capability of a CFI circuit breaker.

Table 4.3 provides an overview of CFI targeting solutions that can be applied to a range of current interruption behaviors, based on the relationship of the current zero crossing timing relations and for different source and load side neutral earthing arrangements.

The work in this thesis has concentrated on development of a CFI solutions for the effectively earthed source and load neutral cases (EE\_0 to EE\_5 in Table 4.3). The current interruption relations listed in Table 4.3 refer to the order of interruption with respect to the timing of the current zero crossings. For example in cases EE\_0 to EE\_2, the currents will interrupt at successive current zeros, effectively independent of each other, and as such can be managed by a “direct” CFI targeting solution aiming at the estimated current zero times in each phase. For case EE\_4 for a phase-to-phase fault, an appropriate phase-to-phase modelling should be applied for estimation of the common interruption current zero time, which can then also be “direct” targeted.

Cases EE\_3 and EE\_4 for three phase earthed and unearthed faults, can apply the “compromise” current zero targeting for the last two phases to interrupt, as described in Figure 4.2, where it is not otherwise possible to reliably discriminate between these cases before the protection system has determined a trip is required. The first phase to interrupt can be directly estimated in both these cases and then the two possible interruption scenarios for the last phases to interrupt can be calculated and the earliest current zero times selected as targets for each of these two phases.

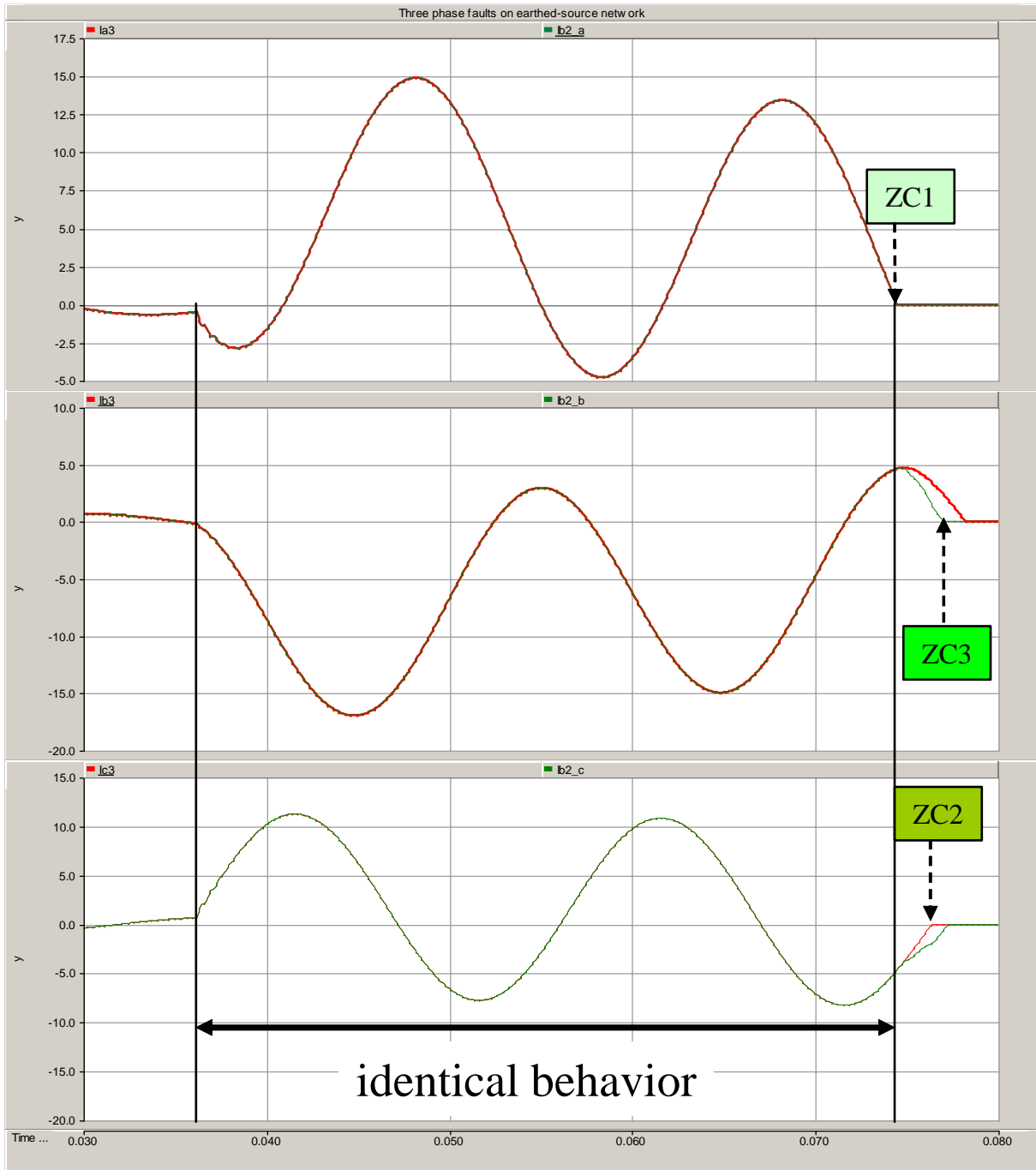


**Figure 4.2: Comparison of interrupted currents for three phase faults, with and without earth connection**

**Table 4.3: Summary of current interruption behaviors with respect to fault type, system earthing and possible CFI targeting solutions**

Case	L1	L2	L3	Fault N	Source N	Load N	Phase shift in 2-3	current interruption relations			CFI solution
								zc1	zc2	zc3	
EE_0	load	load	load	open	earthed	earthed	No	1	2	3	direct
EE_1	fault	load	load	earth	earthed	earthed	No	1	2	3	direct
EE_2	fault	fault	load	earth	earthed	earthed	No	1	2	3	direct
EE_3	fault	fault	fault	earth	earthed	earthed	No	1	2	3	last cz compromise
EE_4	fault	fault	load	open	earthed	earthed	No	1/2	1/2	2/1	direct
EE_5	fault	fault	fault	open	earthed	earthed	Yes	1	2	2	last cz compromise
EO_0	load	load	load	open	earthed	open	Yes	1	2	2	direct
EO_1	fault	load	load	earth	earthed	open	No	1	2	3	direct
EO_2	fault	fault	load	earth	earthed	open	No	1	2	3	direct
EO_3	fault	fault	fault	earth	earthed	open	No	1	2	3	last cz compromise
EO_4	fault	fault	load	open	earthed	open	No	1/2	1/2	2/1	direct
EO_5	fault	fault	fault	open	earthed	open	Yes	1	2	2	last cz compromise
OO_0	load	load	load	open	open	open	Yes	1	2	2	direct
OO_1	fault	load	load	earth	open	open	Yes	1	2	2	direct
OO_2	fault	fault	load	earth	open	open	Yes	1	2	2	direct
OO_3	fault	fault	fault	earth	open	open	Yes	1	2	2	direct
OO_4	fault	fault	load	open	open	open	Yes	1	2	2	direct
OO_5	fault	fault	fault	open	open	open	Yes	1	2	2	direct
OE_0	load	load	load	open	open	earthed	Yes	1	2	2	direct
OE_1	fault	load	load	earth	open	earthed	Yes	1	2	2	direct
OE_2	fault	fault	load	earth	open	earthed	Yes	1	2	2	direct
OE_3	fault	fault	fault	earth	open	earthed	Yes	1	2	2	direct
OE_4	fault	fault	load	open	open	earthed	Yes	1	2	2	direct
OE_5	fault	fault	fault	open	open	earthed	Yes	1	2	2	direct

### 4.3 Prior art and research relevant to CFI

It is not absolutely necessary to implement CFI by seeking to directly estimate and target the interruption current zero times themselves. While achieving an accurate and reliable targeting of fault current zero times is a difficult task, it does provide the most optimum solution if combined with stable and known arcing time behavior.

As described in the licentiate, Pörtl and Fröhlich [2], proposed an alternative targeting strategy using so-called “safepoints”. These safepoints were periodic reference time instants on the current waveform, calculated from the estimation of the fault current phase angle and had the common property of occurring prior to a current zero, hence the safepoints had an inherent safety timing margin built-in, at the expense of being a less optimal overall targeting method. The difference in time between the safepoint and the successive current zero times would vary with the level of DC exponentially decaying offset in the fault current (i.e. “symmetrical” safepoints would eventually converge to the actual current zero times once the DC component had completely decayed).

Pörtl and Fröhlich’s Safepoint method [2] remains the most recent comparable CFI method found in academic literature. There are however a number of patents published that describe methods for either current behavior prediction, with and without the direct objective of some form of controlled fault interruption. While patents tend not to present a detailed analysis of the

performance of their methods and inherently generalized in their descriptions, it is relevant to summarize them here, partly to present alternative CFI approaches and partly to illustrate the interest in CFI development.

Larsson et al [54] describe a method to estimate both the DC component and future current zero-crossing times in order to provide commutation control to a hybrid diode-isolator designed interrupter. The DC component is estimated by taking the difference of selected points on the current wave, e.g. current peak values. Current zero times are predicted using the estimated DC component level.

Niemira et al [55] describe a method for current zero prediction with one objective being to synchronize a circuit breaker to attempt interruption close to the estimated current zero time and thus with a comparatively low level of arcing current. It is not however clear that how the associated circuit breaker would manage the high rates of rise of recovery voltage that would occur interrupting typically inductive fault currents.

Sinha et al [56] describe a method, based in part on applying Fast Fourier Transform, to predict fault current zero-crossing times, including a using residual errors measured between actual and predicted current zero times as “correction factors” to update later current zero time predictions. The method is in part claimed to be directed towards use on contactors and circuit breakers that may in some instance risk seeing fault currents larger than their assigned ratings.

#### 4.4 General CFI and protection system process interactions

As stated in the introduction and the licentiate, *CFI is not proposed as a replacement of existing protection control systems*, but rather as a supplement to achieve a more optimized interruption process from the perspective of the circuit breaker. As described previously in Figure 1.2 it is proposed that a CFI scheme would operate in parallel with the associated protection scheme. Figure 4.3 shows a more expanded process flowchart of the parallel operation of protection and CFI processes, divided into four main stages or sub-processes. Each of these stages will be briefly described here. Later sections of this chapter will then provide functional and method comparisons for the execution of these steps for both protection and CFI systems to identify potential synergies between the two processes.

Stage 1 refers to the management of current and voltage data sampling, that are the main inputs to both the protection and CFI processes. Both processes could utilize the same interface hardware (e.g. filters, analogue-to-digital converters) for the collection of this data.

Stage 2 covers the main data processing carried out by each process. In the case of protection systems, the critical goal is to establish whether or not a protective trip operation is required. This may also involve some form of multi-phase fault type identification to discriminate faulted and healthy phases, particularly where single phase tripping is implemented. For the CFI process, the data processing is focussed on obtaining viable target instants to which the trip commands can be synchronized. As seen from the previous sections in this chapter, the CFI process also requires some form of fault type identification to assist in the target identification process. Section 4.5 provides a further analysis of published techniques for these functions, proposed for use in modern digital relays, that could be adapted to CFI algorithms.

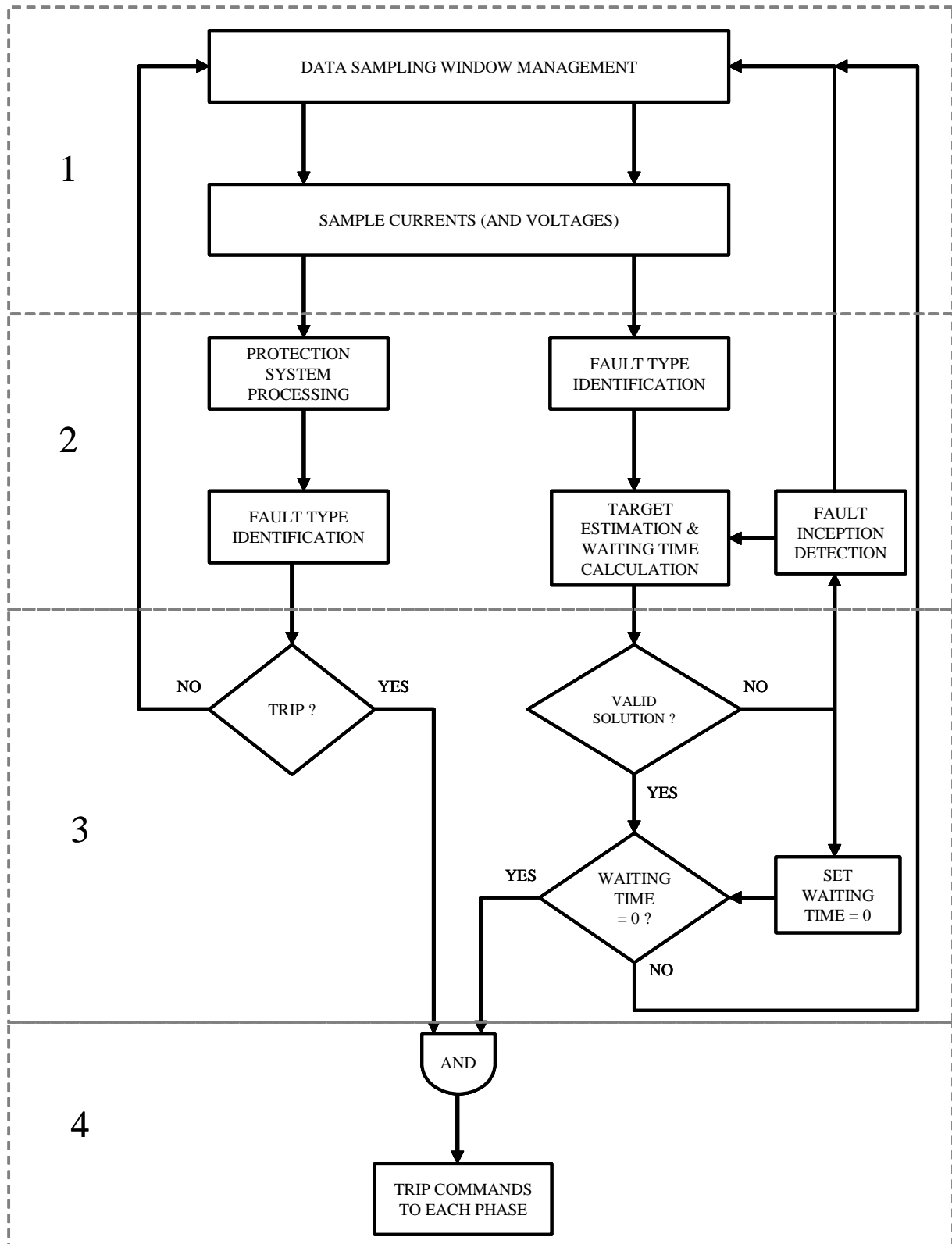


Figure 4.3: Generic flowchart of combined protection and CFI processes

Stage 3 refers to decision validation checks for each process. Specific criteria for issuing a trip command will exist depending on the type of protection system, its location and zones of coverage with respect to the power system.

For the CFI process the decision to issue a trip command is based on two criteria. First is whether a sufficiently confident targeting solution has been obtained and second, whether the resultant waiting time has reached zero. In the event of an insufficient confidence in the targeting solution, the process in Figure 4.3 implements a forced CFI bypass strategy whereby the waiting time is forced to zero. Also included in this stage for the CFI process is the possibility to use the solution validation test as a means of fault inception detection, since when a fault occurs, there will be a deviation from the previously expected normal load current behavior. Fault inception detection is critical to CFI in order to provide both an estimate of the fault inception phase angle,  $\alpha$ , as well as adjustment of the data sampling window to discard pre-fault data.

Stage 4 is where the protection and CFI processes are united with respect to issuing of synchronized final trip commands to the associated circuit breaker. Only when both the protection system has determined that a trip is required *and* the CFI waiting time has reached zero for each phase, is the trip command to each phase of the circuit breaker issued.

## 4.5 CFI and protection system synergies and differences

Having described a general integrated structure for the parallel protection and CFI processes, it is worth assessing in further detail the potential synergies and important differences between these processes.

The synergies between protection schemes and CFI provide indications of the methods that can be adopted by a CFI scheme based on the already extensive research and experience gained from digital protection relay solutions. In addition, this provides guidance on the viability boundaries of application of CFI based on the limitations faced in the application of protection relay techniques.

Though the potential synergies are a valuable resource for CFI development, it is also essential to take account of the important differences in requirements and functionality between digital protection scheme and CFI schemes.

These aspects are assessed in the following sections. The first section, 4.5.1, compares protection and CFI functional requirements and methods with a focus on “algorithm and modelling” aspects affecting both processes. The second section, 4.5.2, will provide a comparison focussed on “hardware” or “auxiliary” system aspects such as measurement device usage and auxiliary component performance. Section 4.6 will present an overall comparison of distance relay protection methods, the “Safepoint” CFI method and the proposed CFI method.



**Table 4.4: Functional performance and method comparisons between protection and CFI processes - models and algorithms**

Characteristic / Feature		Functional performance relevance		Available methods
		Protection systems (e.g. distance protection)	Controlled fault interruption	
1	Fault inception detection	Data sampling window management	Data sampling window management	Comparisons of expected and actual current behavior
			$\alpha$ -value estimation	Moving and adaptive data sampling windows
2	Multi-phase fault type identification	Selective single phase tripping (where applied)	Identification of expected current behavior for correct targeting	Phase specific data processing, possibly with hypothesis testing
				Symmetrical components
				Artificial neural networks
3	Fault current magnitude estimation	Common fault decision criterion	Desirable but not essential. Useful for possible target arcing time selection. Useful for tracking accumulated interrupter wear.	Direct sampling measurement
				Numerical methods e.g. -Least mean squares -Kalman filtering -Discrete Fourier Transform
4	Fault current phase angle estimation	Distance protection fault decision criterion	Critical for estimating expected current zero behavior	Numerical methods e.g. -Least mean squares -Kalman filtering -Discrete Fourier Transform
			Useful for discriminating capacitive and inductive currents for target arcing time selection	
5	Fault criteria validation	Correct selectivity control critical for both operational dependability and security. Should only trip faulted zone, when relevant fault occurs.	Fault decision not relevant to CFI.  Alternatively can consider current modelling and target validation checks.	

**Table 4.4: Functional performance and method comparisons between protection and CFI processes - models and algorithms**

Characteristic / Feature		Functional performance relevance		Available methods
		Protection systems (e.g. distance protection)	Controlled fault interruption	
6	Back-up systems	Provide dependability	Provide dependability	Local “X” and “Y” schemes
				Complementary methods on same operation zone
				Remote back-up by overlapping zones
				Remote back-up by diverted trip signals
7	Primary harmonic distortion	Potential source of mal-operation (e.g. magnetizing inrush currents)	Potential source of mal-operation due to signal distortion	Filtering (analog and digital) Duo-bias CT connections
			Normally insignificant effect on fault currents with respect to interruption capability	Controlled closing to mitigate inrush currents
			Sub-synchronous resonances create difficult targeting problem	Specialized solutions for cases where harmonic distortion is “large” (e.g. > 5-10%)
8	Current zero times	Not normally of direct importance to protection relay operation	Critical for correct circuit breaker and CFI performance	Modelling of estimated current behavior to predict current zero times
9	Fault clearing time	Important for system transient stability	Constraint on total CFI process operation time	Critical fault clearing times normally established by system studies

#### 4.5.1 Synergies and differences in modelling and algorithms

Table 4.4 provides a summary comparison of a range of important characteristics or features pertaining to both protection systems and CFI, together with indications of methods that have been applied or are available to manage the listed tasks. The items listed in Table 4.4 have been selected on their relevance to HV power system level impact, though there are of course overlaps into the secondary data processing level.

The characterization of the fault current behavior and its importance to CFI has already been extensively described in previous sections. Various methods could be applied to obtain estimates of key fault current parameters such as the fault inception angle,  $\alpha$ , and the phase angle,  $\phi$ . As stated earlier, it is not within the scope of this present thesis to provide a detailed

quantitative comparative analysis of published digital protection algorithms, however a brief summary of some of the schemes commonly references in protection system texts [27], [21] is presented here, only to provide some indication of the range of possible techniques that have been proposed for the critical functions of fault inception detection, fault type classification, phase angle estimation and parameter estimate validation.

#### 4.5.1.1 Fault inception detection methods

Digital protection schemes that involve sampling of voltage and current inherently apply some form of data sampling window that is time-shifted and in some cases adjusted in length, depending on the algorithm's ability or dependence on estimating the fault inception instant [21], [27]. The importance of accurate fault inception detection for a model-based CFI scheme, as will be described in Chapter 5, is that in addition to providing data sampling window control, it also provides estimation of the value of the fault inception phase angle term,  $\alpha$ .

Distance protection schemes that required more accurate estimation of the apparent source-to-fault impedance for fault identification and discrimination would benefit from a fault inception detection function to discard pre-fault data and thus provide the impedance estimation function with less corrupted input data. e.g. Fourier and Kalman filter-based algorithms require some form of fault inception instant estimation to minimize their parameter estimation errors [65].

Mann and Morrison [71] proposed a scheme by comparing sampled data points that were one cycle apart and estimating fault inception based on any detected large deviation in the comparison result. Gilchrest et al. [69] proposed a method more closely based on accumulated sample-by-sample deviation detection, which has been applied even in more recent methods also [67]. Gilbert and Morrison [65] propose the use of combination of a median filter, often used in image processing, and a mean filter, as an alternative to sample-by-sample or cycle-by-cycle deviation detectors.

Chowdury et al. [66] proposed fault inception detection by means of hypothesis testing in conjunction with the use of Kalman filtering. Isaksson [29] describes use of the so-called "Hinkley detector", based on looking for a change in the (assumed) mean value of the sampled data beyond a set threshold.

No specific method of fault inception detection was described in the Safepoint method by Pörtl et al. [2], [18]. In the single phase CFI method described in the Licentiate [1], use of the change behavior in the analysis-of-variance tests applied to the modelled current was used as a fault inception detector and a similar use of this approach will be described further in the proposed three phase CFI method in Chapter 5. This use of the analysis-of-variance trend behavior as a fault detector can be considered as a variation on sample-by-sample testing combined with hypothesis testing.

#### 4.5.1.2 Fault type identification methods

Various methods have also been proposed for multi-phase fault type identification (also sometimes referred to as "phase selection" in protection literature). Phadke and Thorpe [27] describe methods following from phase specific fault inception detection e.g. voltage deviation detection in faulted phases, the use of Clarke components transformation and the use of symmetrical components. Girgis and Brown [61] proposed a method of fault type identification

by using Kalman filters to compare the noise variance and co-variance between faulted and unfaulted phases.

Pörtl et al. [18] presented a method using artificial neural networks (ANN) for use in conjunction with the Safepoint CFI method, which provided good results even in the presence of large random signal noise. No fault classification method was presented in the Licentiate work [1] as it only considered single phase CFI cases. In Chapter 5, a method of multi-phase fault type classification and identification is presented based on comparison of analysis-of-variance results for phase-to-earth and phase-to-phase frame-of-reference modelling of the fault currents.

#### 4.5.1.3 Phase angle estimation methods

While both the Safepoint [2] and current zero targeting [1] CFI methods have applied least mean squares (LMS) to obtain phase angle estimates, both methods then have separate methods of utilizing this information to make their synchronizing target estimates and as such are open to applying other phase angle estimation methods such as Kalman filtering or Discrete Fourier Transform (DFT). Distance protection schemes are the most obvious source of phase angle estimation methods that could also be applied to CFI.

Numerous numerical methods have been proposed for use in phase angle estimation for distance protection schemes since the advent of digital relaying in the late 1960's and early 1970's. Andersen [21] and Phadke and Thorpe [27] describe techniques including (discrete) Fourier transforms, Kalman filtering, Walsh transforms, least error (or mean) squares, symmetrical components and general curve fitting techniques. McLaren et al. [57] indicate that amongst the wide range of algorithms proposed for phasor estimation, the full-cycle Fourier filter and the cosine filter tended to be the most common applied in industry.

Altuve et al. [64] presented a comparison of Fourier, Walsh, cosine and sine-cosine filtering techniques and conclude that the latter provided the best overall responses in terms of variable frequency and DC offset effects.

Mann and Morrison proposed methods based on difference (or derivative) methods and also peak value estimation methods to estimate the apparent fault impedance magnitude and phase angle [70], [71]. They reported processing times down to a half-cycle, supporting the possibility for very fast digital protection solutions.

Girgis and co-workers published a number of papers [58], [59], [60] examining the use of Kalman filtering to distance protection. Main advantages proposed by Kalman filtering were its noise robustness and computation efficiency compared to methods such as least error squares regression and DFT. Drawbacks to the Kalman filter technique include its need for a prior estimate of the signal noise co-variance and filter gains, though in its recursive form it has shown ability for a fast convergence rate to update its estimators.

Sidhu et al. [68] present a least error squares (LES) technique combined with method to remove the DC component from sampled data from off-line generated data tables. The method is intended to work with a half-cycle data window for fast protection operation and offered as an alternative to a half-cycle LES method or DFT method combined with a mimic circuit to counter DC offset.

Sachdev and Baribeau [62] proposed use of a LES distance protection algorithm, incorporating a truncated (three term) Taylor series to cater for the exponentially decaying DC component of a fault current. Later Sachdev and Nagpul [63] proposed a modified approach using a recursive least error squares (RLES) approach, offering more computational efficiency. Isaksson also examined and comprehensively investigated the use of RLES [28], [29].

As will be shown in Chapter 5, the proposed three phase CFI method will apply the same (weighted) least mean squares method as was applied in the Licentiate [1], partly for reasons of continuity in the development of the CFI method. It is however to be recognized that alternative and potentially more computationally efficient methods such as RLES could be applied to the proposed CFI method.

#### 4.5.1.4 Parameter and decision validation methods

It is important for operational dependability and security that the protection system responds correctly, even with correct estimations of current magnitude and phase angle. This implies correct operation of the decision process within the protection system based on the programmed fault identification criteria. For CFI, validation of the target estimation and waiting time are more critical and as demonstrated in the licentiate can be managed by analysis of variance between the observed and modelled currents.

It is typical in protection systems to apply different levels of redundancy in order to increase dependability and security. Local back-up methods include the use of “X” and “Y” relay and tripping circuits and the use of complementary protection systems (e.g. overcurrent and distance protection or overcurrent and differential protection, in addition to using relays of different design or make [8]). It is therefore quite feasible to apply similar redundancy approaches to the application of CFI in order to maximize system dependability.

Harmonic distortion of primary currents can occur under both “normal” load conditions e.g. magnetizing inrush to a power transformer and under fault conditions e.g. series compensated line faults. Analogue and digital filtering techniques are one method to reduce the impact of such distortion on relay operations, where the distortion is moderate and the fundamental power frequency behavior is still of prime significance for both proper relay and circuit breaker operation. Load induced harmonic distortion can in some cases be mitigated by controlled closing, such as for power transformers. Cases such as faults on series compensated lines where complex effects like sub-synchronous resonance occur may require specialized solutions.

Actual current zero times are normally not of direct importance to protection relay function, though indirectly they are significant in the context of the total fault clearing time, which is a significant overall operational constraint for the maintenance of power system transient stability. The timing of current zeroes is of course far more critical to CFI schemes, irrespective of their targeting method, as it is these times that ultimately dictate when the circuit breaker should interrupt.

As seen from the above analysis, there are a number of synergies and important differences between the functions and requirements of protection schemes and CFI. It is possible to utilize information obtained from existing protection schemes as data sources to a CFI scheme, including fault inception detection, current magnitude and phase angle estimation. The CFI use of current modelling with validation checking potentially offers complementary methods for fault inception

detection and identification security for protection schemes. Both processes require well designed and understood signal measurement systems.

A potential crossover benefit from CFI to protection systems is the use of CFI current zero time predictions as a means to make more accurate estimation of when the circuit breaker should interrupt and thereby link back to circuit breaker failure detection monitoring. In the event that it is detected that the circuit breaker has failed to interrupt at the predicted current zero time, there is the possibility to activate a back-up trip signal to the next higher level of circuit breakers on the system. This offers the potential for overall reduction in the co-ordination time settings between overlapping protection schemes, that are otherwise based on coarse estimates of the overall expected fault clearing time based on circuit breaker opening and maximum arcing times.

Additional shared benefits could be obtained between the parallel use of CFI with digital protection schemes. The use of current modelling, combined with analysis of variance tests may provide complementary means of fault detection and fault state verification to improve protection system dependability and security.

#### **4.5.2 Synergies and differences at a hardware and auxiliary system level**

Figure 4.4 provides a sketch of the overall protection, auxiliary and circuit breaker components, with the inclusion of an embedded CFI control scheme. This provides an indication of the secondary system features that are shared by protection and CFI schemes, as summarized in Table 4.5.

Circuit breaker opening and arcing times are of course critical parameters in achieving reliable CFI. Modern HV AC circuit breakers generally have very good stability in operating times, or at least well defined behavior for variation in auxiliary power supply voltages and ambient temperature. The arcing time experiments described in Chapter 3 provided evidence of stability in arcing time behavior with a tolerable margin for viable CFI implementation.

Distortion of measurements of voltage and current that are the essential data inputs to the protection and CFI systems is a well known problem, common to all signal processing systems. Management of the measuring process, through careful selection and dimensioning of the primary current and voltage sensors and the interfacing of these devices to the digital signal processing hardware is essential to mitigating the effects of signal distortion on the respective protection and CFI functions. Sources of error in current and voltage transformer measurements are well documented and understood and can mostly be compensated by proper design, testing and calibration.

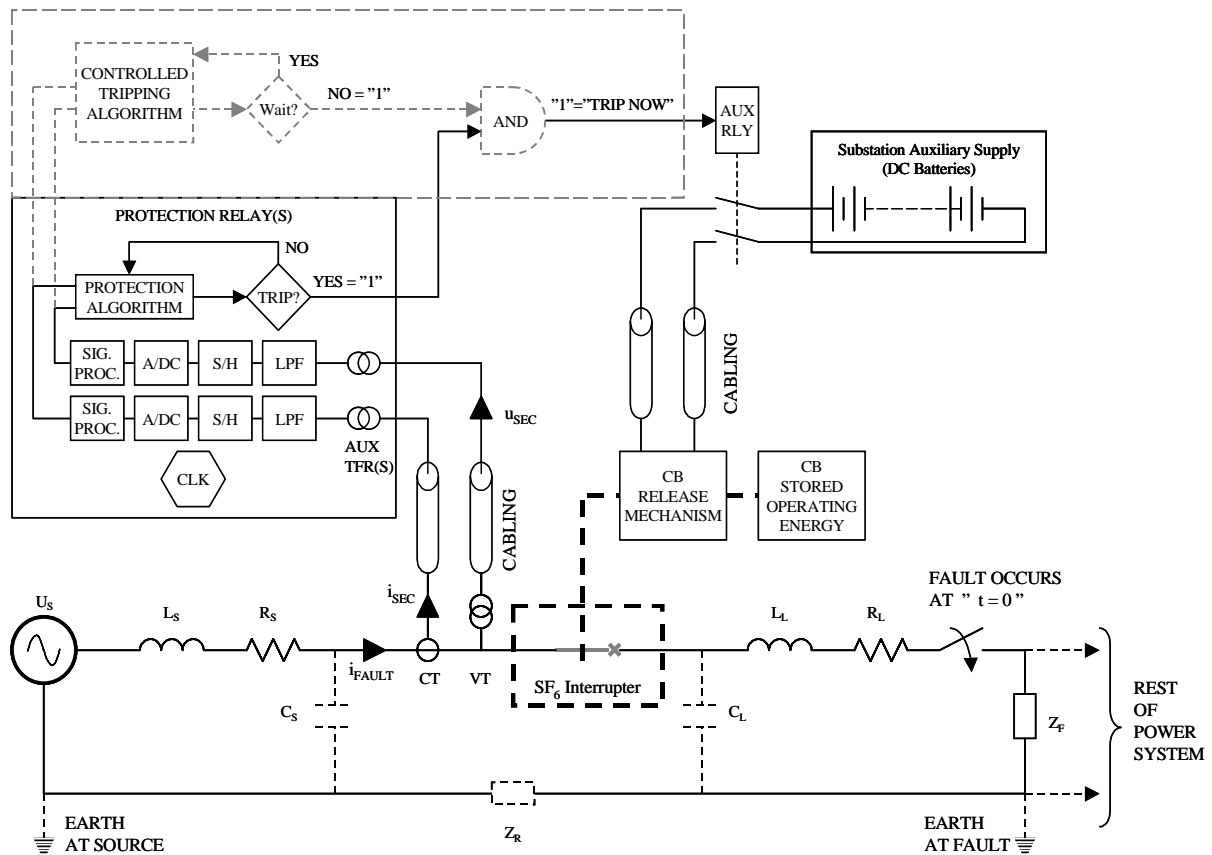


**Figure 4.4: CFI system embedded in conventional digital protection and circuit breaker control scheme**

Verification of the timing synchronization between primary and secondary signals has become more critical with the advent of wide area protection schemes (e.g. GPS-based phasor measurement systems) and the wider use of controlled load switching. It should be recognized that it is possible to make an accurate measurement of the phase angle between current and voltage at a local level and still have a timing error between the primary (HV) and secondary (LV) systems. The inherent signal processing delays of analog-to-digital conversion and numerical data processing will always introduce some level of time delay in the process and need to be well understood so that they can be compensated for, particularly with respect to the estimation of CFI synchronization target instants and associated waiting times.

**Table 4.5: Functional performance and method comparisons between protection and CFI processes at hardware and auxiliary system level**

Characteristic / Feature		Functional performance relevance		Available methods
		Protection systems (e.g. distance protection)	Controlled fault interruption	
1	Circuit breaker opening times	Relevant to remote back-up zone co-ordination settings	Critical to have known and stable opening times for correct target selection and waiting time calculations	Mechanical type testing of circuit breakers
		Relevant to circuit breaker failure protection settings		Knowledge of opening time variation with respect to auxiliary voltage, temperature, idle time, interrupter accumulated wear
2	Circuit breaker arcing times	Relevant to remote back-up zone co-ordination settings	Critical to have known and stable opening times for correct target selection and waiting time calculations	High power type testing of circuit breakers - see Chapter 3
		Relevant to circuit breaker failure protection settings		Knowledge of opening time variation with respect to current magnitudes and accumulated interrupter wear - see Chapter 3
3	Secondary (measurement signal) harmonic distortion	Signal distortion that may lead to maloperation or false tripping	Signal distortion that may lead to maloperation	Filtering
4	Current transformer saturation	Signal distortion that may lead to maloperation or false tripping	Signal distortion that may lead to maloperation	Ultra-fast protection (i.e. $\leq \frac{1}{4}$ cycle) Non-saturating current sensors Large magnetic core CTs
5	Secondary (measurement signal) phase angle error	Moderate local impact if small. Potentially more critical to Wide Area Protection schemes.	Significant impact that should ideally be compensated for.	Calibration tests on CTs  Load flow studies for voltage angle checks
6	Secondary (measurement signal) magnitude (ratio) error	May impact on sensitivity and dependability. Can be compensated for.	Low impact - potentially on arcing time selection. Can be compensated for.	Calibration tests on CTs



**Table 4.5: Functional performance and method comparisons between protection and CFI processes at hardware and auxiliary system level**

Characteristic / Feature		Functional performance relevance		Available methods
		Protection systems (e.g. distance protection)	Controlled fault interruption	
7	Time synchronization of secondary and primary systems	Moderate local impact if small. Potentially more critical to Wide Area Protection schemes.	Critical. Need to compensate difference in waiting time calculations.	Calibration tests

#### 4.6 Overall comparison of CFI and distance protection schemes

Distance protection schemes, with their use of phase angle measurement within their decision making, offer perhaps the closest degree of synergetic potential to CFI schemes. Figure 4.5 presents an overall comparison of distance protection, Safepoint and proposed, current zero targeting, CFI schemes.

All three schemes require an accurate estimation of the current phase angle, though this information is utilized in different ways by each scheme. Least means squares (LMS) regression is one of several methods proposed for use in distance protection schemes. Some protection schemes intentionally try to eliminate the DC component from the fault signal in order to improve the processing performance (e.g. use of mimic circuits within CT secondary circuits [27]).

Safepoint used a LMS method for phase angle estimation, with the assumption of a “fixed” DC component level. This offers advantages in simplicity of the LMS matrix calculation and restriction in the number of degrees of freedom that would assist in noise robustness, though it comes at the expense of accuracy for long data windows or rapidly decaying DC components.

The proposed CFI method also utilizes the LMS method, but with a first order Taylor series approximation of the DC component, as will be described in greater detail in Chapter 5.

Fault inception detection is generally of interest to protection methods as a means for data sampling window control in order to discard pre-fault data from the phase angle calculations. For the proposed CFI method, the fault inception angle has added importance for modelling the fault current accurately. Fault inception detection was not explicitly described in the Safepoint work, though it would have similar importance for data window management, particularly where short data processing response times are required.

Though distance protection and the proposed CFI method both rely on phase angle measurement, they utilize the information in different ways. A distance protection scheme uses the information, combined with current magnitude to decide if the fault threshold criteria are violated and a protection operation is required. The proposed CFI method and Safepoint utilize the phase angle for estimating their synchronization target instants, which potentially requires a higher level of accuracy in phase angle estimation than for protection purposes. Safepoint did not propose any specific validation check of its phase angle estimation, focussing more on the noise robustness of the LMS method.

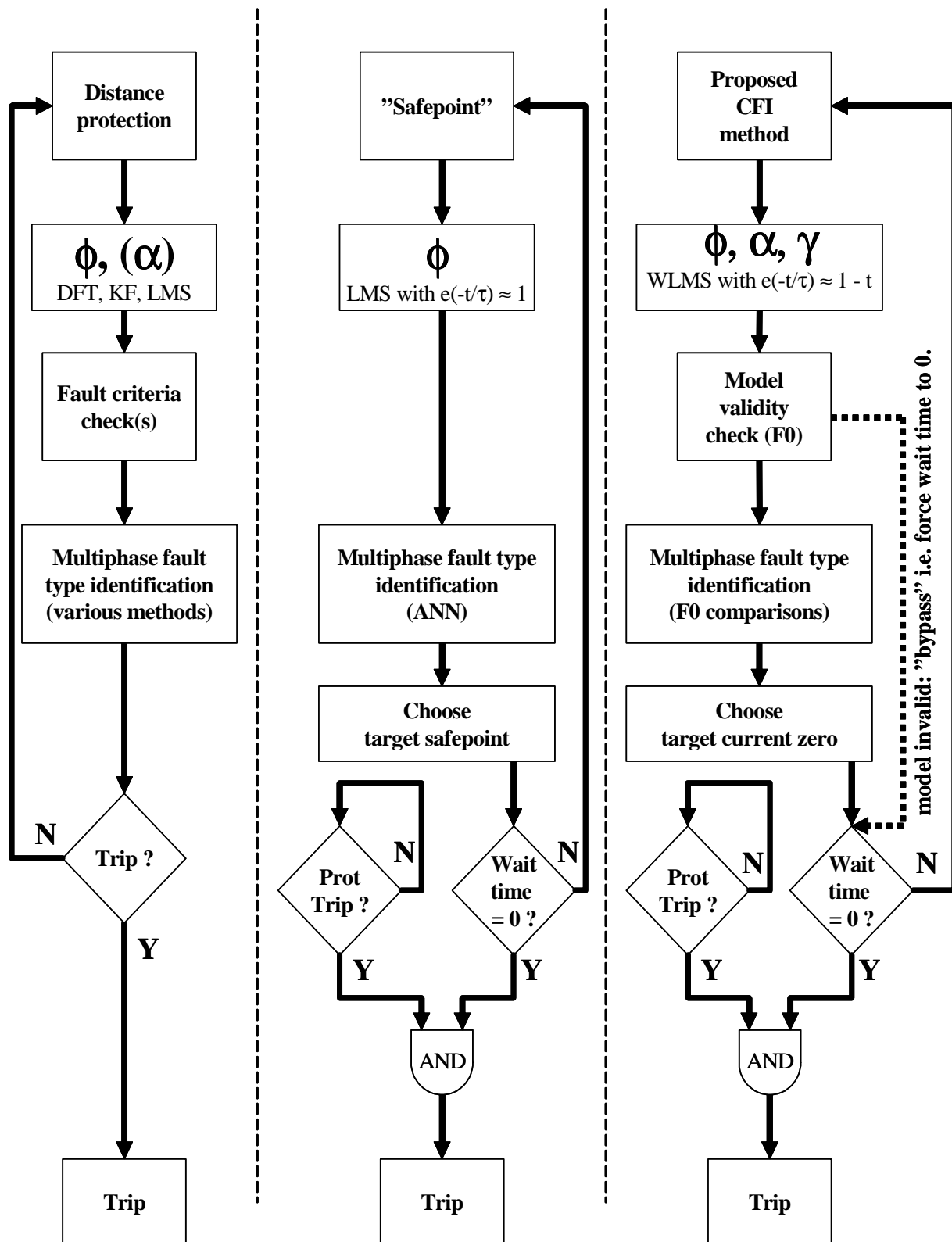


Figure 4.5: Overall comparison of distance protection, Safepoint and proposed CFI schemes

The proposed CFI method has introduced the use of analysis-of-variance testing (F0 test) of its current model against the measured current in order to provide a validity check for added dependability. In the event that an insufficiently accurate model of the current can be obtained, the F0 results permit implementation of bypassing of the CFI control, either by forcing the synchronizing waiting time to zero, or issuing a diversion trip signal to a back-up circuit breaker. The F0 test has additional important uses within the proposed CFI method including fault inception detection and multi-phase fault type identification, as described in the next section.

#### **4.7 Proposed CFI process structure for three phase networks**

The overall structure of the proposed CFI method for three phase networks is described in Figure 4.6 and can be compared to the CFI process described earlier on the right hand side of Figure 4.3. Following from the identified different circuit models for phase-to-earth and phase-to-phase fault models, the three phase CFI scheme executes parallel processing according to both phase-to-earth and phase-to-phase parameter estimations of the fault inception angle ( $\alpha$ ) and relative voltage phase angles ( $\gamma$ ). Each of the models is checked by analysis of variance and the model provides the more accurate result is then used for the target estimation. If neither model can provide a sufficiently accurate result, determined by setting an F0 acceptance value threshold, then the bypass control option can be implemented.

Chapter 5 will present detailed descriptions of the proposed methods for the core CFI process functions of fault inception detection, fault type identification, current model parameter estimation and validation, and target current zero identification within the context of the structure described in Figure 4.6.

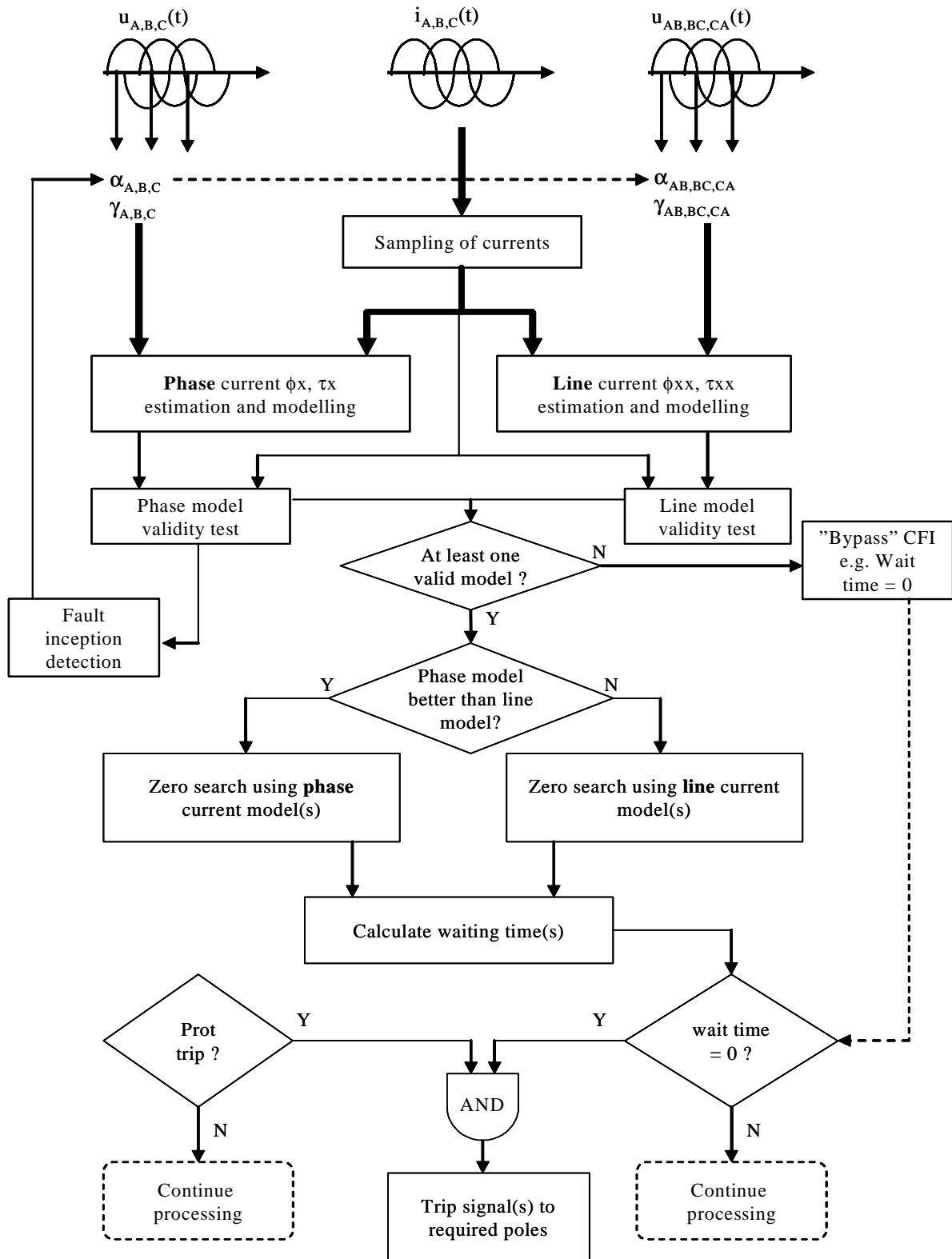


Figure 4.6: Proposed generic three phase CFI algorithm structure

## 5 Three phase controlled fault interruption - Proposed method

The proposed CFI method for three phase networks is based on extension of the method described in the licentiate and is comprised of four main processing steps:

1. Fault inception detection
2. Modelling of fault based on current magnitude, phase angle and time constant estimation
3. Model validation
4. Synchronizing target selection

This chapter will describe the details of the above listed four main processing steps. First an overview of the proposed overall CFI process will be presented. Second the applied current models and main parameter estimation calculation method will be presented. Third the analysis of variance method will be presented with focus on its use for fault inception detection and fault type identification. Fourth the targeting methodology of the three phase CFI method will be presented. Finally, examples of the operation of the algorithm for different milt-phase fault cases will be presented.

### 5.1 Overall proposed CFI process

The proposed CFI method follows from the general approach described in Chapter 4, whereby the synchronizing of the circuit breaker trip commands in each phase is made with respect to estimations of viable interruption current zero times by use of a modelling of the currents.

The model of the current is based on that described in Chapter 2. More generally the modelling of the current can be described as shown in Figure 5.1. The current is a function of many variables, each of which can be estimated by a variety of methods. It is important to note that in the work presented here, a number of the parameters are assumed to remain constant for the duration of the fault (e.g.  $\omega$ ,  $U_{PK}$ ,  $L$ ,  $R$ ).

In reality, effectively all the parameters will be time varying to different degrees due to the true dynamic nature of electric power systems. However factoring in complete power system behavior dramatically complicates the process and potentially detract focus from the primary goals of this work, which has been to provide a suggested process for the implementation of CFI on three phase networks. The impact of the respective dynamic parameter behaviors on their estimation methods and the mode-based CFI approach can then be further investigated in future work, as described in more detail later in Chapter 7.

The proposed overall CFI process is described in the flowchart shown in Figure 5.2. The main difference between the single phase and three phase method is the use of two alternative frame-of-reference models; a phase-to-earth source parameter based model and a phase-to-phase source parameter based model, as outlined in general form in Chapters 2 and 4. The equivalent circuits for each model and the associated reference  $\gamma$  values for the respective driving source voltages are summarized in Table 5.1.

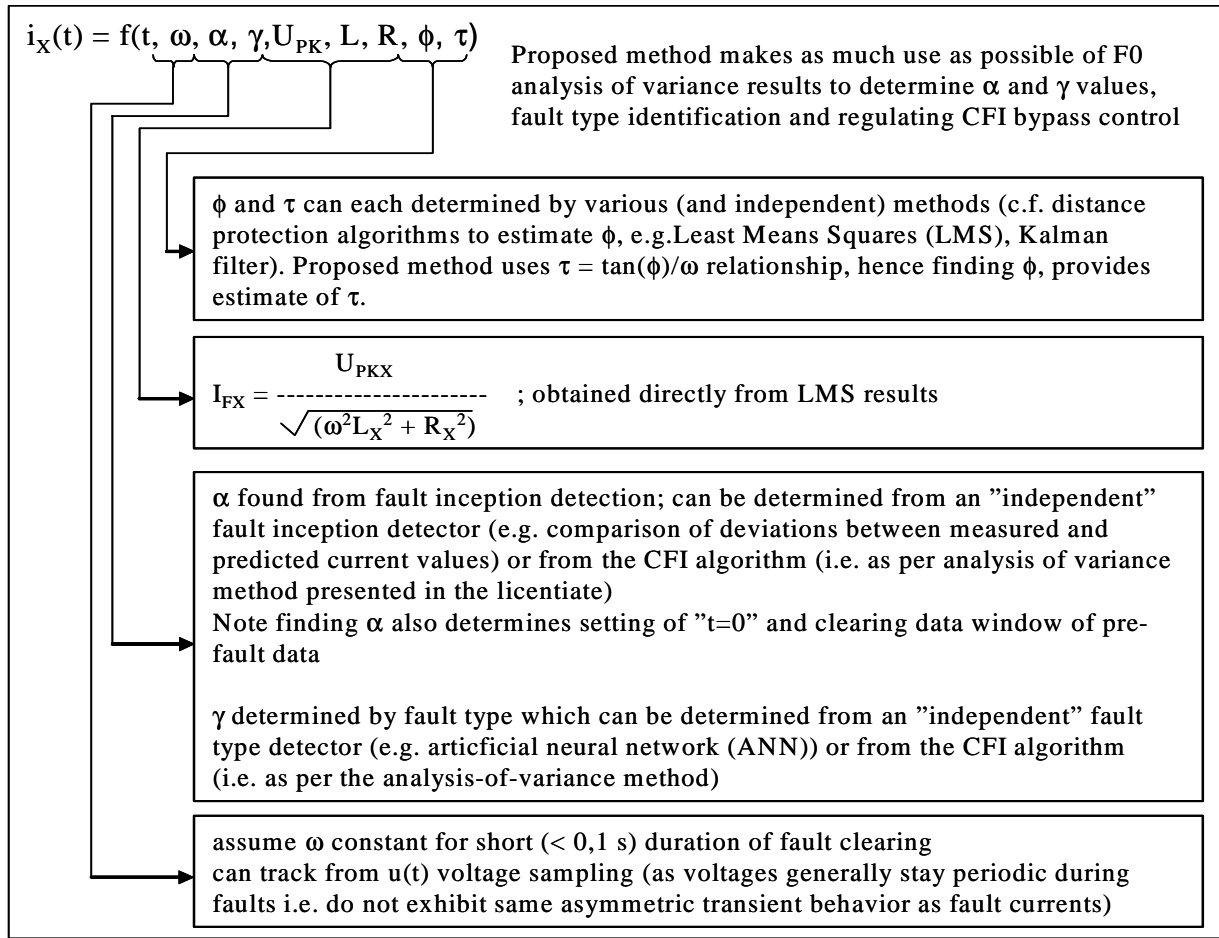


Figure 5.1 : Generalized approach to parameter estimation for fault current model

Table 5.1: Proposed method models and associated  $\gamma$  reference values

Model type	"Equivalent" circuit	$\gamma$ values for A-phase reference A-B-C phase rotation
"Phase" (phase to earth and 3-phase faults)		$\gamma_A = 0$ $\gamma_B = -2\pi/3$ $\gamma_C = -4\pi/3$
"Line" (phase to phase unearthed faults)		$(\gamma_A = 0)$ $\gamma_{AB} = \pi/6$ $\gamma_{BC} = -\pi/2$ $\gamma_{CA} = -7\pi/6$

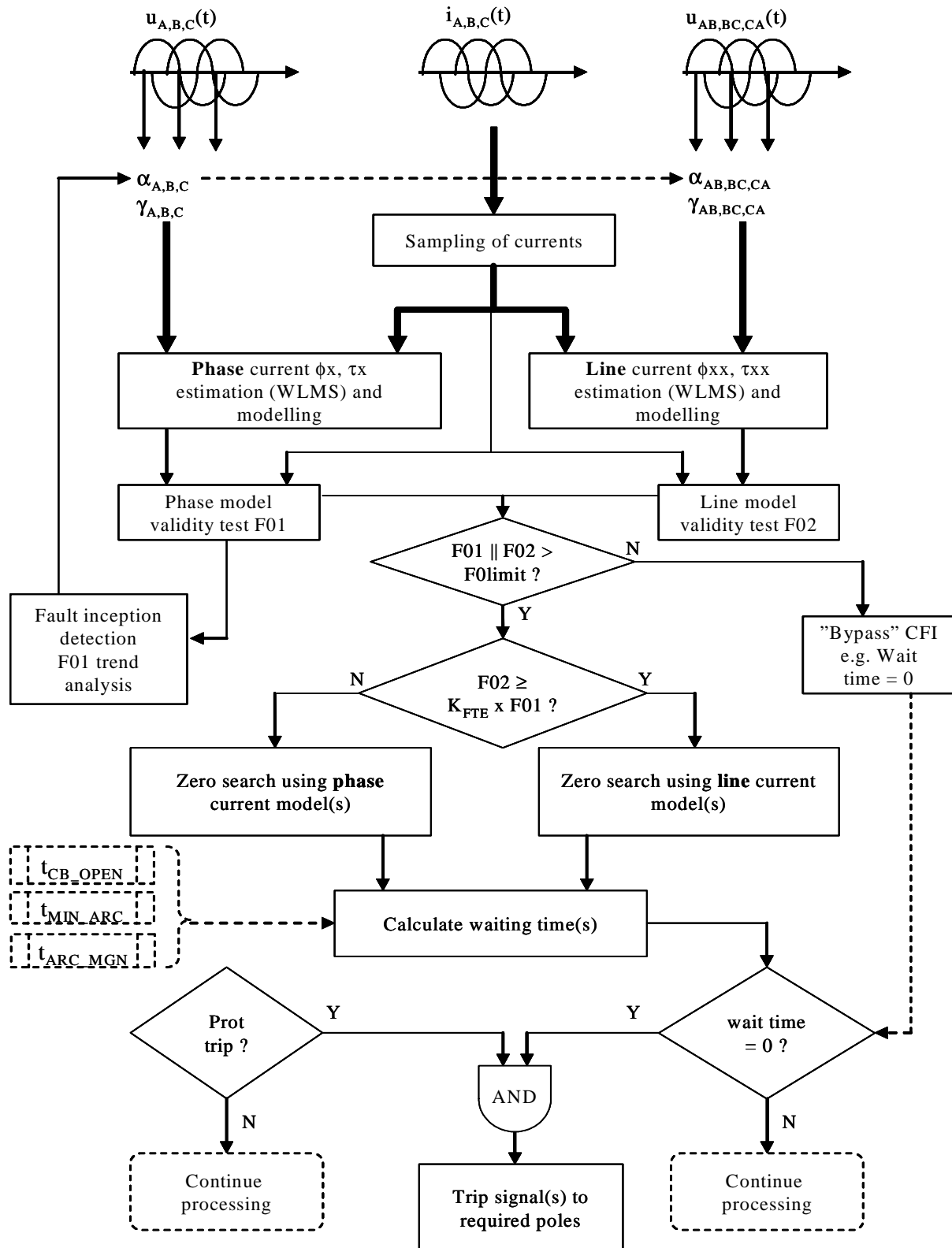


Figure 5.2 : Process flowchart for proposed 3-phase CFI method

Parameters for both models are calculated in parallel and the resultant analysis-of-variance results from each model (i.e. “F01” and “F02”) are compared to select the most appropriate model for subsequent estimation of synchronizing target current zero times. The proposed method also introduces a compromise targeting solution for the last two phases to interrupt on three phase faults, as a means of overcoming the uncertainty of distinguishing between three phase earth and unearthed faults before the first phase is interrupted.

## 5.2 Applied fault current models and parameter estimation method

As described in Chapter 2, fault currents on three phase networks can be generically described by {5.1} and {5.2},

$$u_X(t) = U_{PKX} \cdot \sin(\omega \cdot t + \alpha_X + \gamma_X) \quad \{5.1\}$$

where

$X$  is the associated phase designation,

$\omega$  is the power system angular frequency,

$\gamma_x$  is the reference angle for each phase-to-earth or phase-to-phase voltage with respect to a preselected reference phase,

$\alpha_x$  is the respective source voltage phase angle at which a fault begins (at a time,  $t = 0$ ) in any phase.

$$i_X(t) = I_{FX} \cdot [\sin(\omega \cdot t + \alpha_X + \gamma_X - \phi_X) - \sin(\alpha_X + \gamma_X - \phi_X) \cdot e^{(-t/\tau_X)}] + I_{PF\alpha X} \cdot e^{((-t)/\tau_X)} \quad \{5.2\}$$

where,

$$I_{FX} = U_{PKX}/|Z_X| = U_{PKX}/\sqrt{(\omega^2 L_X^2 + R_X^2)} \quad \{5.3\}$$

$I_{PF\alpha X}$  is the instantaneous value of the pre-fault load current at the moment of fault inception.

$$\phi_X = \tan^{-1}(\omega L_X/R_X) \quad \{5.4\}$$

$$\tau_X = L_X/R_X = \tan(\phi_X)/\omega \quad \{5.5\}$$

$L_X$  is the source to fault inductance and

$R_X$  is the source to fault resistance (including any fault arc resistance).

In a similar manner to that described in the licentiate, weighted least mean squares (WLMS) regression has been used as the means to obtain the estimated  $\phi_X$ ,  $\tau_X$  and  $I_{FX}$  values, based on separately determined  $\alpha_X$  and  $\gamma_X$  values.



The values of  $\alpha_X$  and  $\gamma_X$  for the current modelling in each phase are based on determination of the fault type, using the analysis of variance test results, which will be described later in this chapter. At start up of the CFI algorithm, the same  $\alpha_X$  and  $\gamma_X$  values are used for the phase-to-earth and phase-to-phase models, based on the assumption of the circuit breaker being closed in each phase at controlled voltage phase angles. The current model form described by {5.2} is the same for both the phase-to-earth source and phase-to-phase source frames of reference, and hence the WLMS regression method is also the same for both parameter estimations.

Applying the principle of superposition {5.2} can be orthogonally factorized to give {5.6},

$$i_X(t) = K_{X1} \cdot \sin(\omega \cdot t) + K_{X2} \cdot \cos(\omega \cdot t) - K_{X3} \cdot e^{(-t \cdot K_{x4})} \quad \{5.6\}$$

where

$$K_{X1} = I_{FX} \cdot \cos(\alpha_X + \gamma_X - \phi_X)$$

$$K_{X1} = I_{FX} \cdot [\cos(\gamma_X - \phi_X) \cdot \cos(\alpha_X) - \sin(\gamma_X - \phi_X) \cdot \sin(\alpha_X)] \quad \{5.7\}$$

$$K_{X2} = I_{FX} \cdot \sin(\alpha_X + \gamma_X - \phi_X)$$

$$K_{X2} = I_{FX} \cdot [\sin(\gamma_X - \phi_X) \cdot \cos(\alpha_X) + \cos(\gamma_X - \phi_X) \cdot \sin(\alpha_X)] \quad \{5.8\}$$

$$K_{X3} = I_{FX} \cdot \sin(\alpha_X + \gamma_X - \phi_X) - I_{PF\alpha X}$$

$$K_{X3} = K_{X2} - I_{PF\alpha X} \quad \{5.9\}$$

and

$$K_{x4} = 1/\tau \quad \{5.10\}$$

Applying a 1<sup>st</sup> order Taylor series approximation for the exponential term, equation {5.6} can then be approximated to {5.10},

$$i_X(t) \approx X_{X1} \cdot \sin(\omega \cdot t) + X_{X2} \cdot \cos(\omega \cdot t) - X_{X3} \cdot 1 + X_{X4} \cdot t \quad \{5.11\}$$

The  $X_X$  coefficients in {5.11} can then be found by solving the weighted least means squares matrix as described by {5.12}, {5.13} and {5.14},

$$\begin{bmatrix} X_{X1} \\ X_{X2} \\ X_{X3} \\ X_{X4} \end{bmatrix} = \left( [A]^T \cdot [W]^T \cdot [W] \cdot [A] \right)^{-1} \cdot [A]^T \cdot [W]^T \cdot [W] \cdot \begin{bmatrix} i_X(t_1) \\ i_X(t_2) \\ \dots \\ i_X(t_n) \end{bmatrix} \quad \{5.12\}$$

n is the number of current data sample values processed,

$$[A] = \begin{bmatrix} \sin(\omega \cdot t_1) & \cos(\omega \cdot t_1) & -1 & t_1 \\ \sin(\omega \cdot t_2) & \cos(\omega \cdot t_2) & -1 & t_2 \\ \dots & \dots & \dots & \dots \\ \sin(\omega \cdot t_n) & \cos(\omega \cdot t_n) & -1 & t_n \end{bmatrix} \quad \{5.13\}$$

$$[W] = \begin{bmatrix} 1 & 0 & \dots & 0 \\ 0 & 1 & \dots & 0 \\ 0 & 0 & 1 & \dots \\ 0 & \dots & 0 & 1 \end{bmatrix}, \text{ n x n dimension identity matrix;} \quad \{5.14\}$$

and  $[X_{X1} X_{X2} X_{X3} X_{X4}]^T$  is the vector of unknown coefficients sought.

The key results from the solution of {5.12} are terms  $X_{X1}$  and  $X_{X2}$  which are in the general forms given by {5.15} and {5.16},

$$X_{X1} = I_{FX} \cdot \cos(\gamma_X - \phi_X) \quad \{5.15\}$$

$$X_{X2} = -I_{FX} \cdot \sin(\gamma_X - \phi_X) \quad \{5.16\}$$

The WLMS computation is an orthogonalization of the sampled current vector. The  $X_{X1}$  and  $X_{X2}$  terms provide the orthogonal terms of the symmetrical component of the sampled current, while the  $X_{X3}$  and  $X_{X4}$  terms provide a linearized approximation of the asymmetrical (general) component of the sampled current.

It is of interest to note that the  $\alpha_x$  term does not seem to appear directly in the WLMS computation. However since  $X_{X1}$  and  $X_{X2}$  are coefficients for the symmetrical component of the sampled current are directly related to equations {5.7} and {5.8} for  $K_{X1}$  and  $K_{X2}$  with  $\alpha_X = \pi/2$ , which corresponds to the case of a fault current inception at a positive driving source voltage peak and no resultant transient DC component (i.e.  $\sin(\alpha_X)=1$  and  $\cos(\alpha_X)=0$ ). For the general case, the actual  $\alpha_X$  must be applied to equations {5.7} and {5.8} obtain the relevant  $K_{X1}$  and  $K_{X2}$  coefficients for the particular fault case.  $K_{X4}$  is found directly by using  $X_{X1}$  and  $X_{X2}$  as per {5.17},

$$K_{X4} = 1 / |X_{X2}/X_{X1}| / \omega \quad \{5.17\}$$

The  $K_X$  terms,  $\gamma_X$  and  $I_{PF\alpha X}$  can then be applied to {5.6} (expanded as per {5.18} below) to obtain an approximation of the sampled currents in each phase.

$$i_X(t) = K_{X1} \cdot \sin(\omega \cdot t) + K_{X2} \cdot \cos(\omega \cdot t) - K_{X2} \cdot e^{(-t \cdot K_{X4})} + I_{PF\alpha X} \cdot e^{(-t \cdot K_{X4})} \quad \{5.18\}$$

The approximated currents described by {5.18} are extrapolated in time and hence be used for estimated future current zero times that can be used as targets for controlled fault interruption. It is important to note that the time vector for the current estimation must be reset for  $t=0$  from the estimated fault inception time, corresponding to the  $\alpha_X$  determined for the associated fault case,

thus maintaining the correct frame of reference to the driving source voltage model being applied in this method.

It is important to recognize what assumptions are made in the applied three phase model. While it is assumed that the system has balanced driving source phase voltages, the model and method is sufficiently generic to support unbalance variations in the  $\gamma_X$  values, provided at least one phase voltage is used as a principal reference. Obviously the phase rotation of the system with respect to the main reference phase voltage must be known - though it is reasonable to assume that such information can be supplied at system setup and commissioning and would stay “stable” during the lifetime of the installation / application.

The  $\alpha_X$  and  $I_{PF\alpha X}$  values need also to be known and fed to the algorithm. These are essential not only to extract the final current estimations, but also for the optimum adjustment of data sampling windows at fault inception i.e. the correct discarding of pre-fault from fault current data samples.

### 5.3 Analysis of variance (F0) tests

In the licentiate stage of this work, the “F0-test” was introduced, not only as a means to check the validity of the estimated to sampled current, but also as a means to detect the instant of fault inception and thereby also the  $\alpha_X$  and  $I_{PF\alpha X}$  values. The same analysis of variance “F0” test is used in the proposed three phase CFI method, with the additional application of being used for fault type identification and thereby providing the trigger to update the  $\gamma_X$  values used in the WLMS parameter estimation. The F0-test is defined as follows [46],

$$F_0 = \frac{SS_R/k}{SS_E/(n-p)} \quad \{5.18\}$$

where  $SS_R$  is the regression sum of the squares,  $SS_E$  is the error sum of the squares,  $k$  is number of coefficients used in regression,  $n$  is the number of sampled values tested and  $p$  is the number of terms used in the regression,

$$SS_R = \sum_{i=1}^n (\hat{y}_i - \bar{y})^2 \quad \{5.19\}$$

$$SS_E = \sum_{i=1}^n (y_i - \hat{y}_i)^2 \quad \{5.20\}$$

where

$\hat{y}_i$  = the  $i^{\text{th}}$  estimated model value

$\bar{y}$  = the mean of the sampled values

$y_i$  = the  $i^{\text{th}}$  sampled value

Due to the high numerical value of the F0 results, the base 10 logarithms of the F0 values are used as the values for data processing. When using full one period data window sampling under load current conditions, there can be oscillations in the F0 values, caused by the numerical tolerance of the computer and so once the  $\log_{10}(F0)$  value is above 4, it is simply truncated and kept at 4.

### 5.3.1 Fault type identification using F0-test

The F0 test is performed on both phase-to-earth and phase-to-phase parameter based models of the currents in each phase, at every iteration of the algorithm. The phase-to-earth F0 result is designated “F01” and the phase-to-phase result is designated “F02” for each phase current. Due to the different parameter values used for phase-to-earth and phase-to-phase modelling, each model will have a different F0 result for the same sampled current data set.

If the F01 value is higher than the F02 value for a given phase, then it is concluded that the current in this phase is following a phase-to-earth model. Conversely, a higher F02 than F01 result means that the current is best represented by the phase-to-phase “line” model. For two phase faults, there should be a matching of model type results on the faulted phases. In order to make the process more robust to signal noise, a discrimination factor ( $K_{FTE}$ ) is used in the comparison of F01 and F02 values so that for a phase-to-phase fault case to be determined, F02 must be greater than  $K_{FTE}$  times the associated F01 value for each phase.

Simulations were made on double phase-to-earth fault and phase-to-phase fault cases, with and without noise to ascertain a reasonable value for  $K_{FTE}$ . In simulations without noise,  $K_{FTE}$  can be set to 1.0 and the algorithm correctly discriminated between the double phase-to-earth and phase-to-phase fault cases for all fault inception angles.

A set of simulations with 10% magnitude pseudo-white Gaussian noise were conducted on A-B-E and A-B phase faults for  $K_{FTE}$  values of 1.00, 1.05 and 1.10. For each simulation run, fifteen different WGN data sets were applied to twelve fault inception angles ranging from 0 to 330 electrical degrees in 30 degree steps, resulting in a total of  $15 \times 12 = 180$  simulations per run. The results are summarized in terms of the percentages of respective fault types “identified” by the algorithm in Figure 5.3. Given the reasonably large noise magnitude applied, the method appears to work reasonably well for double phase-to-earth faults. The slightly lower performance for phase-to-phase fault identification can arise from the applied requirement {5.21} being true for the algorithm to estimate the fault as being of the phase-to-phase ungrounded type.

$$F02 > K_{FTE} \times F01 \quad \{5.21\}$$

Though it would be desirable to raise the success of the phase-to-phase fault identification success rate, these are likely to be less frequent than phase-to-earth faults. Nevertheless there is scope for improvement in this part of the algorithm, possibly by reverting to alternative fault type identification methods, for example that utilize a symmetrical components approach. The 0.6% of cases incorrectly identified as three phase earth fault are believed to be due solely to the applied level of WGN, resulting a a false fault inception detection on C-phase. However this is registered in only 1 of 180 simulations. Based on the results shown in Figure 5.3 it was decided to make all further simulations using  $K_{FTE} = 1.10$ .

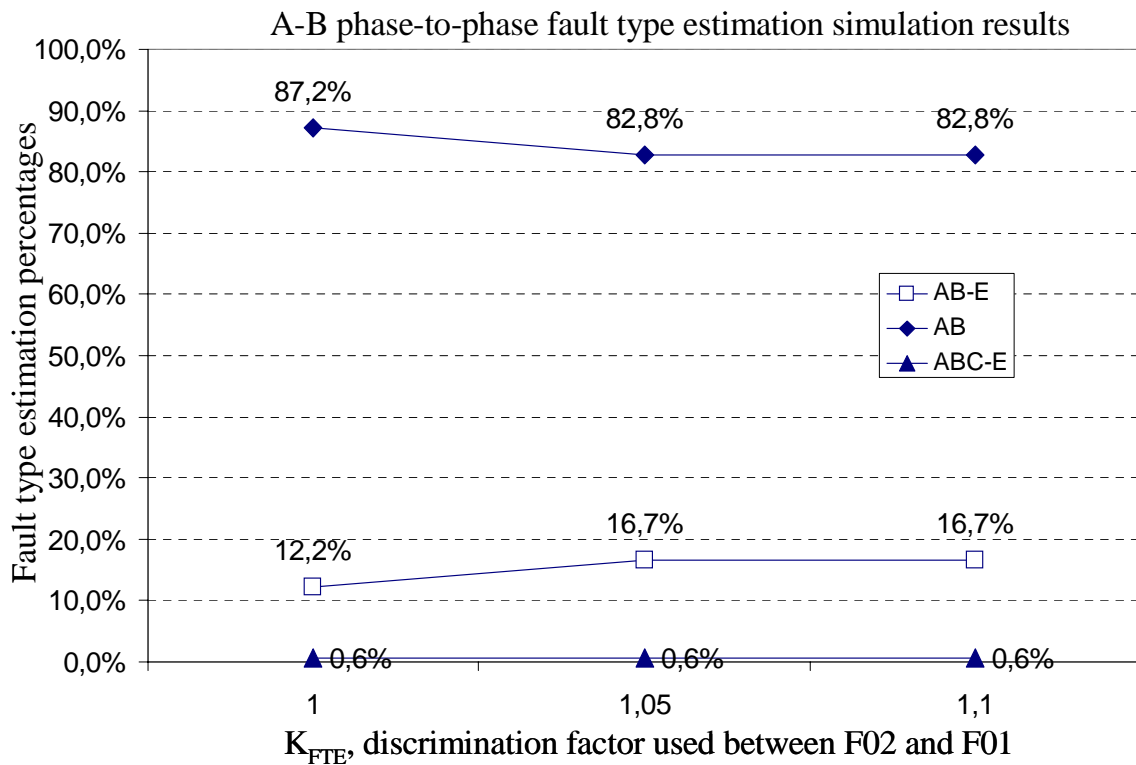
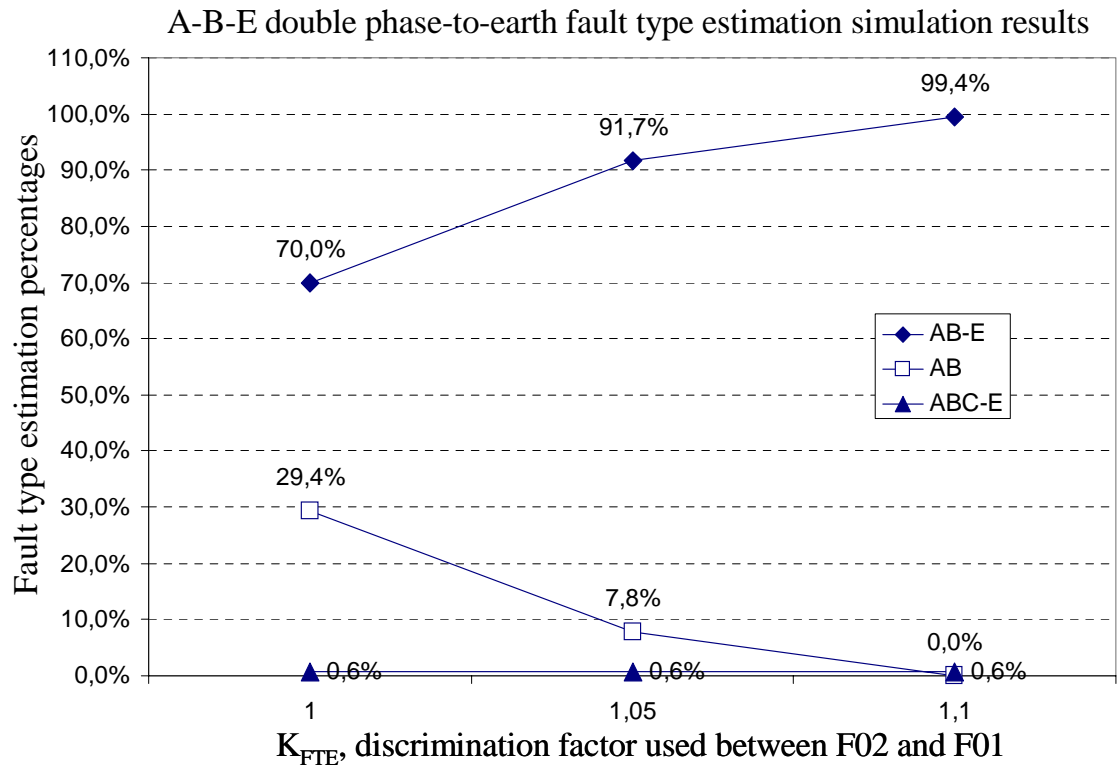


Figure 5.3 : Simulation results to test F0 method to discriminate between double phase-to-earth and phase-to-phase unearthed faults

### 5.3.2 Fault inception detection

As in the single phase CFI method, the F0 results are also used in the three phase method for fault inception detection. In particular, tracking of the trend behavior of the phase-to-earth F01 results in each phase is used for the fault inception detection. As stated earlier, the same  $\alpha_X$  and  $\gamma_X$  values are used for the phase-to-earth and phase-to-phase models at the start up of the CFI process. (The  $\alpha_X$  start up values can be controlled by synchronized closing of the circuit breaker phases). The F01 values are used for fault inception detection as under normal balanced three phase load conditions the currents in each phase should follow the phase-to-earth model, though there is no particular obstacle to using the F02 values for fault inception detection either, as both F0 results will decrease with a change in current behavior, such as a fault occurrence.

An empirical study of the F01 behavior for different fault inception angles was made in order to establish control parameters for setting the fault inception detection threshold, based on the rate of decline of the F01 values with the occurrence of a fault. Figure 5.4 shows examples of the F01 trend behavior about the fault inception instant on A-phase for a three phase earth fault and twelve equally spaced fault inception phase angles ( $\alpha$ ) from 0 to 330 electrical degrees.

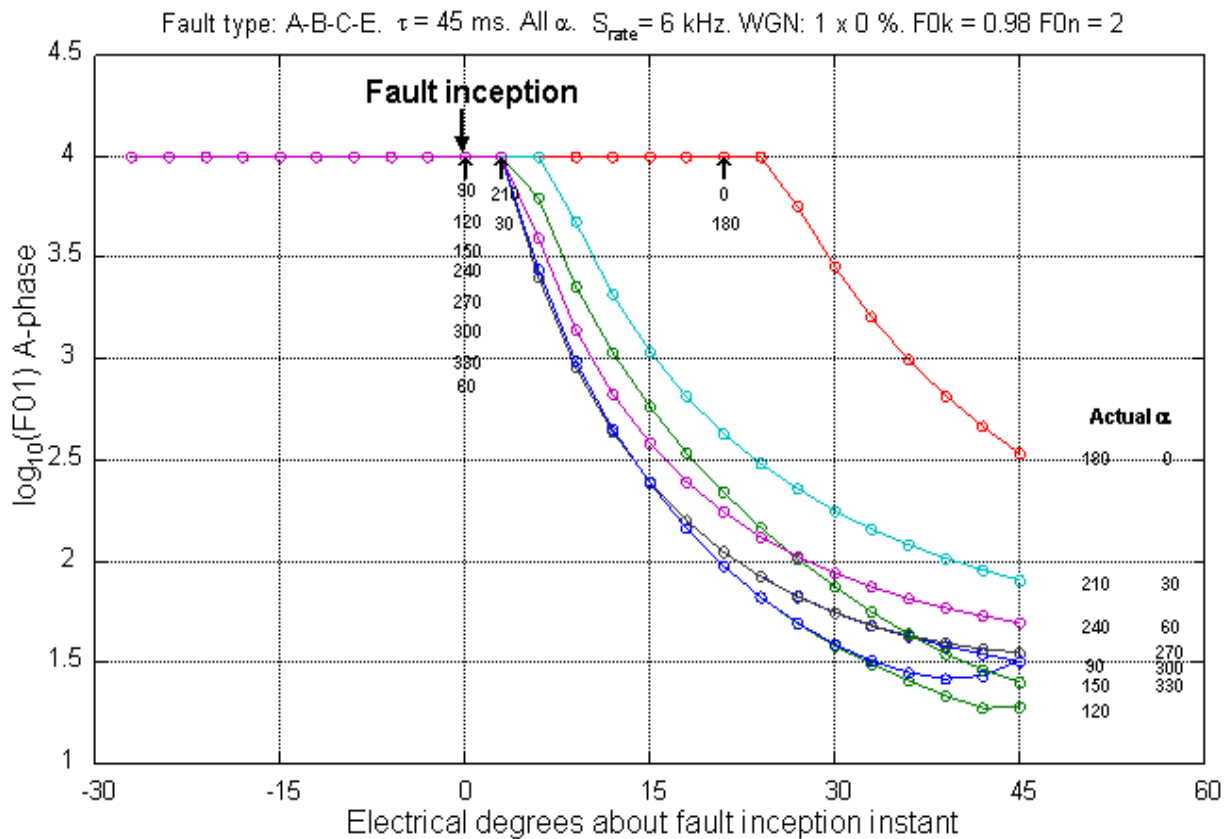


Figure 5.4 : Examples of F01 trend behavior pre- and post-fault inception

The circular points on each curve correspond to a data sample point, which at the 6 kHz simulation rate means that the resolution for fault inception angle estimation is 3 electrical degrees. The actual fault inception angles are indicated to the right end of each F01 trend line and below the arrows that point to the estimated fault inception instant in each case, deduced from the F01 trend analysis. The criteria used for fault inception detection are that once two successive F01 values are found to have fallen by 2% with respect to the preceding F01 value, a fault is determined to have occurred. The fault inception instant is then estimated back to the data sampling point immediately before the start of the F01 decline trend that resulted in the fault detection.

As can be seen in the Figure 5.4 example, the method works well for the majority of fault inception angles, with 0 degree error for eight of the twelve simulated angles, 3 degree error on two of the angles (30 and 210 degrees) and 21 degree error at 0 and 180 degree inception angles. The somewhat larger error at 0 and 180 degree inception angle, corresponds to the  $\alpha$  value that gives maximum asymmetry of the fault current. Though the fault current will develop maximum asymmetry in these cases, the initial development of the fault current is relatively slow and therefore the rate of deviation between the expected (load) current behavior and the fault current is slow and more sample points must be taken before the F01 trend will trigger to the fault inception. Nevertheless the 21 degree error is still relatively “small”, corresponding to 1.16 ms or 5.8% on 360 degrees. As will be shown in the simulations presented later, even with errors in  $\alpha$ -estimation of this order, the algorithm is still able to make reasonably good i.e.  $< \pm 0.5$  ms error, current zero crossing time estimations.

It should be noted that the error in detection of the fault inception instant affects not just the  $\alpha$ -value estimation, but also the data sampling window size and content. At fault inception detection the data sampling window is reset to begin at the estimated fault inception instant and therefore discard all pre-fault data samples.

### 5.3.3 Validation and “Bypass” control

In addition to the fault type and fault inception determinations made, the F0 results are also important in regulating the overall dependability and security control of the algorithm. Only if at least F01 or F02 values are above a predefined threshold limit will the algorithm proceed with using the selected current model for current zero target and waiting time estimation. The threshold for acceptable F0 values is set according to the desired tolerance on current zero time estimation errors. Empirical tests, as shown in the example in Figure 5.5, indicated that a threshold value of  $\log_{10}(F0) = 2$  provides control within  $\pm 0.5$  ms error bound for current zero times.

The data points in Figure 5.5 are for each time step iteration made post-fault and up to the protection operation time (20ms), for a full range of  $\alpha$ -values ranging from 0 to 330 degrees in 30 degree steps. The “WGN = 0%” in the graph header indicates that these simulations were made without any added white Gaussian noise.

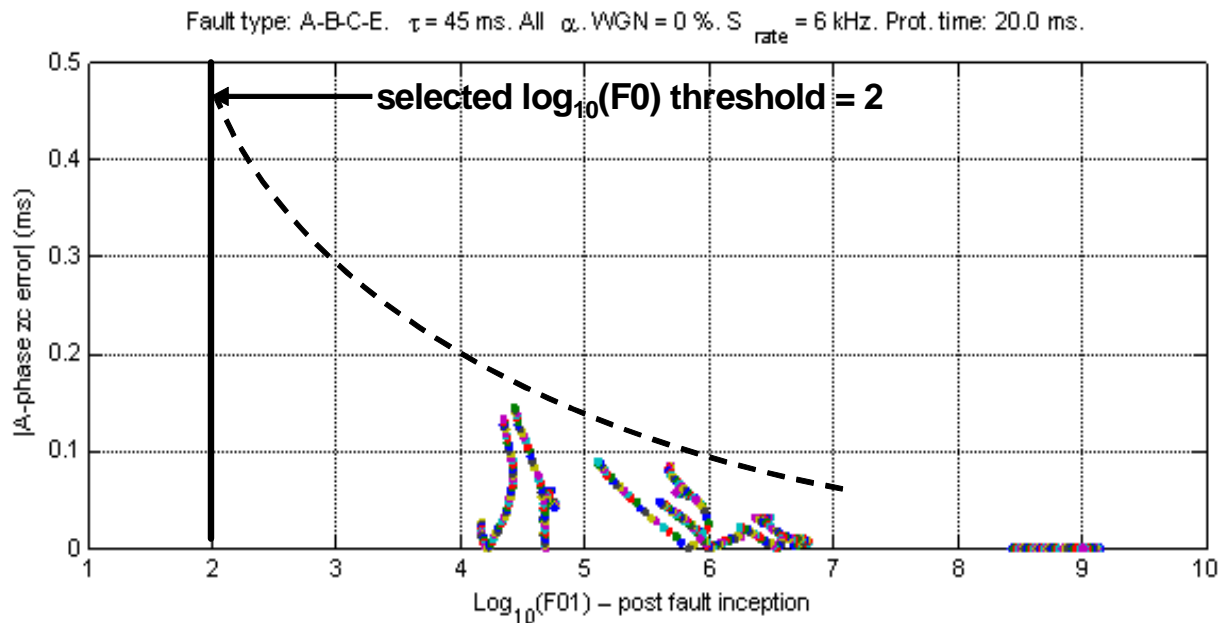


**Figure 5.5 : Absolute value zero-crossing time errors versus post-fault  $\log_{10}(F0)$  values**

The estimation accuracy of  $\phi$  and  $\tau$  is limited in the applied WLMS method by the first order Taylor series approximation of the exponentially decaying DC component. The percentage ratio of the DC component in the fault current, dependent also on the fault inception angle, will affect the accuracy of the overall model result and therefore limit the accuracy in predicting the future current zero times. Figure 5.6 shows the relationship between the target zero crossing time errors and the percentage errors in the estimation of  $\tau$  for the same sets of data as used in Figure 5.5.

It can be seen in the Figure 5.6 results that a fairly large percentage error in  $\tau$  (c. 10%) can be tolerated, while still achieving a low zero-crossing time error ( $< 0.2$  ms). There is no practical direct link between whether the  $\tau$ -error is positive or negative to whether or not the associated zero-crossing time error is also positive or negative as this relation will vary depending on which current zero is being targeted. A positive zero-crossing time error on one current zero will imply a negative error on the following current zero.

However, as the errors cannot be accurately measured before the trip commands need to be sent, there is little benefit that can be utilized by this for the execution of the algorithm. It is however of interest to note the linearity between the zero-crossing time error and percentage  $\tau$  error.



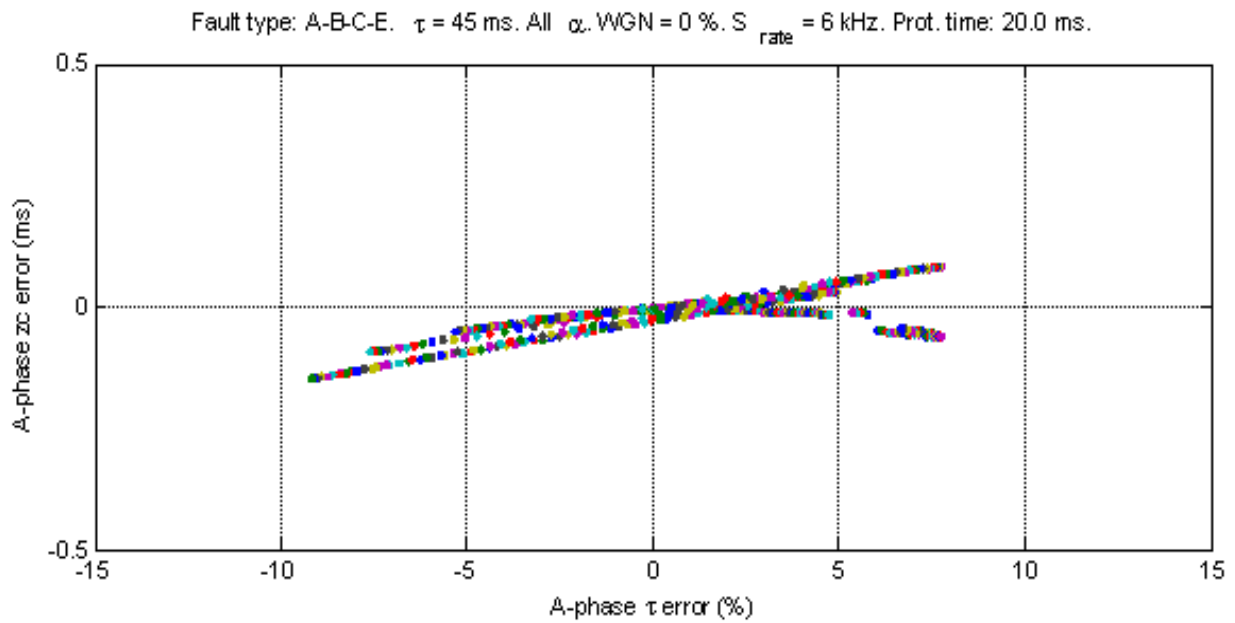


Figure 5.6 : Zero-crossing time errors versus  $\tau$ -estimation percentage errors

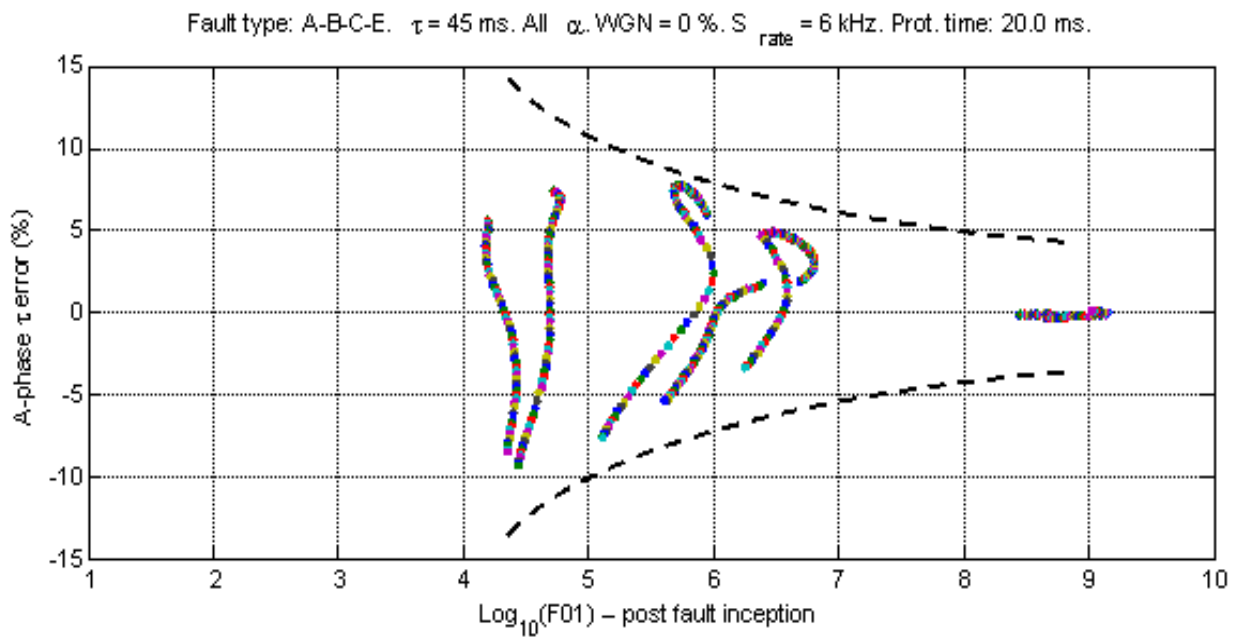


Figure 5.7 : Example of time constant percentage errors versus post-fault  $\log_{10}(F0)$  values

Following from the near linear relationships seen between the zero-crossing time errors and the percentage  $\tau$  errors it is also of interest to see the relations between the F0 results and the percentage  $\tau$  errors, as shown in Figure 5.7 (for the same set of data points as Figures 5.5 and 5.6).

As expected, the lower the  $\tau$  error, the higher the F0 result, for a given percentage DC component within the fault current. As such the F0 test provides a very useful measure of the validity of the model of the current and therefore can be used to regulate the control of the entire CFI process.

If both the F01 and F02 results are below the set threshold level, the algorithm can be structured to implement a “back-up” or “bypass” strategy. The back-up strategy would involve blocking the tripping of the circuit breaker most immediately connected to the CFI control and diverting the trip operation to the next higher level of circuit breakers in the network. Such a strategy would be required for a circuit breaker that was entirely dependent on correct CFI operation to achieve interruption. Existing circuit breaker designs are capable of managing interruption over wide arcing window and so a bypass or “forced trip” strategy, that involves forcing the CFI waiting time to zero can be used, as is described in Figure 5.2.

## 5.4 Synchronizing target selections

While the proposed method uses the estimated current zero times as the synchronizing targets, it is also possible that the method could be combined or used with other target criteria e.g. safepoints as proposed by Pörtl. As indicated in Chapter 4, Table 4.1, there can also be different criteria used for target selection, based on either achieving fastest possible clearing time or maximum saving of the arc current integral (equated to the arc energy). Additional criteria, such as selection of the preferred current zero target based on the  $di/dt$  at the current zero may also be desirable for some interruption cases.

For the purposes of this work, the chosen targets are the earliest viable interruption current zero times, after the minimum clearing time of the circuit breaker, allowing for a small margin (e.g. +1 ms) beyond the minimum arcing time. The search for the target current zero times is managed in the same way as for the single phase CFI method in that a search is made within a one cycle window beyond the CFI minimum clearing time.

For single and double phase-to-earth faults and phase-to-phase unearthed faults the target current zeroes can be identified by the direct extrapolation of the current models for each phase. In the case of three phase faults, earthed or unearthed, the targeting is more difficult due to possibility of phase shift in the last two phases to interrupt and the difficulty to discriminate between the earthed and unearthed cases before the first phase has interrupted. In order to manage this problem, as described in Chapter 4, a “compromise” targeting strategy is applied for the last two phases to interrupt in three phase fault cases.

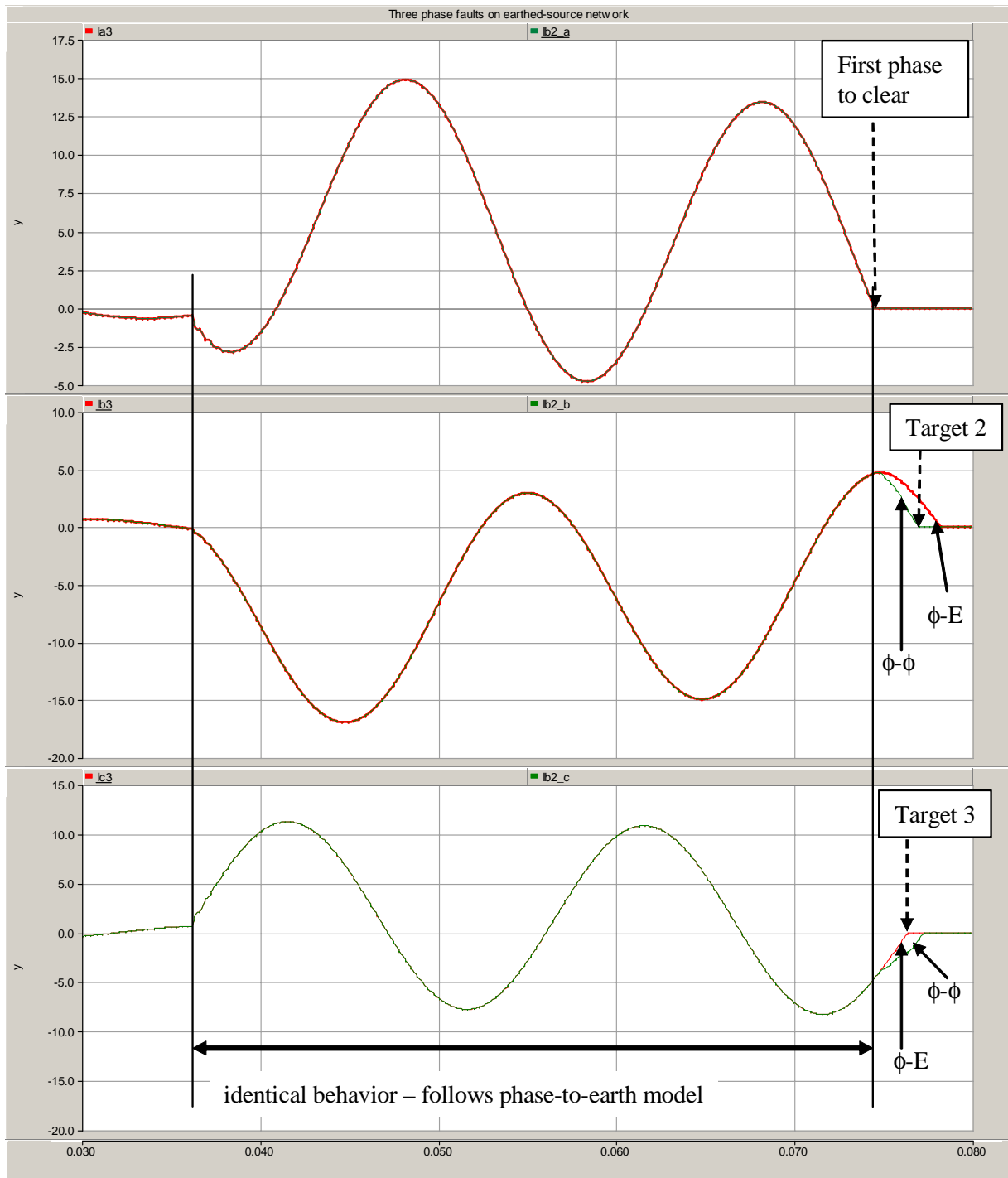


**Figure 5.8 : Compromise targeting strategy for last phases to clear for three phase earthed and unearthed fault cases.**

First the algorithm identifies the first phase to interrupt. Up to this point the algorithm will use the phase-to-earth modelling of the current (i.e. based on F01 results being higher than F02 results in all of the faulted phases). Then the algorithm uses the fact that for a balanced system the L/R ratio of a phase-to-earth fault and phase-to-phase fault at the same location will be the same and therefore the fault current phase angles (each with respect to the correct driving source voltage). The algorithm can then construct an equivalent phase-to-phase current model for the remaining last two phases to interrupt, based on the existing  $\phi$  and  $\tau$  estimations, and appropriately adjusted  $\alpha$  and  $\gamma$  values matching the equivalent phase-to-phase voltage of the affected phases. The “alternative”  $\alpha$  value will be based on the same fault inception time as for the three phase fault.

Searches are then made for viable current zero targets for each of the last two phases using both the phase-to-earth and phase-to-phase models. The earliest current zero time found from both searches is then used as the target for the respective phase. This will have the result that one of the phases will interrupt at the selected target and other will target a point slightly before its actual eventual interruption current zero, as shown in Figure 5.8.

It should be noted that while the scope of this thesis has been focussed on effectively earthed networks, the compromise targeting solution for the last two phases to clear will work equally for non-effectively earthed source systems where there is no zero sequence path.

## 5.5 Simulation examples of proposed method

The overall CFI process has been modelled and simulated in MATLAB [30]. Some examples of are presented here to demonstrate the process, prior to a more comprehensive summary of investigative simulations that will be presented in Chapter 6.

The “actual” fault currents generated for the simulations are based on the general fault current equation described by {5.2}. The A-phase phase-to-earth voltage is used as the base reference for the  $\gamma$  values for B and C phases, assuming a positive A-B-C phase rotation. A 6 kHz sampling rate has been used, forming also the basic iteration time step of 0.167 ms. For all the simulations a protection response time of 20 ms was used, as this provides a reasonable window to observe the algorithm behavior, though shorter protection response times, down to ¼-cycle, are possible, as was shown in the licentiate. A circuit breaker opening time of 20 ms was used, as is typical for modern HV SF<sub>6</sub> circuit breakers. An absolute minimum arcing time of 10 ms was used, together with an arc margin time of 1 ms, giving a CFI target arcing time of 11 ms.

The fault current time constant is 45 ms. The simulations shown here are without any simulated white Gaussian noise.

Figure 5.9 shows an example of a double phase-to-earth fault involving A and B phases. The top graph shows the phase-to-earth voltages and the currents ( $i_A$ : O;  $i_B$ : [];  $i_C$ :  $\Delta$ ). The grey shaded areas immediately prior to the current interruptions are the envelopes of the estimated currents for each phase for the CFI controlled arcing times. The direct protection trip circuit breaker opening time is shown by the vertical line (c. 0.08 s). The errors in the prediction of the target current zero times are shown in the upper left hand corner, together with the savings in arcing time achieved by the CFI operation compared to a direct protection trip operation. At the upper right hand side the difference in total fault clearing time between the CFI and direct protection trip operations is shown - in this case there is no difference. The actual and estimated

fault inception angles ( $\alpha_X$ ) for each phase are shown above the graph. Even with a 21 deg  $\alpha$ -error in A-phase, the resultant A-phase target time error is only 0.15 ms. Though there is no fault in C-phase, the  $\alpha$ -values reflect a synchronized closing of C-phase at the start of the simulation.

The middle graph shows the data window size and the  $\log_{10}$  F01 (phase-to-earth model) and F02 (phase-to-phase model) results for each phase. The initial data window is set at 5 ms and incrementally increased to 20 ms, whereupon it is shifted with each iteration until the fault is detected. At fault detection the start of the data windows in the fault phases are reset to the estimated fault inception instant (i.e. nearest associated time step) and then WLMS processing of the faulted phases is resumed once their data windows have reached the 10 ms minimum. As described earlier, under normal load conditions the phase-to-earth and phase-to-phase models use the same  $\alpha$  and  $\gamma$  values and so the F01 and F02 results remain the same until the fault is detected and the  $\alpha$  and  $\gamma$  values in the faulted phases updated accordingly. In this case the fault involves two phases to earth and so the F01 values are correspondingly higher than the F02 values for A and B phases and the target current zero times are predicted based on the phase-to-earth parameter based models in those phases.

The bottom graph shows the control signals and calculated waiting times for each phase. Active control signals have a value of “1” and an inactive value of “0”. At the top of this graph the common three phase protection trip signal is shown, occurring 20 ms after the fault inception. For each of the phases there is a “status” control signal that is driven by the F01 and F02 validation checks. Status is “1”, meaning “OK” if at least one of F01 or F02 is above the acceptance threshold value (i.e.  $\log_{10}(F0) = 2$ ), otherwise it is set to zero and the waiting time is then correspondingly set to zero. It will be noted that once the fault is detected the waiting times in all three phases are set to zero, until the status is “OK” in all three phases. Though it is assumed that there is single phase operation control of the circuit breaker, it is also assumed that all trip operations will be three phase, hence even the unfaulted C-phase waiting time is forced to zero in this short interval of uncertainty.

It can be seen that prior to the fault the waiting times in each phase cycle uniformly from 10 ms to 0 ms, with a 60 degree shift between them, corresponding to the 60 degree difference between successive current zeroes of the three phases under stable, balanced load conditions. The final CFI waiting times in each phase after the protection trip goes active are indicated in the test to the right hand side of the graph.

For comparison, Figure 5.10 shows an unearthed phase-to-phase CFI fault interruption, also involving A and B phases and with the fault starting at the same simulation time instant (i.e.  $t = 0.04$  s) as for the example shown in Figure 5.9 for the double phase-to-earth fault.

Two main differences can be observed between the CFI algorithm results for the double phase-to-earth and phase-to-phase fault cases. First, in the phase-to-phase case, the fault inception angles for A and B phases are now those referred to the  $U_{AB}$  phase-to-phase (or “line”) voltage and are 180 electrical degrees apart, reflecting the relative polarity of the current flows with respect to  $U_{AB}$ .

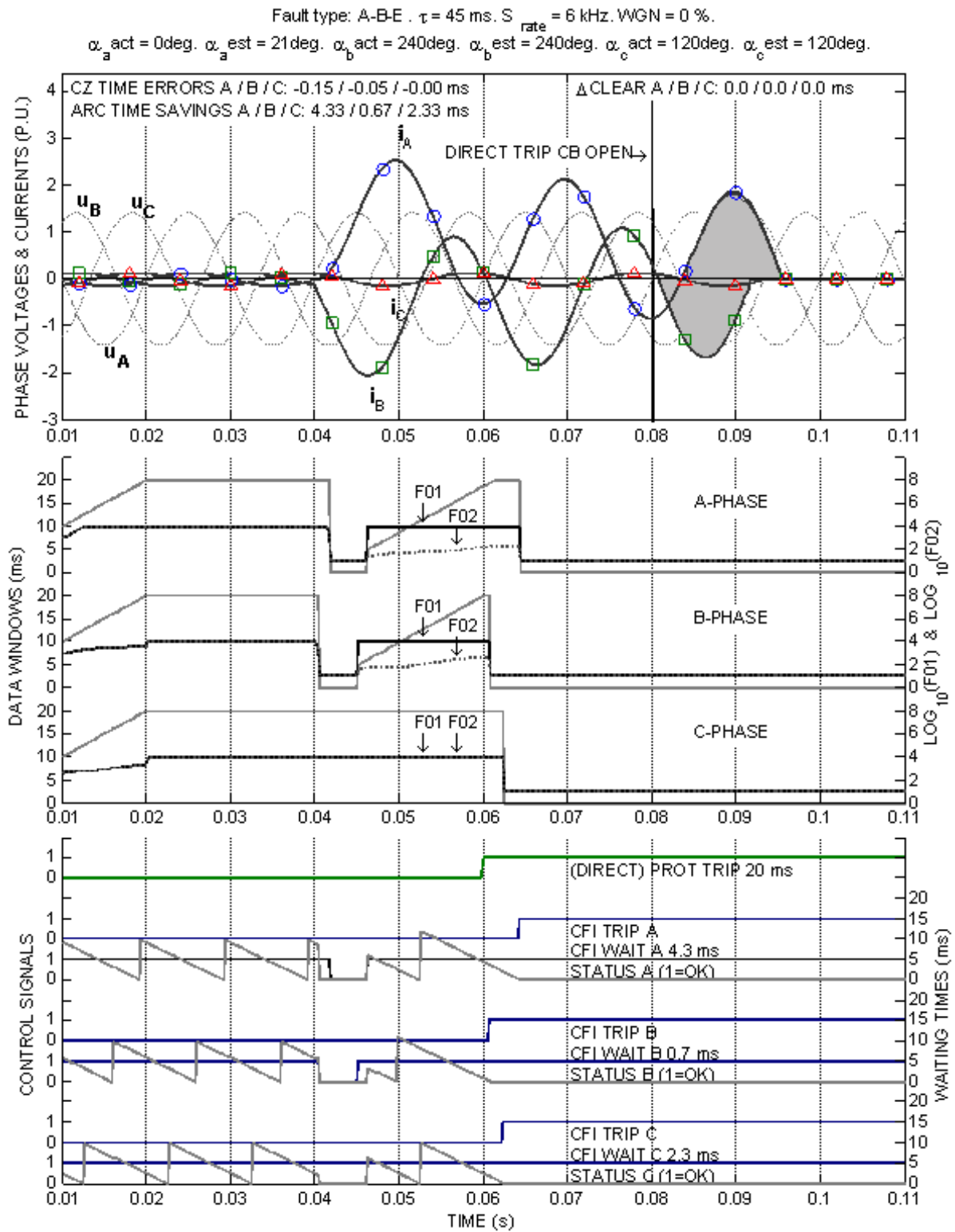
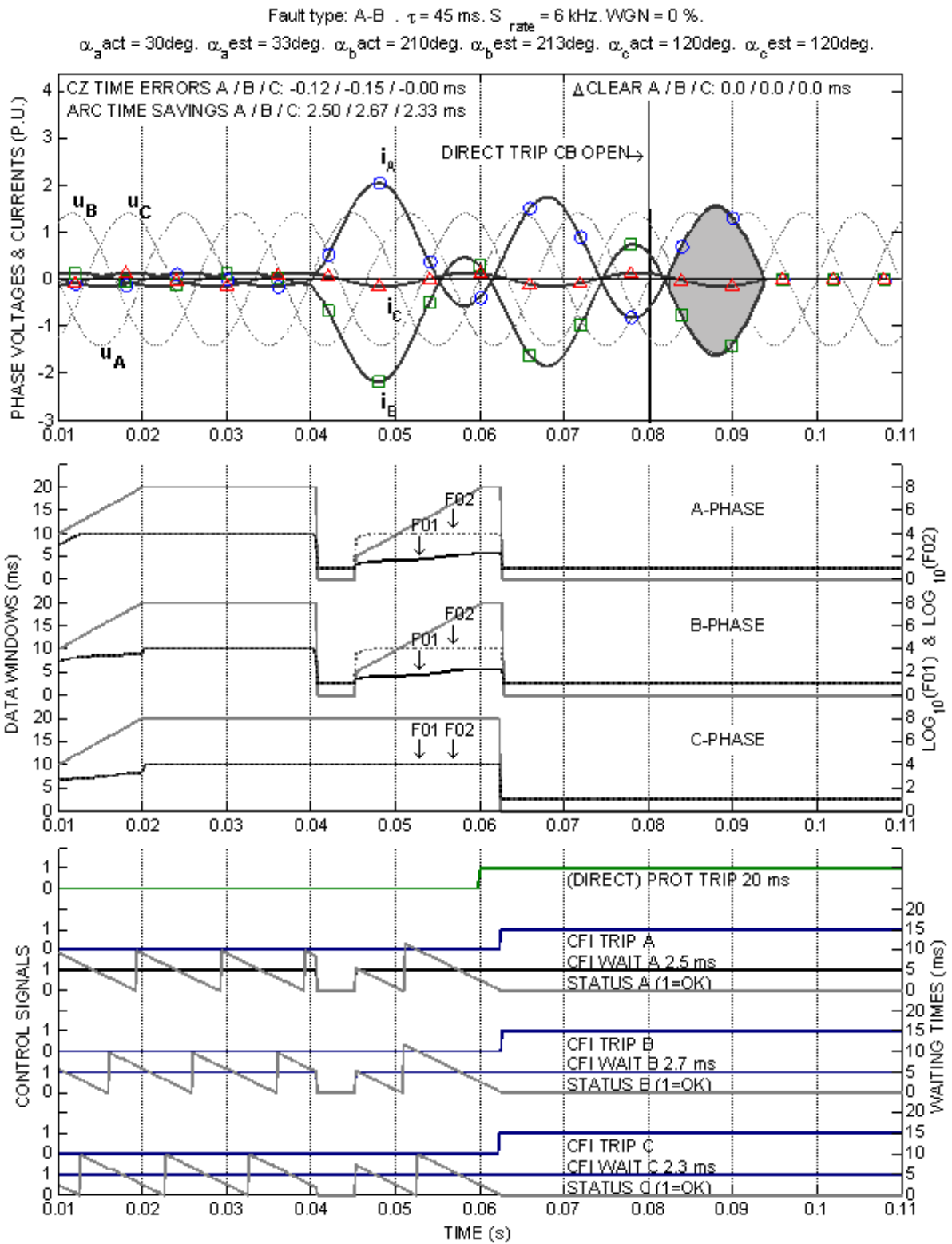


Figure 5.9 : Example A-B-E double phase-to-earth fault CFI interruption



**Figure 5.10 : Example A-B phase-to-phase unearthed fault CFI interruption**

Second, it can be clearly seen that in the post-fault F0 results that the F02 values in A and B phases are higher than their corresponding F01 values, indicating the algorithm has (correctly) identified the phase-to-phase unearthed fault type.

Two final examples of the algorithm performance are shown in Figures 5.11 and 5.12 for three phase earthed and unearthed faults respectively. The essential difference in both cases is the actual current zeroes that interruption occurs. C-phase is the first phase to interrupt in each example. The compromise target current zero times used for the last two phases (A and B) to interrupt are the same in both cases, but the actual interruption current zeroes differ according to the earth or lack of earth connection.

The impact of the compromise targeting on the current zero error is significant in only one of the phases in each case. In the earth fault case, A-phase targets what would otherwise be its unearthed fault interruption current zero point, but then interrupts in the earth fault case, 1.4 ms later.

In the unearth fault case, B-phase targets what equates to its earth fault current zero and then interrupts at the unearthed current zero point, 1.7 ms later. While these errors are significantly higher than the desired 0.5 ms error limit for all other fault cases, it is still within the a nominal 3 ms boundary that was explored in the high power experiments for a restricted CFI arcing window.

It should also be remembered that three phase faults are relatively uncommon on most transmission systems.

It can also be seen in these simulations how the waiting times are updated and change in each phase while the CFI algorithm waits for the protection trip signal to go active as the algorithm continuously updates which phase is expected to interrupt first and thereafter which phases are required to use the compromise targeting solution.



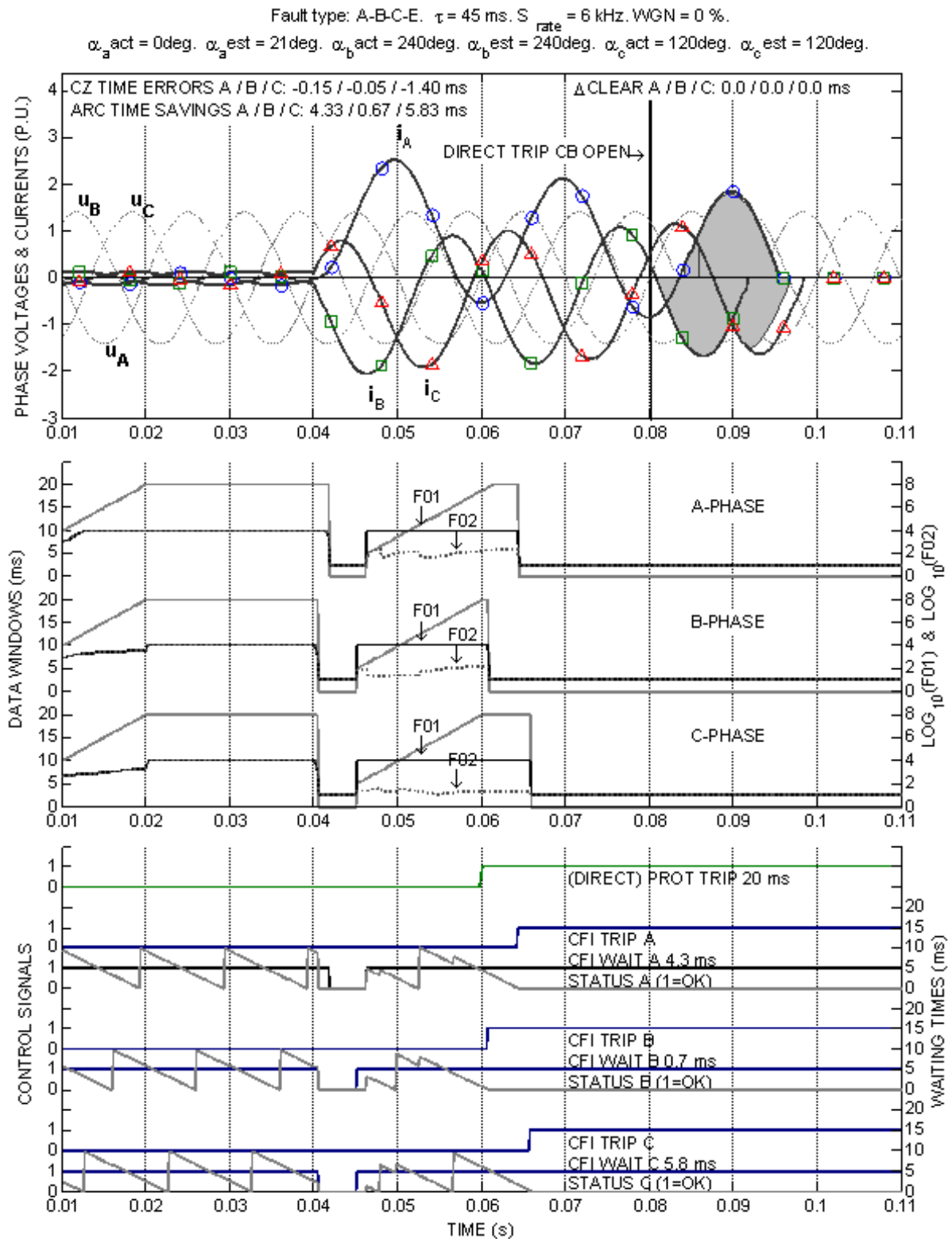


Figure 5.11 : Example of A-B-C-E three phase earth fault CFI interruption

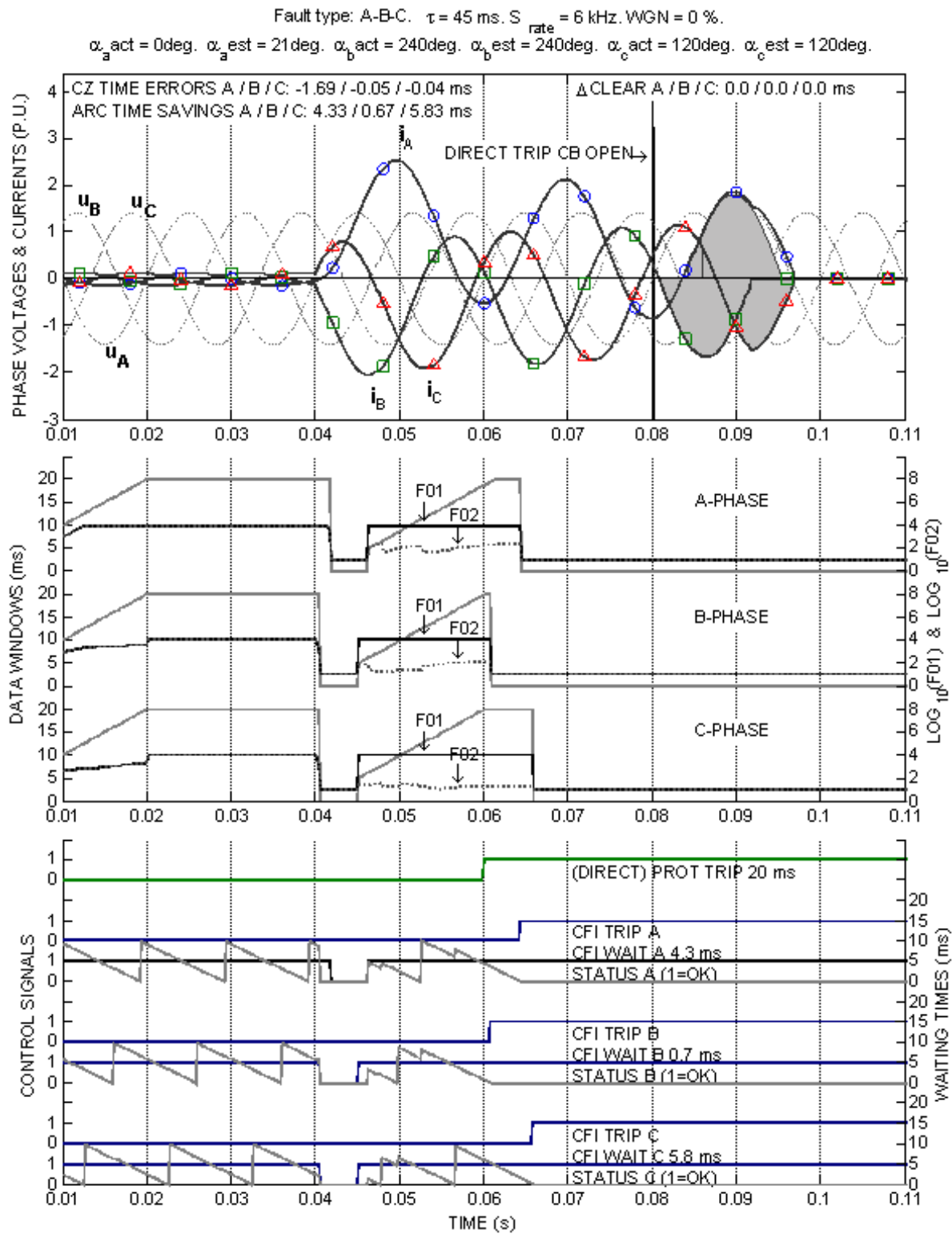


Figure 5.12 : Example of A-B-C three phase unearthed fault CFI interruption

## 6 Three phase controlled fault interruption - Simulation tests

The proposed CFI algorithm has been tested through a wide range of simulations made using MATLAB® [30]. The purpose of the simulations has been to verify the functionality of the algorithm for its intended applications and to investigate the sensitivity and robustness of the algorithm to both changes in power system parameters (e.g.  $\alpha$ ) and simulated disturbances (e.g. pseudo-random signal noise). Similar simulations were made for the single phase CFI algorithm described in the licentiate thesis [1], but then with a focus on the performance of the algorithm over both a range of time constants and fault inception angles. Naturally the range of possible simulation conditions grows by nearly an order of magnitude if considering three phase system fault cases and it is therefore necessary to restrict the scope of the simulations presented in this thesis to those that provide a sufficiently representative picture of the algorithm's performance.

First a brief description of how the simulations have been conducted will be given, followed by a summary of the performance indicators applied to assess the algorithm's performance. Then an explanation of which parameters have been varied and to what extent, will be given. Some single parameter set simulation examples will be presented and discussed, followed by summary results of larger scale parameter set multiple run simulations will be given. The final part of this chapter presents and discusses aspects not included in the simulations made within this work, together with recommendations for further simulation development.

### 6.1 Description of simulation program structure

The simulation program is essentially made up of three parts; fault current generation with an option for addition of random signal noise, CFI calculation, including modelling of the fault currents with the estimated parameter values (indicated by '^') and finally results extraction, as described in Figure 6.1. A common discrete sampling rate of 6 kHz was applied as this is similar to higher sampling rates used in modern digital protection relays [27] and provided convenient application of  $\alpha$  and  $\gamma$  values in steps of 30 electrical degrees.

The modelled system for the fault simulations was quite simple as the intention has been to verify the basic performance of the algorithm for single specific fault current cases. Essentially it was assumed that the system had an effectively earthed, infinite bus source with a specific and stable source-to-fault inductance and resistance, as described by Figure 6.2. This allowed focus on assessment of the basic "core" performance of algorithm and the effectiveness of the LMS method for parameter estimation and the F0 function for algorithm control, fault inception detection and fault type identification. The last section of this chapter will discuss the limitations of this power system model and the impact of the simplifications it involves with respect to possible "real world" application of the proposed CFI algorithm.

### 6.2 Performance indicators used for CFI algorithm assessment

In a similar approach to that described in the licentiate thesis [1], the performance of the algorithm for different parameter conditions has been assessed through the use of a set of performance indicators, each of which is defined below. Some additional performance measures have been developed for the assessment of the algorithm within the three phase network application.

### 6.2.1 Target current zero time error

One of the most critical measures of performance is the error in the estimation of target current zero times. This measure,  $\Delta t_{CZT}$ , is defined as the difference between the estimated current zero time,  $t_{CZE}$ , and the actual current zero time,  $t_{CZA}$ , as stated below:

$$\Delta t_{CZT} = t_{CZE} - t_{CZA}; \quad (\text{units: milliseconds}) \quad \{6.1\}$$

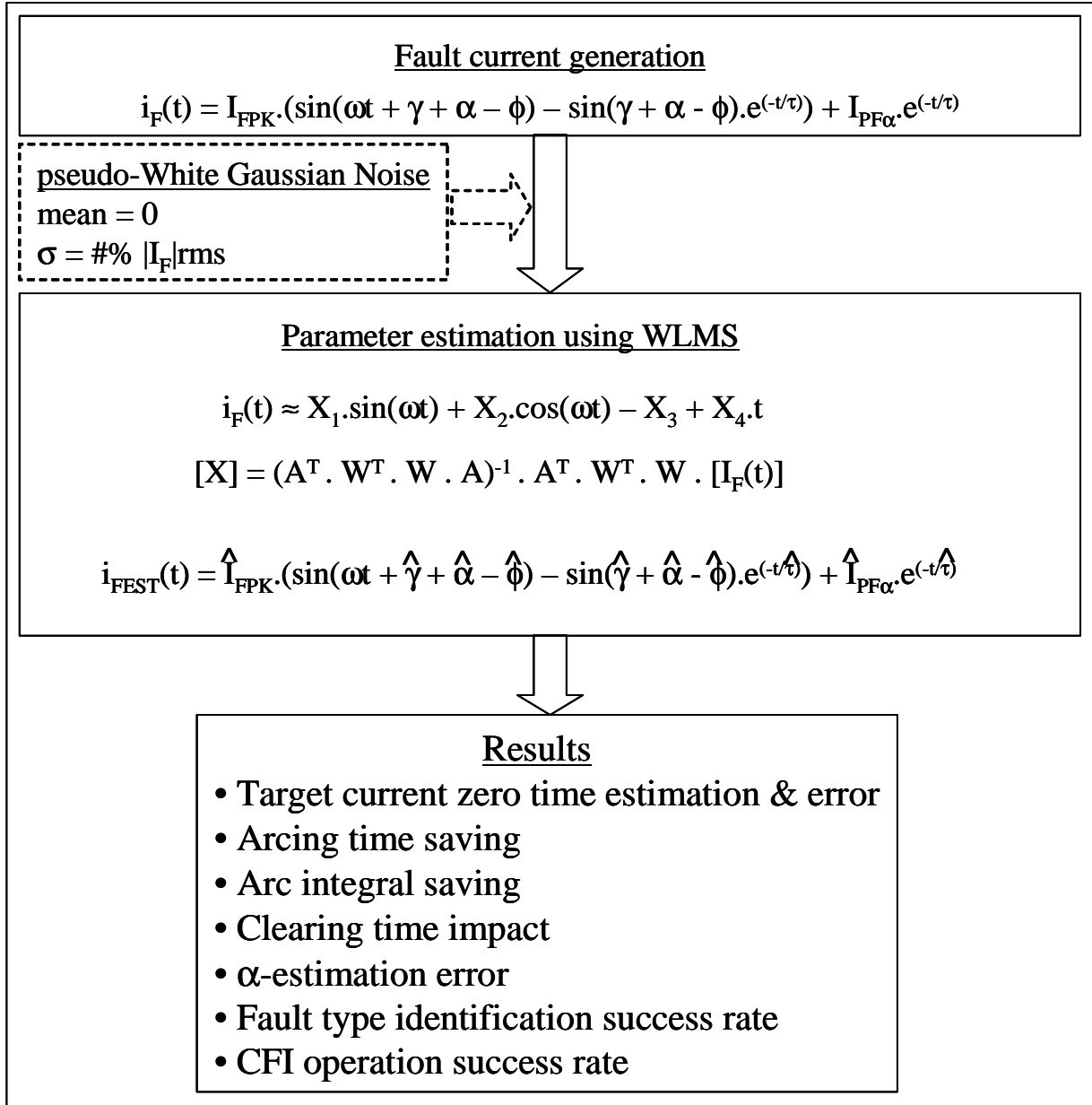


Figure 6.1 : Summary description of main steps applied in CFI simulations

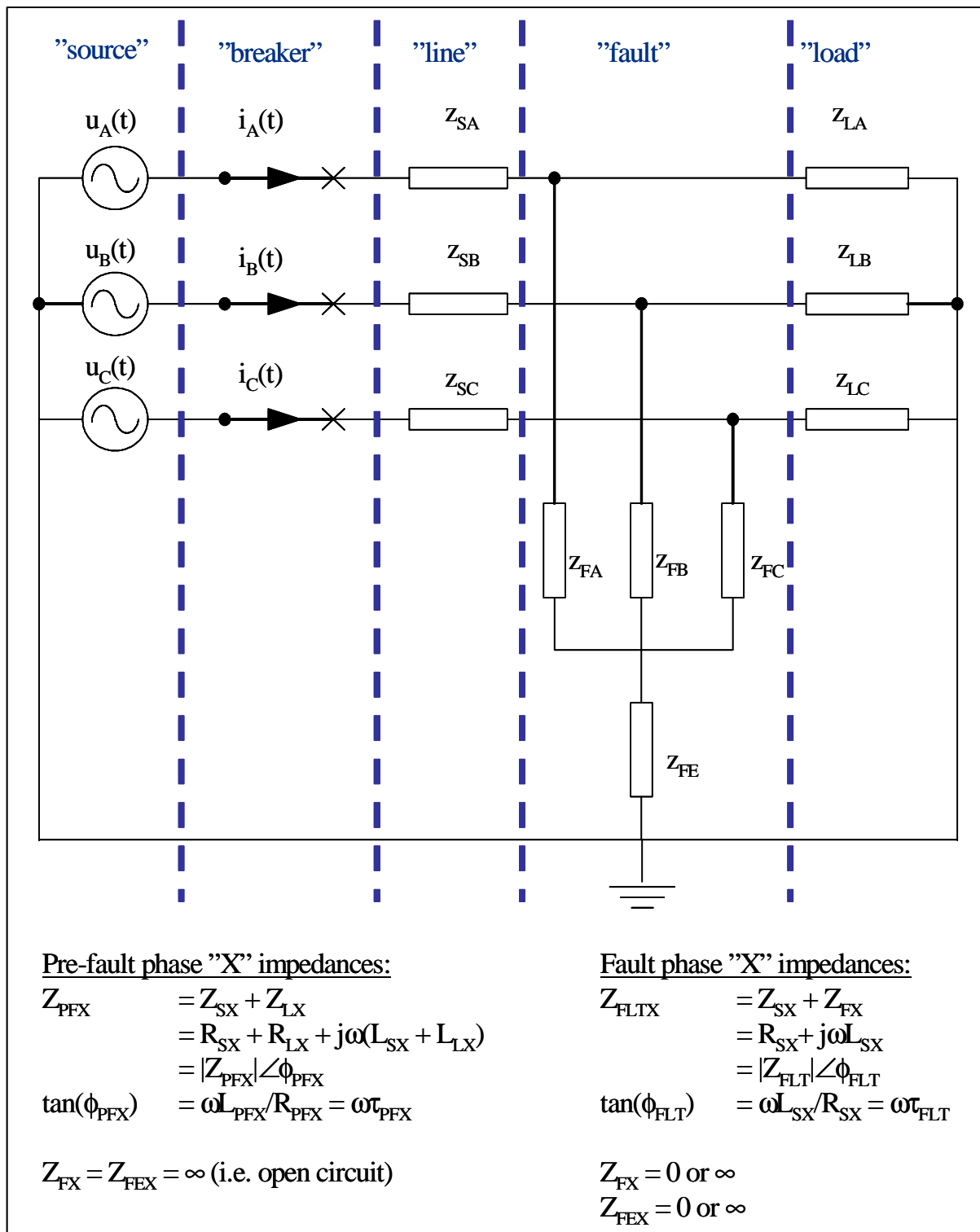


Figure 6.2 : Equivalent circuit for simulations

### 6.2.2 $\alpha$ -estimation error

This is a measure, in electrical degrees, of the error in estimation of the fault inception phase angle on the associated driving source voltage for a specific fault, as defined below:

$$\Delta\alpha = \alpha_{\text{EST}} - \alpha_{\text{ACT}}; \quad (\text{units: electrical degrees}) \quad \{6.2\}$$

### 6.2.3 Fault type identification success rate

The success rate of the algorithm to correctly identify the type of multi-phase fault is defined as the ratio,  $\text{SR}_{\text{FI}}$  (in percent) between the number of correctly identified faults,  $N_{\text{I}}$ , over the total number of faults simulated for a particular simulation batch run,  $N_{\text{T}}$ :

$$\text{SR}_{\text{FI}} = 100 \times N_{\text{I}} / N_{\text{T}}\% \quad \{6.3\}$$

### 6.2.4 CFI operation success rate

As mentioned in the licentiate, this measure could be defined in several ways, depending on the specific application interest of the CFI technique. Here a very basic definition has been applied, as the percentage ratio,  $\text{SR}_{\text{FI}}$ , between the number of operations executed as CFI,  $N_{\text{CFI}}$ , without resort to zero waiting time bypass operation, over the total number of faults simulated for a particular simulation batch run,  $N_{\text{T}}$ :

$$\text{SR}_{\text{FI}} = 100 \times N_{\text{CFI}} / N_{\text{T}}\% \quad \{6.4\}$$

### 6.2.5 Arcing time saving

The saving in arcing time,  $\Delta t_{\text{ARC}}$ , by using CFI,  $t_{\text{CFI\_ARC}}$ , compared to direct, non-synchronized tripping,  $t_{\text{DIRECT\_ARC}}$ , is one of the primary goals of CFI and as such forms an important measure of algorithm performance. The level of saving is dependent on both the minimum arcing time of the circuit breaker,  $t_{\text{MIN\_ARC}}$  and the arc margin time,  $t_{\text{ARC\_MGN}}$ , applied by the CFI algorithm and as such the savings presented in these simulations can only be taken as “indicative” of the specific circuit breaker and system parameters applied here.

$$t_{\text{CFI\_ARC}} = t_{\text{MIN\_ARC}} + t_{\text{ARC\_MGN}} \quad \{6.5\}$$

$$\Delta t_{\text{ARC}} = t_{\text{DIRECT\_ARC}} - t_{\text{CFI\_ARC}} \quad (\text{units: milliseconds}) \quad \{6.6\}$$

It should be noted that it is possible for  $\Delta t_{\text{ARC}}$  to be negative, up to a duration equal to  $t_{\text{ARC\_MGN}}$ . This occurs for the cases where the direct tripping of the circuit breaker would result in interruption with an arcing time between  $t_{\text{MIN\_ARC}}$  and  $t_{\text{CFI\_ARC}}$ .

### 6.2.6 Arc integral saving

The energy released by the arc in the interrupter can be evaluated by the integral of the arc power over the arcing time. If the arc voltage is assumed to be constant, which is generally a reasonable assumption for high current arcs (Flurschein, 2.3.11 [40]), then the integral of the arc current over the arcing time provides an equivalent relative measure of arc energy. The released arc energy is an important factor in both interrupter performance and contact wear and as such, the saving or reduction in the arc integral by restricting the arcing time is an important measure of the performance and impact of the use of CFI.

The arc integral saving is defined as described in the licentiate. Let  $A_1$  denote the arc integral for non-controlled fault interruption and  $A_2$  denote the arc integral for controlled fault interruption:

$$A_1 = \int_{t_{O1}}^{t_{I1}} |i_{arc}(t)| dt \quad \{6.7\}$$

$$A_2 = \int_{t_{O2}}^{t_{I2}} |i_{arc}(t)| dt \quad \{6.8\}$$

where

$t_{O1}$  = Non-CFI breaker opening time

$t_{O2}$  = CFI breaker opening time

$t_{I1}$  = Non-CFI fault interruption time

$t_{I2}$  = CFI fault interruption time

Then the arc integral saving,  $S_{AI}$ , is defined as the following percentage

$$S_{AI} = \left( 1 - \frac{A_2}{A_1} \right) \cdot 100 \% \quad \{6.9\}$$

Provided ( $A_2 < A_1$ ) then ( $S_{AI} > 0$ ), else for ( $A_2 > A_1$ ), then ( $S_{AI} < 0$ ). **The most desirable result from the application of controlled fault interruption is ( $S_{AI} > 0$ ), in addition to  $t_{I2} = t_{I1}$ ,** implying that the arc integral value is reduced compared to non-controlled interruption, but without any prolongation of the total fault clearing time.

### 6.2.7 Clearing time impact

In order to maintain power system transient stability in addition to mitigating the potential damage they may cause, fault currents must be interrupted quickly. Hence the total fault clearing time is an important parameter in the design and performance of the protection of the power system. This places a major constraint on CFI, as ideally the total fault clearing time using CFI should be no greater than for direct protection tripping.

For the single phase CFI method the clearing time impact was simply defined as the difference between the CFI clearing time,  $t_{I1}$ , and the direct trip clearing time,  $t_{I2}$ , as per {6.10},

$$\Delta t_{clear} = t_{I1} - t_{I2} \quad \{6.10\}$$

For three phase network CFI the above definition could be modified to be the difference in clearing times in the last phases to interrupt for both CFI and direct tripping. Due to the addition of an error time margin to the minimum arcing time in setting the targeted CFI arcing time, there will be a certain proportion of clearing times in each phase that will be longer using CFI than direct tripping. However in the three phase case this proportion will be lower for a given number

of interruptions as prologations will be spread over the three phases. Provided the CFI error time margin can be kept small (e.g. 1 ms) with respect to the nominal minimum arcing time (e.g. 10 ms) the overall proportion of prolonged clearing times can be expected to be also small (e.g. less than 10%) and can be factored into protection co-ordination settings to minimize the impact on contingency planning for maintaining power system transient stability.

### 6.3 Parameter values used for CFI simulations

There are over a dozen main parameters, some with considerable ranges of values, that could be varied within the structure of the CFI simulation program and for practical reasons the range and combinations of applied values must be restricted. Selection of the parameter values tested was made with a view towards using values representative of “typical” HV circuit breakers, HV protection systems and faults. A minimum set of combinations was applied to provide verification of the most important features of the proposed algorithm. A brief description of the values used in the simulations for the most significant parameters is given below.

#### 6.3.1 Fault types

There are eleven (11) main combinations faults involving the three phases and earth, as described in Chapter 2 earlier. Simulations are possible for all of these fault types, however the results presented here have been limited to selected examples of four fault cases that illustrate key features of the extension of the CFI algorithm from the single phase version described in the licentiate to the three phase version presented in this thesis. The presented fault cases here include:

1. A-B phases-to-earth
2. A-B phase-to-phase fault, without earth connection
3. A-B-C phases-to-earth
4. A-B-C three phase fault, without earth connection

Single phase earth faults are not included in the results here, though are possible to simulate, as the performance of the CFI algorithm for such faults has already been extensively described in the licentiate thesis. Simulation of the two phase fault cases, involving and not involving earth provide a means of illustrating the performance of the algorithm to discriminate between these two cases using comparison of the F0 ANOVA results for both the phase-to-earth and phase-to-phase parameter models.

The three phase fault simulation cases will show how it is not possible for the proposed algorithm to discriminate between the earthed and non-earthed fault case due to the similarity in fault current behavior prior to the interruption in current in one phase. As such it will be shown how the algorithm implements its “compromise” targeting solution for the last two phases to interrupt and the impact of this strategy on the algorithm performance indicators.

Though in reality there is a non-uniform probability distribution of different fault types (see Table 2.1), it has been assumed for these simulations that all faults have an equal probability of occurrence.



### 6.3.2 Fault and load current magnitudes, $I_F$ and $I_{LOAD}$

Though the proposed algorithm is primarily directed towards application on HV and EHV systems and has been developed with HV SF<sub>6</sub> circuit breakers in mind, no consideration of specific fault current levels has been made. Rather the simulations have been conducted using per unit values of current, with 1 per unit being defined as the r.m.s. (symmetrical) fault current magnitude.

Typically there is approximately a 10:1 ratio between the fault current interruption rating of a circuit breaker and its normal load current rating [5], [9]. As such a similar ratio has been applied here, with the pre-fault simulated load current having a 0.1 p.u. r.m.s. magnitude. This reflects the simulation of the algorithm within a “strong” (infinite bus), effectively earthed network, typical for HV and EHV transmission systems worldwide. As will be discussed later, the performance of the algorithm in weaker or non-effectively earthed networks, where the ratio between fault and load current magnitudes is closer to 1:1, needs to be further examined.

### 6.3.3 Power system frequency, $f$

While there is no inherent limitation to the power frequency to which the proposed CFI algorithm can be applied, subject to an appropriate sampling rate, all the presented simulations have been made using 50 Hz, as this is the most common power frequency used.

It is worth noting that one of the interesting potential applications of the proposed CFI method for circuit breaker performance enhancement, is “railway” applications, where 16 2/3 or 25 Hz systems exist. The majority of modern (SF<sub>6</sub>) HV AC circuit breakers are designed for use on 50 or 60Hz systems. In order to use such circuit breakers on lower frequency systems, it is necessary to slow down their contact separation speed in order to ensure at least one current zero can be encountered before contact travel has ceased. This slowing down of the circuit breaker contact (and puffer) system, results in a reduction in the interrupting capability of the circuit breaker and therefore the circuit breakers must typically be correspondingly de-rated for use on lower than 50Hz systems. As the CFI algorithm can predict current zero times, it should be possible to apply the CFI algorithm to the control 50 / 60 Hz circuit breakers used on 16 2/3 and 25 Hz systems to target arcing times at “normal” (i.e. 50 / 60 Hz) opening speeds and thus avoid reduction in the circuit breaker current interruption rating.

### 6.3.4 3-phase voltage reference angles, $\gamma_X$

On the basis of the simulated power system being a “strong”, infinite bus, it has been also assumed that the driving source voltages maintain their relative phase differences, even during fault conditions. It should be noted that the simulated system assumes the measured voltage references supplied to the algorithm are the “ideal” references from the source and do not reflect the angular difference between voltages measured and “ideal” (zero impedance) source at the circuit breaker i.e. the impact of the angular difference in the voltages due to the ideal source to circuit breaker impedance is neglected. The possible impact of this assumption is discussed later in the last section of this chapter.

For the presented simulations an A-B-C positive sequence phase rotation has been used, with A-phase-to-earth voltage used as the reference phase. The resultant phase-to-earth and phase-to-phase  $\gamma$  values are therefore as shown in Figure 6.3 below.

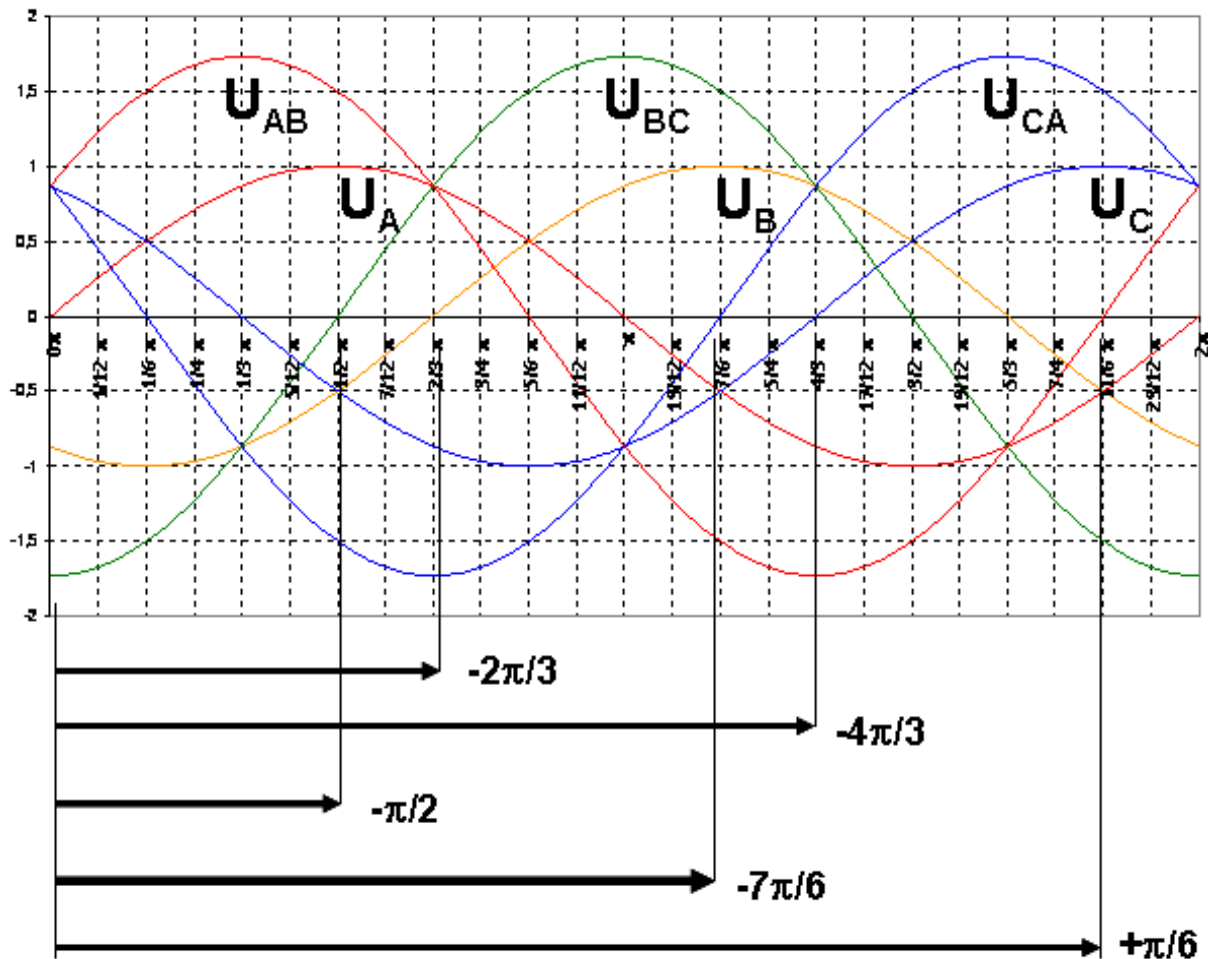


Figure 6.3 : Values of  $\gamma$  using A-phase reference voltage for A-B-C phase rotation

### 6.3.5 Fault inception voltage angles, $\alpha_X$

As faults are random, they can theoretically occur at any angle,  $\alpha$ , with respect to the associated driving source voltage. The main impact of the  $\alpha$ -value is the level and polarity of the transient asymmetry exhibited by the fault current. In order to limit the number of simulations, yet provide a comprehensive picture of algorithm performance over a full cycle range of  $\alpha$ -values, a range of 0 to 330 electrical degrees in 30 degree steps has been used.

### 6.3.6 Fault phase angle, $\phi$ , and time constant, $\tau$

A comprehensive range of time constants were tested and presented in the licentiate work, examining among other things, the effectiveness of the first order taylor series approximation of the exponential components used in the WLMS parameter estimation. As the algorithm presented here uses the approximation method, it was decided to limited simulations only to  $\tau = 45\text{ms}$  and  $\phi = 86\text{ deg}$  for 50Hz as this value of time constant corresponds to the basic standard values used for asymmetrical fault interruption type testing of HV AC circuit breakers in accordance with IEC standards [5].

### 6.3.7 Protection response time, $t_{\text{PROT}}$

In the licentiate work, protection response times of 5 ms and 20 ms were used in the simulations (See Chapter 7 in [1]), in order to see the response of the algorithm to “ultra-fast” and “nominal” protection system response times. For the purposes of investigating the effectiveness of the F0-based fault type identification method under a prolonged period, only a 20 ms protection response time has been used in the three phase network simulations. The “status” control flag that is set by either of the F01 and F02 values being above the F0 threshold provides an indication of how quickly the algorithm can achieve viable target current zero estimations and the simulations have shown, even under “noisy” signal conditions, that the three phase algorithm can perform well down to at least a 10 ms “fast” protection response time. Without signal noise, the algorithm can perform well even down to 5 ms or quarter cycle protection response times. For such short protection response times the performance of the algorithm could be made more noise robust by reverting to the 0-order approximation of the exponential component (i.e.  $e^{(-t/\tau)} \approx 1$ ) as used by Pörtl, however it should be noted that this lower order approximation will not work as well for longer data sampling windows or rapidly decaying DC components.

### 6.3.8 Circuit breaker opening time, $t_{\text{CB\_OPEN}}$

A fixed circuit breaker opening of 20 ms has been used, comparable to typical opening times of modern HV SF<sub>6</sub> circuit breakers, as described in the licentiate (2.3.2) [1].

### 6.3.9 Circuit breaker minimum arcing time, $t_{\text{MIN\_ARC}}$

A fixed circuit breaker minimum arcing time of 10 ms has been used. As seen from the data presented in Chapter 3, this corresponds to a typical minimum arcing time for a modern HV SF<sub>6</sub> circuit breaker, interrupting at its full symmetrical current rating.

### 6.3.10 Target CFI arcing time, $t_{\text{CFI\_ARC}}$ , and arc margin, $t_{\text{ARC\_MGN}}$

In order to simulate nominal variations that may occur in practice for circuit breaker opening times, minimum arcing times and errors in the estimation of target current zero times by the CFI algorithm, a target arcing time margin of 1 ms has been used, resulting in a total target arcing time of 11 ms.

### 6.3.11 Pseudo-White Gaussian Noise (WGN)

In order to investigate the robustness of the proposed method to signal distortion, simulated pseudo-random noise vectors, mimicing White Gaussian Noise, were generated using the MATLAB “randn” function. The nominal intended characteristics of each noise vector were a normal probability distribution with a zero mean and 1 per unit standard deviation ( $\sigma$ ). An example of one of the noise vectors and a histogram of its values is shown in Figure 6.4.

The noise vectors were only applied from the time of fault inception and scaled in percent with respect to the 1 per unit nominal fault current magnitude i.e. “10%” noise would have a nominal 0.1 per unit standard deviation.

### 6.3.12 Sample rate

A 6 kHz sampling and time step rate was used in all the simulations presented here. This is consistent with typical sampling rates used in modern digital protection relays [21],[27] and

provided convenience both in implementing a range of  $\alpha$  values from 0 to 330 degrees in 30 degree steps, as well as 3 degrees resolution in estimation of  $\alpha$  estimation errors.

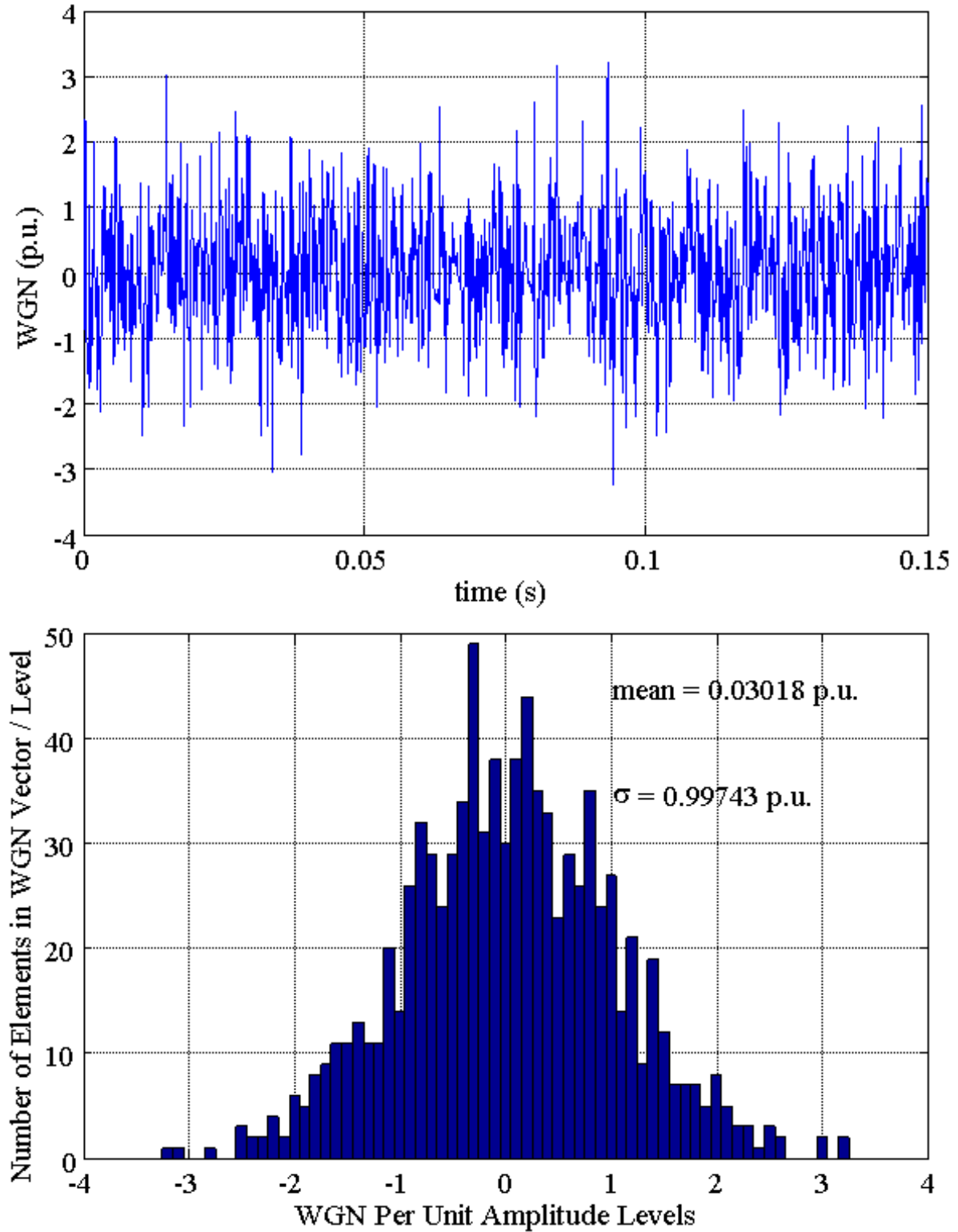


Figure 6.4 : Example of pseudo-random noise vector and associated histogram

## 6.4 Single parameter set CFI simulation examples

Examples of single  $\alpha$ -value CFI simulations will now be presented for two and three phase fault cases, with and without earth connection. The purpose of these examples is to illustrate how the algorithm manages multiple phase faults, with the addition of the simulated WGN, as a prelude to multiple run CFI results that focus on the robustness of the algorithm when tested with the pseudo-random WGN. The single parameter simulations are in the same format and present the same fault cases without WGN, as were shown at the end of Chapter 5.

### 6.4.1 Double phase-to-earth fault

Figure 6.5 shows a fault between A and B phases and earth, starting at  $\alpha_A = 0$  deg at time  $t = 0.04$  s. This simulation includes pseudo-WGN (mean = 0,  $\sigma = 0.1$  p.u.) signal noise applied from the fault inception instant, until the protection trip is active, corresponding to the main data processing time for updated parameter estimation. The top plot shows the phase voltages (dotted) and currents for all three phases. The shaded areas prior to current interruption indicate the CFI arcing times. The vertical line at  $t = 0.08$  s, indicates the opening time of the circuit breaker for non-controlled, direct protection tripping.

The middle plot shows, for each of the three phases, the size of the data sampling windows and the results of the F0 tests made for the phase-to-earth (F01) and phase-to-phase (F02) parameter estimation current models. Note that the minimum data window size is set at 5 ms. As this fault case involves earth, the phase-to-earth parameter estimations provide the more accurate model and therefore the F01 values are higher than the F02 values during the fault and the algorithm therefore uses the phase-to-earth parameter model to estimate the target current zero times for implementing CFI.

The bottom plot shows the protection trip signal, the calculated waiting times for the CFI trip signals for each phase, together the eventual per phase CFI trip signals and the status control signals for each phase. It can be seen that the WGN affects the WLMS process and status signals in the faulted phases are not able to consistently return to the “OK” status before approximately 8 ms after fault inception. However, this would still permit the algorithm to function with a protection response time down to a 10 ms level.

There is not a significant difference in the target current zero estimation times between the simulation shown in Figure 6.5 and the same simulation without WGN shown earlier in Figure 5.9. There are differences in the errors in the  $\alpha$  estimation values for the faulted phases, though in the case of the signal noise it actually results in a reduction in the error as the F01 value drops faster due to the signal distortion - such a trend may not be the same in the event of pre- and post-fault inception signal distortion.

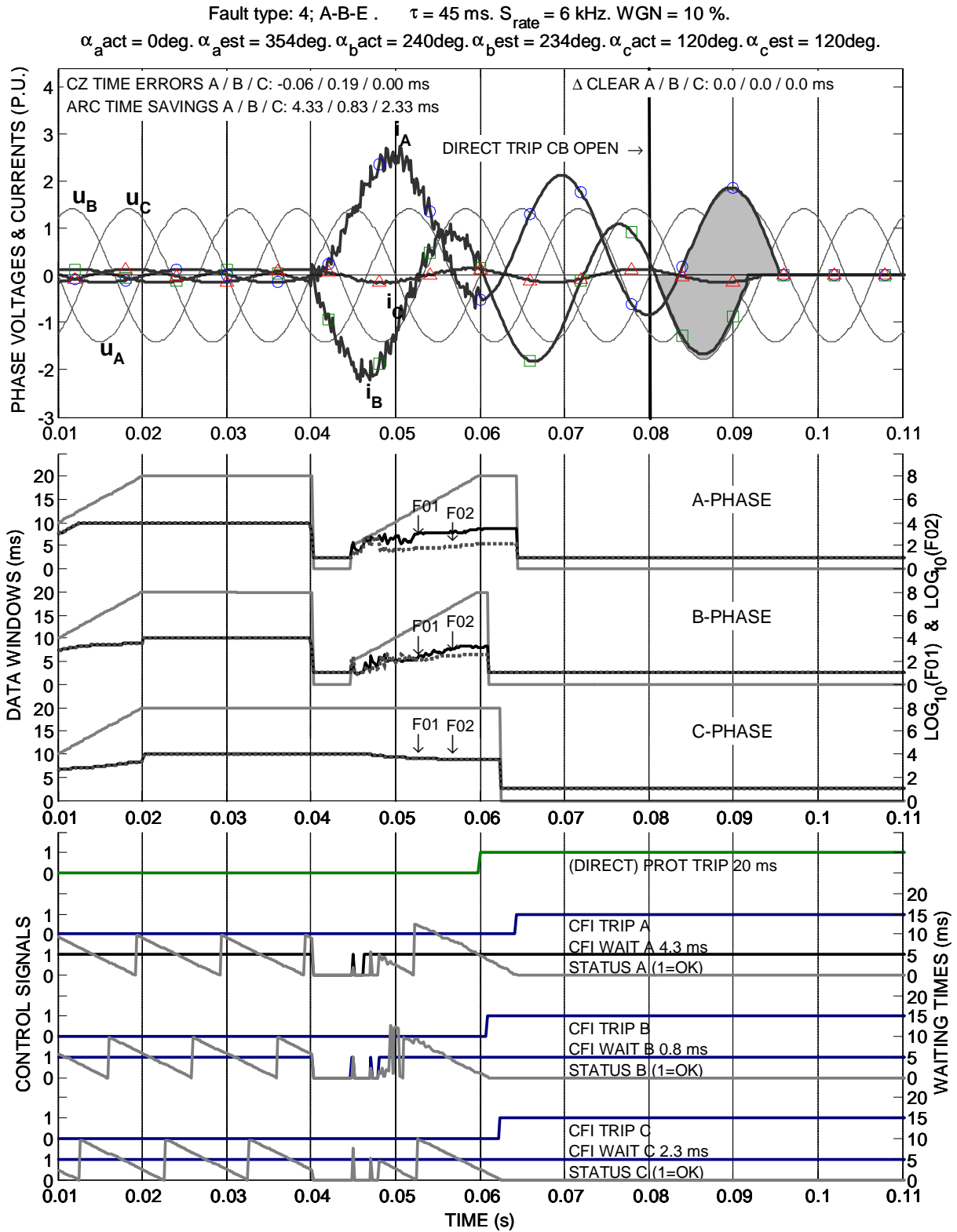


Figure 6.5 : A-B-E double phase-to-earth fault simulation with 10% WGN

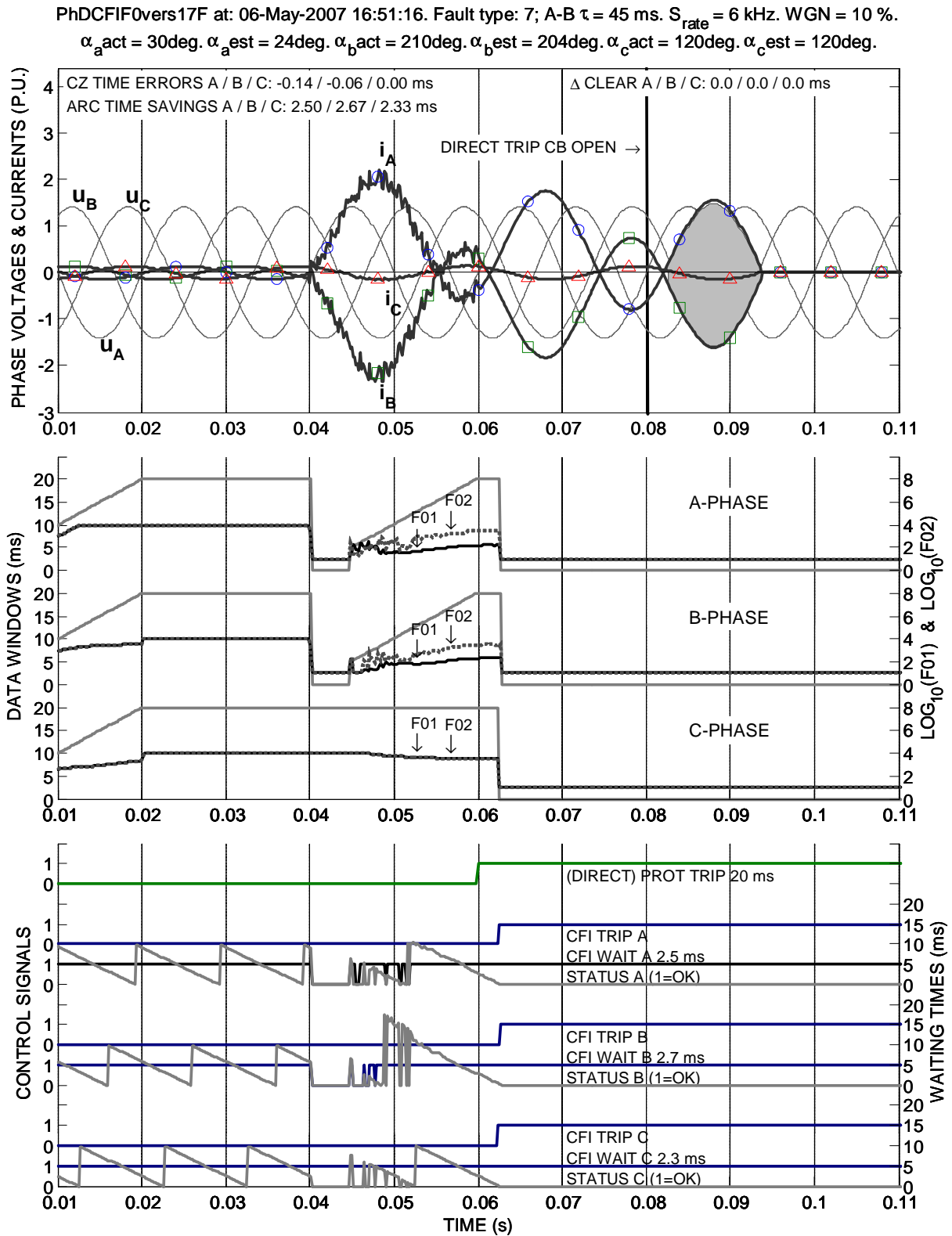


Figure 6.6 : A-B phase-to-phase fault simulation with 10% WGN

### 6.4.2 Phase-to-phase fault without earth

Figure 6.6 shows a phase-to-phase fault without earth for the same phases (A and B), fault inception time and equivalent  $\alpha_A = 0$  deg fault inception angle as simulated in 6.4.1 and for the simulation without WGN shown earlier in Figure 5.10.

Again there are only small differences in the eventual target current zero time errors between the simulation with and without 10% WGN, and only minor differences in the  $\alpha$  value estimation. The minimum response time of the CFI algorithm, after fault inception and when “stable” results are obtained above the F0 threshold is also approximately 8 ms in the faulted phases, supporting the case that the algorithm could be used in conjunction with a “fast” half cycle protection system, even under “noisy” signal conditions.

### 6.4.3 Three phase fault with and without earth connection

Figures 6.7 and 6.8 show simulations of the three phase to earth and three phase without earth fault cases, with 10% WGN, respectively. Both have similar (6 deg) errors in  $\alpha$  estimation for all three phases and the minimum CFI response time is approximately 8 ms as for the earlier simulations. The target current zero crossing time errors are consistent with the earlier simulations of the same type without WGN, shown in Figures 5.11 and 5.12.

Overall the algorithm shows good performance under noisy signal conditions for the WLMS stage of the CFI process, though the results suggest that the performance is limited for applications with a protection response time down to 10 ms or half a power frequency cycle. The final section of this chapter will present results of multiple run simulations, over a complete period range of fault inception  $\alpha$  angles, conducted for a consistent set of WGN simulated noise vectors.

The WLMS method can be noise and data window size sensitive and it should not be overlooked that other numerical methods may provide a more robust estimation of the fault phase angle with a larger noise tolerance. Further studies of the noise withstand robustness of the algorithm could be made, considering pre- and post- fault inception noise and developing a signal noise model more representative of that observed from field fault recordings.



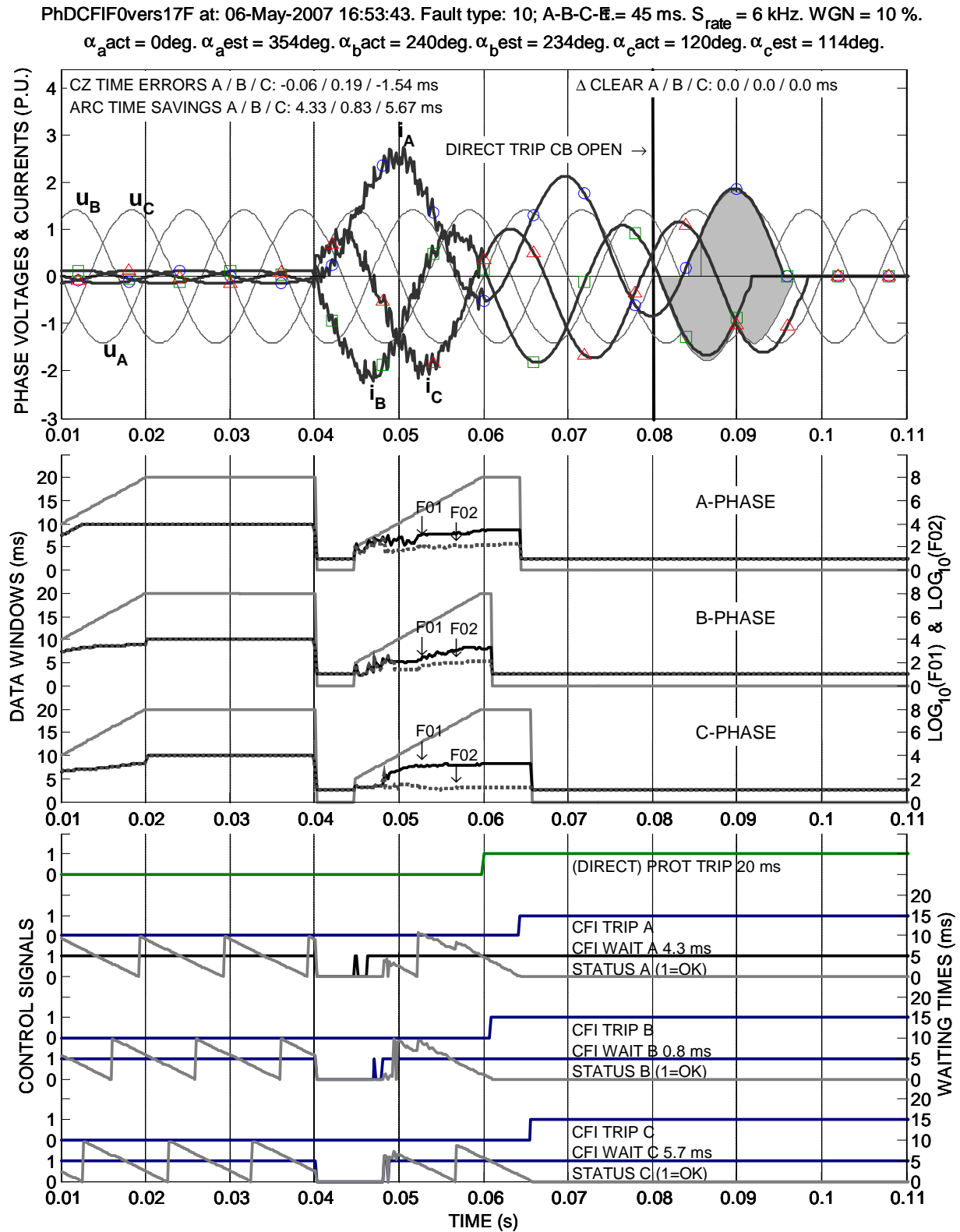


Figure 6.7 : A-B-C-E three phase-to-earth fault simulation with 10% WGN

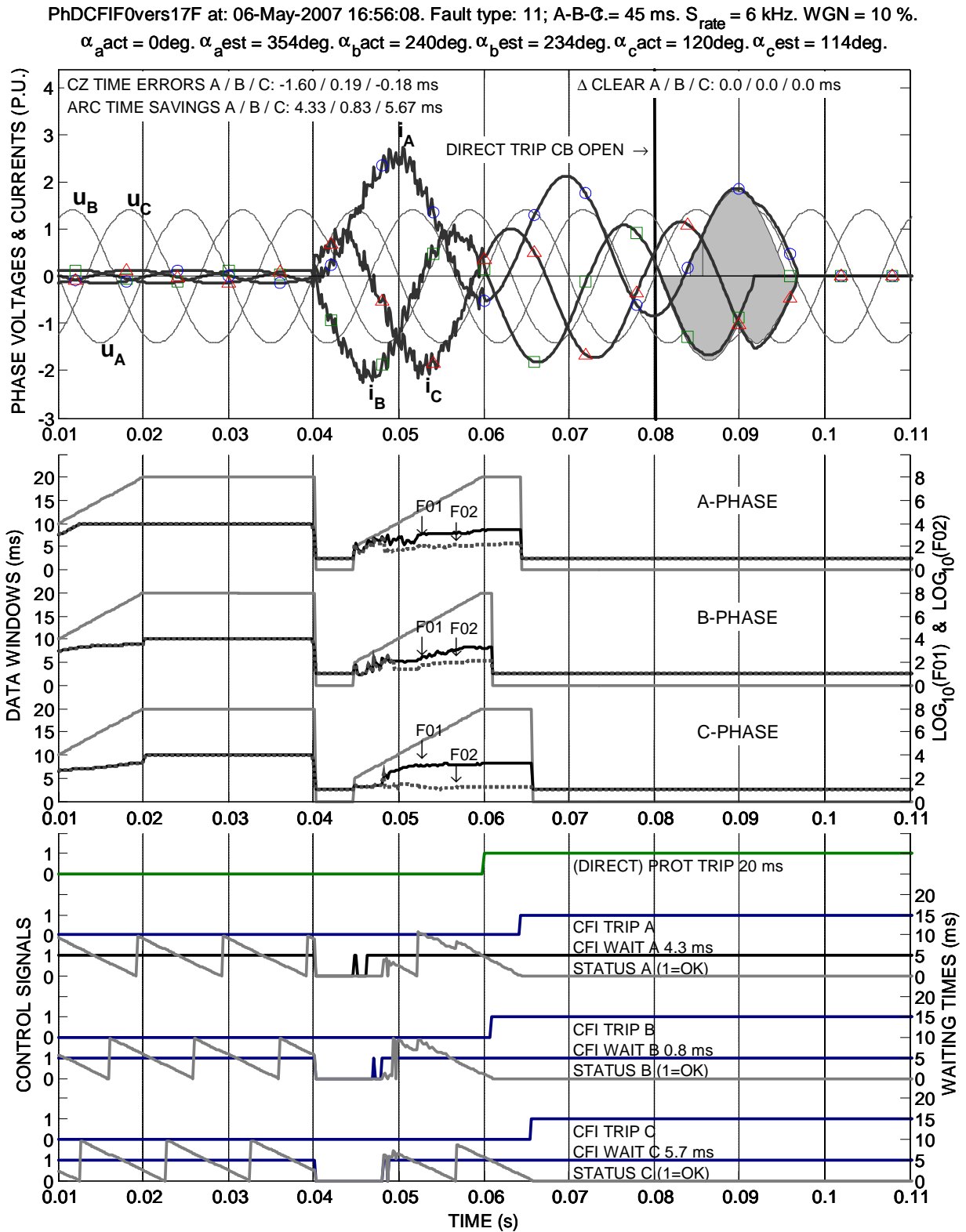


Figure 6.8 : A-B-C three phase fault without earth simulation with 10% WGN

## 6.5 Baseline “ideal” CFI simulation results

Prior to presenting the summarized performance of the proposed CFI algorithm for multiple combinations of fault type, fault inception angle and signal noise, it is of interest to summarize the potential “baseline” results that could be obtained from an “ideal” CFI algorithm. The ideal CFI method is defined as a control scheme that could predict the target current zero instants exactly for phase-to-earth and phase-to-phase faults, but only implement a compromise targeting solution for three phase faults.

The assessment of the ideal CFI method performance has been focussed on the arcing time and arc integral savings that can be obtained for all eleven multi-phase faults types, based on a range of fault inception angles (0 to 330 electrical degrees in 30 degree steps), but restricted to a nominal 45 ms time constant, 20 ms protection response time, 20 ms circuit breaker open time, 10 ms minimum arcing time and 1 ms CFI arc margin. These results also provide a basis for comparison and assessment of the performance of the proposed CFI method when subjected to random signal noise, presented in the next section.

Figure 6.9 shows the average arcing time and arc integral savings for all multiphase fault cases. The single and double phase-to-earth cases show comparable results for the faulted and healthy phases, as should be expected, given the single phase processing approach applied. The minor differences in the faulted phase savings for the phase-to-phase unearthed faults is due to the impact of the pre-fault load current on the respective faulted phase currents. Both of the three phase fault case average results are affected by the compromise targeting solution applied to the last two phases to interrupt, which results in an inherent “error” in the targeting for one of the phases. The differences in the savings results for each of the three phase fault cases is due to the combination of the compromise targeting method and the difference in the current behaviors of the last two phases to interrupt between the earthed and unearthed fault cases.

Figure 6.10 and Figure 6.11 show provide more detail of the arcing time and arc integral savings for four selected fault cases; A-B-E, A-B, A-B-C-E and A-B-C. The results are presented as histograms for each fault case, for which twelve evenly spread fault inception angles have been used. The savings in arcing time and arc integrals can be seen to be reasonably uniformly spread, consistent with the uniform distribution of fault inception angles. The deviations from complete uniformity in the savings can be attributed to the transient asymmetry inherent in the simulated fault current, which causes the current zero times to be non-periodic.

A comparison of the Figure 6.9 to 6.11 results to those arising from multiple noise case simulations will be presented in section 6.6.7.

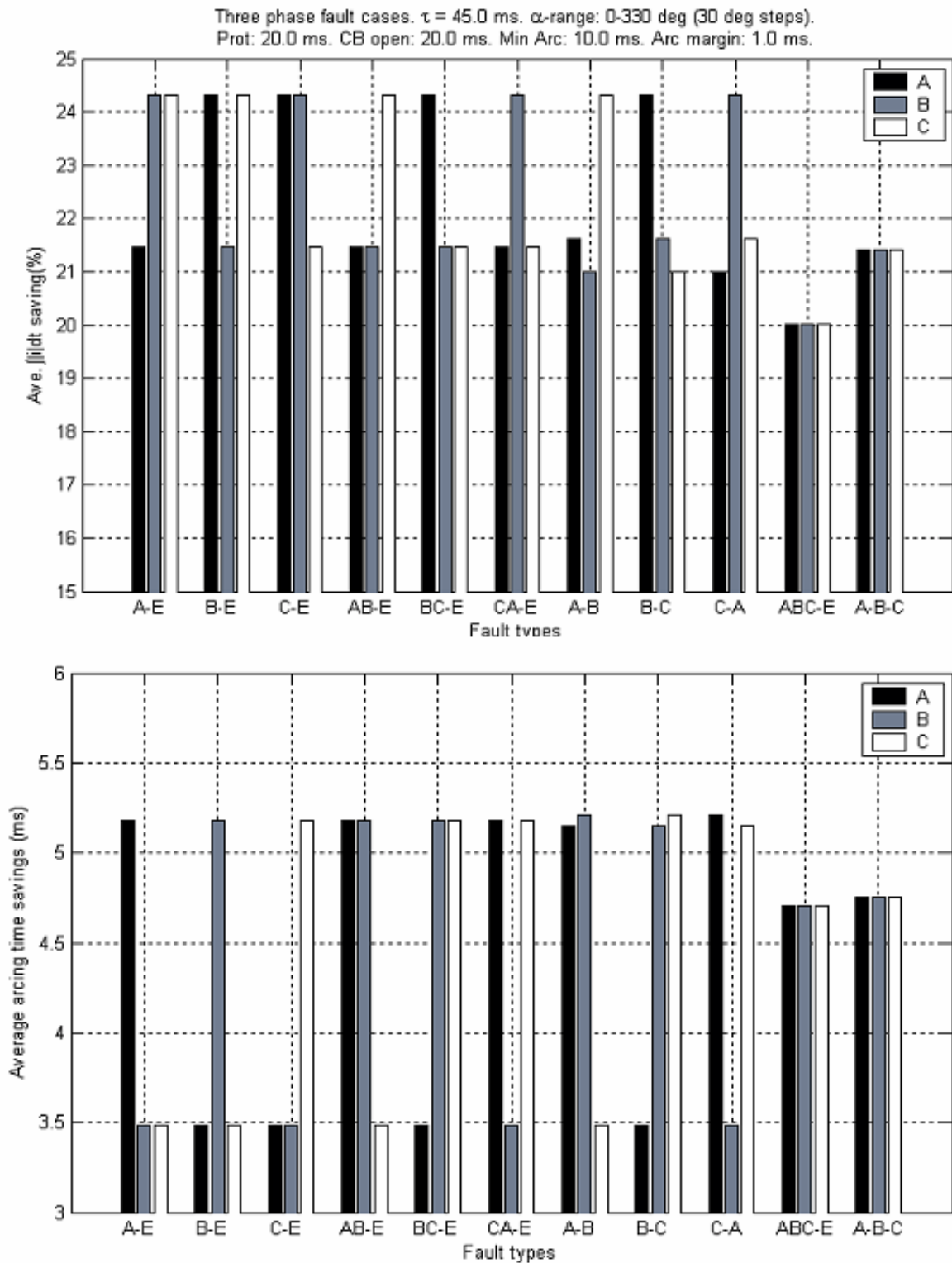


Figure 6.9 : Average arc integral and arcing time savings using “ideal” CFI for given operational parameters

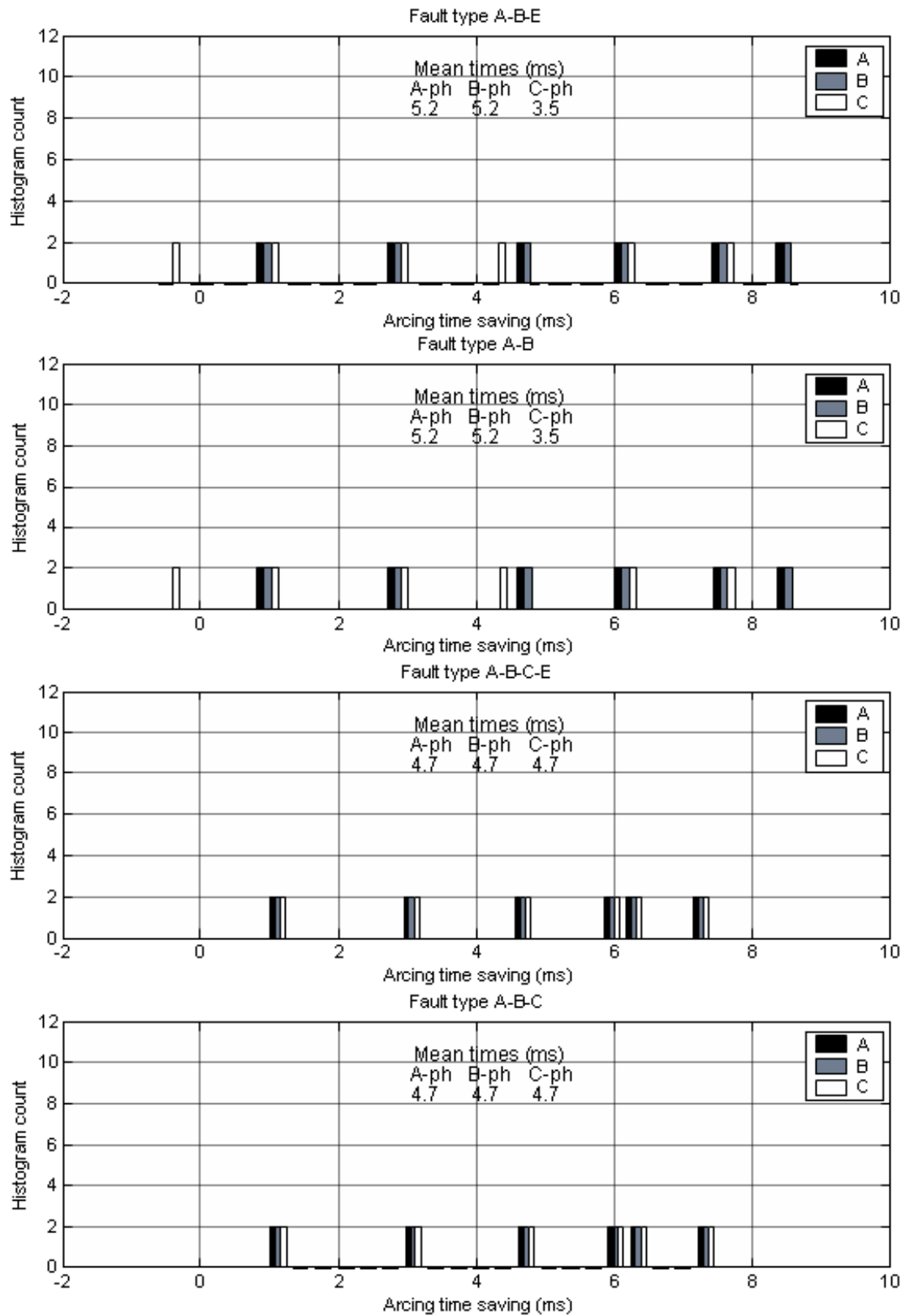


Figure 6.10 : Arcing time saving histograms for “ideal” CFI

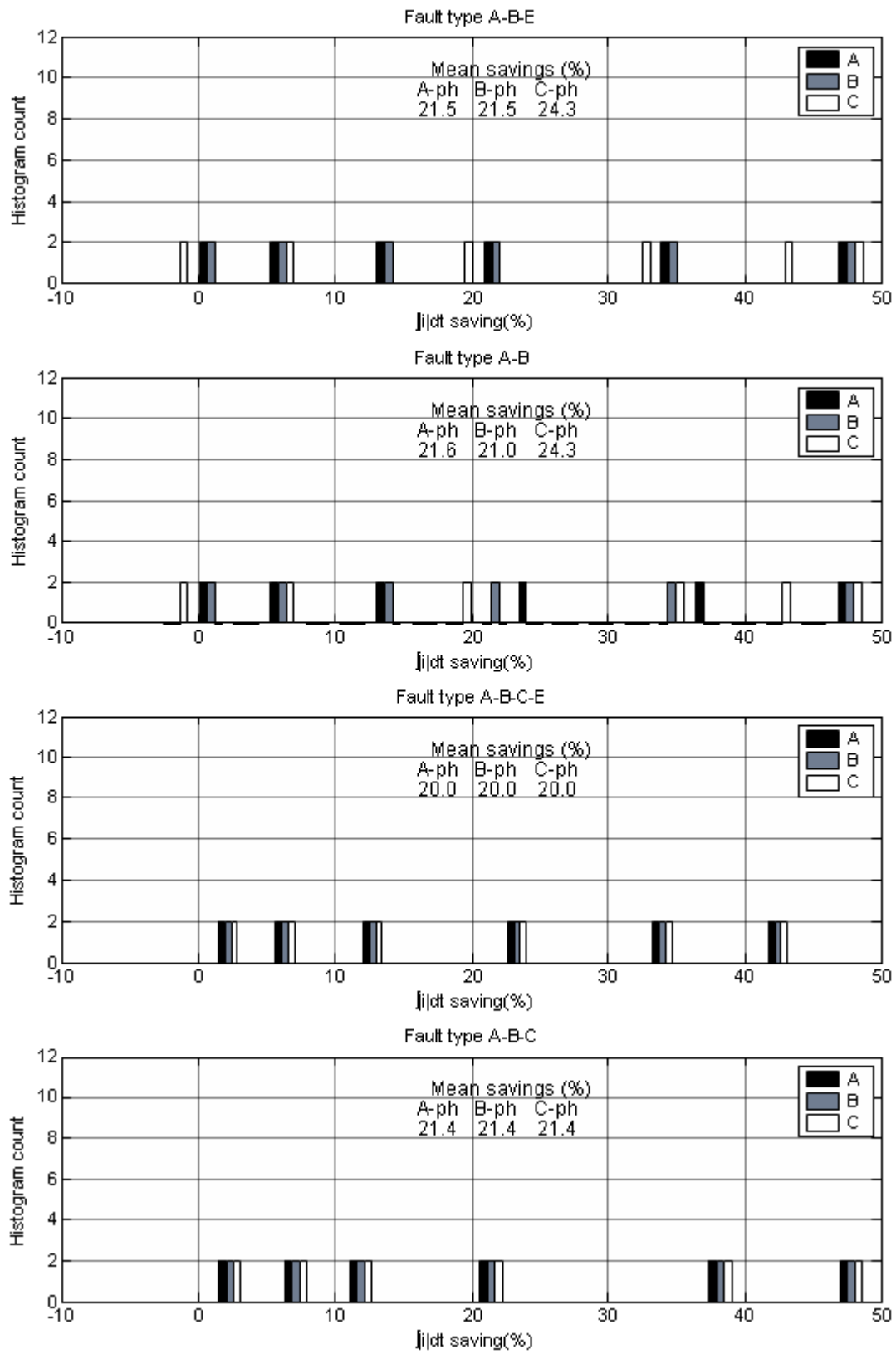


Figure 6.11 : Arc integral saving histograms for “ideal” CFI

## 6.6 Multiple run parameter set CFI simulation results - with signal noise

The following section presents the results of multiple simulation runs, made with twenty-five (25), 10% WGN vectors applied to the same four fault type cases shown previously, over the range of  $\alpha$  values from 0 to 330 degrees in 30 degrees steps (Figures 6.12 to 6.19). In total this amounts to 300 simulations for each fault case. All other simulation parameter values are as described earlier in this chapter.

The purpose of these simulations has been to obtain measures of the general performance of the proposed algorithm, with respect to the performance measures described at the start of this chapter, in the presence of signal noise applied during the main WLMS data processing period from fault inception until the protection system trip signal is active.

The results are mostly presented in the form of histogram or percentage counts, depending on the characteristic of the algorithm performance that is measured. Six performance results have been collated, in two groups of three graphs, for each of the four fault cases:

1. Errors in targeted zero-crossing times, per phase
2. Savings in arcing time using CFI, per phase
3. Savings in arc current time integral, per phase
4. Fault inception angle,  $\alpha$ , errors, per phase
5. Fault type detection percentage rate
6. CFI operation success rate in percent, per phase

Observations on each of the above performance results, relative to the different fault cases are summarized in the sub-sections below. It should be noted that the following results are valid for the particular combination of time constant, protection and circuit breaker operating and arcing times used in the simulations. Different values of the aforementioned parameters will affect the specific values, and potentially also the distributions of the results shown. For further details of the affects of variation in these parameters, the single phase simulations presented in the licentiate provide a comprehensive summary.

### 6.6.1 Target zero-crossing time errors

Recalling that the simulated WGN is based on a normal probability distribution with zero mean, it can be seen that the zero-crossing error histograms generally fall into a norm-like pattern, with an approximate  $3\text{-}\sigma$  boundary of 0.5 ms. This consistency between the zero-crossing error distribution and the WGN distribution reflects the impact of the noise on the WLMS estimation of  $\phi$  and  $\tau$ , which in turn influence the eventual error in the estimation of the zero-crossing times.

There seems at first to be an exception to this trend for the three phase fault cases, with a “tail” of zero-crossing time errors grouped around -1.5 ms; this however is slightly misleading from the perspective of assessing the accuracy of the WLMS results. The errors grouped near -1.5 ms, reflect the impact of the “compromise” targeting method used for the last phases to interrupt in the case of three phase faults, whereby one of the phases will interrupt at its targeted current zero time, while the other phase will be targeting a slightly earlier estimated current zero time, based on the algorithm’s estimations for the three phase fault being either earthed or unearthed. As these errors are “negative”, it implies the algorithm is making an “early” estimation of the

current zero target, which is “safe”, provided that the circuit breaker has an arcing window margin in the order of 2...3 ms, and so can tolerate the occasional -1.5 ms target estimation error in any phase.

### 6.6.2 Arcing time savings

The arcing time savings generally follow a uniform distribution, which while allowing the the residual fault current asymmetries in each phase at the interruption current zero times, is to be expected given that the simulations cover a complete periodic range of fault inception angles.

Notably there are cases of negative arcing time savings, principally on the non-faulted phase for the two phase fault cases. This reflects the effect of the 1 ms arc margin included in the CFI target arcing time, where in some cases the direct tripping of the circuit breaker would be achieved in the minimum arcing time.

### 6.6.3 Arc current time integral savings

The arc integral results also generally follow uniform distributions, allowing for the asymmetrical effects of the fault current. It is clear from both the arcing time and arc integral saving results that there is considerable potential for benefits to be gained in both contact wear and arc energy savings from the application of CFI, using single phase operated circuit breakers.

### 6.6.4 Fault inception angle, $\alpha$ , errors

The fault inception angle errors follow a similar pattern for each of the simulated fault types, with the errors generally linearly increasing from -9 to + 6 degrees, with very few outlying exceptions. The “ramped” pattern of these errors is a characteristic of the applied F01 trend analysis method that is used in the proposed algorithm for fault inception detection. The position of the ramp about the zero error point can, to some extent, be adjusted by altering the time step offset used in conjunction with the fault inception triggering criteria. However the overall simulation results, coupled to analysis of the single parameter set simulations shown earlier, suggest that the applied fault inception and  $\alpha$  estimation control parameters provide a good overall performance of the algorithm. Even with up to a 20 degree  $\alpha$  estimation error, the algorithm is capable of still making target zero crossing time estimations within  $\pm 0.5$  ms.

### 6.6.5 Fault type detection percentage rates

These results reflect the algorithm’s ability to correctly identify the faulted phases and classify the fault type. The specific results summarized here are those taken at the time the protection system trip signal goes active. It should be recalled that the main discrimination criteria applied in the proposed method is based on comparison of the F01 (phase-to-earth parameter based model) and F02 (phase-to-phase parameter based model) results. If F02 is greater than 1.1 times the F01 value, the algorithm will classify the fault in the associated phase as being of the phase-to-phase type, otherwise it will apply the phase-to-earth parameter values. The 1.1 factor was applied to provide some additional discrimination margin under noisy signal conditions between the F01 and F02 results.

For the double phase-to-earth case, the algorithm identifies the fault case correctly for all 300 simulations. For the phase-to-phase fault case, the performance is less ideal, with the algorithm mistaking the phase-to-phase fault for a double phase-to-earth fault. However the identification of the phases identified in the fault is correct in all cases. Closer examination of



individual cases of this type indicated that at certain fault inception angles the phase-to-earth fault behavior is sufficiently similar to the phase-to-phase fault behavior that the algorithm is unable to clearly discriminate between them. However as can be seen also by the zero-crossing error and CFI success rate results, the algorithm was still able to execute a reasonably accurate CFI operation in the 17% of cases of fault type mis-identification. Inclusion of a zero sequence detection function in conjunction with the proposed F0 comparison method may improve the two phase fault discrimination performance of the algorithm.

In the three phase fault cases it can be clearly seen that the algorithm is unable to distinguish between the earthed and unearthed cases, due to the identical behavior of the currents in both cases, up until the first phase interrupts. This confirms the requirement to implement the compromise targeting solution for the last two phases to interrupt for three phase faults. Nevertheless the algorithm was capable of identifying the faults as being of a general three phase type in all simulations made.

### 6.6.6 CFI operation success rates

For all the simulations conducted for the four fault types the algorithm was able to execute CFI operations for all phases. This is an excellent result given the relatively high level of simulated noise applied to the processed current signals.

### 6.6.7 Comparison to “ideal” CFI baseline results

In section 6.5, Figures 6.9 to 6.11, baseline results were presented for an “ideal” CFI, able to predict current zero times without error, while still applying the “compromise” targeting solution for the last two phases to interrupt on three phase faults. Table 6.1 presents a summary comparison of these baseline results to those of the simulations with the proposed algorithm with random signal noise.

**Table 6.1: Comparison of “ideal” baseline CFI to proposed CFI with WGN**

Fault type	Phase	Mean arcing time saving (ms)			Mean arc integral saving (%)		
		"Ideal" CFI	Proposed CFI (with  10%  WGN)	Difference	"Ideal" CFI	Proposed CFI (with  10%  WGN)	Difference
A-B-E	A	5.2	4.9	-0.3	21.5	21.1	-0.4
	B	5.2	4.9	-0.3	21.5	21.1	-0.4
	C	3.5	3.2	-0.3	24.3	23.8	-0.5
A-B	A	5.2	4.9	-0.3	21.6	21.5	-0.1
	B	5.2	4.9	-0.3	21.0	20.7	-0.3
	C	3.5	3.2	-0.3	24.3	23.8	-0.5
A-B-C-E	A	4.7	4.5	-0.2	20.0	19.6	-0.4
	B	4.7	4.5	-0.2	20.0	19.6	-0.4
	C	4.7	4.4	-0.3	20.0	19.4	-0.6
A-B-C	A	4.7	4.5	-0.2	21.4	21.0	-0.4
	B	4.7	4.5	-0.2	21.4	21.0	-0.4
	C	4.7	4.4	-0.3	21.4	20.8	-0.6

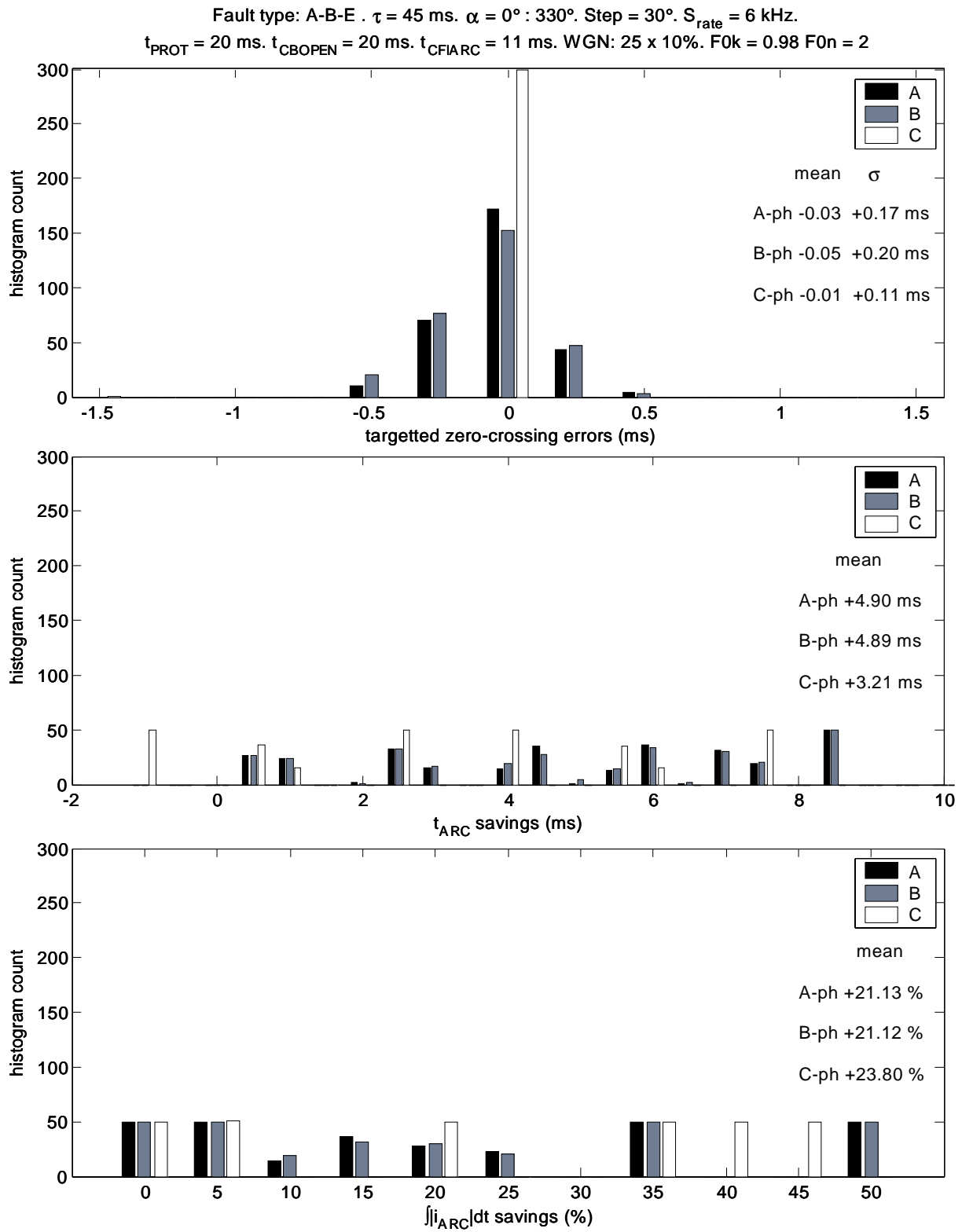


**Figure 6.12 : A-B-E fault; 25 x 10% WGN multi-run simulation result histograms - zero-crossing time errors, arcing time savings and arc current integral savings**

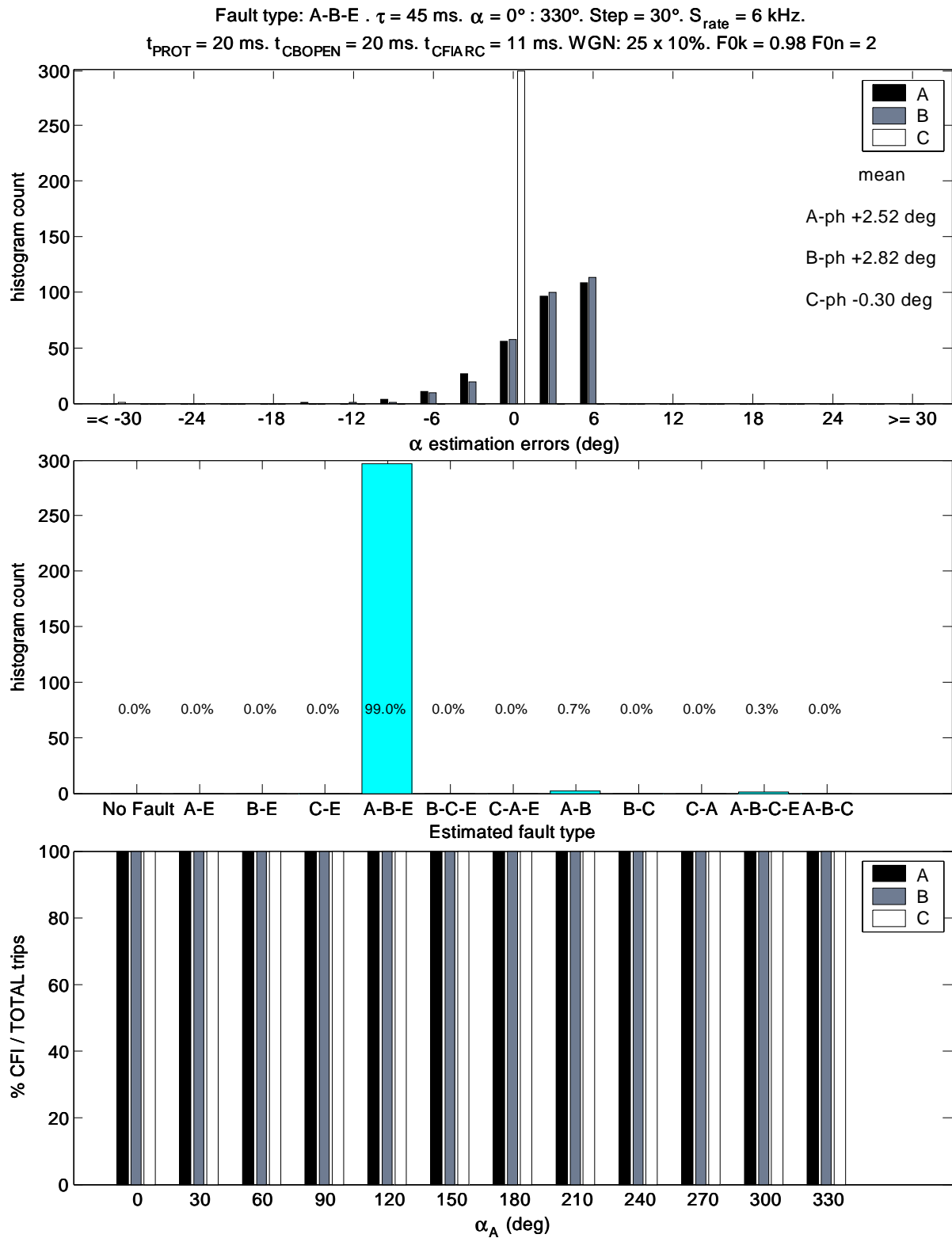
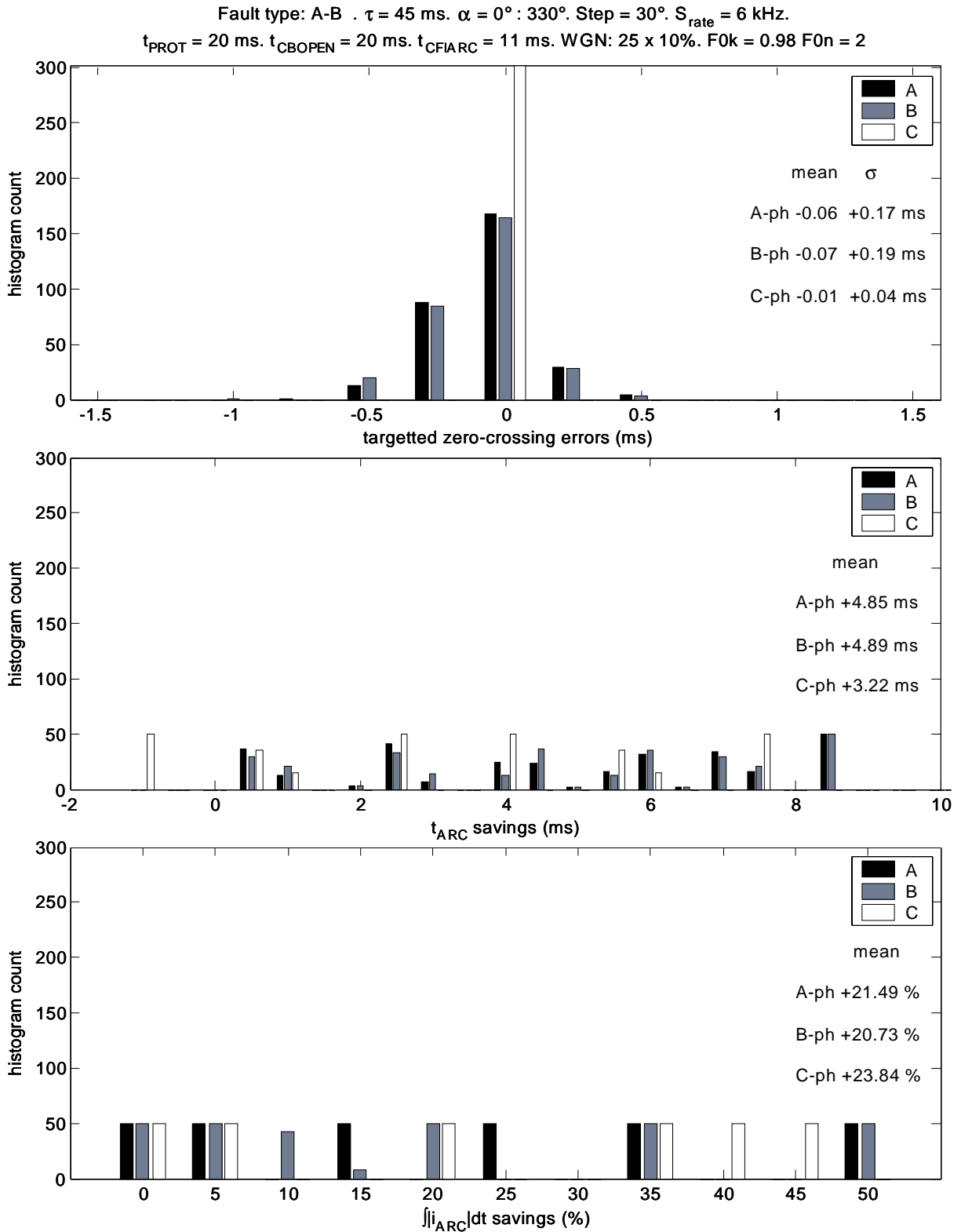


Figure 6.13 : A-B-E fault; 25 x 10% WGN multi-run simulation result histograms -  $\alpha$  estimation errors, fault type identification and CFI success rates



**Figure 6.14 : A-B fault; 25 x 10% WGN multi-run simulation result histograms - zero-crossing time errors, arcing time savings and arc current integral savings**

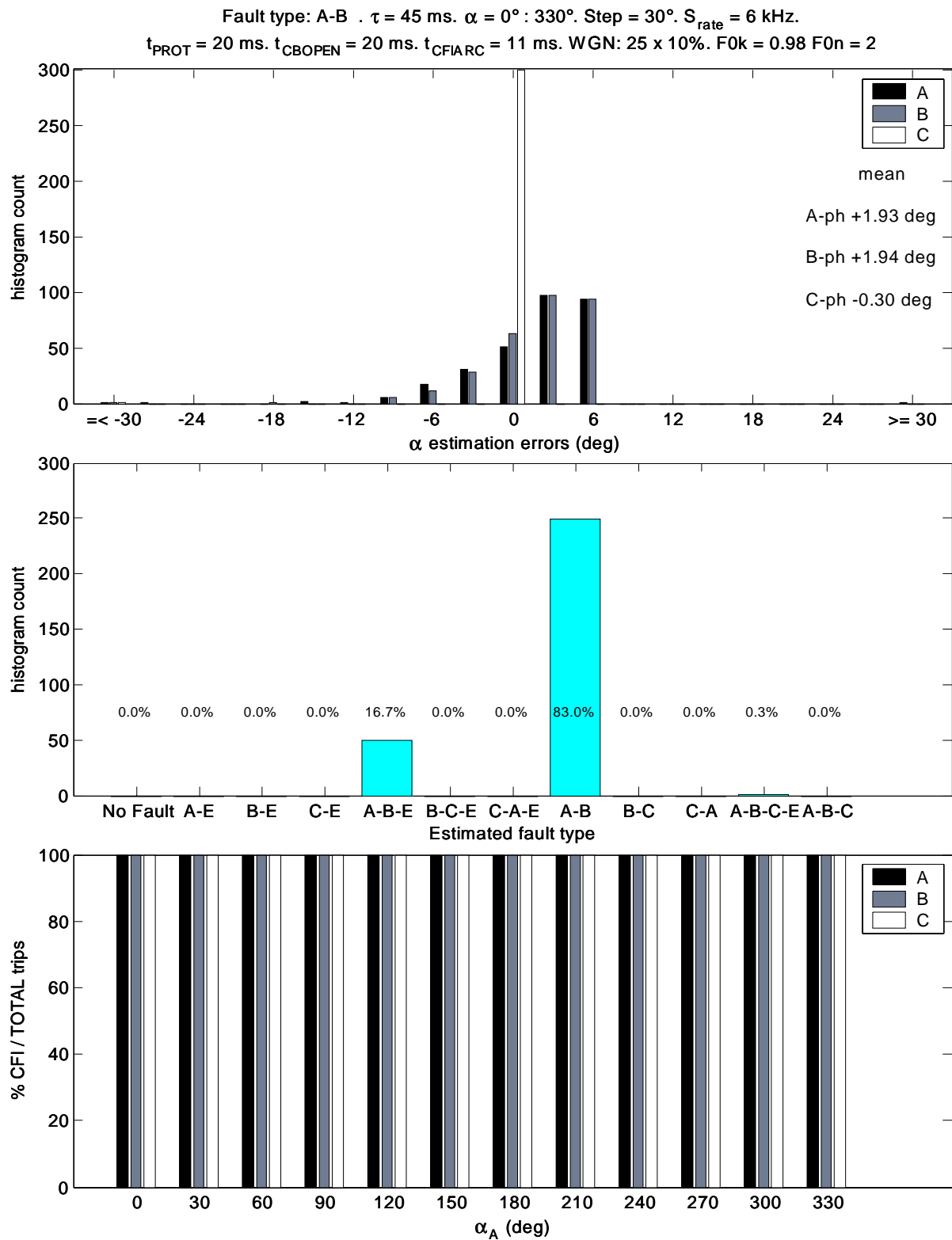
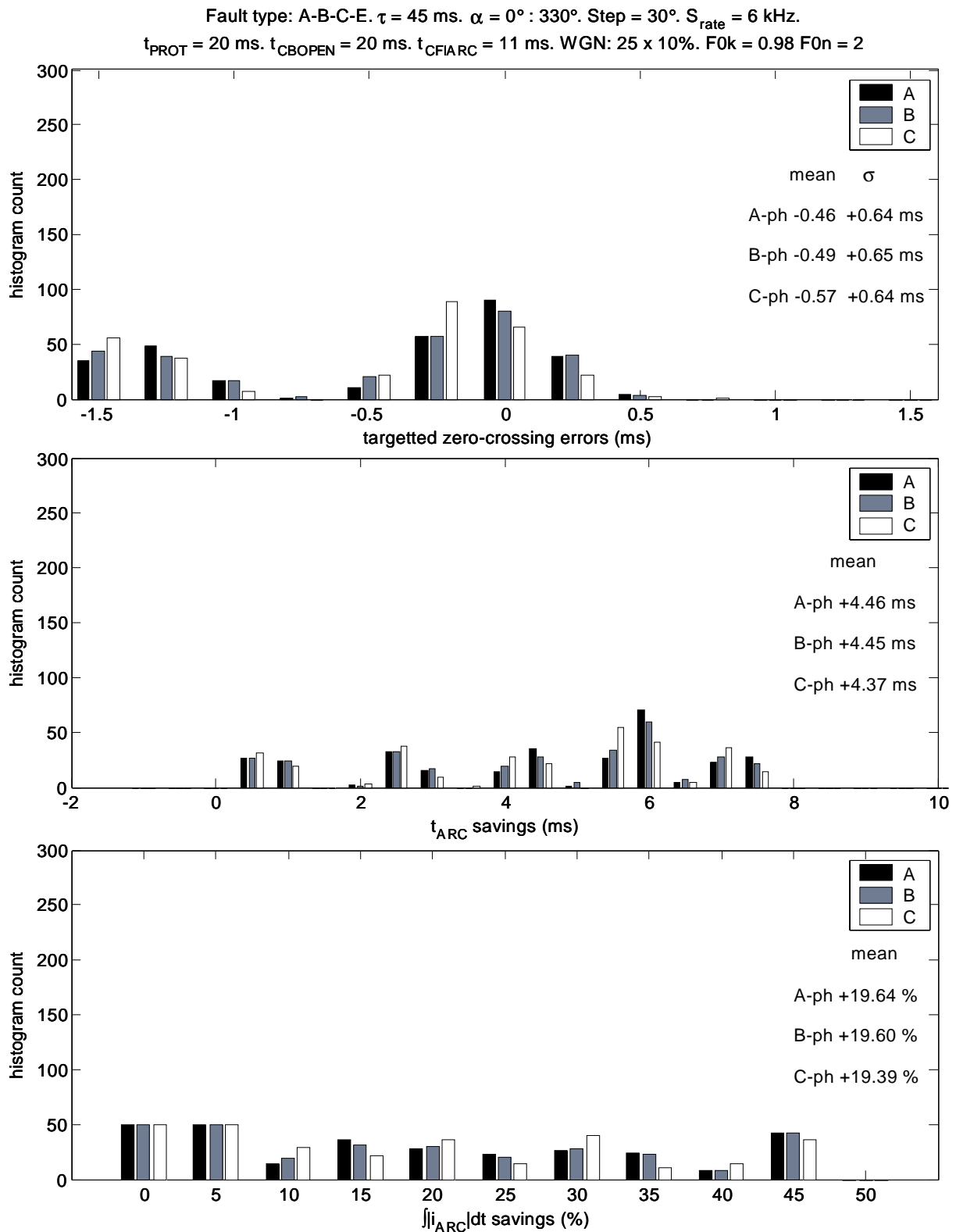
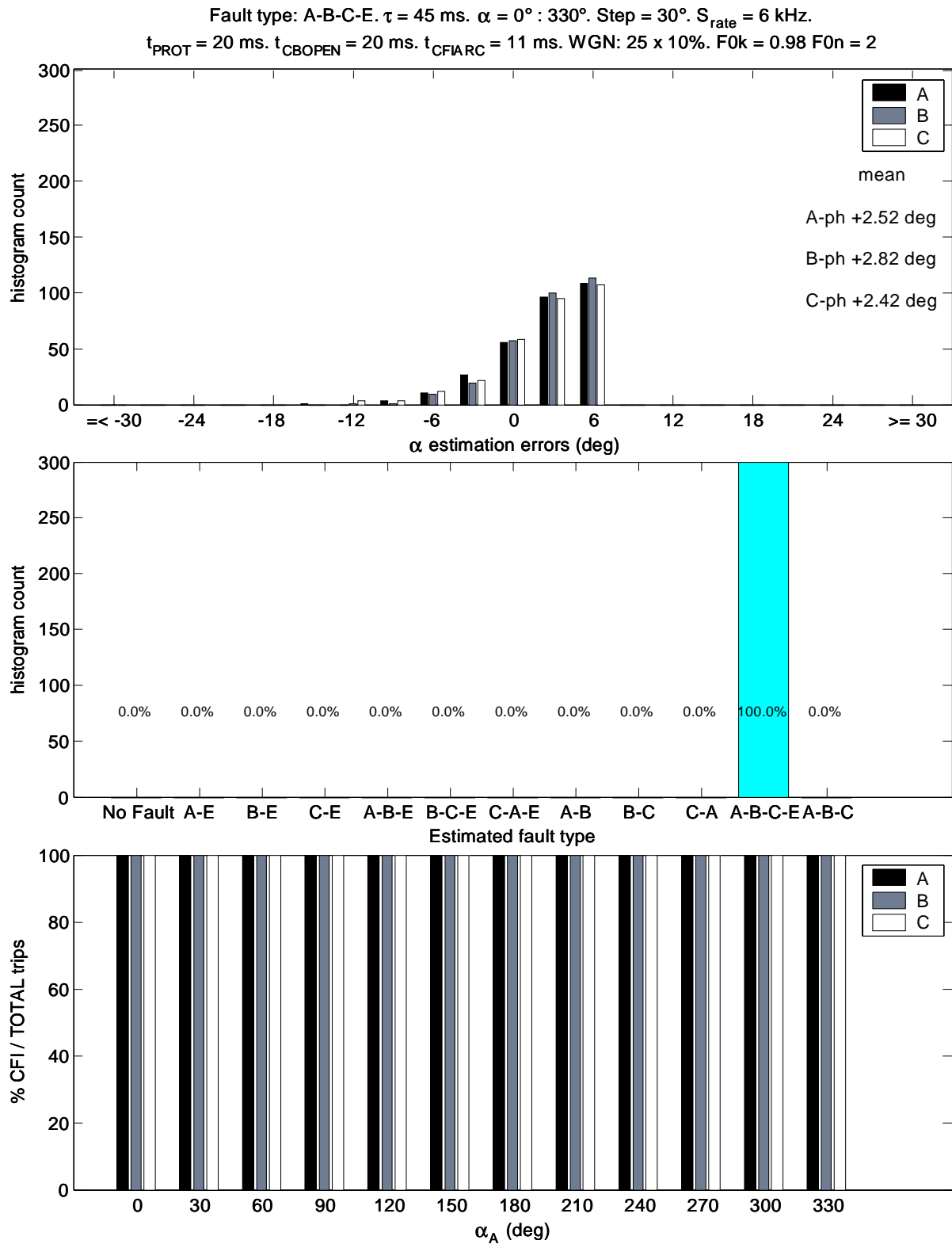


Figure 6.15 : A-B fault;  $25 \times 10\%$  WGN multi-run simulation result histograms -  $\alpha$  estimation errors, fault type identification and CFI success rates



**Figure 6.16 : A-B-C-E fault; 25 x 10% WGN multi-run simulation result histograms - zero-crossing time errors, arcing time savings and arc current integral savings**



**Figure 6.17 : A-B-C-E fault; 25 x 10% WGN multi-run simulation result histograms -  $\alpha$  estimation errors, fault type identification and CFI success rates**

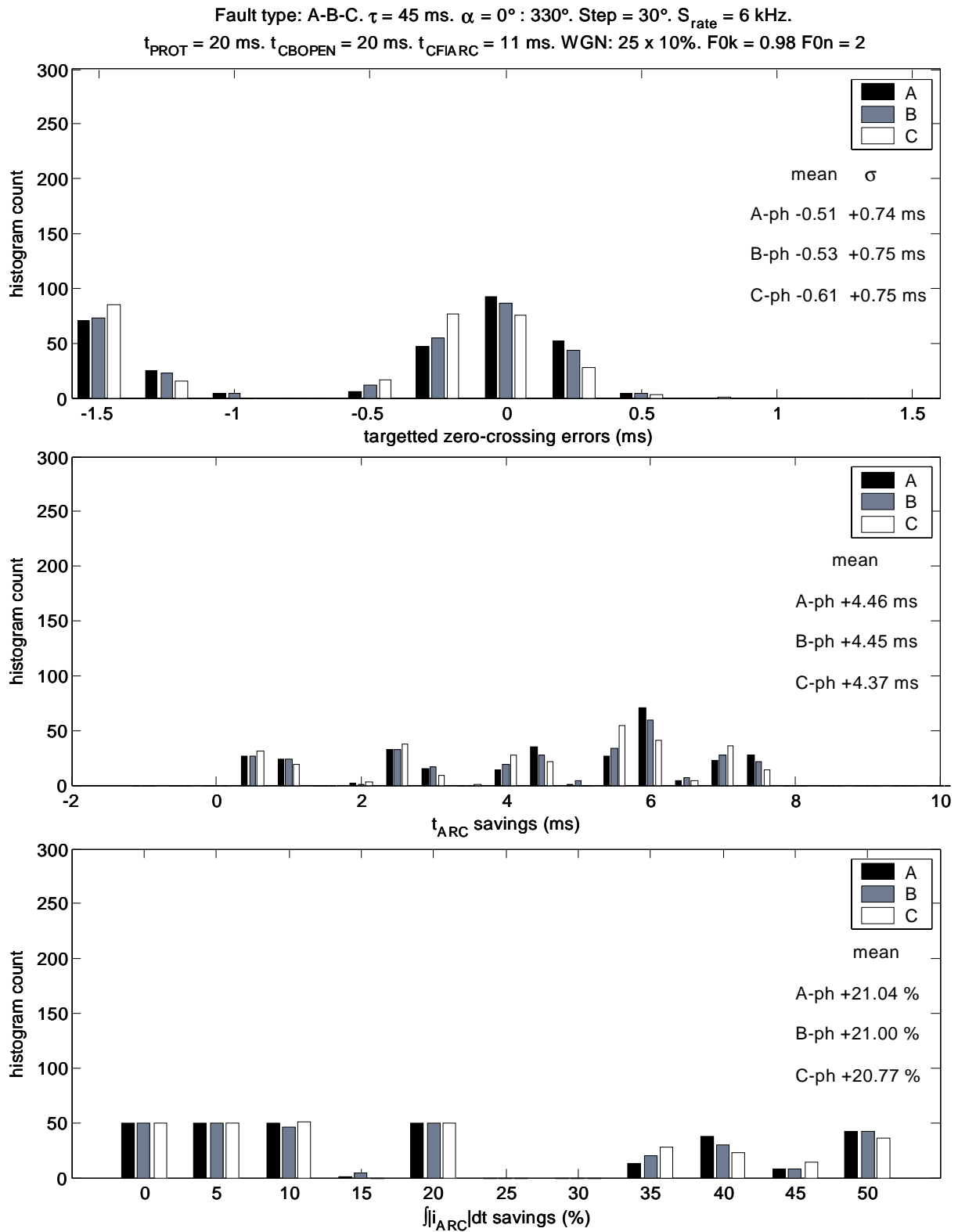


**Figure 6.18 : A-B-C fault; 25 x 10% WGN multi-run simulation result histograms - zero-crossing time errors, arcing time savings and arc current integral savings**



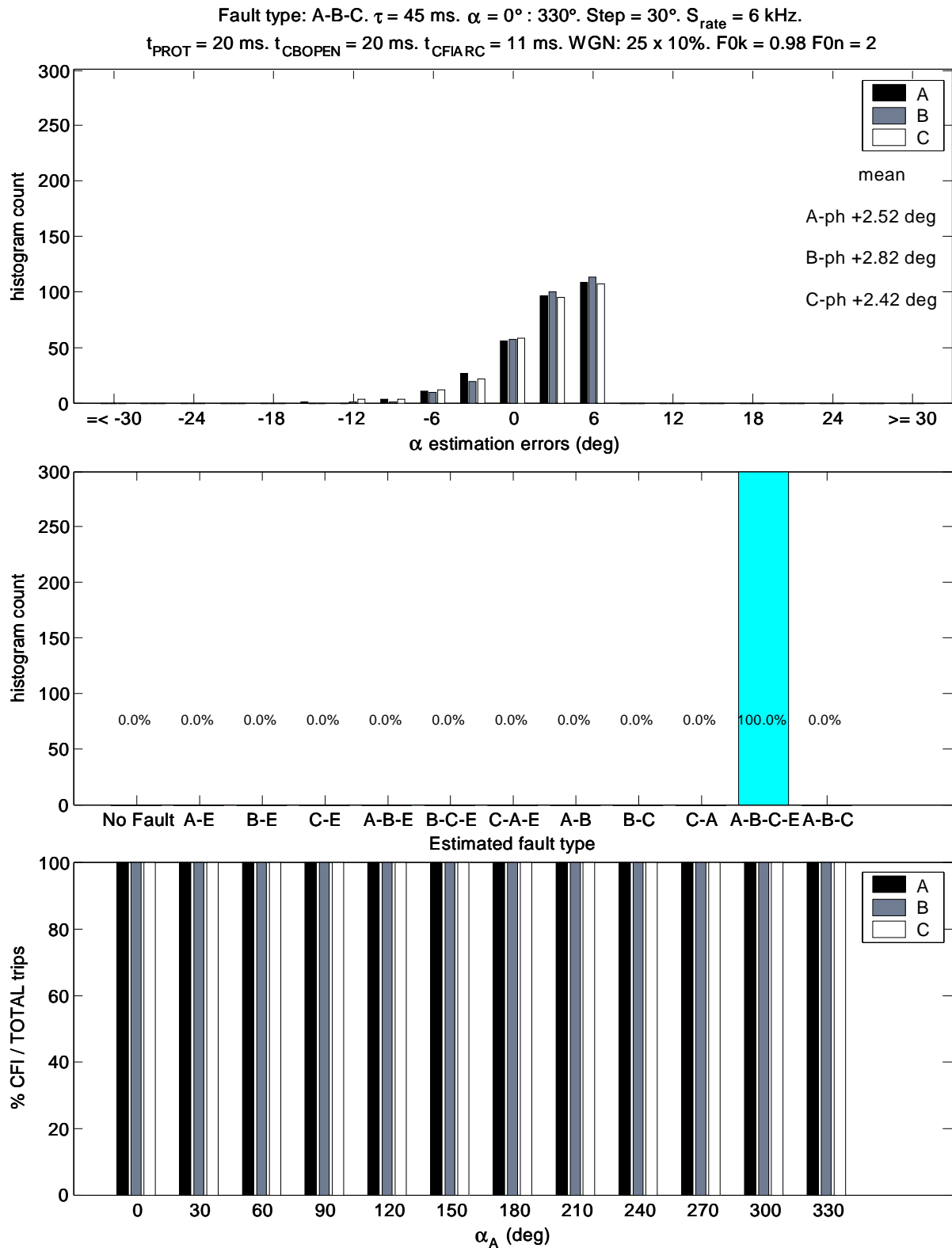


Figure 6.19 : A-B-C fault; 25 x 10% WGN multi-run simulation result histograms -  $\alpha$  estimation errors, fault type identification and CFI success rates

The results in Table 6.1 suggest that the proposed algorithm performs very well in comparison to an “ideal” CFI, able to predict target current zero times without error. However it must be observed that the fault type discrimination between double phase-to-earth and phase-to-phase faults is less than might be desired, allowing for the relatively high level of signal noise applied in the simulations. There remains scope for improvement in the detailed processes used for both the fault inception detection and fault type identification. It must also be recognized that both the “ideal” baseline and the proposed method simulations are made using a fault generator that is based on the same basic fault current model. As presented earlier this model does have limitations in its potential scope applicability and the performance of the proposed algorithm under “real world” conditions needs to be further investigated. This aspect and others is outlined in greater detail in the following chapter of future work proposals.

## 7 Future work proposals

As there has only been limited previous published work focussed on controlled fault interruption, there remains significant scope for further work in this area. This chapter outlines proposals for possible future research areas grouped into five main areas, though not in any specific order of importance:

1. Fault current model and parameter estimation development and comparison studies
2. Parameter variation sensitivity analyses
3. CFI implementation and simulation testing in large scale power system models
4. Field trialing of current prediction method
5. Investigation of current interruption technologies based on CFI

While grouped in the above manner, these future work suggestions could of course be combined in various ways. The grouping has only be made in order to provide some clarity of specific issues of importance with respect to the further research and development of viable CFI methods. Summaries of prior work, the contributions of this thesis and proposals for future work in each of the topic areas are included in each of the sub-sections of this chapter, for comparative reference and to provide some context to the continuation of work in this area.

Depending on the intended application of the current behavior prediction method, either as a method for circuit breaker control or as an augmentation to protection schemes, there would also remain substantial work to be done in terms of defining standardized performance and testing requirements. However, in order for any such productification work to be made, it remains necessary to complete the background concept research in order to establish the viabilities and limitations of different potential implementation techniques.

One additional important subject area is that of the cost-benefit analysis of applying CFI. The high power experiments included in this thesis indicated that there is possibly scope for the optimization of circuit breaker design through the use of CFI to restrict the required arcing window for different interruption duties. There also remains the potential application of the CFI method in conjunction with alternative interrupter technologies such as power electronic devices. While these aspects provide motivations to further study CFI, any such benefits must be weighed against the various costs of implementing CFI. As stated in the Introduction, modern HV SF<sub>6</sub> and vacuum circuit breakers are very reliable devices.

### 7.1 Fault current model and parameter estimation technique comparisons

Table 7.1 provides a summary of the main items presented in this and the following sub-section, relating to past, present and future work on the application of fault current models, parameter estimation and algorithm robustness.

As summarized in Chapter 4 there are a number of synergies to be found between the parameter estimations required for CFI and for protection schemes such as distance protection.

**Table 7.1: Summary of CFI algorithm development proposals**

Work packages		Prior CFI methods (e.g. Pörtl "Safepoint" method)	Proposed CFI method	Future work proposals	
CFI Algorithm	Models of current	Single time constant, classical fault model, no pre-fault current	Single time constant, classical fault model, including pre-fault current	Faults with sub-transient reactance effects i.e. exponential changing current magnitude and missing current zero periods Out-of-phase currents	
	Parameter estimation	LMS, "constant" DC component	(W)LMS with 1st order Taylor series exponential approximation	WLMS with weight estimation functions Recursive LMS Kalman filters	
	Parameter sensitivities	Phase angle	Phase angle	Phase angle (and time constant)	Dynamic phase angle sensitivity ( $d\phi/dt$ )
		Pseudo-white gaussian noise	Pseudo-white gaussian noise	Fault inception angle	Dynamic frequency sensitivity ( $df/dt$ )
				Pseudo-white gaussian noise	High load-to-fault magnitude ratio
				Pseudo-white gaussian noise	Harmonic distortion (primary and secondary) Current and voltage phase angle error Current signal saturation
	Application scope	Eleven (11) "classical" multiphase fault types.	Eleven (11) "classical" multiphase fault types.	Currents with missing current zero periods (e.g. sub-transient reactance effects, series compensated lines) Also out-of-phase interruption cases.	
		Asymmetrical fault currents with missing current zero periods		Management of special load cases e.g. capacitive or inductive load interruption, integrated to CFI algorithm. Integration of protection parameter estimation methods to CFI process. Also use of ANOVA in protection applications.	
	Computation efficiency	Implied, not quantified. 10 kHz nominal sampling rates, down to 1/4 cycle response time.	Implied, not quantified. 2...6 kHz nominal sampling rates, down to 1/4 cycle response time.	Quantification of processing times with respect to processor speed, memory and sampling rates for different core parameter estimation methods	
				Comparisons of algorithm accuracy, robustness and processing time versus sampling rate and minimum response time	
	Fault inception detection	Not specified	Use of analysis of variance (ANOVA) trend behavior	Investigate use of existing alternative methods	
	Fault type identification	Artificial neural network (ANN)	Use of ANOVA in conjunction with comparison of phase- to-earth and phase-to- phase driving source voltages frames of reference	Investigate use of existing alternative methods. Include symmetrical components analysis to improve discrimination between earthed and unearthed faults.	
	Robustness control	No specific self- checking. Implied robustness from noise sensitivity simulations	Use of ANOVA to verify suitability of modelled current	Investigate alternative ANOVA methods	
			Inclusion of "bypass" control in event of unacceptable ANOVA result	Utilize ANOVA or residual analysis to provide iterative improvement to model or estimated parameter values i.e. "feedback control" modelling	

While the proposed method described in this thesis applied least mean squares regression for estimation of the fault current phase angle, a wide range of other numerical techniques exist in the literature and in principle could also be applied to the general CFI method. In addition there exist various techniques for fault inception detection and fault type identification that could be investigated in the same context.

The implementation of the online analysis-of-variance check in the proposed CFI method is somewhat novel in the context of HV power systems control and protection, though the applied test is based on only one of many that exist in the area of regression analysis. It is possible that other feedback control techniques could also be applied to facilitate a level of both continuous parameter estimation improvement as well as regulatory control to maintain system dependability and security (e.g. the “bypass” control option included in the proposed method).

A comparison of methods for each of four main CFI method tasks including, parameter estimation, fault inception detection, fault type identification and (online) result validation would provide a useful reference for the further research and development. It can also be considered that the use of the analysis-of-variance test within the CFI algorithm could be further investigated for use within other power system on-line control processes, including protection algorithms e.g. as a means of validating operational decisions and increasing dependability and security.

### **7.1.1 Mutual coupling**

Mutual coupling not considered in the modelled current or simulations, but as the algorithm processes and estimates parameters based on individual phase current measurements, the effects of mutual coupling on the parameter estimation should be minimal. However a more detailed investigation of the potential impact of mutual coupling, in addition to parallel circuit lines (such as where two or more circuits share common towers) should be investigated.

### **7.1.2 Out-of-phase current interruption**

The main IEC standard [5] requires that circuit breakers be type tested for out-of-phase making and interruption for “worst case” conditions with the voltage across the open circuit breaker being 180 degrees out-of-phase. However during cases of power system transient instability, circuit breakers might be required to interrupt and reclose while parts of the system are “separating”, giving rise to a (dynamic) range of possible angles between the voltages on either side of a circuit breaker. This would pose a particular problem to the proposed CFI method and current model that is based on having relatively stable and known reference voltage measurements (effectively only one single phase voltage required from one side of the circuit breaker) in order to provide both the  $\alpha$  and  $\gamma$  term values to the least means squares regression calculation. In the worst case, the algorithm may revert to the zero waiting time “bypass” solution, assuming no viable result is determined within the protection response time. Alternatively to manage such cases, possibly a dynamic model is required that could estimate the current behavior based on an estimation of the rate of voltage angle change between either side of the circuit breaker.

### **7.1.3 Sub-transient reactance effects - “missing” current zeros**

The effects of sub-transient reactance in large synchronous generators leading to high fault current asymmetries and periods of “missing” current zeroes is a well known and documented phenomenon [26]. It could be possible to adapt the proposed fault current model to incorporate

additional terms to estimate such effects, though at the cost of the degrees of freedom and increased signal noise sensitivity if using the least means squares regression method.

Though specially designed generator circuit breakers are normally used for the direct protection of large generators [10], including management of missing current zeros, it can remain of interest to have an algorithm that could predict the duration of missing current zero periods, or even estimate “near” current zero times, for improved synchronized interruption control in such cases.

#### **7.1.4 Series-compensated lines - Sub-synchronous resonance (SSR) cases**

Series-compensated lines can give rise to quite complex fault current behaviors, characterized by sub-synchronous oscillation modes and even missing current zero periods [52]. Such behavior appears to be analogous in some respects to that seen with sub-transient reactance of large synchronous generators and there could be synergies in development of a current model for CFI targeting estimation to manage both of these cases, possibly with development application specific solutions.

One interesting potential benefit of CFI in conjunction with SSR is the possibility to select the current loop for interruption in order to mitigate the SSR mechanical torsional stress seen by generators affected by a fault on series compensated line[51].

#### **7.1.5 Impact of system earthing and zero-sequence equivalent circuit on proposed algorithm**

While the proposed CFI method presented in this thesis assumed a solidly earth system, the method included the compromise targeting solution to manage the phase shift in last phases to clear on unearthed three phase faults. Such phase shift behavior during three phase interruptions is also to be seen in non-effectively earthed networks due to the nature of the zero sequence path. Further investigation of the behavior of the algorithm for different system earthing arrangements would be beneficial. System earthing will effect not only the interruption behavior of the last two phases to clear, but also limits the prospective fault current magnitude on earth faults. As such the behavior of fault inception detection methods would also be of significance in connection to the application of the CFI method to non-effectively earthed systems and a comparative evaluation of existing techniques e.g. including symmetrical components, may be of interest in this context.

#### **7.1.6 Processing time requirements**

CFI has critical and limited operating time constraints, similar to that for protection systems. As described in Chapters 1, 4 and 5 the proposed CFI method has been developed with a view to utilize potential synergies with modern digital distance protection schemes in data sampling and parameter estimation and as such be a system that could be embedded in the same hardware platform as a distance protection algorithm. In this respect the simulations of the algorithm, both in the Licentiate and this thesis have been made using data sampling rates between 2 to 6 kHz, consistent with those found in modern digital relays.

There are a number of trade offs to be evaluated between algorithm speed, accuracy, security, sampling rates and data conditioning. The proposed method assumes that each iteration of the CFI process, including parameter estimation, analysis of variance testing, model extrapolation, target identification and waiting time calculations can be made within the time of each acquired data sample. This requires careful thought with respect to selection of the most

appropriate calculation methods that provide the required combination of efficiency, accuracy and reliability. Applying a high sample rate may permit obtaining an accurate solution within a shorter data window, but in order to capitalize on the short total sampling time the iteration processing must be correspondingly fast(er).

It is possible to adapt the least mean squares (LMS) method applied in this thesis to a recursive form and include a large degree of pre-calculation of the regression matrices, provided the processing platform is equipped with sufficient memory. Other methods for estimation of the fault current parameters, as for example applied or proposed for distance protection could be comparatively assessed for their efficiency, accuracy and reliability or robustness in the context of CFI application. Such comparisons would also benefit from inclusion of any numerical data pre-conditioning or filtering techniques being similarly assessed.

### 7.1.7 Data sampling and filtering delays and distortions

In addition to the overall data processing time constraint, CFI is critically dependent on an accurate understanding of the time synchronization between the primary and secondary voltage and current waveforms - possibly to an even more critical extent than for protection system applications. There will be inherent, cumulative and unavoidable delays between the primary and secondary waveforms due to measurement and filtering. Similarly there is inherent waveform distortion errors between the primary and secondary levels. A detailed mapping of the primary to secondary signal process will permit identification, modelling, quantification and management of these effects - see Figure 4.4.

Delays and distortion caused by the measurement sensors used can normally be managed through the correct specification of voltage and current transformers with reference to relevant international standards (e.g. IEC 60044 [74], [75], [76], [77]) that specify measurement accuracy classes based on limits for ratio and phase angle errors. A particular problem for current measurement can be distortion due to core saturation, which can be exacerbated in some cases by residual flux in CT cores, e.g. during rapid auto-reclosing onto a permanently faulted line. Non-magnetic core current sensors (e.g. Rogowski coils) can avoid this problem.

Delays and distortion caused by digital hardware sampling can also normally be well modelled and correlated by experimentation. Nevertheless, effects caused by cable connections between the primary sensors and the relay can be more difficult to generically model as they may vary from installation to installation.

The performance of the measurement and filtering system should also be tested for its performance under transient asymmetrical fault conditions. Ultimately it is important to the CFI application that the total expected time delay between the primary and secondary waveforms can be quantified to a value of acceptable confidence and error margin. Such a delay can then be incorporated into the waiting time calculation for the trip commands issued by the CFI process.

## 7.2 Parameter variation sensitivity analyses

The performance of the proposed method has been tested in simulations for a complete range of fault inception,  $\alpha$ , angles and a comprehensive range of DC component time constants,  $\tau$ . However there can exist additional fault current model parameter variations that can arise under both normal and faulted power system conditions that should be investigated in respect of their

effects on the algorithm performance. This can provide an additional quantitative assessment of algorithm robustness, beyond the generic pseudo-random noise tests presented thus far.

### 7.2.1 $d\omega/dt$ changes during faults

Changes in network frequency (and therefore also network angular frequency) are typical during faults. Maintaining system frequency within defined limits (e.g. 49.5 to 50.5) is of course critical to many aspects of power system operation and electrical equipment use. Extreme swings, outside the prescribed normal operation tolerances, in large, strong and interconnected networks tend to be “slow” by comparison to the typical expected and planned interruption times for faults. However it cannot be ignored that frequency changes are inherent to fault situations and the effect of such changes should be investigated, possibly on the basis of applying different simulating  $df/dt$  rates (e.g. 0.5 Hz/s to 2 Hz/s) and observing the impact on the CFI algorithm success rate and zero crossing errors. It should also be considered that non-zero  $df/dt$  rates will impact on the value of the current phase angle and magnitude (due to dependence on  $\omega L$ ).

### 7.2.2 $d\phi/dt$ changes pre-fault

The potential problems (e.g. for distance protection) arising from gradual changes in current phase angle due to swings in the power flow on a network are well known and documented, leading to mitigation methods such as power swing detection. Current phase angles will change continuously during normal system operation simply due to the dynamic supply and demand nature of the power system. It is therefore important to investigate the sensitivity of the proposed method to  $d\phi/dt$  changes, possibly in similar manner to that proposed above for  $df/dt$  change sensitivity.

### 7.2.3 Load-to-Fault current magnitude and load magnitude fluctuations

As mentioned above in 7.1.5, earth faults in non-effectively earthed systems will have limited fault current magnitude which can make fault detection difficult. In addition, normal power system operation will see continuous changes in current magnitude as loads are connected and disconnected. Both these effects may cause difficulties for the fault inception detection method based on analysis-of-variance testing, as the proposed method effectively reacts to any “significant” changes in current behavior. A large change in load may trigger the fault inception detection, causing the algorithm to update its  $\alpha$  values. This is not necessarily a problem, provided that the load change is also characterized by a (significant) change in current phase angle(s), the algorithm will nevertheless need to adjust its  $\phi$  estimation in order to maintain accurate prediction of potential current zero target times. Nevertheless the sensitivity of the algorithm to current magnitude changes should be further investigated.

### 7.2.4 Harmonics

Harmonics in power systems and their impact on protection and control is complex issue and the subject of much literature and research, not least within the area of power quality monitoring and control. Two main areas could be considered for the study of the impact of harmonics in the context of CFI; primary and secondary level harmonics.

“Primary” system harmonics refers to “real” harmonic distortion of the primary currents to be interrupted. Observation of fault recordings (see licentiate Chapter 8) seems to indicate that the level of obvious harmonic distortion is not normally a problem and certainly not to a level where



the current zero behavior is altered to an extent that may result in “premature” interruptions (e.g. by introducing very short current loops). In extreme distortion cases there may exist a risk for current chopping. Transformer magnetizing inrush currents can exhibit extreme harmonic distortion and present a challenge for effective interruption without reignition by an HV circuit breaker. However inrush currents are not a fault case and the level of the inrush can be mitigated through correct use of controlled switching for the energization of a transformer [14].

Primary harmonic distortion can be difficult to simulate, especially if relying on accurate models of magnetic devices as a source of the distortion. There are several consequential effects of harmonics that need to be considered based on their associate effect on the angular frequency of the system and thus inductive and capacitive reactance values. The time constant of a switched or fault current should not be affected as it is defined by the L/R ratio which is independent of frequency,  $f$ . This is relevant to the presently applied method for time constant estimation based on the phase angle,  $\phi$ , and the angular frequency,  $\omega$ .

“Secondary” system harmonics is distortion introduced by the data measurement and sampling systems e.g. CT saturation effects. These effects can normally be more easily modelled based on analysis of the behavior of specific devices in the data processing system. Such an analysis can lead to specifying requirements for signal processing and CT core characteristics needed for CFI to work acceptably.

### **7.2.5 Current transformer issues: saturation, remanence, phase angle error, ratio error**

As mentioned several times previously in this thesis and in the licentiate the current measurement device plays a major role in the accuracy and overall performance of the CFI algorithm. So far in this work, only a completely ideal current measurement system has been assumed, though with the background consideration that the current sensor used would be adequately designed according to relevant standards(e.g. IEC 60044 [74], [77]) for faithful representation of asymmetrical fault currents within the rated requirements relevant at any specific installation. The IEEE Working Group C-5 has produced a useful paper describing possible software models for instrument transformers that might be considered in this context [72], [73].

It is however important that the potential sources for error due to the current measurement process be adequately defined and investigated for their impact on the performance of the CFI algorithm. Two critical aspects of the current sensor performance are phase angle error (time synchronization between primary and secondary currents) and exponential DC component transformation. Though the above aspects of current sensor performance are generically relevant to power system control and protection applications, the importance for CFI performance is especially critical given the narrow margins of timing error tolerance desired to achieve maximum benefit from the process.

Such a study should not be limited to any particular type of current sensor. Though non-saturating designs exist (e.g. Rogowski coils or optical Faraday effect type sensors), the majority of in service and still manufactured current sensors are the traditional magnetic core, wound current transformer type.

### 7.2.6 Impact of error in voltage phase angle measurement

As described in Chapter 2 the fault current model applied in the proposed system is based on an “ideal”, driving source voltage, whereas the actual measured source voltage at or near to the circuit breaker location will have an inherently different relative phase angle. The impact of voltage phase angle error has not been studied in detail in this work so far. Such an error will affect the accuracy of the fault inception angle, phase angle and time constant estimations, when applying the method as described in this thesis. The impact of errors in the estimation of these parameter values has been described in more general terms, specifically in regard to current zero-crossing time estimation errors, based on simulations made with pseudo-random noise. It would however be beneficial to investigate and quantify independently the impact of the voltage reference angle error on the CFI algorithm performance, together with possible error mitigation methods, such as inclusion of estimated voltage angle error based on system load flow and fault studies.

### 7.2.7 Statistical variation of CB opening and arcing times

Most HV SF<sub>6</sub> circuit breakers in production today are equipped with spring operating mechanisms that have been shown to be very consistent in their operating times, with  $3\sigma$  values in the order of 0.5 ms seen during extensive mechanical endurance tests [1], [53]. However such tests are normally based on frequent operation, whereas most circuit breakers are infrequently operated and in connection with fault interruption the idle times between operation of a circuit breaker can be substantial (e.g. months or even years) and varied. Ito [53] reports for spring operated circuit breakers of variation ranges due to idle time in the order of +/- 1.0 ms. Variation in circuit breaker opening times with respect to variations in operating control voltage and ambient temperature are also well documented (see Table II in [11]).

As described in Chapter 3, (published) data on the stability of the minimum arcing time behavior HV circuit breakers tends to be inherently limited, in part due to the cost of high power testing and the minimum requirements laid down by the relevant international circuit breaker standards. Though the Chapter 3 results are limited and made operating a circuit breaker well below its designed opening speed, it was shown that there is a general relationship between interrupted current magnitude and minimum arcing time duration and that a manageable level of stability in minimum arcing time behavior can be found, even for an accumulation of interruptions. Nevertheless, it must be assumed that there will be certain level of statistical spread in minimum arcing time durations, even on the same circuit breaker, as well as within a population of circuit breakers of the same design.

The simulations of the proposed algorithm have so far used fixed values of both the circuit breaker opening time and minimum arcing times for simplicity, in order to provide a clearer indication of the base performance of the proposed algorithm, without too many concurrent variabilities. Now having presented such an analysis, it would be of interest to expand the simulation model to include selective variations in both the opening and minimum arcing times. In addition the algorithm could be tested with a more sophisticated (and “independent”) power system model in order to test performance with different fault current magnitudes, including a functional relation between detected current magnitude and targeted arcing time.

### 7.3 CFI implementation and simulation on large scale power system models

Table 7.2 below summarizes the existing and proposed power system models applied for the development of CFI methods. The proposed CFI method has only been developed and tested using a very simple power system model, intentionally chosen as a starting point for the research. However, any practical application of CFI requires that the algorithm be developed and tested with power system models that reflect both the scale and dynamics of large scale power systems.

**Table 7.2: Summary of power system models for CFI development**

Work packages	Prior CFI methods (e.g. "Safepoint" method)	Proposed CFI method	Future work proposals
Power system modelling	"Simple", single (infinite bus) source. Stable impedances, voltages and frequency (EMTP)	"Simple", single (infinite bus) source. Stable impedances, voltages and frequency (MATLAB)	Multi-source, multiple line model, for investigation of parallel breaker operations. Model in EMTDC, PSS or EMTP and embed algorithm for direct simulation testing.
			Specific modelling for "special" cases e.g. near large generators / machines, series compensated lines, distributed generation
			Modelling of mutual line coupling, frequency and voltage changes during faults, dynamic current phase angle behavior, "ideal" versus "actual measured" reference voltages for fault current modelling

The following sub-sections expand upon particular challenges for CFI implementation that can be more adequately addressed by more comprehensive power system models than have hitherto been applied in the CFI research.

#### 7.3.1 Evolving faults

Evolving faults are those where the magnitude and behavior of the fault current changes, other than following the basic transient asymmetry, due to changes in the overall source to fault impedance, driving source voltage, or even number of phases or earth connection involved. Typically the evolving fault interest has focussed its occurrence at or just after a circuit breaker's contacts have parted, but not yet interrupted the arc (pp 481-482 [40]). The concern was based on the impact of the altered stress placed on the interrupter due to a change in arc current behavior as the circuit breaker attempts to interrupt e.g. a sudden increase in current magnitude would place additional thermal stress on the interrupter and could, theoretically at least, lead to the circuit breaker requiring a longer arcing time (or later current zero) to interrupt.

From the perspective of CFI, the evolving fault problem can be more complex, as the very nature of the phenomenon means that the fault current behavior is not stable and therefore more difficult to predict. In the extreme, one can argue that any fault can take on "evolving" and non-predictive characteristics and therefore make CFI based on predictive current behavior non-viable. However, it should be taken into consideration that most modern HV circuit breakers are capable of interrupting evolving faults, due in part to the consistency and stability of their arcing time behaviors over the wide range of current duties for which they are tested.

It would however be useful to test the performance of a CFI algorithm to manage a range of evolving fault cases e.g. single phase faults evolving to double or triple phase faults within the first power frequency cycle or impact on change in source-to-fault impedance to target current zero accuracy, as can occur with parallel breaking described below.

### 7.3.2 Parallel breaking

Typically all lines, or protected equipment are connected directly to two or more circuit breakers, which are not necessarily of same type or design and therefore can exhibit different opening and minimum arcing time behaviors. All the circuit breakers directly connected to a faulted section of a network, particularly a meshed network, would be expected to open and interrupt their respective currents that are contributing to the overall current at the fault location. Such operations of multiple breakers interrupting the same fault is referred to as parallel breaking.

It is possible, again in meshed or partly meshed networks that as each circuit breaker interrupts, particularly if they do not interrupt at the same current zero, the currents being conducted by the yet to interrupt circuit breakers will change, due to the change in network configuration due to each circuit breaker interrupting. Parallel breaking is a “special case” of “evolving fault”, as seen from the perspective of changes in current behavior flowing through the circuit breaker. Using large, meshed, multi-source power system models will allow simulation of parallel breaking for CFI.

### 7.3.3 Current magnitude dependent minimum arcing times

The results in Chapter 3 show evidence that HV AC SF<sub>6</sub> circuit breakers can exhibit a general relationship between current magnitude and minimum arcing time, at least for inductive current interruption from nominal load current level up to 100% fault interruption rating i.e. the larger the current the longer the arcing time and since the proposed algorithm also estimates the current magnitude the target arcing times could be adjusted according to the determined current magnitudes. This permits scope for a more comprehensive range of simulations of the algorithm, in particular for studies that look to the accumulated arc integral savings for a given combination of interruptions occurring on a specific circuit breaker with an associated probabilistic mix of fault cases over a defined, simulated service time interval. In this respect, studies such as [25], provide useful guidance as to the percentage mix of fault current magnitudes that could be modelled statistically for such studies.

### 7.3.4 Fault type probabilities

The work published so far on CFI has tended to assume a uniform probability distribution of all fault types. Surveys, such as that conducted for the IEC 62271-310 electrical endurance testing technical report [7], indicate that the probability of different faults types is understandably not uniform. The combination of fault types varies with system voltage level and may also be expected to vary with network topology and construction (e.g. proportion of overhead to cable network, rural versus urban network concentrations), as such factors can influence the type of faults that might be caused by natural (external) causes, system age and stress or externally caused damage to the network.

Less well known is the distribution of fault cases described in terms of interruption stresses (e.g. terminal, short-line, out-of-phase conditions). In some cases certain assumptions could be made on the probability of certain faults types not occurring in certain locations e.g. no short-line

fault conditions on cable connected circuit breakers, capacitor banks or transformer bays. Some surveys do provide useful guidance to the probability of fault current magnitudes with respect to circuit breaker ratings [25], however such surveys must be taken in the context of the network(s) from which the data has been obtained.

The available statistics on fault type probabilities could be combined within large scale power system simulations to provide a more “realistic” assessment of the benefits and performance of a CFI algorithm in terms of arc integral savings and reliability of operation versus fault types.

### **7.3.4 Circuit breaker and interrupter models used in power system simulators**

The circuit breaker models found in power system simulation software (e.g. EMTDC/PSCAD) tend to be extremely simple, without inclusion of arc models or arcing time limitations within the circuit breakers. This is understandable in the context that first, power systems are typically populated by a wide variety of circuit breaker types and makes and second, it is difficult to find a truly “generic” interruption arcing model valid for all interruption cases. The most commonly referred basic arc models of Cassie and Mayr were based on different base assumptions and are best only applied to certain extremes of arc magnitude and behavior (e.g. constant arc resistance or constant arc voltage) [40].

It should however be possible to create comparatively “simple” circuit breaker models within power system simulators that are programmed to react with certain minimum arcing times for given current magnitudes and possible current phase angles (e.g. for discrimination between capacitive and inductive current interruption behaviors). Such models might also be adapted to simulate simple arc voltage models for given current levels also. The use of such models would be restricted to assessing the effect on CFI predictive current models and efficacy of an algorithm adapting to different current levels with different arcing windows. As such they should not necessarily be used assess circuit breaker performance, per se. The circuit breaker models could also be enhanced to provide simulation of the statistical variation in both opening and arcing time behaviors, and thus provide a basis for CFI algorithm performance as described earlier in 7.2.7.

## **7.4 Field trialing of current prediction method**

Despite the range of issues to be further investigated for the development of CFI, the proposed method has been proven through the simulations to operate with a good level of robustness for extensive ranges of fault asymmetry and onerous signal noise. However simulation testing is limited by the inherent approximations used in the power system and component modelling and as such it is important to also gain information on the performance of the method under “real world” conditions. Table 7.3 presents a summary of proposals for the progressive implementation of CFI algorithm(s) through staged field trial approaches.

### **7.4.1 Simulation testing using fault recordings**

Chapter 8 of the licentiate thesis provided single phase examples of the algorithm performance using fault recordings provided by power utilities and demonstrated that the algorithm was able to perform adequately, even for a range of sampling rates from 1 to 6 kHz.

While fault recordings are a useful alternative source for simulation testing, it is difficult to obtain a comprehensive set of such data for all possible fault cases. In addition, sampling rates

and methods used by different fault recorders can vary widely and in order to conduct an efficient and comprehensive testing using fault recordings can involve a substantial amount of preparatory work to survey and collate the recordings into formats that can be then readily used for simulation purposes. In addition, there can often be the problem that not all the operational data relating to a fault case and its interruption are readily available from the one data source e.g. circuit breaker and protection system data may not be always directly included in recordings focussed only on current and voltage waveform recording. Consideration should also be made of the phase angle and measurement ratio errors that are inherent in the recording system.

**Table 7.3: Summary of staged field trialing for CFI development**

Work packages		Prior CFI methods (e.g. "Safepoint" method)	Proposed CFI method	Future work proposals
Field trialing	Simulations with fault recordings	None	Single phase simulations with selected fault recordings	Build "reference library" of actual field fault recordings for use in simulation testing and comparison to artificial power system fault modelling performance
	Passive trialing	None	None	Embed algorithm in digital (distance) protection relay and observe current zero prediction accuracy and overall algorithm robustness.
	Active trialing	None	None	Embed algorithm in digital (distance) protection relay and set-up for actual CB control for mitigation of electrical wear, using "bypass" control for CFI algorithm "failure".  Alternatively embed algorithm as a supplementary breaker failure protection tool.

However the increasing importance of post fault investigation in the operation of liberalized power networks, coupled with the increasing inclusion of fault recording facilities within digital relay platforms should mean that an increasingly comprehensive set of "real world" fault data exists and could be harnessed to provide a useful comparative analysis of the performance of the CFI algorithm.

#### 7.4.2 Passive real-time field trialing

As the method has been developed with the view of being able to be embedded in the same hardware platform as an existing digital distance protection relay, it is possible that the method could be trialed in such devices, without actually executing any direct control commands. The proposed objective of such an implementation would be to test the algorithm "on-line" for its ability to detect and correctly identify fault cases, in addition to checking its accuracy for current zero time predictions. It would also be possible to verify the ability of the algorithm to execute its designated processing steps within the response time of the associated protection algorithm(s).

While proposed as a "passive" trialing, meaning that the algorithm is excluded from any control of trip commands to a circuit breaker, consideration would need to be made as to the correct selection of digital relay platform within which the algorithm was embedded (e.g. processor speed and memory) so that implementation of the algorithm does not lead to any

unacceptable degradation of the protection system performance. An alternative (though more expensive) approach would be to simply embed the algorithm in such a relay, installed as an additional (passive) device within a bay.

Due to the random (and hopefully infrequent) nature of fault occurrences, in order for such passive trialling to provide a useful and credible amount of data, it would be ideal if the algorithm could be easily embedded in a number of digital relays on the same network and operated over a two to three year period, with periodic review of events. Such an implementation may also provide a useful means to test and compare alternative data processing methods on-line e.g. for fault inception detection, fault type identification, phase angle estimation. The observed performance of the CFI method from such trials would provide a valuable reference for further assessment of the viability of CFI control both in general and for any possible application of such a technique for use with “optimized” circuit breaker designs that would be critically dependent on the correct function of the CFI algorithm.

### 7.4.3 Active real-time field trialling

Assuming reasonable accuracy and robustness is found from passive trialling of a CFI algorithm as described in 7.4.2, the next logical step in the introduction of CFI would be to proceed to selective active trialling, where by the CFI algorithm is permitted to interact directly in the control and protection system. A first step in such active trialling could be the use of the CFI algorithm as a tool to improve circuit breaker interruption failure detection, whereby the algorithm predicts the current zero that the circuit breaker should interrupt and could issue a back-up trip command signal if current was still observed to flow within a defined time error margin after the predicted interruption time. This may provide for shorter margins in protection system time grading between “primary” and “back-up” protection, which is typically based today on conservative estimates of the “worst case” clearing time for the given circuit breaker type.

## 7.5 Current interruption technologies based on CFI

Table 7.4 provides a summary of possible research threads directed towards the development of interruption technologies based on integrated dependent use of CFI in such designs.

Work packages		Prior CFI methods (e.g. Pörtl "Safepoint" method)	Proposed CFI method	Future work proposals
Interrupter development research	Arc-based interrupters	No investigation	Some investigation on minimum arcing time behavior operating at 20% lower than designed opening speed.	Investigate benefits (or limitations) in designing interrupter for a "restricted" arcing window for full range of standardized interruption duties.
	Power electronic interrupters	No investigation	No investigation	Some work already published. Investigate application of CFI algorithm as tool to facilitate commutation control of power electronic based interrupter for high voltage application.

**Table 7.4: Summary of interruption technology research areas based on CFI**

The experiments presented in Chapter 3 of this thesis aimed to provide both information on the stability minimum arcing times of HV SF<sub>6</sub> circuit breakers in addition to exploring the effect of reducing the opening energy used by such a circuit breaker on the minimum arcing time boundary. While the results were promising in both respects, there remains significant scope for further work in the area of interrupter design to quantify the viable benefits that might be obtained in arc-based interrupter design using CFI, including possibly the use of alternative, more environmentally friendly interrupting media than SF<sub>6</sub>. As also stated earlier in the thesis, interrupters not based on an arc design, such as power electronic interrupters [54], could be developed to high voltage levels through the use of CFI.

Development of a CFI-dependent interrupter raises a number of critical issues, not least in terms of the reliability of such a design compared to today's non-CFI dependent circuit breakers. This places a high demand on the benefits to be proven using a CFI-dependent design so as to justify either the possibly reliability limitations or the additional measures required to maintain an acceptable level of reliability in such a device. Interrupter design itself normally involves disciplines outside of electrical power engineering, such as plasma physics, but in the broader context of CFI should involve a multidisciplinary approach. Such work also normally involves a level of investment, laboratory and computer resources that requires the support if not direct involvement of a major circuit breaker manufacturer.

It would be nevertheless beneficial for further research in this particular potential for the utilization of CFI in order to establish a more comprehensive understanding of the risks and benefits arising from the pursuit of CFI.



## 8 Conclusions

A method for implementation of controlled fault interruption has been presented, based on synchronizing the trip commands to each phase of a three phase circuit breaker with respect to selected current zero times that are estimated from a model of the sampled currents in each phase. The presented work has shown that while there are significant challenges in implementing a viable CFI scheme, there are interesting potential benefits, not only for reduction in the interrupter wear rate or optimization of circuit breaker design, but also possibly vicarious benefits for the further development of protection algorithms and circuit breaker failure detection.

### 8.1 Fulfilment of thesis goals

As declared in Chapter 1, two main goals were set for this thesis work:

1. Extension of the single phase CFI method outlined in the licentiate thesis to three phase application with associated simulation analyses of algorithm performance under a range of system fault conditions.
2. High power experiments to investigate aspects of circuit-breaker performance related to both the application and potential benefits of controlled fault interruption.

The proposed CFI method has been shown to reliably predict the target current zero times for a wide range of multi-phase fault cases within a three phase network, within +/- 0.5 ms, even in the presence of large simulated signal noise and without prolongation of the total fault clearing time. The analysis of variance tests have been applied to facilitate fault type identification in addition to their roles for fault inception detection and CFI solution validation control. Further work is required to develop and test the proposed method for more specialized fault cases such as those near large generators or on series compensated lines.

The high power experiments conducted as part of this thesis have provided valuable insight into the minimum arcing time behavior of an HV SF<sub>6</sub> circuit breaker, in addition to showing the potential for circuit breaker optimization through the use of CFI to allow a restricted arcing window. While the results covered only a limited range of interruption duties, in general the arcing times were found to be sufficiently consistent to suggest that CFI is viable using a target arcing time based on a type tested minimum arcing time with an added 1 ms arcing time margin. The results were obtained operating the circuit breaker at 20% below its designed opening speed. While the observed arcing times were correspondingly slightly longer than for the normal opening speed, the changes were moderate (within 3 ms) and the consistency in the accumulated interruption minimum arcing time limits were good. Exception results were obtained on the short-line fault tests, but this provides a valid indication that the need to fully optimize an interrupter if operational energy savings are to be effectively gained from the use of CFI. It was also shown that it is possible obtain a useful model of the interrupter wear rate and thereby provide a CFI algorithm with a means to update its expected opening and arcing times with accumulated interruptions.

## 8.2 Novel contributions of the work

While prior methods for CFI have been proposed, the work contained in the Licentiate and this thesis has sought to augment the area of CFI research in a number of important ways. The five main novel contributions of this work, within the context of CFI, include:

### 1. Proposed structure for CFI strategy classification

First outlined in Chapter 5 of the Licentiate thesis [1], the structural classification of CFI application strategy types, presented in Table 8.1 (see also Table 4.1 in this thesis), is considered an important contribution to guiding the continued development of CFI methods, both in terms of defining objectives and assessment of performance.

**Table 8.1: Classification structure for CFI strategy types (as per Table 4.1)**

CFI "Type":	1	2	3	4
Arcing time	NON-CRITICAL		CRITICAL	
Optimization	Clearing Time	Arc Energy	Clearing Time	Arc Energy
Accuracy	Moderate e.g. $\pm 1\text{ms}^*$	Moderate	High e.g. $\pm 0.1\text{ms}^*$	High
Security	Moderate e.g. $>95\%^*$	Moderate	High e.g. $>99.9\%^*$	High
Signal Noise Tolerance	Low e.g. $\leq 5\%   \text{WGN}^*$	Low	High e.g. $\leq 20\%   \text{WGN}^*$	High
Response Time	Fast e.g. $\frac{1}{4}\text{-}\frac{1}{2}\text{ cycle}^*$	Moderate e.g. $\frac{1}{2}\text{-}1\text{ cycle}$	Fast	Moderate

\* Note: Examples for "tolerances" shown above are indicative suggestions only.

### 2. Generic structure for CFI implementation

A generic structure has also been proposed for the integration of CFI into the existing control and protection systems used in modern power systems with digital relay platforms, as shown in Figure 8.1 (originally as per Figure 4.6). Importantly the CFI algorithm has been used as a complement to the protection system and provided with a means of self-checking and by-pass control in order to maintain robustness of the overall current interruption process.

The proposed method offers a generic structure for the development of CFI, independent of specific methods for the prediction of the current behavior or methods to estimate current parameters, fault inception or fault type and thus is open to utilizing alternative methods for all of these parts of the process and maximizing the synergies to be gained from existing digital protection scheme methods.

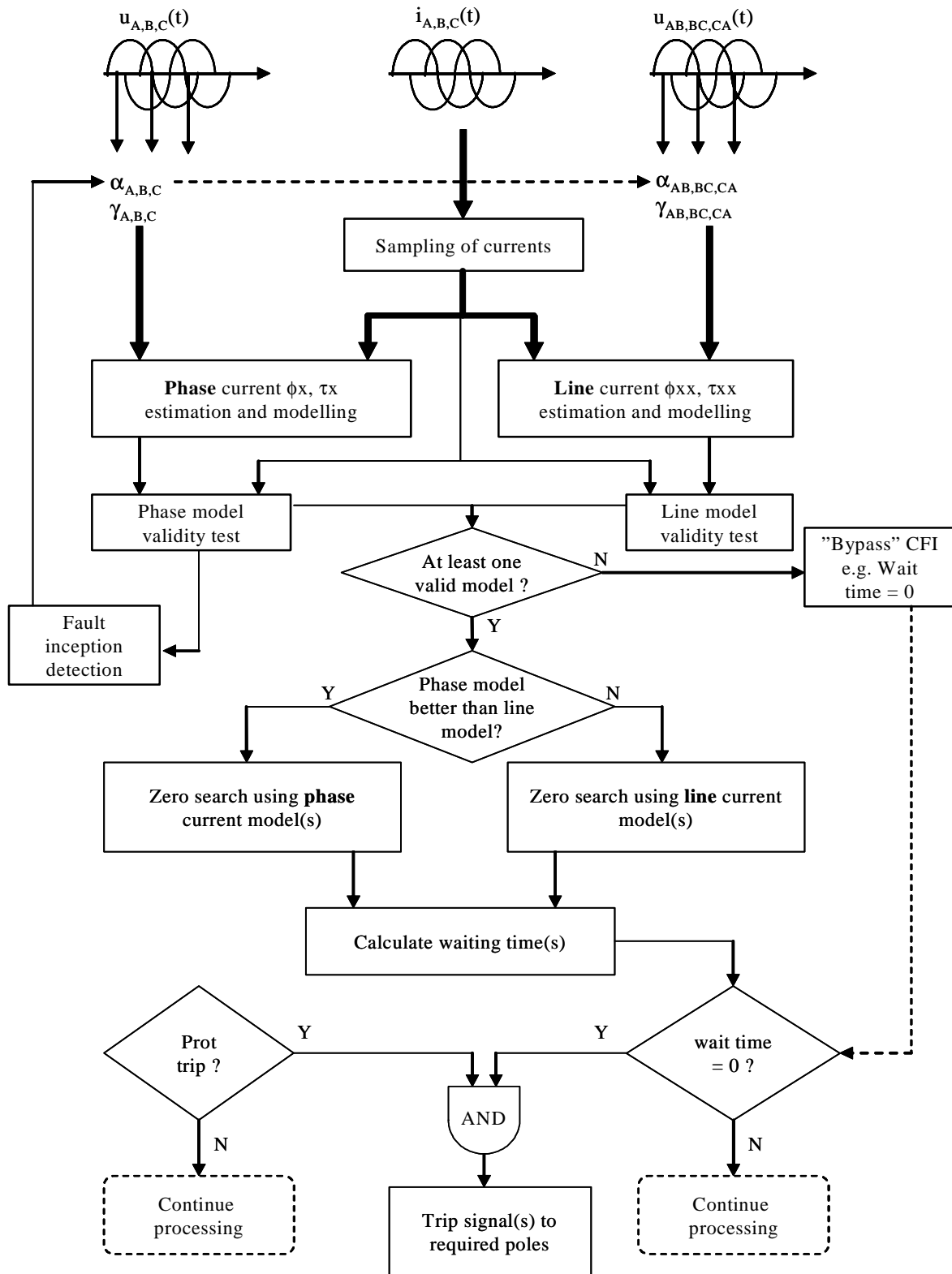


Figure 8.1: Proposed three phase CFI algorithm structure (as per Figure 4.6)

### 3. Defined measures for assessing CFI method performance

A number of important CFI performance measures have been defined and applied during the course of this work in order to provide a quantified basis for assessing various aspects of the proposed method. The measures have been defined with a focus on the CFI method performance with respect to the critical functions and objectives of the algorithm and included:

- a. error in predicted current zero times
- b. savings in arc integral using CFI compared to direct tripping
- c. impact on total fault clearing time (compared to direct tripping)
- d. error in estimation of fault inception instant
- e. fault type identification success rate
- f. overall CFI operation success rate

### 4. Use of analysis-of-variance test

The introduction of the analysis-of-variance (ANOVA) test to the CFI algorithm is novel in the context of power system control and protection. It is a critical part of the proposed method in terms of maintaining operational security and facilitating bypassing of the algorithm in the event of its inability to achieve an acceptable modelling of the current. This application of ANOVA may also have potential in the wider context of protection system robustness control if applied for verification of phase angle and other parametric estimations. The ANOVA test has also been shown to be a means for fault inception detection and fault type identification.

### 5. Information on minimum arcing time behavior of an HV SF<sub>6</sub> circuit breaker

The particular high power tests made for this thesis work were conducted on a circuit breaker operated at 20% below its normal opening speed, representing a significant reduction in the operating energy of the circuit breaker. While the measured arcing times were slightly longer compared to those obtained during type tests at 100% normal opening speed, the difference was reasonably small (2-3 ms) and the stability of the minimum arcing times, even after 6 to 12 interruptions provides encouraging evidence that the minimum arcing time of an HV SF<sub>6</sub> circuit breaker is sufficiently stable to support CFI.

Nevertheless it was found that for short-line fault interruptions, the minimum arcing time at reduced opening speed was significantly longer than for the other fault interruption duties. While this difference was not unexpected, due to the high thermal stress associated with short-line fault interruption, it is a noteworthy reminder that optimization of a circuit breaker by lowering of operating energy, in conjunction with use of CFI, will involve modification to the overall interrupter design in order to provide the necessary arcing time predictability and consistency required for CFI implementation.

Each of the above contributions are extensions in the structure and implementation of CFI beyond the Safepoint method presented by Pörtl. Nevertheless, Pörtl's concept of the Safepoint approach still provides a useful approach to the CFI problem and it is feasible that the additional features presented above could be incorporated with the Safepoint approach to provide an even more robust CFI solution.

### 8.3 Results summary

The proposed algorithm has been shown to perform well according to its intended functions, within the modelled framework that it has so far been tested. Current zero-crossing times were predicted with errors less than  $\pm 0.5$  ms, within 10...20ms protection response times, even for comparatively large (10% magnitude) random signal noise.

The F0, ANOVA test, introduced in the licentiate was shown again to be an effective means for fault inception detection. The use of F0 trend analysis provided fault inception instant detection within six electrical degrees, even for 10% magnitude random signal noise simulations. In some cases the error in fault instant detection ranged up to 20 electrical degrees, but the algorithm was still able to provide target current zero time predictions within  $\pm 0.5$  ms in such cases.

The combined use of the phase-to-earth and phase-to-phase source voltage parameter models, together with the ANOVA tests were able to effectively discriminate between earthed and unearthed multiphase faults for all cases, except for three phase earthed and unearthed faults, where the behavior of the fault currents is identical until the first phase is interrupted. However the compromise targeting solution for the last two phases to interrupt in three phase fault cases was shown to be reasonably effective, resulting in a targeting error in only one of the phases in the order of -1.5 ms. Though larger than the general error range of  $\pm 0.5$  ms, the -1.5 ms error is acceptable, provided the circuit breaker can interrupt with an arcing window in the order of 3 ms wide. The negative zero crossing error means that the CFI algorithm uses an "early" targeting point, and thus avoids the risk of a "late" target estimation that may result in a failure to interrupt at the desired current zero and lead to an additional forced current loop before interruption can be attempted.

The arc integral savings observed during the simulations were consistent with those seen for the single phase CFI simulations presented in the licentiate for the same values of protection response time, circuit breaker operating times, time constant and fault inception angle values, being in the range of 0 to 50%.

### 8.4 Areas for further development

In addition to the future work proposals described in Chapter 7, there remain aspects of the algorithm performance that can be improved. While the F0 ANOVA test has been usefully applied for algorithm control, fault inception detection and fault type identification, its performance in the last two functions could be improved. The F0 trend analysis method for fault inception detection has been shown to be somewhat sensitive to the fault inception angle, particularly for angles near  $n\pi$  ( $n: 0,1,2$ ), where while the asymmetry is maximum, the rate of change of the current from the load to fault state is gradual and therefore leads to a longer data sampling set required before the F0 trend method reacts to the state change.

It should also be noted, as described in Chapter 7, that alternative ANOVA methods may prove more robust or suitable to a CFI algorithm. Consideration could also be given to utilizing ANOVA results, e.g. residuals analysis, in a more active way for improvement of the characteristic parameter estimations, in particular the phase angle, time constant and fault current magnitude estimates. In this respect the incorporation of some form of feedback control integrated to the CFI algorithm may prove useful, particularly with respect to its performance under more realistic dynamic system operating conditions with continuous changes in phase angle and current magnitude.

While using the ANOVA tests for several functions within the algorithm offers some advantage in terms of maximizing return on the computational investment and maintain some inherent simplicity in the structure of the algorithm, this should not preclude using separate methods for fault inception detection or fault type classification. The presented method of computing both phase-to-earth and phase-to-phase frame-of-reference parameter values is somewhat inefficient and given that the phase-to-phase model case should only arise in connection with a phase-to-phase unearthed fault, the calculation of this case could be “suppressed” until a fault is detected. Equally, alternative methods for fault type identification could be used to reduce the need for parallel parameter set calculations and so reduce the computational effort required.

## 8.5 Closing remarks

The idea to being able to control the operation of a circuit breaker to coincide with a targeted current zero for interruption has existed virtually since the start of circuit breaker development. The concept itself appears at first, almost obvious, if not simple, but the reality of achieving such a control has been often considered too difficult to be viable. The past century has seen development of a wide range of ingenious and reliable arc-based interrupters that have been designed to circumvent the difficulty of achieving CFI with acceptable reliability and cost. While arc-based interrupters have served the power industry very well over time, the advances in digital control schemes now allow us to revisit the possibility of achieving CFI, equipped with new and powerful tools.

While potential direct benefits to circuit breaker operation and development have been identified from the application of CFI, it is possible that continued research in this area may provide additional benefits in associated areas. The best measure of this thesis will be if it stimulates further research in this area to lead not only to better solutions, but also an improved body of reference material with respect to current interruption and circuit breaker control in support of reliable, cost effective and sustainable electrical power utilization.

# References

## References

Titles of referenced journal articles, conference papers or technical reports are presented within “quotation marks”.

Titles of referenced standards are presented in *italics*.

Titles of referenced books are presented in ***bold italics***.

- [1] Thomas R., “Controlled Switching of High Voltage SF<sub>6</sub> Circuit Breakers for Fault Interruption”, Technical report No. 514L, Chalmers University of Technology, Sweden, 2004.
- [2] Pörtl A., Fröhlich K., “A New Algorithm Enabling Controlled Short Circuit Interruption”, IEEE Trans. Power Delivery, Vol. 18, No. 3, pp802-808, July 2003.
- [3] Garzon R. D., ***High Voltage Circuit Breakers: Design and Applications***, Marcel Dekker Inc, New York, 1997
- [4] Horowitz S. H., Phadke A. G., ***Power System Relaying***, 2nd edition, Research Studies Press Ltd., Baldock, England, 1995.
- [5] IEC 62271-100:2001, *High-voltage switchgear and controlgear - Part 100: High-voltage alternating-current circuit-breakers*, International Electrotechnical Commission, Geneva, May 2001.
- [6] IEC 60427:2000 Third Edition, *Synthetic testing of high-voltage alternating current circuit-breakers*, International Electrotechnical Commission, Geneva, April 2000.
- [7] IEC TR 62271-310:2004 First Edition, *Technical Report - High-voltage switchgear and controlgear - Part 308: Electrical endurance testing for circuit-breakers of rated voltage 72,5 kV and above*, International Electrotechnical Commission, Geneva, April 2004.
- [8] CIGRÉ Brochure 140, “Reliable fault clearance and back-up protection”, CIGRÉ, Paris, April 1999.
- [9] ANSI C37.06-1987, *AC High-Voltage Circuit Breakers Rated on a Symmetrical Current Basis - Preferred Ratings and Related Required Capabilities*, American National Standards Institute, Inc. New York, 1987.
- [10] ANSI C37.013-1997, *Standard for AC High-Voltage Generator Circuit Breakers Rated on a Symmetrical Current Basis*, American National Standards Institute, Inc. New York, 1997.
- [11] CIGRÉ Task Force 13.00.1 of Study Committee 13, “Controlled Switching - A State-of-the-Art Survey (Part 1)”, Electra No. 162, Oct. 1995, CIGRÉ, Paris.
- [12] CIGRÉ Task Force 13.00.1 of Study Committee 13, “Controlled Switching - A State-of-the-Art Survey (Part 2)”, Electra No. 164, Feb. 1996, CIGRÉ, Paris.

## References

- [13] CIGRÉ Working Group 13.07, “Controlled Switching of HV AC Circuit Breakers: Guide for application lines, reactors, capacitors, transformers (1st Part)”, Electra No 183, Apr 1999, CIGRÉ, Paris.
- [14] CIGRÉ Working Group 13.07, “Controlled Switching of HV AC Circuit Breakers: Guide for application lines, reactors, capacitors, transformers (2nd Part)”, Electra No 185, Aug 1999, CIGRÉ, Paris.
- [15] CIGRÉ Working Group A3.07, “Controlled Switching of HV AC Circuit Breakers: Guidance for further applications including unloaded transformer switching, load and fault interruption and circuit-breaker uprating”, Jan 2004, CIGRÉ, Paris.
- [16] CIGRÉ Working Group A3.07, “Controlled Switching of HV AC Circuit Breakers: Benefits & economic aspects”, Jan 2004, CIGRÉ, Paris.
- [17] CIGRÉ Working Group A3.07, “Controlled Switching: non-conventional applications”, Electra No 214, Jun 2004, CIGRÉ, Paris.
- [18] Pörtl A., Fröhlich K., “Two New Methods for Very Fast Fault Type Detection by Means of Parameter Fitting and Artificial Neural Networks”, IEEE Trans. Power Delivery, Vol. 14, No. 4, pp1269-1275, Oct. 1999.
- [19] Fortescue, C.L., “Method of Symmetrical Coordinates Applied to the Solution of Polyphase Networks”, Trans. AIEE, Vol. 37, pp 1027-1140, 1918. (See also [27], Appendix II.)
- [20] Greenwood, Allan, *Electrical Transients in Power Systems*, 2nd edition, John Wiley & Sons Inc., New York, 1991.
- [21] Anderson P. M., *Power System Protection*, IEEE Press, John Wiley & Sons Inc., New York, 1999.
- [22] Pons A., Sabot A., Babusci G., “Electrical Endurance and Reliability of Circuit-Breakers - common Experience and Practice of Two Utilities”, IEEE Trans. Power Delivery, Vol. 8, No. 1, pp168-174, Jan. 1993.
- [23] Blez B., Henry J.C., Martin J., “Essais d’endurance électrique des disjoncteurs HT: les alléger sans diminuer leurs représentativité”, RGE 7, 1987. (Referenced from [22] above).
- [24] Jeanjean R., Salzard C., Migaud P., “Electrical Endurance Tests for HV Circuit-Breakers: EDF Experience”, IEEE, pp294-298, 2002.
- [25] Neumann C., Balzer G., Becker J., Meister R., Rees V., Sölver C-E., “Stress of HV Circuit-Breakers During Operation in the Networks - German Utilities Experience”, Paper 13-304, CIGRÉ, Paris, Aug. 2002.



## References

- [26] Satou T., Nishio M., Kawakita K., Baba S., Kamei K., Hirano Y., Kobayashi A., Nakamoto T., Hirasawa K., Yuichiro Y., "Influence of the time constant of D.C. component on interrupting duty of GCB", IEEE Power Engineering Society Winter Meeting, Columbus Ohio USA, Vol 1, pp300-305, IEEE 2001.
- [27] Phadke A.G., Thorp, J.S., *Computer Relaying for Power Systems*, Research Studies Press Ltd, Baldock, England, 1988.
- [28] Isaksson A., "A Study of methods for digital protective relaying", Report LiTH-ISY-I-0769, Linköping University, Linköping, Sweden, 1985.
- [29] Isaksson A., "Digital protective relaying through recursive least-squares identification", IEE Proceedings, Vol 135, Part C, No. 5, Sept. 1988.
- [30] MATLAB<sup>®</sup> Version 6.5.1.199709 Release 13 (Service Pack 1), Copyright 1984-2003, The Mathworks, Inc. (Licensed No 188486, ABB Power Technology Products AB).
- [31] Johannesson T., Ingemansson D., Messing L., "The probability of a large fault current DC component", Preferential subject 3, CIGRÉ Colloquium SIBIU, Romania Sept 10-14, 2001.
- [32] van der Sluis, L., Rutgers W. R., Koreman C.G.A., "A physical arc model for the simulation of current zero behavior of high voltage circuit breakers", IEEE Trans. Power Delivery, Vol. 7, No. 2, April 1992.
- [33] Habedank U., Knobloch, H., "Zero-crossing measurements as a tool in the development of high voltage circuit breakers", IEE Proc. Sci. Meas. Technol., Vol. 148, No. 6, Nov. 2001.
- [34] Mazza G., Michaca R., "The First International Enquiry on Circuit Breaker Failures & Defects in Service", CIGRÉ - ELECTRA No. 79, Dec 1985, pp21-91.
- [35] Heising C.R., Colombo E., Janssen A.L.J., Maaskola J.E., Dialynas E., "Final Report on High-Voltage Circuit Breaker Reliability Data for Use in Substation and System Studies", Paper 13-201, CIGRÉ, Aug 28 - Sept 3, 1994, Paris.
- [36] Janssen A.L.J., Degen W., Heising C.R., Bruvik H., Colombo E., Lanz W., Fletcher P., Sanchis G., "A Summary of the Final Results and Conclusions of the Second International Enquiry on the Reliability of High-Voltage Circuit Breakers", Paper 13-202, CIGRÉ, Aug 28 - Sept 3, 1994, Paris.
- [37] Canadian Electricity Association, "Forced Outage Performance of Transmission Equipment - for the Period January 1, 1993 to December 31, 1997", CEA, 1998.
- [38] Bosma A., Koerber F-J., Cameroni R., Thomas R., "Motor Drive with Electronic Control for HVAC Circuit Breakers", Paper 13-203, August Session, 2002, CIGRÉ, Paris.

## References

- [39] Bosma A., Thureson, P-O., "A New Reliable Operating Mechanism for HVAC Circuit-Breakers", Transmission and Distribution Conference and Exposition, 2001 IEEE/PES, Vol. 1, Oct 28 - Nov 2, 2001.
- [40] Flurscheim C.H.(Editor), *Power circuit breaker theory and design*, Peter Peregrinus Ltd. on behalf of IEE, London, Revised Edition 1982.
- [41] Knobloch H., Marin H., Schramm H-H., Stenzel P., Kirchesch P., Schiemann A., de Hessel M., Möller K., von Starck R., "Technological Trends in High-Voltage Circuit-Breakers", Paper 13-106, CIGRÉ, Paris, Aug 2000.
- [42] Dufornet D., Ozil J., Sciullo F., Ludwig A., "New interrupting and drive techniques to increase high voltage circuit breaker performance and reliability", Paper 13-104, CIGRÉ, Paris, Aug. 1998.
- [43] Aeschbach H., Blatter J., Dufournet D., Christen J., "Arc Modelling Application to High Voltage Circuit Breaker Development", Paper 13-102, CIGRÉ, Paris, Aug-Sept 1994.
- [44] Nakanishi K., Hirasawa K., Yanabu S., Yoshizumi T., "Analysis and Application of Interrupting Arc and Gas Flow in SF<sub>6</sub> Gas Circuit Breaker", Paper 13-104, CIGRÉ, Paris, Aug-Sept 1994.
- [45] Möller K., Claessens M., Thiel H.G., Rütten U., Stechbarth J., "Progress in Modelling of Circuit-Breaker Arcs Considering Gas Flow Interaction", Paper 13-108, CIGRÉ, Paris, Aug-Sept 1994.
- [46] Montgomery Douglas C., Runger George C., *Applied Statistics and Probability for Engineers*, 2nd Edition, John Wiley & Sons, Inc., New York, 1999.
- [47] CIGRÉ Brochure 11, "Evaluation of characteristics and performance of power system protection relays and protective systems", CIGRÉ, Paris, January, 1986.
- [48] EMTDC/PSCAD Professional © (2005) by Manitoba Hydro Research Centre Inc. Version 4.2.0, License No 479028.
- [49] Lehmann K., Zehnder L., Chapman M., "A Novel Arcing Monitoring System for SF<sub>6</sub> Circuit Breakers", Paper 13-301, CIGRÉ, 2002, Paris Aug. 2002.
- [50] Kuhn M., Hadorn P., Heinemann Th., "In Service Operating Times of High Voltage Circuit Breakers with Spring Operating Mechanisms", Paper 13-101, CIGRÉ, Paris, Aug-Sept 1994.
- [51] Anderson P.M., Farmer R. G., *Series Compensation of Power Systems*, PBLSH! Inc., Encinitas, USA, 1996.

## References

- [52] Bui-Van Q., Khodabakhchian B., Landry M., Mahseredjian J., Mainville J., “Performance of Series-Compensated Line Circuit Breakers Under Delayed Current-Zero Conditions”, IEEE Trans. Power Delivery, Vol. 12, No. 1, pp227-233, Jan. 1997.
- [53] Ito H., “Controlled Switching Technologies, State-of-the-Art”, IEEE Transmission and Distribution Conference and Exhibition 2002: Asia Pacific. IEEE/PES, pp1455 - 1460, Vol. 2, 6-10 Oct. 2002.
- [54] Larsson P., Backman M., Jonsson L., “Method and Device for Prediction of a Zero-Crossing Alternating Current”, United States Patent No. US 7,010,436 B2. Patent date: March 7, 2006. PCT Publication date: June 14, 2003.
- [55] Niemira J. K., O’Leary R. P., “Predictive Control Circuit and Method for Circuit Interrupter”, United States Patent No. US 5,793,594. Patent date: Aug 11, 1998. Filed: Dec 21, 1995.
- [56] Sinha G., Premerlani W. J., Vlatkovic V., “Method and System for Real-Time Prediction of Zero Crossings of Fault Currents”, United States Patent No. US 6,597,999 B1. Patent date: Jul. 22, 2003. Filed: Dec 20, 1999.
- [57] McLaren P.G., Mustaphi K., Benmouyal G., Chano S., Girgis A., Henville C., Kezunovic M., Kojovic L., Marttila R., Meisinger M., Michel G., Sachdev M. S., Skendzic V., Sidhu T. S. and Tziouvaras D., “Software Models for Relays”, IEEE Trans. Power Delivery, Vol. 16, No. 2, April 2001.
- [58] Girgis A. A., Brown R. G., “Application of Kalman Filtering in Computer Relaying”, IEEE Trans. Power Apparatus and Systems, Vol. PAS-100, No. 7, July 1981.
- [59] Girgis A. A., “A New Kalman Filtering Based Digital Distance Relay”, IEEE Trans. Power Apparatus and Systems, Vol. PAS-101, No. 9, Sept. 1982.
- [60] Girgis A. A., Brown R. G., “Modelling of Fault-Induced Noise Signals for Computer Relaying Applications”, IEEE Trans. Power Apparatus and Systems, Vol. PAS-102, No. 9, Sept. 1983.
- [61] Girgis A. A., Brown R. G., “Adaptive Kalman Filtering in Computer Relaying: Fault Classification Using Voltage Models”, IEEE Trans. Power Apparatus and Systems, Vol. PAS-104, No. 5, May 1985.
- [62] Sachdev M.S., Baribeau M.A., “A New Algorithm for Digital Impedance Relays”, IEEE Trans. Power Apparatus and Systems, Vol. PAS-98, No. 6, Nov./Dec. 1979.
- [63] Sachdev M.S., Nagpul M., “A Recursive Least Error Squares Algorithm for Power system Relaying and Measurement Applications”, IEEE Trans. Power Delivery, Vol. 6, No. 3, July 1991.

## References

- [64] Altuve H. J. F., Díaz I. D., Vázquez E. M., “Fourier and Walsh Digital Filtering Algorithms for Distance Protection”, IEEE Trans. Power Systems, Vol. 11, No. 1, Feb. 1996.
- [65] Gilbert D. M., Morrison I. F., “A Statistical Method for the Detection of Power System Faults”, Electrical Power & Energy Systems, Vol. 19, No. 4, pp. 269-275, 1997.
- [66] Chowdury F. N., Christensen J. P., Aravena J. L., “Power System Fault Detection and State Estimation Using Kalman Filter with Hypothesis Testing”, IEEE Trans. Power Delivery, Vol. 6, No. 3, July 1991.
- [67] Sidhu T. S., Ghotra D. S. and Sachdev M. S., “An Adaptive Distance Relay and its Performance Comparison With a Fixed Data Window Distance Relay”, IEEE Trans. Power Delivery, Vol. 17, No. 3, July 2002.
- [68] Sidhu T. S., Zhang X., Balamourougan V., “A New Half-Cycle Phasor Estimation Algorithm”, IEEE Trans. Power Delivery, Vol. 20, No. 2, April 2005.
- [69] Gilcrest G. B., Rockefeller G. D., Udren E. A., “High-Speed Distance Relaying Using a Digital Computer - Part I: System Description”, IEEE Trans. Power Apparatus and Systems, Vol. PAS-91, pp. 1235-1243, 1972.
- [70] Mann B. J., Morrison I. F., “Digital Calculation of Impedance for Transmission Line Protection”, IEEE Trans. Power Apparatus and Systems, Vol. PAS-90, No. 1, Jan/Feb. 1971.
- [71] Mann B. J., Morrison I. F., “Relaying a Three Phase Transmission Line With a Digital Computer”, IEEE Trans. Power Apparatus and Systems, Vol. PAS-90, No. 2, Mar/Apr 1971.
- [72] Tziouvaras D.A., McLaren P., Alexander G., Dawson D., Estergalyos J., Fromen C., Glinkowski M., Hasenwinkle I., Kezunovic M., Kojovic L., Kotheimer B., Kuffel R., Nordstrom J., Zocholl S., “Mathematical Models for Current, Voltage and Coupling Capacitor Voltage Transformers”, IEEE Trans. Power Delivery, Vol. 15, No. 1, Jan. 2000.
- [73] Swift G., “Discussion on “Mathematical Models for Current, Voltage and Coupling Capacitor Voltage Transformers””, IEEE Trans. Power Delivery, Vol. 16, No. 4, Oct. 2001.
- [74] IEC 60044-1:2003 Edition 1.2, *Instrument transformers - Part 1: Current transformers*, International Electrotechnical Commission, Geneva, Feb. 2003.
- [75] IEC 60044-2:2003 Edition 1.2, *Instrument transformers - Part 2: Inductive voltage transformers*, International Electrotechnical Commission, Geneva, Feb. 2003.
- [76] IEC 60044-5:2004 Edition 1.0, *Instrument transformers - Part 5: Capacitor Voltage transformers*, International Electrotechnical Commission, Geneva, Apr. 2004.

## References

- [77] IEC 44-6:1992 Edition 1.0, *Instrument transformers - Part 6: Requirements for protective current transformers for transient performance*, International Electrotechnical Commission, Geneva, Mar. 1992.



**Project settings:**

Characteristic	Value	Units
Solution time step	50	$\mu\text{s}$
Channel plot time step	50	$\mu\text{s}$

**Source:**

Characteristic	Value	Units
Base voltage	24	kV
Base MVA (3-phase)	10 000	MVA
Base frequency	50	Hz
Source control	Fixed	-
Specified parameters	At the terminals	-
Voltage input time constant	0.001	s
Zero sequence differs from positive sequence	Yes	-
Positive sequence series resistance	0.1	$\Omega$
Positive sequence parallel resistance	0.2	$\Omega$
Positive sequence parallel inductance	0.5	H
Zero sequence parallel resistance	4.0	$\Omega$
Zero sequence parallel inductance	0.15	H

**Source Transformer:**

Characteristic	Value	Units
Primary / Secondary voltages	24 / 420	kV
Power rating	2 000	MVA
Frequency	50	Hz
Ideal transformer model	No	-
Positive sequence leakage reactance	0.01	p.u.
No load losses	0.01	p.u.
Copper losses	0.00	p.u.

**Load Transformer:**

Characteristic	Value	Units
Primary / Secondary voltages	420 / 24	kV
Power rating	750	MVA
Frequency	50	Hz
Ideal transformer model	No	-
Positive sequence leakage reactance	0.05	p.u.
No load losses	0.02	p.u.
Copper losses	0.00	p.u.



**Circuit breaker:**

Characteristic	Value	Units
Open resistance	$10^6$	$\Omega$
Closed resistance	0.005	$\Omega$
Open possible on any current?	No	-
Current chopping limit	0.00	kA

**Load (per phase):**

Characteristic	Value	Units
Voltage	245	kV
Frequency	50	Hz
Rated active power	350	MW
Rated reactive power	40	MVA <sub>r</sub>
dP/dV (index)	2	-
dQ/dV (index)	2	-
dP/df (index)	0	-
dQ/df (index)	0	-

**Transmission lines:**

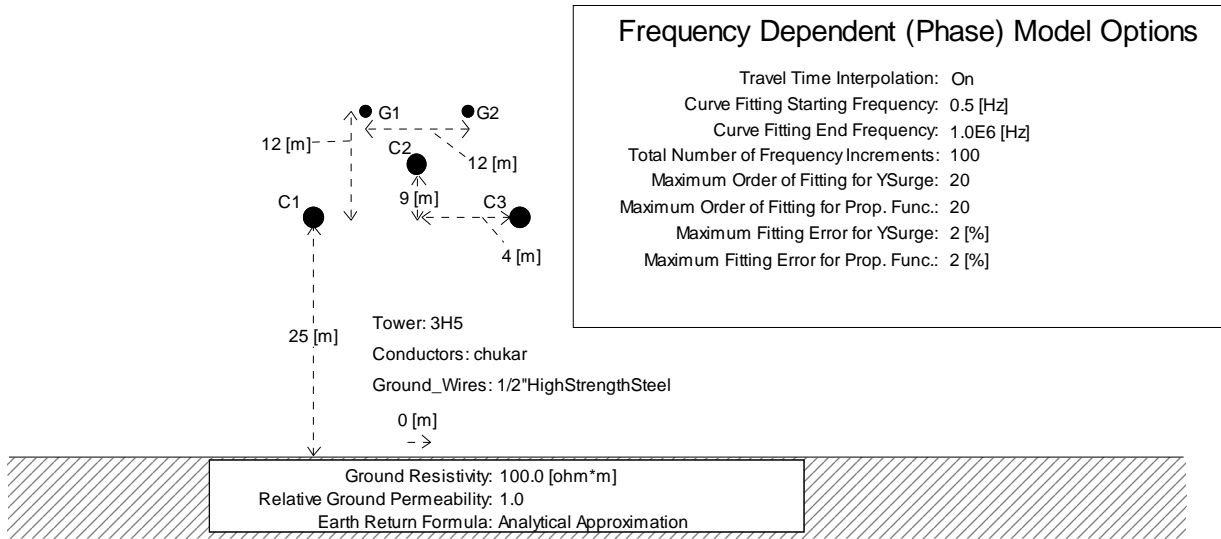


**Figure A.2 : EMTDC/PSCAD transmission line section details**

**Transmission line “TLine1” - circuit breaker to fault location:**

Characteristic	Value	Units
Voltage	420	kV
Frequency	50	Hz
Length	50	km
Conductors per phase	1	-

**Transmission line “Tline2” - fault location to load:**

Characteristic	Value	Units
Voltage	420	kV
Frequency	50	Hz
Length	150	km
Conductors per phase	1	-

**Multi-phase fault generator:**

Characteristic	Value	Units
Fault on resistance	0.01	$\Omega$
Fault off resistance	$10^6$	$\Omega$

===||===